SECOND MESSENGER SYSTEMS IN ALZHEIMER'S DISEASE: A QUANTITATIVE AUTORADIOGRAPHIC STUDY

KAREN J. HORSBURGH, B. Sc. (HONS)

A thesis submitted for the Degree of Doctor of Philosophy
to the Faculty of Medicine, University of Glasgow

Wellcome Surgical Institute &
Hugh Fraser Neuroscience Laboratories,
University of Glasgow,
Garscube Estate,
Bearsden Road,
Glasgow G61 1QH.

ProQuest LLC.
789 East Eisenhower Parkway
P.O. Box 1346
Ann Arbor, MI 48106 – 1346

CONTENTS

PAGE NOS.

PAGE NOS.

PAGE NOS.

APPENDICES

TABLES

PAGE NOS.

FIGURES

ACKNOWLEDGEMENTS

It has been a great pleasure for me to work with all of the staff at the Wellcome Surgical Institute. During my three years, I have benefited from the kindness and generosity of everyone, and I thank them all.

I would like to extend my warmest gratitude to Professor James McCulloch, whose constant enthusiasm was a source of inspiration for me, (most of the time). The freedom he allowed in following my research interests and insistent demands for experimental rigour are now fully appreciated, and I recognise the firm neuroscientific background with which he has afforded me. I hope his daunting task of supervising a student whose awareness of neuroanatomy was confined to the knowledge of a front, a middle and a back have not been effortless.

Thanks are also extended to Professor Murray Harper for both his moral support throughout my studies and the provision of excellent laboratory facilities, not to mention the luxurious office which was provided for the preparation of this thesis. I would also like to thank Sue Browne, Dr. Deborah Dewar, Fiona Inglis, Dr. Mhairi Macrae, Mark McLaughlin, Mike Robinson and Brian Ross who have guided me in the laboratory and scientifically, (and even from the pub!).

The excellent assistance of the technical staff of the biochemical laboratories is graciously acknowledged and I would like to thank Hayley-Jane Dingwall, Lindsay Dover, Michael Dunne, Mairi Law, Margaret Roberts, Marion Steele, Joan Stewart and Margaret Stewart, (in alphabetical order, not increasing age!).

I am particularly grateful to the technical staff for the measurement of cholineacetyltransferase activity and for the provision of cryostat sections of postmortem human brain which were of an exceptionally high standard.

Thanks are also extended to Margaret Crossling, Peter Johnston, Gordon Littlejohn and all the animal nurses. I would also like to thank Dave Love, the whizz-kid of the computers, for converting my disks and the frequent lifts from work.

I am also grateful to Professor D.I. Graham and colleagues for histological staining and to Mr. A. Shand and Mrs. A. Lynch for plaque quantification, at the Department of Neuropathology, Southern General Hospital; to Dr. B. Murphy and colleagues for clinical diagnosis of AD patients at Gartnavel Royal Hospital and to my colleague, Fiona Inglis, for lesioning the rat medial septum and provision of the histology data in this study (also for danish pastries and gin!).

The expert secretarial assistance provided by Mrs. Anne-Marie Colquhoun and Mrs. Jean Pearce was greatly appreciated. The artwork presented in this thesis was photographed with artistic flair by Allan May of the Department of Photography.

The accuracy and speed with which Lyndsay Graham typed the thesis was astounding. The encroachment of her personal time and yet her constant patience during this period deserve my especial thanks.

Finally, I would like to thank all my friends. To Morag and Vince, I am eternally grateful for their friendship and tolerance throughout my studies. To my parents, who had faith in me, and were constantly morally and financially supportive, I am indebted.

SUMMARY

Quantitative ligand binding autoradiography was used to map key components of second messenger systems in the CNS. [^{3}H]-Forskolin binding to G_s-adenylate cyclase and [^{3}H]-phorbol 12,13 dibutyrate (PDBu) binding to protein kinase C was investigated in human postmortem brain of control patients and patients with Alzheimer's Disease (AD). Disruption of glutamatergic and cholinergic systems may contribute to the pathology of AD. In view of this, alterations in ligand binding sites following selective lesions of glutamatergic and cholinergic pathways in rat brain were used as a framework on which to elucidate possible plastic modifications of second messenger systems in AD. Since the primary lesion in AD occurs within the cortex, ligand binding to second messenger systems was investigated following excitotoxic lesion of the rat cerebral cortex.

Second Messenger Ligand Binding in Alzheimer's Disease

In two separate series, [^{3}H]-forskolin binding was investigated in a total of 15 controls and 16 age-matched patients dying with AD in middle frontal and temporal cortices and in the hippocampal formation. AD brains contained numerous neuritic plaques in both cortical areas and the hippocampal region, whilst controls had minimal neuritic plaques. Choline acetyltransferase (ChAT) activity was significantly reduced (>50%) in AD compared to control subjects in both cortex and the hippocampus. [^{3}H]-Forskolin binding was significantly reduced by approximately 50% in all layers of the middle frontal cortex in AD brain compared to controls. There was a positive correlation between [^{3}H]-forskolin binding and ChAT activity in each layer of frontal cortex (correlation coefficient, r = 0.662 - 0.712) when data from control and AD brain

were combined. [^{3}H]-Forskolin binding was minimally altered in 1 of the 11 discrete regions examined in the hippocampus in AD brain compared to control. ChAT activity and [^{3}H]-forskolin binding were unrelated in any region of the hippocampus ($r = 0.42 - 0.6$). In the temporal cortex and the molecular layer of the dentate gyrus, there was evidence that [^{3}H]-forskolin binding was lower in AD patients compared to control subjects. Whether these changes achieved the probability level of 5% was a reflection of group size, variability of measurements, and the errors of sampling heterogeneous populations. There was no association between the number of neuritic plaques and [^{3}H]-forskolin binding in any brain region examined.

The effect of 5'guanylimidodiphosphate (Gpp(NH)p) on [^{3}H]-forskolin binding was examined in adjacent sections from the same group of control and AD patients. In control brain, basal levels of [^{3}H]-forskolin binding were significantly increased in layers I-III of middle frontal cortex (28%) and middle temporal cortex (30%) in the presence of Gpp(NH)p. In AD brain, the ability of Gpp(NH)p to enhance [^{3}H]-forskolin binding from basal levels in cortical layers (I-III) was conserved. Gpp(NH)p had no effect on the level of [^{3}H]-forskolin binding within each region of the hippocampus in the control or AD group.

In a separate study, both quantitative autoradiography and homogenate binding to particulate and cytosolic fractions were employed to investigate [^{3}H]-PDBu binding in middle frontal and temporal cortices, and the hippocampal region of nine control and nine AD subjects. All AD brains exhibited extensive signs of the pathology classically associated with the disease, namely numerous

neuritic plaques and a profound reduction in ChAT activity (<60%) in both cortical areas and the hippocampus. Quantitative autoradiographic analysis of [^{3}H]-PDBu binding showed there was no significant difference between control and AD sections in all areas examined within the middle frontal and temporal cortices and hippocampal formation. In adjacent sections to those used for [^{3}H]-PDBu autoradiography, [^{3}H]-forskolin binding was markedly reduced in all layers of middle frontal and temporal cortex (at least 30%) and in the molecular layer of the dentate gyrus (38%) in AD when compared with control subjects. In a parallel study, [^{3}H]-PDBu binding to homogenate preparations of control and AD brain confirmed that there was no significant difference in [^{3}H]-PDBu binding in either the particulate or cytosolic fraction.

Second Messenger Ligand Binding with Selective Neuronal Lesions in the Rat Brain

Selective neuronal lesions in rat brain were used to examine possible plastic alterations of ligand binding to second messenger systems after disruption of a glutamatergic pathway (retinofugal fibres), an excitotoxic lesion of the cerebral cortex, and a lesion of a cholinergic pathway (septo-hippocampal pathway).

Quantitative autoradiography of [^{3}H]-forskolin and [^{3}H]-PDBu binding was examined in the rat visual system at 1, 5, 10 and 20 days after unilateral orbital enucleation. Local cerebral glucose utilisation was determined in the same animals using [^{14}C]-2-deoxyglucose autoradiography as an index of local functional activity. There were no significant alterations in ligand binding to second messenger systems at 1 day post-enucleation. At 5 days post-lesion,

[^{3}H]-forskolin binding was significantly reduced in the visually-deprived superior colliculus (-14%) and dorsal lateral geniculate body (-8%), and these reductions persisted until 20 days post-lesion. There were no significant alterations in the amount of [^{3}H]-PDBu binding in any region in the visually-deprived hemisphere following enucleation. Function-related glucose use was significantly reduced throughout the visual pathway at all time points after enucleation.

The effect of Gpp(NH)p on [^{3}H]-forskolin binding was examined in adjacent sections 10 days after unilateral orbital enucleation. In the presence of Gpp(NH)p, differential effects on the levels of [^{3}H]-forskolin binding in each area studied were displayed. In the presence of Gpp(NH)p, the number of [^{3}H]-forskolin binding sites was significantly increased by 10% in layer IV of visual cortex in both hemispheres. No asymmetry in [^{3}H]-forskolin binding was uncovered in visual cortex. Similarly Gpp(NH)p significantly increased [^{3}H]-forskolin binding (37%) in both hemispheres of the superior colliculus. Thus the asymmetry of [^{3}H]-forskolin binding in this region was maintained. In the visually-deprived dorsal lateral geniculate body, Gpp(NH)p had no effect on [^{3}H]-forskolin binding in the visually-intact dorsal lateral geniculate body. However, in the visually-deprived dorsal lateral geniculate body, symmetrical [^{3}H]-forskolin binding was restored despite the enucleation.

[^{3}H]-Forskolin and [^{3}H]-PDBu binding were examined using quantitative autoradiography, 21 days after unilateral lesioning of the rat visual cortex using ibotenic acid. In the same animals, functional deficit was assessed using

[^{14}C]-2-deoxyglucose autoradiography. Post-lesion [^{3}H]-forskolin binding was significantly reduced in each layer of the lesioned hemisphere of visual cortex by at least 40% of the control hemisphere. Significant reductions in [^{3}H]-forskolin binding were observed in the superior colliculus (15%) and dorsal lateral geniculate body (12%) ipsilateral to the lesioned cortex. [^{3}H]-PDBu binding was significantly reduced in the lesioned visual cortex (layers V-VI) by 34%, compared with the control hemisphere. There were no significant alterations in [^{3}H]-PDBu binding in any other brain regions. In sham-treated animals, a significant reduction in glucose use was observed in the lesioned visual cortex (layer IV) by 9%. Following ibotenate-induced lesioning of the visual cortex, glucose use was significantly reduced throughout the lesioned cortex by at least 25%. There was a small, but significant, reduction in glucose use in the dorsal lateral geniculate body ipsilateral to the lesioned cortex.

Quantitative autoradiography of [^{3}H]-forskolin and [^{3}H]-PDBu binding were examined 21 days following ibotenate lesion of the rat medial septum. A significant reduction in [^{3}H]-forskolin binding was observed at the lesion site (-19%) compared to the sham-treated group. A significant increase in [^{3}H]-forskolin binding was demonstrated in the polymorph layer of the dentate gyrus (19%) whilst in all other brain regions, [^{3}H]-forskolin binding remained unaltered post-lesion. [^{3}H]-PDBu binding was significantly increased in the superficial layers (I-III) of entorhinal cortex (27%) following lesion of the medial septum, and remained unaltered in all other brain regions post-lesion.

The stability of [^{3}H]-PDBu binding and the consistent reduction of [^{3}H]-forskolin binding, indicates the relative vulnerability of these two binding sites in AD. For [^{3}H]-forskolin binding, there appears to be a regional hierarchy of loss in AD ranging from the frontal cortex (in which it is consistently reduced in AD) to most of the hippocampal formation (in which it is minimally reduced), with temporal cortex and molecular layer of the dentate gyrus intermediate. Such data suggest that the loss of G_s-adenylate cyclase in discrete brain areas may contribute to the pathology of AD, and may complicate the use of treatments directed at cyclase linked receptors. In contrast, the levels of protein kinase C appear to be exceedingly robust in AD. The reductions in second messenger ligand binding sites after orbital enucleation and excitotoxic cortical lesions provide, with the most conservative interpretation, evidence of their anatomical localisation in these model neuronal systems. With septo-hippocampal lesions, the nature of the alterations in both ligand binding sites (namely elevations) are supportive of plastic modifications of second messenger systems following cholinergic denervation.

PREFACE AND DECLARATION

This thesis primarily represents results from ligand binding studies in human postmortem brain and rat brain. Quantitative ligand binding autoradiography *in vitro* was the principal technique used in the investigation of ligand binding to second mesenger systems. Local cerebral glucose utilisation was measured *in vivo* to assess functional deficits within the rat visual system using the [^{14}C]-2-deoxyglucose technique.

Investigations were conducted in three broadly defined areas:

(1) to examine possible alterations of ligand binding to second messenger systems in postmortem tissue from patients dying with Alzheimer's Disease,

(2) to assess ligand binding sites and cerebral function in the rat visual system following lesion of retinofugal and corticofugal fibres,

(3) to assess ligand binding sites following lesion of the septo-hippocampal pathway.

Results from these studies are presented and discussed separately. In the final overview, I have attempted to highlight the advantages and limitations of assessing neurochemical alterations in human postmortem brain using quantitative autoradiography. Additionally, the relevance of animal models as a basis for

elucidating the mechanisms underlying alterations in ligand binding sites in Alzheimer's Disease is discussed.

This thesis comprises my own original work and has not been presented previously as a thesis in any form.

CHAPTER I

INTRODUCTION

1. HISTORICAL OVERVIEW OF SECOND MESSENGER SYSTEMS

The molecular mechanisms by which cells communicate with each other are of intrinsic importance to the normal physiological functioning of multicellular organisms. Receptor recognition of a neurotransmitter is only the first step in a cascade of events by which transmitter recognition is translated into altered cellular function via systems of regulatory and catalytic proteins known collectively as "second messenger systems". There are two major receptor-regulated second messenger systems currently thought to be active in the brain, namely the adenylate cyclase-cyclic adenosine monophosphate (cAMP) system and the phosphoinositide (PI) cycle.

1.1 Adenylate Cyclase and G-Proteins

cAMP was first discovered by Sutherland and colleagues (1957) as a co-factor enabling adrenaline and glucagon to initiate glycogen breakdown in the liver. In this system, and in subsequently elucidated systems, a hormone or neurotransmitter binds to a specific receptor, on the cell surface, which stimulates the enzyme to form cAMP. Acting as an intracellular second messenger, cAMP activates a protein kinase which alters cellular activity. In 1971, Martin Rodbell and colleagues discovered that guanosine trisphosphate (GTP) was essential for hormones to activate adenylate cyclase. The GTP dependency of hormonal action was found to be due to a specific GTP-binding protein, guanine-nucleotide regulatory protein (G-protein) which is quite distinct from either the receptor or adenylate cyclase. The essential mechanism for regulation of adenylate cyclase activity was to promote the GTP-dependent association of this regulatory protein (now

termed G_s) with adenylate cyclase itself (Ross et al. 1978; Northup et al. 1980; Sternweis et al. 1981).

G-Proteins that function in transmembrane signalling are now known to be heterotrimer proteins, subunits being designated α, β and γ, respectively. Prior to receptor activation, G_s is complexed with guanosine diphosphate (GDP) on the α-subunit and is unable to stimulate adenylate cyclase activity. Neurotransmitter receptor activation of G_s enhances its affinity for GTP relative to GDP (Cassel et al. 1978). GTP causes dissociation of the G-protein α-subunit from $\beta\gamma$, and it is the G-protein α-subunit that interacts with, and regulates, adenylate cyclase. The α-subunit contains a high affinity (nM) binding site for guanine-nucleotides, and can hydrolyse GTP to GDP by an intrinsic GTPase activity. Deactivation of adenylate cyclase follows nucleotide hydrolysis, resulting in a regenerated GDP-G_s complex (see Figure 1). The rates of these processes are crucial elements in the function of this guanine-nucleotide-controlled mechanism. Four forms of $G_s\alpha$ are known to exist (Bray et al. 1986), the products of alternative splicing of precursor RNA. Although betweem them there is a high degree of homology (Kozasa et al. 1988), the functional significance of these distinct G-proteins is unclear. Receptors that stimulate G_s-adenylate cyclase include β-adrenergic, dopamine (D1), and adenosine (A2) (Levitzki, 1987).

An analogous system pertains for receptor-mediated inhibition of adenylate cyclase except that a distinct G-protein, G_i (inhibitory protein) for adenylate cyclase, is involved (see Figure 1). Three highly homologous forms

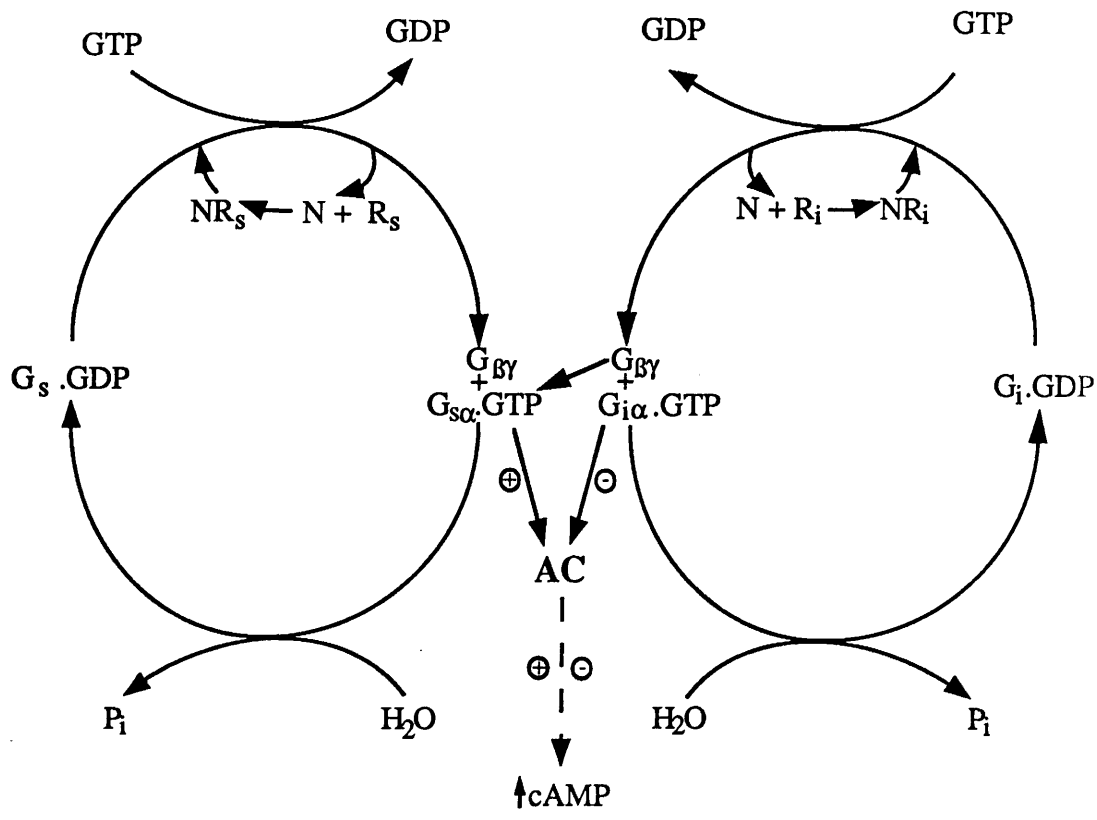

FIGURE 1
DUAL REGULATION OF ADENYLATE CYCLASE

Schematic diagram of neurotransmitter activation and inhibition of adenylate cyclase. Neurotransmitter (N) association with a receptor (R) induces a conformational change in either a stimulatory G-protein (G_s) or an inhibitory G-protein (G_i) and enhances the affinity of the G-protein for GDP relative to GTP. GTP causes dissociation of the G-protein α-subunit from the βγ-subunit. The α-subunit interacts with and regulates adenylate cyclase (AC) activity to either activate or inhibit the production of cyclic adenosine monophosphate (cAMP). GTP is hydrolysed to GDP resulting in a regenerated GDP-G-protein complex.

of this protein are now recognised as products of distinct genes, and although their mode of interaction with effector molecules is quite similar, there is a subtle difference in their interactions with receptors (Itoh et al. 1988). Activated G_i can inhibit adenylate cyclase activity directly or may act indirectly by reducing the activity of G_s. Inhibition of adenylate cyclase is attributed, in part, to the capacity of $\beta\gamma$, released on activation of G_i, to interact with, and deactivate, $G_{s\alpha}$. An increasing number of G-proteins have now been identified, each of which may have a distinct function in transmembrane signalling. Thus, the possibility exists that activation of one pathway can cause inhibition of effectors that are controlled by other G-protein α-subunits if the concentration of $\beta\gamma$ in the membrane is raised sufficiently (Gilman, 1984). It has also been proposed that $\beta\gamma$ can inhibit adenylate cyclase directly (Katada et al. 1987). Receptors that inhibit adenylate cyclase activity include adrenergic (α_2), adenosine (A_1), γ-aminobutyric acid ($GABA_B$), muscarinic (M_2) and dopaminergic (D_2) receptors.

The discovery of forskolin, a diterpene isolated from the roots of the Indian herb Coleus forskohlii, markedly potentiated the mechanistic insight of the adenylate cyclase system. Forskolin was originally isolated based on its ability to produce cardiotonic effects, possessing both a positive ionotropic action and potent vasodilatory action (Bhat et al. 1977). These unique actions were later found to be due to its ability to directly interact with the catalytic subunit of adenylate cyclase (Seamon et al. 1981) and hence increase cAMP levels. The presence of G-proteins, although not

necessary for this action of forskolin, has been implicated as important for the expression of full enzymatic activity of adenylate cyclase (Daly et al. 1982). This direct stimulation of adenylate cyclase normally occurs at forskolin concentrations in the micromolar range (Seamon et al. 1981). However, at much lower concentrations, in the nanomolar range, forskolin can also act synergistically with hormones that activate adenylate cyclase to greatly increase the generation of cAMP (Barovsky et al. 1983; Seamon et al. 1984). These two actions of forskolin have been explained as a consequence of two distinct binding sites: a low affinity binding site in which forskolin directly activates the catalytic subunit, and a high affinity binding site, the location of which is unknown. Occupancy of this high-affinity binding site by forskolin is associated with the coupling of the stimulatory G-protein (G_s) to the catalytic subunit (C). Other conditions that promote G_s-C coupling include Mg^{2+} and guanyl nucleotides. The use of affinity chromatographic techniques with immobilised forskolin, pioneered by Pfeuffer and Metzger (1982), allowed adenylate cyclase to be purified from brain tissue (Smigel, 1986; Yeager et al. 1985). Adenylate cyclase is a polypeptide glycoprotein with a molecular weight of approximately 150KDa. A cDNA clone has been isolated specific for one form of adenylate cyclase (Graziano and Gilman, 1987). Adenylate cyclase is comprised of two alternating sets of hydrophobic and hydrophilic regions. Each of the two hydrophobic regions contains six transmembrane spans, whilst each of the hydrophilic domains includes a stretch of amino acid residues that is homologous with the putatitive catalytic domain of guanylate cyclase. The overall topology of adenylate cyclase resembles those of various membrane channels and transporters

suggesting that adenylate cyclase may be multifunctional, serving as both the catalyst of cAMP synthesis and the transporter that exports cAMP from cells (Gilman, 1989).

At least two forms of adenylate cyclase are known to exist (Mollner and Pfeuffer, 1988) differing on their relative sensitivity to calmodulin. In brain, the expression of a calmodulin-sensitive adenylate cyclase (Brostom et al. 1975; Cheung et al. 1975) appears to be unique. Calmodulin appears to mediate the calcium-dependent stimulation of adenylate cyclase by binding directly to the catalytic subunit of the enzyme (Smigel, 1986). Although this interaction does not require the presence of GTP or GTP-binding proteins, there appears to be a potentiative interaction between calmodulin and either hormones, neurotransmitters or guanyl nucelotides in the stimulation of adenylate cyclase. In brain, there is evidence that G_s can enhance the stimulation of adenylate cyclase by Ca^{2+}/calmodulin (Harrison et al. 1989).

In most brain regions, such as the cerebellum, adenylate cyclase activity displays sensitivity to Ca^{2+}/calmodulin, although this does not appear to be true for areas such as the caudate putamen, where adenylate cyclase is less sensitive to stimulation by Ca^{2+}/calmodulin. Recent evidence suggests that there may be a selective association of calmodulin-independent and calmodulin-dependent adenylate cyclase with different forms of G_s proteins (Cooper et al. 1990).

1.2 Phosphoinositide Cycle and Protein Kinase C

A role for phospholipids in mediating the effects of acetylcholine has been investigated since the demonstration by Hokin and Hokin (1953) that acetylcholine stimulates phospholipid turnover in the pancreas. Subsequently it was observed that all receptors which elicit Ca^{2+}-dependent responses shared the common ability to enhance the breakdown of phosphoinositide (PI), an anionic phospholipid. This observation led Michell (1975) to postulate that the degradation of PI was associated, in some causative manner, with the mobilisation of intracellular calcium.

Detailed clarification of the PI cycle, and appreciation of its widespread role in mediating effects of hormones and neurotransmitters, has only been quite recent (Berridge,1984; Berridge and Irvine, 1984; Hokin, 1985; Nishizuka, 1984). Neurotransmitter receptors which regulate cellular activity via the phosphoinositide system include muscarinic, $5HT_2$, α-adrenergic and glutamatergic. According to currently accepted concepts, neurotransmitter interaction with a receptor hydrolyses the membrane phospholipid, phosphatidylinositol 4,5 bisphosphate. This compound is cleaved by phospholipase C to release diacylglycerol (DAG) and inositol 1,4,5 trisphosphate (IP_3). Both products seem to function as second messengers; DAG remains within the plasma membrane where it activates protein kinase C (Nishizuka, 1984) leading to phosphorylation of proteins, whilst IP_3 diffuses into the cytosol to release calcium from the endoplasmic reticulum (Berridge, 1984). IP_3 is thought to act on a specific receptor associated with a non-mitochondrial Ca^{2+} store within the cell to open a Ca^{2+} channel (see Figure

2). This system is very much analogous to receptor stimulation of adenylate cyclase. In both cases, a highly phosphorylated precursor is cleaved by an enzyme (which functions as a signal amplifier) to release second messengers. An additional feature, common to both the phosphoinositide and adenylate cyclase systems, is the presence of a G-protein (Cockcroft and Gomperts, 1985; Smith et al. 1986). At present, it is unknown which G-protein acts to stimulate the PI system in the brain.

In keeping with the proposed role of DAG and IP_3 as second messengers, they are rapidly inactivated once the external signal is withdrawn. The neutral DAG which operates within the plane of the membrane can either be rapidly phosphorylated by DAG kinase to phosphatidic acid (PA), which in turn is converted to CDP-DAG by cytidyl transferase and then via de novo synthesis to PI, or it can be converted to arachadonic acid by DAG lipase. There are also two pathways for degrading IP_3. First, IP_3 can be dephosphorylated to free inositol through a stepwise series of phosphatases. Alternatively, IP_3 can be phosphorylated to form inositol 1,3,4,5 tetrakisphosphate. This latter inositolphosphate was first identified in brain cortical slices and appears to be the precursor of inositol 1,3,4 trisphosphate. IP_3 can thus flow along two separate routes, a degradative pathway to form free inositol or via a novel pathway to generate other inositol polyphosphates. Some of these inositol phosphates have been suggested to have second messenger functions.

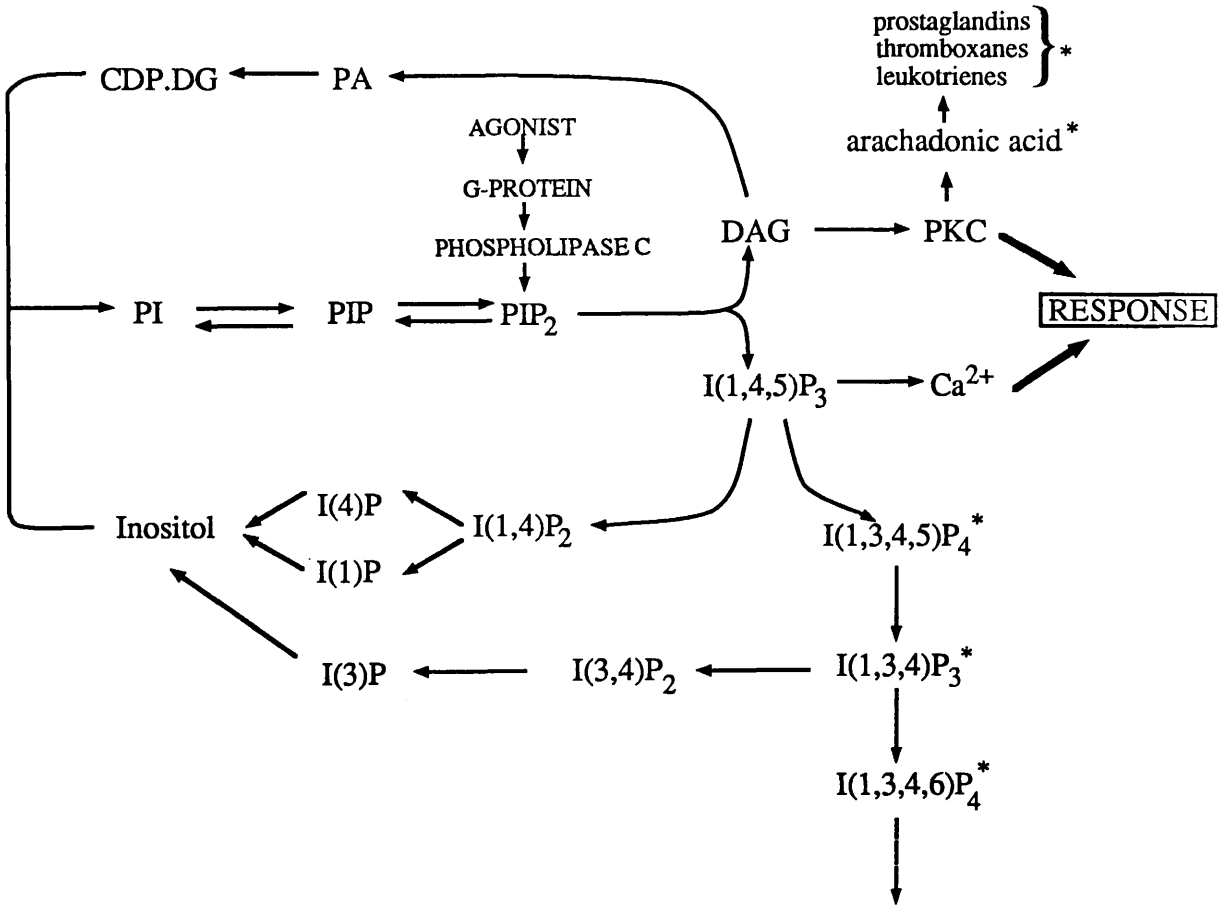

FIGURE 2
PHOSPHOINOSITIDE SYSTEM

Schematic diagram of agonist-dependent phosphoinositide system. The key event is the hydrolysis of phosphatidylinositol 4,5 bisphosphate (PIP_2) to yield diacylglycerol (DAG) and inositol 1,4,5 trisphosphate (IP_3). Both DAG and IP_3 have second messenger functions; DAG activates protein kinase C (PKC), whilst IP_3 mobilises intracellular Ca^{2+} stores. DAG and IP_3 may be converted to other metabolites or inositol phosphates (IP) which have been reported to have additional second messenger functions denoted by *. See text for further details and abbreviations.

Protein kinase C (PKC) was identified in 1977 as a proteolytically-activated protein kinase (Inoue et al. 1977), and is now known to be ubiquitous in tissues in organs. In particular, PKC is especially abundant in the brain. The purified enzyme consists of a single polypeptide chain with a molecular weight of approximately 80KDa (Kikkawa et al. 1982). The transient production of diacylglycerol in response to PI hydrolysis is the major physiological pathway for the activation of PKC. In the presence of phosphatidylserine, diacylglycerol and calcium, PKC is fully activated. Diacylglycerol increases the apparent affinity of the enzyme for phospholipid and decreases the concentration of calcium required for full activation of PKC to a concentration range of calcium which is within the basal levels of most cells (Kikkawa et al. 1982). In brain, PKC is associated mainly with synaptic membranes and, to a lesser extent, is found in the cytosol (Kuo et al. 1980). Activation of PKC by diacylglycerol is associated with a translocation of the enzyme from the cell cytosol to the plasma membrane (Kraft and Anderson, 1983). Similarly, an increase in intracellular calcium may promote translocation of PKC. Phorbol esters, one of the most potent classes of tumor promoters, have been invaluable tools in the study of PKC. Phorbol esters mimic the action of diacylglycerol to stimulate PKC; the phorbol ester binding site has been suggested to be identical to PKC (Kikkawa et al. 1983; Niedel et al. 1983; Blumberg et al. 1984). Similar to diacylglycerol, phorbol esters dramatically increase the affinity of PKC for Ca^{2+}. However, unlike diacylglycerol which is transiently produced in response to receptor activation, phorbol esters are minimally degraded.

Molecular cloning of several cDNAs of PKC (Nishizuka, 1988; Coussens et al. 1986) and isolation of multiple PKC isozymes (Huang, 1986) have established the molecular diversity of this enzyme family. There are at least seven subspecies of PKC designated as α, βI, βII, γ, ε, and ζ, all of which are composed of a single polypeptide chain but with differing sensitivies to Ca^{2+}, phospholipid and diacylglycerol. Within the central nervous system, differential distributions of some of these isoforms of PKC have been identified (Girard et al. 1985; Stichel and Singer, 1988; Tsujino et al. 1990, Wood et al. 1986).

2. ROLE OF SECOND MESSENGER SYSTEMS IN MODULATING SYNAPTIC PLASTICITY

Many of the definitive studies which determined the mechanisms of signal transduction signalling were examined in the peripheral nervous system. In the past decade both the adenylate cyclase system and protein kinase C (PKC), as a key enzyme in the phosphoinositide system, have been demonstrated to play a major role in the CNS, in particular in modulating many aspects of synaptic plasticity such as the regulation of neurotransmission, cellular growth and differentiation, neurodegeneration and learning and memory.

Increased levels of intracellular cAMP enhances neurite extension in embryonic rat cortical cells (Shapiro, 1973) and hippocampal pyramidal neurons (Mattson,1988). Similarly in neuroblastoma cell lines and hybrids, elevated levels of cAMP potentiates both neurite outgrowth and synapse formation (Mattson et al. 1988). In the case of PKC, phorbol esters were found to promote neurite outgrowth in sensory ganglia neurons and neuroblastoma cells (Ishii, 1978; Spinelli and Ishii, 1983). Following axotomy, stimulation of neurite sprouting has been observed in response to phorbol ester exposure in Helisoma neurones (Barnes, 1986). Moreover, in the same study, glutamate, known to activate PKC, stimulated sprouting in these neurones. An increasing awareness of an integral role for PKC in mediating glutamate-induced responses such as neuronal growth and degeneration is becoming apparent (Sladeczek et al. 1988; Favaron et al. 1990). PKC can also suppress neuronal growth after prolonged exposure of neuronal cultures

to phorbol esters. In cultured hippocampal pyramidal neurones, phorbol esters, in nanomolar concentrations, inhibit axonal and dendritic outgrowth (Mattson, 1988).

cAMP and PKC are now believed to be involved in learning and memory processes as shown in several model systems. The simple nervous system of the mollusc Aplysia, where changes in membrane properties of single neurones can be directly related to altered behaviour, is often used as a model of learning. A learning paradigm, referred to as sensitisation, is associated with adenylate cyclase activity induced by serotonin activation (Kandel and Schwartz, 1982). Sensitisation can also be mimicked by intracellular injection of the catalytic fragment of adenylate cyclase. In the hippocampus, long term potentiation (LTP), used as a model of memory, can be blocked by removing noradrenergic inputs and can be restored either by exogenous noradrenaline (acting at β-receptors coupled to adenylate cyclase) or by direct activation of adenylate cyclase (Stanton and Sarvey, 1985). Hypoxia induced in animals immediately after learning has been widely employed as an agent for the depletion of short-term memory (Sara and Lefevre, 1972). Delayed memory dysfunction by transient hypoxia was reported to be prevented by forskolin, a potent activator of adenylate cyclase (Ando et al. 1987). Further, increased tissue cAMP levels in ischaemic myocardium prevents ventricular arrhythmias in rat hearts (Thandroyen et al. 1988). This may support a role for increased cAMP to restore neuronal transmission which is supressed by hypoxia (Okada et al. 1989).

An apparent involvement of PKC in LTP induced by glutamate (Routtenberg, 1986) has been suggested. Induction of hippocampal LTP associated with an increase in glutamate and intracellular Ca^{2+} enhances the translocation of PKC from the cytosol to the membrane where it can enhance subsequent stimuli. Thus PKC appears to sustain LTP and may represent a form of "memory".

Sustained PKC translocation has been implicated in mediating glutamate-induced neurotoxicity in cell cultures (Favaron et al. 1988; Manev et al. 1989; Ogura et al. 1988; Favaron et al. 1990). More recently, in ischaemic brain, enhanced translocation of PKC has been suggested to play a pivotal role in post-ischaemic modulation of synaptic efficacy in the hippocampus and neuronal death in the CA1 field which is putatively associated with excessive glutamate release (Onodera et al. 1986, 1989; Hara et al. 1990). Interestingly, exposure of hippocampal slices to anoxia in vitro induced an increased sensitivity of the PI system to glutamate receptor stimulation (Ninomiya et al. 1990).

Although the existence of second messenger systems has been recognsed for several years, the availability of selective and potent agents which act on individual elements of these systems are exceedingly limited. Two of these compounds which have been extensively used to facilitate examination of signal transduction mechanisms are forskolin and phorbol esters, known to be potent activators of adenylate cyclase and protein kinase C respectively (see Figures 3 and 4). Furthermore, the recent availability of these

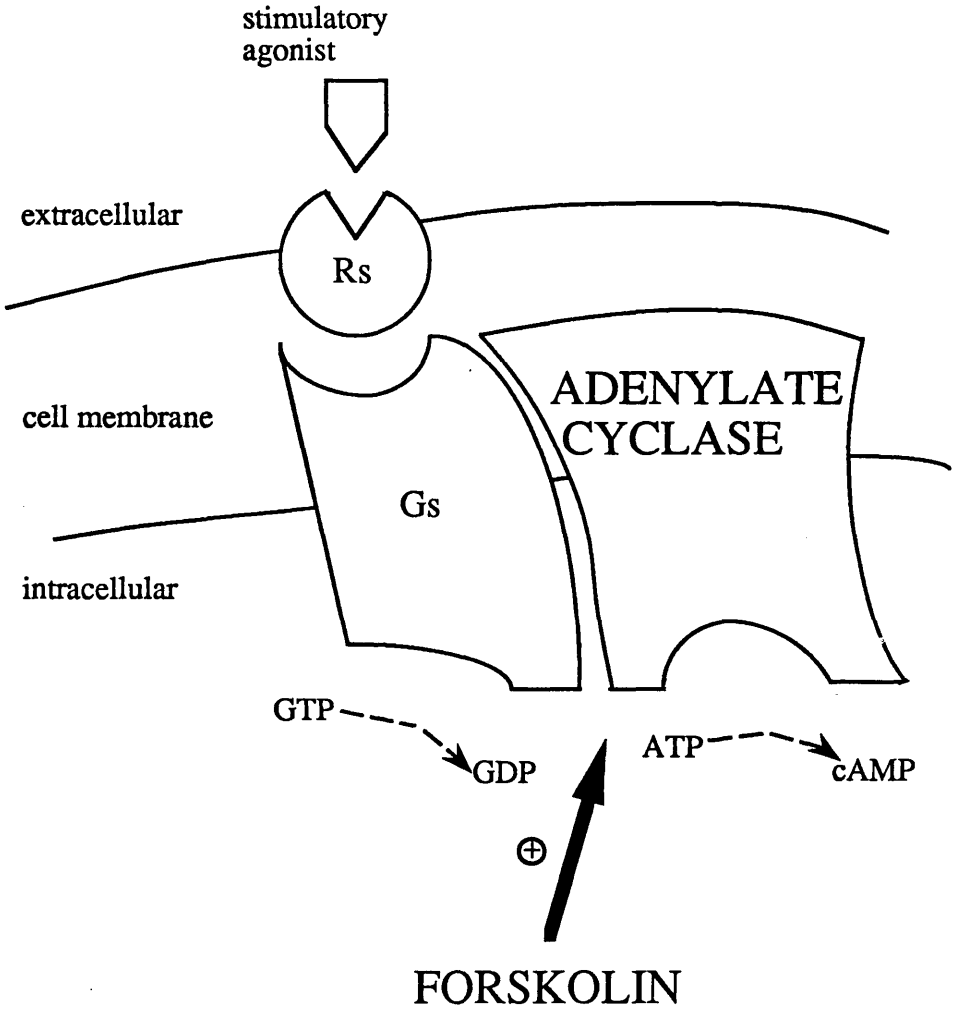

FIGURE 3
FORSKOLIN ACTIVATION OF ADENYLATE CYCLASE

Schematic view of the stimulatory receptor regulated adenylate cyclase signalling system. Activation of a specific receptor, on the cell membrane, by an agonist enhances the coupling of the stimulatory guanine triphosphate (GTP)-binding regulatory protein (G_s) with adenylate cyclase. Adenylate cyclase activation yields the formation of the second messenger, cyclic adenosine monophosphate (cAMP).

Forskolin directly activates adenylate cyclase at high concentrations (μM). At nanomolar concentrations, forskolin enhances the stimulatory interaction of G_s with adenylate cyclase.

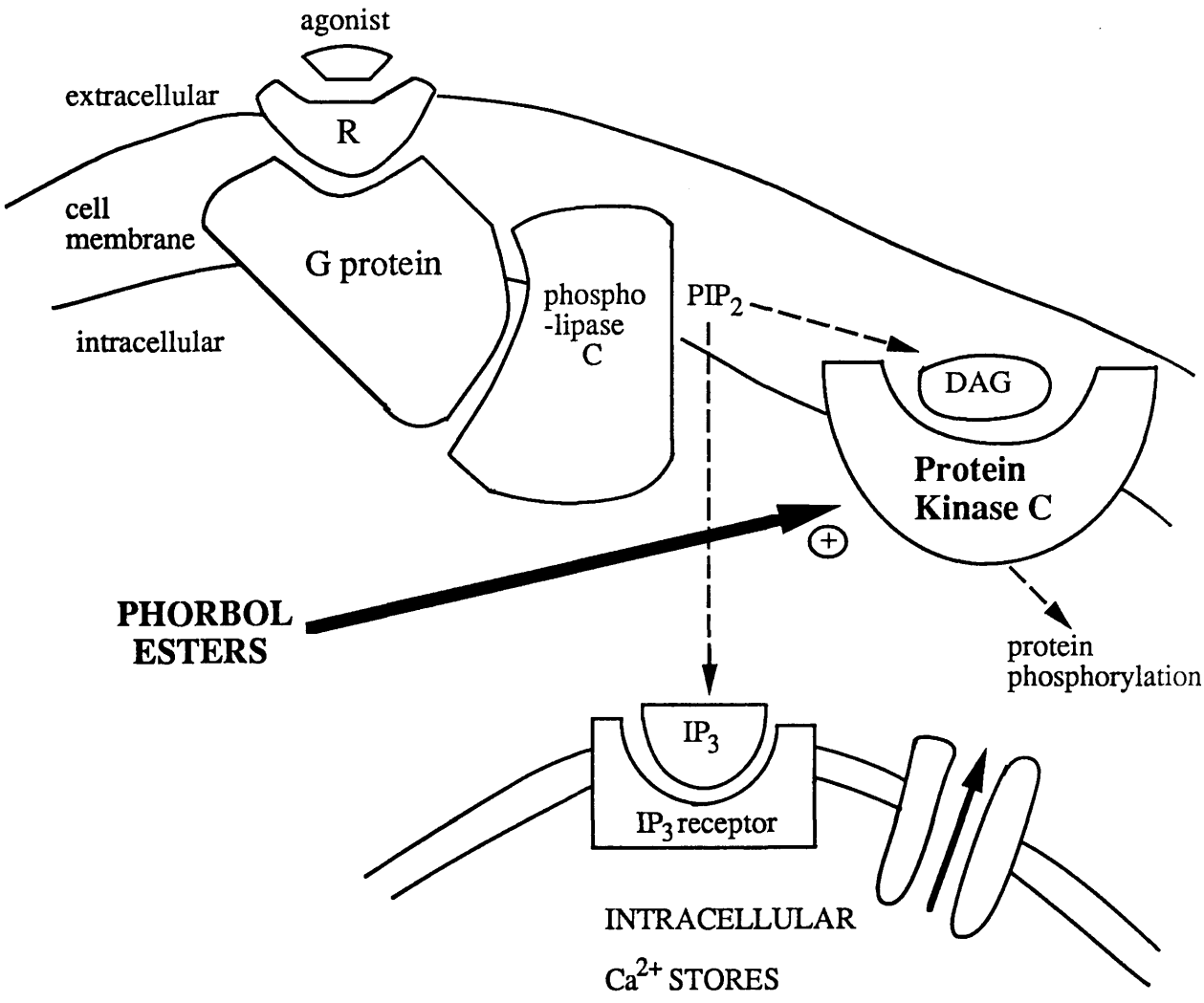

FIGURE 4
PHORBOL ESTER ACTIVATION OF PROTEIN KINASE C

Schematic illustration of receptor-mediated phosphoinositide turnover. Binding of a neurotransmitter or agonist to a specific receptor on the cell membrane activates a G-protein (G). In turn this stimulates phospholipase C leading to the hydrolysis of phosphatidylinositol 4,5 bisphosphate (PIP_2) and the generation of two second messengers, inositol 1,4,5 trisphosphate (IP_3) and diacylglycerol (DAG). IP_3 causes the release of calcium from intracellular stores, whilst DAG activates protein kinase C which phosphorylates a broad range of substrates. Protein kinase C can also be found in the cell cytosol.

Phorbol esters mimic the action of DAG by stimulating protein kinase C.

compounds in a tritiated form has allowed a novel approach to examination of second messenger systems in the CNS (Young and Kuhar, 1979; Unnerstall et al. 1982). Receptor autoradiography has demonstrated the anatomical mapping of a multitude of neurotransmitter receptors in the CNS such as α-adrenergic, β-adrenergic, 5HT, GABA and glutamate subtypes.

Quantitative autoradiography has an advantage over other ligand binding techniques in that it allows non-prejudicial examination of recognition sites in discrete brain areas with a high degree of spatial resolution. Ligand binding techniques, essentially similar to those used for receptor autoradiography, now permit the distribution of second messenger systems to be mapped in the CNS. Quantitative autoradiography of [^{3}H]-forskolin binding to G_s-adenylate cyclase, [^{3}H]-phorbol dibutyrate (PDBu) binding to PKC and [^{3}H]-IP_3 binding to IP_3 receptor (Worley et al. 1986 a,b and 1987) has demonstrated the heterogeneity in binding densities of second messenger ligands in well-defined neuroanatomical components of the rat CNS. The pattern of [^{3}H]-forskolin and [^{3}H]-PDBu binding is striking within the cerebellum, hippocampus and caudate-putamen of rat brain (Figure 5). Lesion studies have shown both [^{3}H]-forskolin and [^{3}H]-PDBu binding to be localised in the molecular layer of the cerebellum but whilst G_s-adenylate cyclase is associated with granule cell terminals, PKC is associated with Purkinje cell dendrites (Worley et al. 1986a). Within the hippocampus [^{3}H]-forskolin binding is highly localised in granule cells in the polymorph layer of dentate gyrus and CA3 field whereas [^{3}H]-PDBu binding is concentrated in the intrinsic neurons of CA1-CA4 fields. [^{3}H]-Forskolin binding is particularly

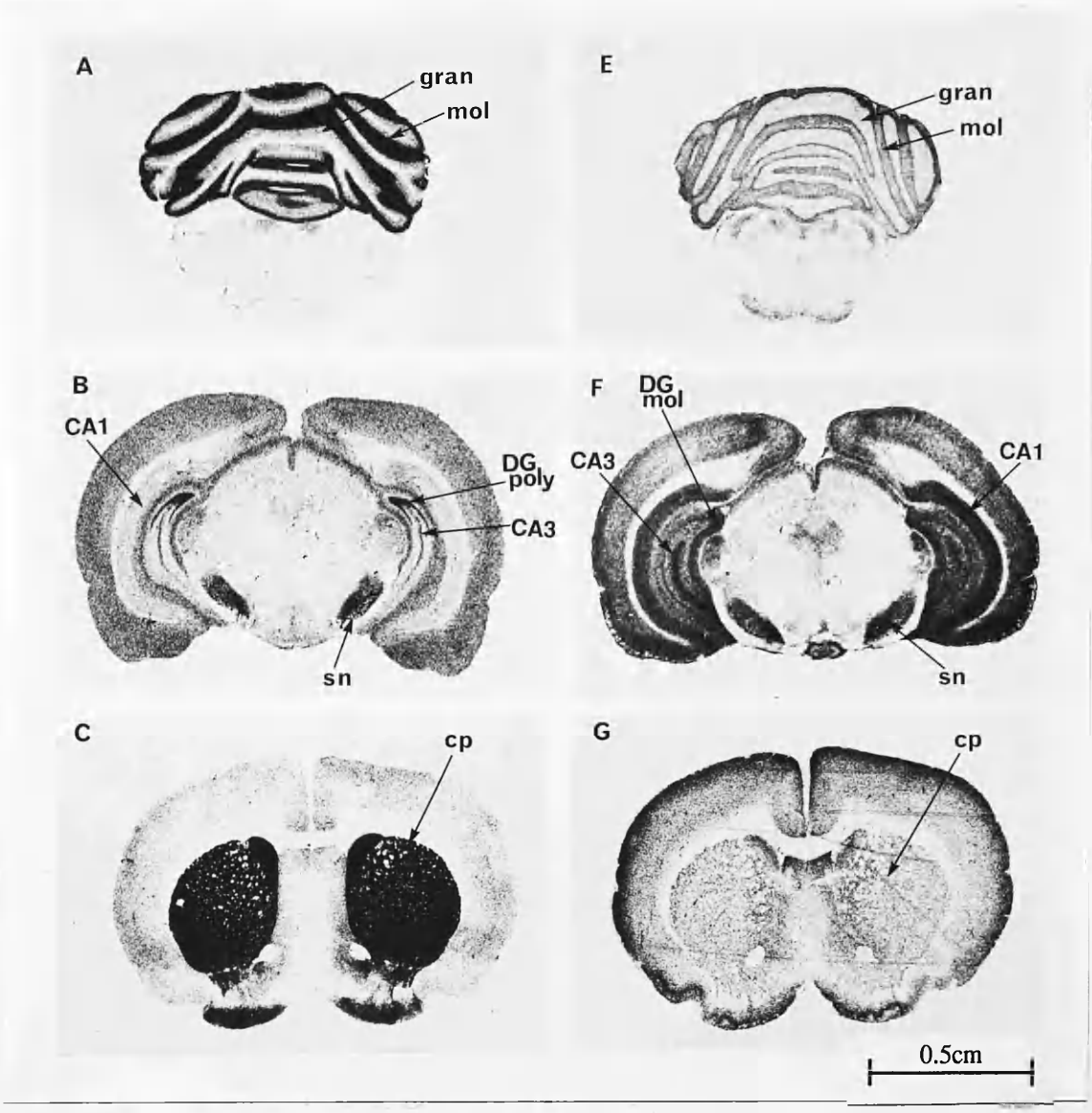

FIGURE 5
AUTORADIOGRAPHIC IMAGES OF [^{3}H]-FORSKOLIN AND [^{3}H]-PDBu BINDING IN RAT BRAIN

Representative autoradiograms of [^{3}H]-forskolin binding (A-C) and [^{3}H]-PDBu binding (E-G) in rat brain sections at the level of the cerebellum (A,E), dorsal hippocampus (B,F) and caudate putamen (C,G). Abbreviations are: molecular (mol) and granular (gran) layer of the cerebellum; CA1, CA3, CA4 fields in hippocampus; polymorph (poly) layer of dentate gyrus (DG), substantia nigra (sn) and caudate putamen (cp). Note the heterogeneous pattern of ligand binding to second messenger systems.

concentrated in the caudate putamen.

One of the major disadvantages of ligand binding autoradiography is that not all binding sites are necessarily functional. Thus, alterations in ligand binding to second messenger systems in neurodegenerative brain may not represent changes in functional circuitry. However, this does not apply in all brain regions. [^{3}H]-Forskolin binding is intense in the striatum and caudate nucleus paralleling the density of dopamine-sensitive adenylate cyclase in the striato-nigral pathway. Thus, the level of functional activity in this system is reflected by the concentration of [^{3}H]-forskolin binding to G_s-adenylate cyclase. Most studies to date have employed biochemical assays to examine second messenger system activity or function in response to agonist stimulation in homogenate preparations of brain tissue. However, in such studies, the lack of anatomical resolution limits the mechanistic insight of second messenger alterations in diseased brain. Further, in human postmortem tissue, the use of neurochemical assays to measure functional activity of second messenger systems is limited by the instability of second messenger systems following long postmortem delay intervals and freezing of brain tissue (Candy et al. 1984; Saitoh and Dobkins, 1986; Danielsson et al. 1988; Dodd et al. 1988).

In addition to constructing maps of intraneuronal messenger systems in the CNS, quantitative autoradiography of ligand binding to second messenger systems may provide a novel approach to examine the relationship between second messenger systems and neurodegenerative conditions.

3. NEUROPATHOLOGICAL AND NEUROCHEMICAL FEATURES OF ALZHEIMER'S DISEASE

Alzheimer's disease (AD) is a dementing disorder of insidious onset and characterised by a progressive deterioration of memory and cognitive function. AD is now recognised as the most common cause of adult-onset dementia, affecting at least 10-15% of individuals over the age of 65 (Henderson, 1986). Diagnostic ambiguities and uncertainties limit pre-mortem diagnosis of AD at present. Symptomatic overlap between AD and other dementing disorders such as multi-infarct dementia and mixed dementia is problematic. Macroscopically, the traditional feature associated with AD is brain atrophy in particular affecting frontal and temporal lobes associated with widening of gyri and narrowing of sulci with concomitant ventricular enlargement (Perry and Perry, 1982). At present, however, diagnosis of AD status requires neuropathological confirmation. The classical hallmarks of AD are characterised neuropathologically, as first described by Alzheimer (1907), by the presence of numerous neuritic plaques and neurofibrillary tangles in specific areas of the neocortex and hippocampus.

Quantification of neuritic plaques provides the definitive means of distinguishing AD from ageing changes in non-demented aged subjects according to criteria set by Khachaturian (1985). Plaques are described histologically as being composed of an amyloid core surrounded by degenerating neurites (presynaptic nerve terminals) and glial processes (Brun, 1983). Wisniewski and Terry (1973) proposed the evolution of plaques to be in three distinct stages: (1) the "immature" plaque composed of dystrophic

neurites and glial processes with minimal amyloid in the core, (2) the "mature" plaque composed of a central core of amyloid surrounded by numerous degenerating neurites, (3) the "burned-out" plaque which describes the final stage of a plaque in which the central amyloid core remains devoid of encompassing neurites.

Neuritic plaques accumulate in abundance in AD brain, predominantly in frontal and temporal cortex, hippocampus and amygdala, and to a much lesser extent in the remaining neocortex (Mann, 1988). In the neocortex, plaques appear to be associated with intracortical fibres and, in general, do not appear to be limited to one particular neurotransmitter system.

Unlike plaques which occur in the neuropil, neurofibrillary tangles are found mainly within the perikarya of affected neurons. Similar to plaques, tangles are present in high numbers in neocortex and hippocampus but they can also be found in archicortical areas such as raphé nuclei, nucleus basalis of Meynert and locus coeruleus (Mann, 1985; Perry, 1986). In neocortex, the presence of tangles appears to be closely associated with pyramidal neurons especially in layer III. At the ultrastructural level, neurofibrillary tangles in AD often contain fibres that appear to be a tightly adherent pair of helically wound filaments, referred to as paired helical filaments (Kidd, 1963). It remains unclear whether paired helical filament protein represents a modification of normal cytoskeleton elements or the synthesis of some new abnormal protein. However, the microtubular system is linked immunochemically to neurofibrillary tangles; considerable cross-reactivity has been

shown between tangles and microtubule-associated proteins, MAP2 and tau.

The functional significance of neuritic plaques and tangles in AD brain is largely unknown. The detection of relatively abundant aluminium and silicon concentrations in plaque cores by x-ray and electron probe analysis, and evidence of aluminium concentration in tangles initiated a putative link between aluminium toxicity and the pathogenesis of Alzheimer's disease. More recently, intensive investigation has focused on the amyloid β protein, the major component of amyloid deposits in AD brain. Discovery that the gene encoding the amyloid precursor protein is located on chromosome 21, associated with trisomy 21 disorders (Down's Syndrome), has potentiated this flurry of investigation. More recently, part of the amyloid precursor protein has been shown to be potentially neurotoxic (Yankner et al. 1989).

Perhaps the most invariant and pervasive disruption in AD brain involves the cholinergic system. Selective degeneration of cholinergic neurons originating in the nucleus basalis of Meynert, vertical diagonal band and septal nucleus and projecting to the cerebral cortex and hippocampus, is a consistent feature in AD brain. Reduced acetylcholine concentrations (Richter et al. 1980) and synthesis (Sims et al. 1980) in AD cortex have been shown. In the hippocampus and neocortex of AD brain, the high affinity uptake mechanism for choline is markedly deficient (Rylett et al. 1983). Undoubtedly the most consistent feature of AD is a profound reduction in ChAT activity with losses up to 95% from control values in cortical and sub-cortical regions (Perry et al. 1978; Mountjoy et al. 1984). Most severely

affected are areas such as hippocampus, temporal, parietal and frontal cortex although ChAT deficits may extend to areas not directly innervated by cortical projecting neurons such as cerebellum, hypothalamus and pons (Davies, 1979). In the neocortex, the reduction in ChAT is laminar specific, being most extensive in the granular layers II and IV (Perry et al. 1984).

Increasing severity of ChAT deficiency in AD neocortex and hippocampus is quantitatively correlated to the numbers of neuritic plaques and tangles in these regions (Perry et al. 1978). Moreover, the reduction in ChAT appears to be intimately related to impaired cognitive function and in particular memory (Perry, 1986).

Pharmacological intervention to try to restore cholinergic transmission either presynaptically by stimulating production of acetylcholine in surviving neurons or inhibiting the destruction of acetylcholine at the synapse, has been relatively ineffective to date (Etienne, 1983). Another approach, namely direct action on the post-synaptic receptors using muscarinic agonists, is dependent on the presence of cholinergic receptors in the brain of AD patients. However, despite a consistent neurochemical abnormality of the cholinergic system in AD, the status of muscarinic receptors remains controversial. Normal densities of muscarinic receptors with unaltered pharmacological properties have been found in AD brain (Bartus et al. 1982; Davies and Verth, 1978; White et al. 1977), whilst other groups have reported a reduction in muscarinic receptors in the neocortex (Reisine et al. 1978; Shimohama, 1986; Wood et al. 1983). Differentiation between subtypes of

muscarinic receptors has demonstrated a selective decrease in M_2 receptors (presumably presynaptic autoreceptors) whilst M_1 receptors are unaltered in cortex of AD brain (Mash et al. 1985). Another group has shown the ratio of muscarinic receptors per pyramidal cell to be significantly increased in the hippocampus of AD brain (Probst et al. 1988).

A multitude of neurochemical deficits, now reported in AD brain, dispute the cholinergic disruption as being exclusive in AD. Biochemical indices have demonstrated reductions in the noradrenergic, dopaminergic, serotonergic, GABAergic and glutamatergic systems (Lowe et al. 1988; Hardy et al. 1985; Quirion et al. 1986; Rossor & Iversen, 1986) in cerebral cortex and hippocampus of AD brain. Additionally, a profound reduction in somatostatin has been demonstrated in AD neocortex (Rossor et al. 1980), as well as alterations in other peptides such as cholecystokinin and corticotropin releasing factor (Beal et al. 1986; De Souza et al. 1986). An increasing role for excessive glutamatergic activity has been implicated in the aetiology of AD. Glutamate is putatively the major excitatory transmitter of cortical pyramidal neurons which mediate intracortical and corticofugal neurotransmission (Jones, 1981). A prominent feature of AD pathology is a loss of cortical pyramidal cells (Mountjoy et al. 1983; Pearson et al. 1985). It is now understood that the primary lesion in AD occurs within association cortex rather than subcortical projections to cortex (Pearson et al. 1985; Mann et al. 1986). Thus, cortical glutamatergic dysfunction may be a contributory factor in the pathophysiological progression of the disease. In support of this hypothesis, application of N-methyl-D-aspartate (a glutamate

receptor agonist) to the cerebral cortex induced retrograde degeneration of cholinergic neurons in the nucleus basalis of rodents (Sofroniew & Pearson, 1985). Glutamate, when applied to human spinal cord neurons in culture, has been shown to induce the formation of structures almost identical to paired helical filaments, components of neurofibrillary tangles which are a hallmark of AD (De Boni & Crapper-McLachlan, 1985).

Dysfunction in a variety of neuronal systems is also associated with receptor alterations in AD. Ligand binding techniques have been used extensively to study neurotransmitter receptors in AD brain. Demonstration of neurotransmitter receptor abnormalities in AD brain include α_1, α_2, β_1, β_2 (Shimohama et al. 1986, 1987); nicotinic (Nordberg et al. 1988); $5HT_1$ and $5HT_2$ (Bowen et al. 1983; Perry et al. 1984; Cross et al. 1986 and 1988), $GABA_A$ and $GABA_B$ (Chu et al. 1987); benzodiazepine (Shimohama et al. 1988) and glutamate (Greenamyre et al. 1987). Statistical correlations have been found between many of these neurotransmitter receptor abnormalities and neuropathological changes in AD (see Mountjoy, 1986). Thus no one system can be regarded as responsible for the disorder. Furthermore, the functional significance of such diverse neurochemical abnormalities in AD remains unclear.

Although there has been intensive investigation of neurotransmitter receptor densities in AD brain, to date there have been few attempts to assess the functional status of these receptors. It is the integrity of neurotransmitter receptors with their associated signal transduction

mechanism which determines normal cellular responses. In view of the ineffectiveness, to date, of receptor targeted drug therapy in Alzheimer patients, the assessment of signal transduction systems of receptors, as well as their distribution in Alzheimer's disease, is vitally important if the possibilities of drug treatment for this condition are ever to be realised.

4. SECOND MESSENGER SYSTEMS IN DISORDERS OF THE CENTRAL NERVOUS SYSTEM

There has been minimal attention placed on second messenger systems in Alzheimer's disease. However, it has been proposed that functional disturbances in intraneuronal signal transmission distal to neurotransmitters play a vital role in the aetiology of several disorders.

Probably the definitive example of a disease in which interruption of second messenger systems is well characterised is pseudohypoparathyroidism (type 1A). This illness is caused by a dominantly inherited deficiency of the GTP-binding protein (G_s) which couples the parathyroid hormone receptor to stimulation of adenylate cyclase (Spiegel et al. 1982 & 1985). Recent evidence suggests a functional dysbalance of second messenger systems in affective disorders. In depression, hypofunction of the adenylate cyclase pathway with a relative dominance of the phosphoinositide (PI) system is proposed to occur with the converse resulting in mania (Wachtel, 1988, 1989). Therapeutically, lithium has been used effectively in treating depressive illnesses. Evidence indicates that lithium, at concentrations used clinically, inhibits inositol-1-phosphatase (Hallcher & Sherman, 1980) thereby increasing levels of inositol phosphate in the brain and preventing resynthesis of phosphatidylinositol 4,5 bisphosphate (see Figure 2). Alternatively, lithium within the therapeutic range, inhibits adenylate cyclase (Newman et al. 1983) by competing with sites for Mg^{2+} on the G_s-adenylate cyclase complex (Newman & Belmaker, 1987). Lithium has also been indicated to interfere with neurotransmitter receptor coupling with G-proteins (Avissar et al. 1988).

Thus, therapeutically, lithium may act, in the case of depression, by inhibiting the PI system and, in mania, by blocking the overactive adenylate cyclase system.

Second messenger system abnormalities are proposed in epilepsy. Epilepsy is characterised by spontaneous recurrent epileptic seizures in the absence of a known precipitatory cause or illness. Electroconvulsive shock and a number of convulsants markedly elevate concentrations of cAMP in the brain which can be reduced by anticonvulsants (Wasterlain & Dwyer, 1983). Interestingly, [^{3}H]-forskolin binding has been shown to be increased in the substantia nigra, pars reticulata following electroconvulsive shock in the rat (Fochtmann et al. 1988). This increase in [^{3}H]-forskolin binding parallels the upregulation of D_1 receptor binding in the substantia nigra, which may be associated with some of the anti-parkinsonian effects of electroconvulsive therapy. Furthermore, during seizures the PI system is activated which possibly involves activation of protein kinase C (PKC). Enhanced PKC activity may be putatively linked to neuronal death which is often seen around epileptic foci in human brain (Wasterlain, 1989). An increased involvement of PKC activation in neuronal death has also been implicated in ischaemic brain (Onodera et al. 1989). In gerbils, ischaemic damage in the CA1 subfield of the hippocampus can be prevented by pretreatment with a PKC antagonist (Hara et al. 1990).

Dysfunction of second messenger systems may be implicated in the pathophysiology of a number of disorders. The ability of pharmacological

intervention directed towards intraneuronal signalling is evident. Thus, it is essential that second messenger systems should be characterised in AD brain, an area to which, hitherto, minimal attention has been directed.

5. ANIMAL MODELS OF ALZHEIMER'S DISEASE ?

There are, to date, no animal models of Alzheimer's Disease (AD). As yet, it has been impossible to model in animals a disease which is heterogeneous not only in terms of symptomatology, but also in terms of the diversity of neurpathological and neurochemical abnormalities. In order to interpret possible alterations of second messenger systems in such an exceedingly complex neurodegenerative disease as AD, it is fundamental that the understanding of second messenger systems be explored in simple neuronal pathways in animal brain.

In AD, it is indisputable that the disruption of presynaptic cholinergic innervation of cerebral cortex and hippocampus is the most invariant neurochemical feature of the disease (Perry et al. 1978; Mountjoy et al. 1984; Perry, 1986; personal observations). Additionally, there is increasing evidence which implicates a glutamatergic dysfunction in the pathophysiological progression of AD (Greenamyre, 1986; Maragos et al. 1987). Furthermore, it is now believed that the primary degeneration in AD occurs within association cortex rather than subcortical regions (Pearson et al. 1985; Mann et al. 1986). On the basis that cholinergic and glutamatergic systems may have an integral role in AD, selective lesions of these specific neuronal pathways in rodent brain were used to investigate possible alterations of ligand binding to second messenger systems. As such, the retinofugal, corticofugal and intracortical fibres of the rat visual system are wholly glutamatergic, whilst the medial septal pathway to the rat hippocampus is principally cholinergic. Since the cortex is the site of

primary degeneration in AD, the investigation of ligand binding sites in cortical projection areas following lesioning of the rat visual cortex may provide a basis for the elucidation of second messenger systems in AD.

In addition to providing a framework for interpreting second messenger system alterations in AD, selective lesions of retinofugal and corticofugal efferents and the septo-hippocampal pathway would extend the limited awareness of the localisation of second messenger systems in neuronal pathways. Since the early studies of Worley and colleagues (1986a) employing lesioning techniques to examine specific neuronal localisations of ligand binding to second messenger systems in the rat striatum, hippocampus and cerebellum, there has been minimal expansion of research in this field.

5.1 Lesion of Retinofugal Fibres

The rat visual system provides an ideal polysynaptic pathway, being anatomically well-defined and, easily, completely, and reproducibly lesioned. In hooded rats, 97-98% of efferent retinal fibres are directed towards the contralateral hemisphere (Jeffrey, 1984). Thus, unilateral orbital enucleation of the rat visual system allows the ipsilateral (visually-intact) hemisphere to act as the reference against which changes in the visually-deprived (left) hemisphere can be compared.

The main anatomical components and connections of the primary visual system of the rat are illustrated in Figure 5. The axons of the retinal ganglion cells provide the only output from the retina, and hence determine

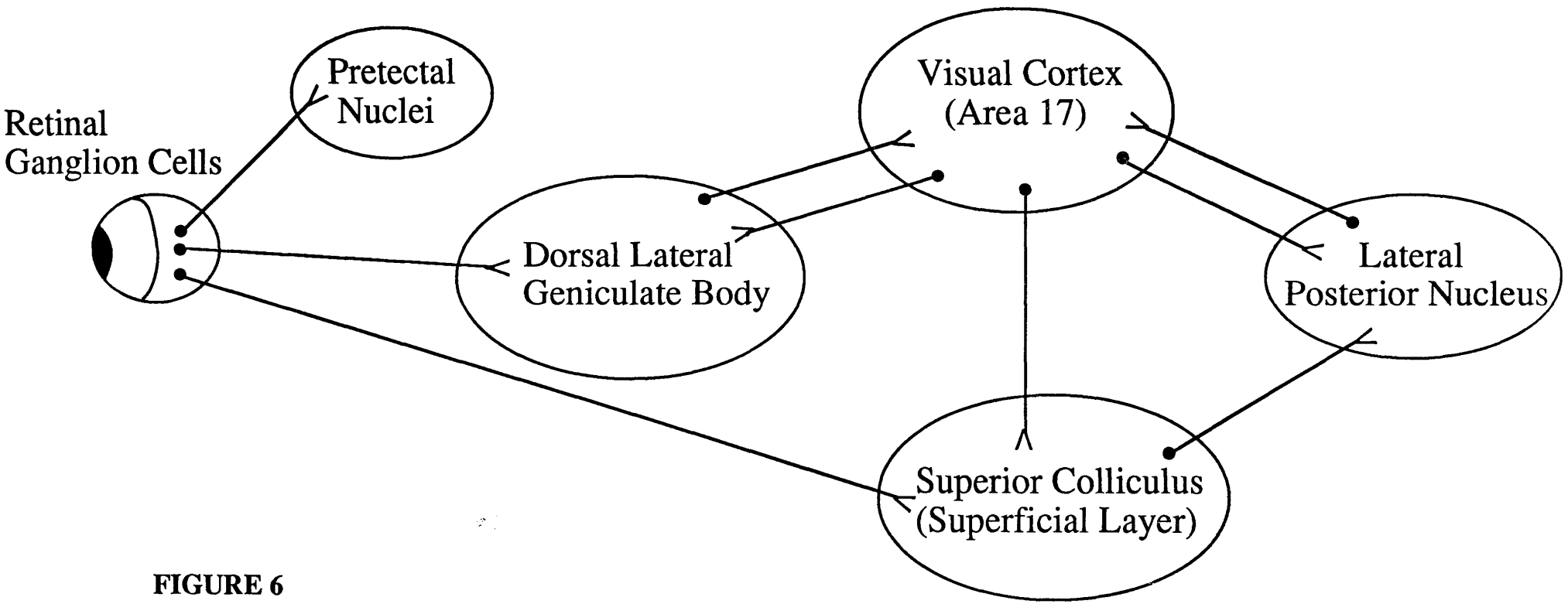

FIGURE 6

DIAGRAMMATIC REPRESENTATION OF THE PRIMARY VISUAL SYSTEM

the nature of the information supplied to each of the retinorecipient brain regions. The ganglion cells of the retina project via the optic nerve and in hooded rats it has been estimated that the optic nerve contains 120,000 axons (Hughes, 1977). The majority of these axons, approximately 65% (Toga & Collins, 1981), are targeted to the superior colliculus. The superior colliculus is horizontally laminated, being composed of layers designated zonal, superficial gray, optic, intermediate gray and white, deep gray and white (Huber & Crosby, 1943). However, only the superficial layers of the superior colliculus are directly innervated by retinal axons. Cells in these layers project to the deeper layers where other sensory systems are represented (Stein, 1981). Cells from the superficial layers of the superior colliculus project to subcortical visual structures such as the dorsal lateral geniculate body (Pasquier & Villar, 1982), pretectal nuclei and the lateral posterior nucleus (Takahashi, 1985). Although there are no direct projections from the superior colliculus to the visual cortex, the superior colliculus receives cortical efferents.

A smaller portion of retinofugal fibres (15%) project to the dorsal lateral geniculate body (Toga & Collins, 1981), which lies in the dorsolateral part of the thalamus. The dorsal lateral geniculate body, in contrast to the superior colliculus, relays information directly to the primary visual cortex (area 17). The major termination layer for geniculo-cortical projection fibres is layer IV (Sefton & Dreher, 1984). Unlike the superior colliculus, there are no projections from this structure to subcortical regions except for a minor projection to the reticular thalamic nucleus (Hale et al. 1982). However,

there are projections to the dorsal lateral geniculate from retinorecipient areas such as pretectal (Pasquier & Villar, 1982) and the superior colliculus (Takahashi, 1985). There is also a non-visual projection to the dorsal lateral geniculate arising from the locus coeruleus (Kromer & Moore, 1980).

The pretectal nuclei lie at the most rostral pole of the midbrain, bordering the thalamus. The pretectal nuclei consist of a number of distinct nuclear groups; nucleus of the optic tract; olivary pretectal nucleus; anterior pretectal nucleus and posterior pretectal nucleus (Scalia, 1972). In hooded rats, only 13% of the retinofugal axons terminate in the contralateral pretectal nuclei (Toga & Collins, 1981). There are projections from the pretectal nuclei to the superior colliculus, dorsal lateral geniculate body and lateral posterior nucleus (Sefton & Dreher, 1985; Mackay-Sim et al. 1983).

The lateral posterior nucleus, in the lateral thalamus, lies medially and caudally to the dorsal lateral geniculate body. This structure receives a relatively minor input from retinal ganglion cells (4%) in comparison to other retinorecipient regions. However, these nuclei receive a significant projection from the superior colliculus and visual cortex (area 17). In turn, the lateral posterior nucleus projects to primary visual cortex (area 17).

5.2 Lesion of Corticofugal Fibres

Detailed information on the cortical inputs and synaptic connectivity of the primary visual cortex (area 17) was demonstrated by use of autoradiography, and light and electron microscopy (Feldman & Peters, 1978;

Peters & Feldman, 1976, 1977; Peters et al. 1982). The primary visual cortex (area 17) is a typical granular cortex and approximately 85% of neurons in this area are pyramidal cells. Although non-pyramidal neurones are present in all layers, they are concentrated in layer IV (Parnavelas et al. 1977). The great majority of thalamic efferents, principally arising in the dorsal lateral geniculate body, terminate in layer IV of the visual cortex. Most of the thalamic terminals synapse with dendritic spines of apical and basal dendrites of pyramidal neurons, sparsely spined stellate cells and spiny non-pyramidal cells in layers III-IV. To a lesser extent, thalamic terminals synapse on the shafts of apical dendrites or on smooth stellate cells (Sefton & Dreher, 1985). Pyramidal cells in cortical layers II/III are responsible for cortico-cortical projections (Cusick & Lund, 1981), whilst those in layers V-VI are responsible for projections to subcortical visual structures (Olavarria & Van Slutyers, 1982; Sefton et al. 1981). The primary visual cortex sends afferents to all subcortical structures as outlined in this chapter (section 5.1).

Biochemical and electrophysiological studies have implicated a major role for glutamate in visual pathways. Visual cortex ablation in rats demonstrated a marked reduction in high affinity glutamate uptake and endogenous glutamate in the dorsal lateral geniculate body, superior colliculus and lateral posterior nucleus (Lund-Karlsen & Fonnum, 1978; Fosse et al. 1986; Fosse & Fonnum, 1987). Glutamate was also found to be the major neurotransmitter in the projections from the cortex to the lateral geniculate body, arising from layer IV of visual cortex, and in the projection within the visual cortex from layer VI to layer IV (Baugham & Gilbert, 1981).

Additionally, excitatory postsynaptic potentials evoked by electrical stimulation of the optic tract have been demonstrated to be reversibly inhibited by a glutamate receptor antagonist (Crunelli et al. 1987), Alteration of visual input by monocular deprivation affects glutamate binding in the lateral geniculate body (Schliebs et al. 1984). Investigation of glutamate receptor subtypes has suggested NMDA receptors play an important modulatory role in cortical neurotransmission in the rat visual cortex (Artola & Singer, 1987). This evidence supports a major role for glutamate as a transmitter in both retinofugal and corticofugal fibres to the superior colliculus and dorsal lateral geniculate body, and as a transmitter within visual cortex.

In addition to glutamate, a number of other neurotransmitters have been implicated in the visual circuitry. Of these, within the visual cortex, γ amino-butyric acid (GABA) has been shown to be an inhibitory transmitter of a number of intrinsic interneurons including aspinous and spiny stellate cells and chandelier cells (Houser et al. 1984). In subcortical visual structures, several types of GABAergic neurons are present in the superficial layer of the superior colliculus (Mize et al. 1982). The dorsal lateral geniculate body has also been shown to use GABA as a neurotransmitter (Fitzpatrick et al. 1984) in addition to the projections of the reticular thalamic nucleus to the geniculate body which provide local inhibitory control of relay neurone activity (Kayama, 1985). Monoaminergic involvement has also been demonstrated in the primary visual system. In the dorsal lateral geniculate body, the noradrenergic input from the locus coeruleus has a

powerful facilitatory action on activity, whereas serotonergic projections from the dorsal raphé nucleus have an equally potent depressant effect (Rogawski & Aghajanian, 1980). In contrast, both noradrenaline and serotonin have been shown to exert an inhibitory control over superior colliculus neurons (Sato & Kayama, 1983; Lai et al. 1978). Within the primary visual cortex, noradrenaline has an important modulatory role in controlling cortical plasticity which has also been shown for acetylcholine (Kasamatsu & Pettigrew, 1979; Bear & Singer, 1986). The dorsal lateral geniculate body and superior colliculus contain high quantities of acetylcholine, acetylcholinesterase and cholineacetyltransferase (Hebb & Silver, 1956; Phillis et al. 1967). Acetylcholine is reported not to be involved in relaying retinal input to the dorsal lateral geniculate (Curtis & Davis, 1962; Kemp & Sillito, 1981), but is instead associated with an excitatory input from the nucleus cuneformis (Hoover & Jacobowitz, 1979).

Ligand binding techniques have been used successfully to investigate the plasticity of neurotransmitter receptors in the visual pathways. Monocular deprivation was demonstrated to reduce [^{3}H]-glutamate binding selectively in the ipsilateral dorsal lateral geniculate body associated with a down-regulation of glutamate binding sites in response to enhanced functional activity in the non-deprived eye of rats (Schliebs et al. 1984 & 1986). [^{3}H]-DHA binding to β-adrenergic receptors was shown to increase in both the deprived and non-deprived dorsal lateral geniculate body following monocular deprivation (Schliebs et al. 1982). Quantitative autoradiography has been used to localise neurotransmitter receptors in the visual system of the cat

(Fox et al. 1989), rat (Chalmers & McCulloch, 1990) and monkey (Rakic et al. 1988). During the critical period, abnormal visual experience can alter neuronal properties of the visual cortex (Hubel & Wiesel, 1970). Quantitative autoradiographic studies of neurotransmitter binding sites have demonstrated marked increases in GABA and muscarinic receptors in visual cortex of cats indicative of the plasticity of visual cortex during this period. Additionally, quantitative autoradiography has demonstrated the heterogeneity of neurotransmitter receptor alterations in the rat visual system following unilateral denervation of the rat visual pathway (Chalmers & McCulloch, 1990).

5.3 LESION OF SEPTO-HIPPOCAMPAL PATHWAY

Since the cholinergic deficit has been most consistently implicated in AD, manipulation of this system has been widely investigated in animal models. In view of the major cholinergic projection to the rat hippocampal formation which arises primarily from the medial septum and diagonal band of Broca, lesion of the medial septum affords an ideal system in which to examine the functional consequences following denervation of this cholinergic pathway to the hippocampus.

The anatomical organisation of the hippocampal formation, although well-defined, is functionally complicated by the extensive intrinsic and extrinsic circuitry. This section will deal solely with the principal connections of the septo-hippocampal pathway (for further details see Swanson et al. 1987; Witter et al. 1989) and functionally-related structures (see Figure 7). The medial division of the septal region consists of the medial septal nucleus and the diagonal band of Broca which form a more or less a continuous mass. Degeneration, autoradiographic and retrograde studies (Swanson & Cowan, 1979; Mellgren & Srebo, 1973; Alonso & Köhler, 1984) have demonstrated that neurons in the medial septum innervate all fields of the hippocampal formation. The hippocampal formation is comprised of four cortical regions; the dentate gyrus, Ammon's Horn (CA1, CA2, CA3 and CA4 subfields), the subicular complex (subiculum, presubiculum and parasubiculum) and the entorhinal cortex. Inputs to the dentate gyrus from the medial septum are particularly dense and are concentrated in the polymorph (hilar) region (Rose et al. 1976) forming asymmetric synapses upon dendrites. In Ammon's Horn,

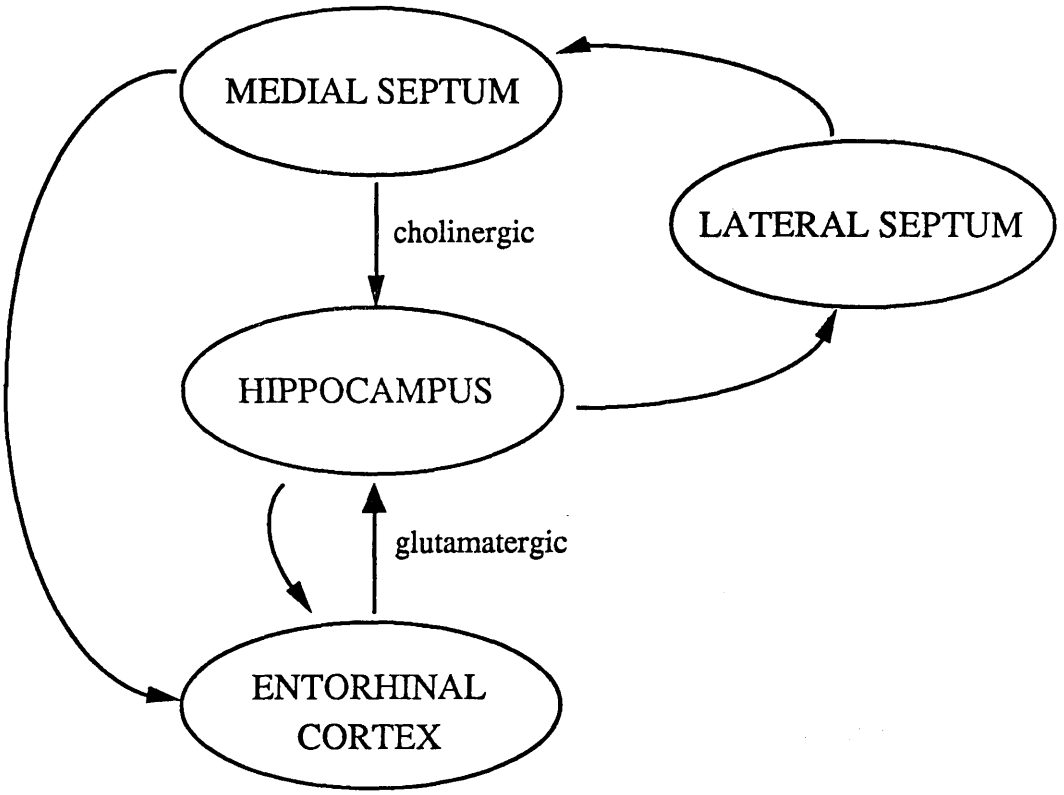

FIGURE 7
SEPTO-HIPPOCAMPAL PATHWAY

Simple diagrammatic representation of the septo-hippocampal pathway in the rat.

septal fibres appear to end predominantly in the stratum radiatum and oriens of CA3 subfield and, to a lesser degree, in the stratum oriens of CA1 subfield. All layers of the subiculum receive inputs from the medial septum. Additionally, there is a major input from the medial septum to entorhinal cortex, in particular to layers II, IV and VI.

The medial septum receives a modulatory input from the lateral septum, (Swanson & Cowan, 1979) which itself receives input from Ammon's Horn and the subiculum. Thus, the lateral septum acts as a link in a feedback system from the hippocampus to the medial septum. Other inputs to the medial septum arise from the hypothalamus and brainstem.

There is now substantial evidence which determines the projection from the medial septum to the hippocampus as being mainly cholinergic. Massive depletions of choline acetyltransferase (ChAT) activity, up to 80-90%, and acetylcholine levels in the hippocampus following medial septum lesions have been demonstrated (Storm-Mathisen, 1970; Lewis et al. 1967; Mellgren & Srebro, 1973). Furthermore, combined retrograde tracing with immuno-histochemistry of ChAT has confirmed this pathway to be mainly cholinergic (Rye et al. 1984; Woolf et al. 1984). A smaller number of neurons, distinct from cholinergic neurons, have now been identified as being GABAergic (Brashear et al. 1986), whilst a subpopulation of cholinergic neurons are immunoreactive with galanin (Melander et al. 1985). ChAT has been localised in all layers of the dentate gyrus, subiculum and Ammon's Horn and is particularly concentrated in the stratum lacunosum moleculare (Houser et al.

1983). The distribution of acetylcholinesterase coincides with the degeneration pattern following a septal lesion (Lynch et al. 1972). Cholinergic interneurons are present to a much lesser extent in the hippocampal formation and, as yet, their function is unclear.

There has been intensive investigation of the excitatory pathway, the perforant pathway, which projects from the entorhinal cortex to the molecular layer of the dentate gyrus and, to a lesser extent, the stratum lacunosum moleculare of the hippocampus (Steward, 1976; Swanson et al. 1987). The projection to the dentate gyrus arises mainly from layer II of entorhinal cortex, whilst fibres to the lacunosum moleculare are mainly from layer III. These fibres form asymmetric synapses on the spines of granule cell dendrites. The perforant pathway continues with the mossy fibre pathway from the dentate gyrus to CA3 field, and ends with the Schaffer collateral (commisural) projection from CA3 to CA1 field. The CA1 field projects back to all layers of the entorhinal cortex.

The perforant pathway has been demonstrated to be wholly glutamatergic (Storm-Mathisen, 1977; White et al. 1977). The terminal fields of the perforant pathway contain high densities of receptors for glutamate, particularly those of the N-methyl-D-aspartate-preferring receptor subtype which plays an important role in the induction of long-term potentiation in the hippocampus (Collingbridge & Bliss, 1987). Ligand binding autoradiography in the rat hippocampus has demonstrated an abundance of other glutamate receptor subtypes such as kainate and AMPA (Greenamyre

et al. 1985; Monaghan et al. 1985), which additionally may have specific roles to play in hippocampal LTP (Izumi et al. 1987; Collingbridge & Singer, 1990).

6. AIMS OF THESIS

6.1 Human Postmortem Studies

The use of quantitative autoradiography to map neurotransmitter receptors in postmortem brain is well-established. Currently available are novel radioligands which are specific for second messenger systems. Thus, quantitative autoradiography can be used to localise the distribution and density of second messenger systems in discrete areas of human brain with a high degree of spatial resolution. The primary aim of these studies was to apply two of these ligands, [^{3}H]-forskolin and [^{3}H]-phorbol 12,13 dibutyrate, to investigate the distribution of adenylate cyclase and protein kinase C respectively in postmortem human tissue sections using quantitative autoradiography.

Increasingly evident is the demonstration of multiple neurotransmitter receptor abnormalities in AD. Effective drug therapy targeted at neurotransmitter receptors is dependent on the integrity of the coupling of neurotransmitter receptors with effector systems. Another aim of the human postmortem studies was to use quantitative autoradiography to examine possible alterations in ligand binding to second messenger systems in a group of Alzheimer subjects compared to controls. The studies are focused on three brain regions which are differentially affected in Alzheimer's disease (AD) namely middle frontal cortex, middle temporal cortex and the hippocampal formation. Additionally, in the same patients in which ligand binding autoradiography was applied, the degree of local neuropathological and neurochemical abnormalities was measured as an index to the severity

of AD in these patients.

6.2 Studies in the Rat Brain With Selective Neuronal Lesions

Disruption of glutamatergic and cholinergic systems may have a major role in Alzheimer's disease. Thus, selective lesions of these specific neuronal pathways were examined in rat brain. Glutamatergic pathways of retinofugal (following unilateral orbital enucleation), corticofugal and intracortical fibres (following stereotaxic lesion) were investigated in the rat visual system. The cholinergic pathway of the rat septo-hippocampus was examined following stereotaxic lesion of the medial septum. Three main aims of these studies were to:

(1) localise ligand binding to second messenger systems in specific neuronal pathways in rat brain,

(2) investigate possible plastic modifications of ligand binding sites associated with lesioning glutamatergic and cholinergic pathways,

(3) provide a framework for the elucidation of alterations in ligand binding sites in Alzheimer's Disease.

Quantitative autoradiography in vitro was used to examine [^{3}H]-forskolin binding to G_s-adenylate cyclase and [^{3}H]-PDBu binding to protein kinase C in rat brain following lesion. Functional deficit within the visual system was assessed, in parallel, in the same animals in vivo by measuring the rat of

local cerebral glucose utilisation with [^{14}C]-2-deoxyglucose autoradiography (Sokoloff et al. 1977).

CHAPTER II

METHODS

1. AUTORADIOGRAPHY

1.1 In Vitro Ligand Binding Autoradiography

1.1.1 Theory

Autoradiography is simply the localisation and quantification of radioisotopes in discrete brain areas. The method is based on the principle that radioactive ligands (which are highly specific for certain recognition sites) emit energy to produce a photographic image when placed in contact with radiation-sensitive film. The blackness of the image is related to the density of binding sites which can be quantified by reference to a set of standards containing a known amount of radioactivity. Autoradiography permits sensitive quantification of ligand binding sites in well-defined neuroanatomical areas of the CNS with a high degree of spatial resolution.

Ligand binding techniques are based on the kinetics of ligand-receptor interaction. The simplest type of binding can be expressed as a reversible reaction,

$$L + R \underset{K_{-1}}{\overset{K^{+1}}{\rightleftharpoons}} [L\ R] \qquad (1)$$

where: L = Ligand R = Receptor

LR = Ligand Receptor Complex

K+1 = Rate Constant for Association

K-1 = Rate Constant for Dissociation

At equilibrium, the dissociation constant K_D can be defined:

$$K_D = \frac{K^{-1}}{K_{+1}} = \frac{[L]\ [R]}{[LR]} \qquad (2)$$

Since the total number of binding sites B_{Max} equals the sum of free receptors [R] and receptors bound to ligand [LR], that is:

$$B_{Max} = [LR] + [R]$$

substitution redefines equation (2) as:

$$K_D = [L]\ \frac{(B_{Max} - [LR])}{[LR]} \qquad (3)$$

or

$$\frac{B}{F} = \frac{B_{Max} - B}{K_D} \qquad (4)$$

This equation (4) is known as the Scatchard equation (Scatchard, 1949). If the concentration of ligand bound and free are known at equilibrium, then the maximum number of binding sites, B_{MAX} and the dissociation constant of the ligand K_D can be determined.

More commonly, in ligand binding studies, this equation is applied by plotting the ratio of [B] to free [L] against the concentration of bound ligand. This yields a straight line that has a slope equal to the negative reciprocal

of the dissociation constant ($-1/K_D$) and an intercept on the abscissa equal to the total concentration of receptors (B_{Max}). An advantage of using Scatchard analysis is that it provides an estimate of the total concentration of receptors without requiring saturating concentrations of radioligand. In addition, the Scatchard plot provides insight into whether or not a simple bimolecular reaction adequately describes the interation between ligand and receptor. Curvature of a Scatchard plot implies that this interaction is complex.

1.1.2 Practice

The general outline of the method for quantitative in vitro ligand binding autoradiography is outlined in Figure 8. In brief, fresh brain tissue is frozen and cut into 20μm thick sections using a cryostat microtome. The tissue sections are thaw-mounted onto subbed slides. The sections are then incubated in the appropriate buffer medium containing the ^{3}H-ligand specific for the recognition site to be mapped. In adjacent sections, non-specific binding (binding to sites other than the recognition sites such as glass, constituents in tissue) is defined in the presence of excess unlabelled ligand or displacer. After an optimal incubation time at which equilibrium is achieved, unbound radioactivity is washed off. The radiolabelled sections are dried rapidly or they can be wiped off the slides using microfilter discs and the radioactivity bound counted by liquid scintillation analysis. The dried sections are exposed to radiation-sensitive film and the resultant autoradiograms analysed using computer-assisted densitometry.

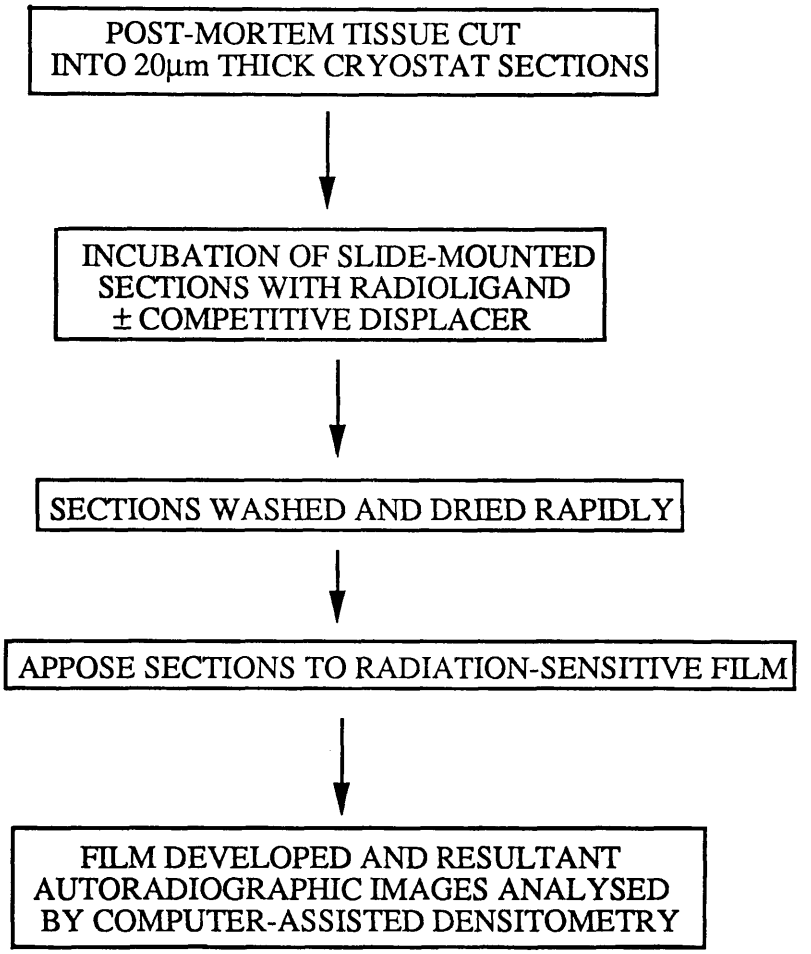

FIGURE 8
IN VITRO LIGAND BINDING METHOD

General outline of the method for quantitative in vitro ligand binding autoradiography.

The protocols for ligand binding to second messenger systems, used in this thesis, are slightly modified versions of well-established methods and are listed in Table 1.

The concentration of radioligand used in routine binding experiments was applied in close range to the equilibrium dissociation constant and was never applied at a saturating concentration of ligand. By applying radioligands near K_D concentrations, this allows sensitive detection of a small change in the number of binding sites.

1.1.3 Methodological Considerations

Several extrinsic factors possibly influence the amount of ligand binding to sections in different experiments. Increased variability between sections may arise from variation in the temperature of incubation and rinsing, differences in the buffer medium, e.g. pH, salt concentration and most importantly, alterations in the concentration or specific activity of the radiolabelled ligand in the incubation medium.

The additive effect of these factors on ligand binding was minimised by undertaking binding studies from the same experimental series on the same day. This enabled all tissue sections, in a random order, to be labelled with the radioligand from the same batch and concentration and at the same temperature. This method ensured the variability of ligand binding within the same series was internally consistent although variation between different experimental studies is not excluded.

TABLE 1

PROTOCOLS FOR LIGAND BINDING

LIGAND	DISPLACER	BUFFER	INCUBATION TIME	WASHES IN DIST. H20	REFERENCE
[^{3}H]-Forskolin (20nM)	forskolin (20μM)	50mM Tris-Acetate (pH 7.5) + 10mM $MgCl_2$	20 min. (R.T.)	2 x 1 min. (4°C)	Gehlert et al. 1985 Worley et al. 1986a
[^{3}H]-Phorbol 12,13 Dibutyrate (2.5nM)	phorbol 12,13 dibutyrate (2μM)	50mM Tris-HCl (pH 7.7) + 1mM $CaCl_2$	90 min. (R.T.)	2 x 2 min. (4°C)	Worley et al. 1986 a,b

R.T. = room temperature

1.2 In Vivo [^{14}C]-2-Deoxyglucose Autoradiography

1.3.1 Theory

There are two basic principles which provide the conceptual basis for the utility of the [^{14}C]-2-deoxyglucose technique. Firstly, the energy requirements of cerebral tissue under normal conditions are derived almost exclusively from the aerobic catabolism of glucose (Sokoloff, 1982). Secondly, the functional activity and energy requirements are intimately and directly related within any region of the central nervous system.

2-Deoxyglucose, a structural analogue of glucose, differs only in the replacement of the hydroxyl group on the second carbon atom by a hydrogen atom. It is this single structural difference which is responsible for the chemical properties that make the use of 2-deoxyglucose suitable for this method. The systems of brain uptake and phosphorylation are common to both deoxyglucose and glucose (Figure 9). However, glucose-6-phosphate dehydrogenase which converts glucose-6-phosphate for further metabolism in the glycolytic pathway is unable to act upon the anomalous structure of 2-deoxyglucose. As a result, 2-deoxyglucose-6-phosphate is essentially "trapped" within the cerebral tissues. The rate at which 2-deoxyglucose-6-phosphate accumulates in any cerebral tissue is equal to the rate of phosphorylation of 2-deoxyglucose by hexokinase and this may be directly related to the rate at which glucose is phosphorylated over the same period of time.

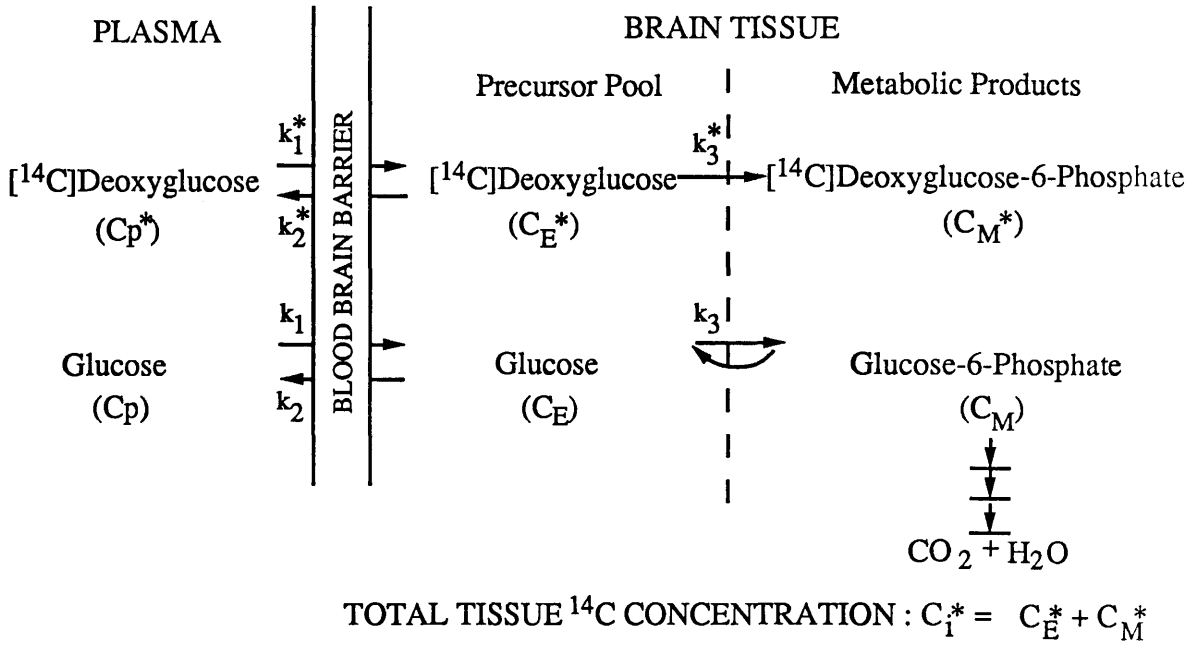

FIGURE 9
DIAGRAMMATIC REPRESENTATION OF THE THEORETICAL MODEL.

Cp* and Cp represent the concentrations of [^{14}C]-deoxyglucose and glucose in arterial plasma whilst C_E* and C_E represent their respective concentrations in the tissue precursor pool. C_M* represents the concentration of [^{14}C]-deoxyglucose-6-phosphate in the tissue. The constants k_1*, k_2* and k_3* represent the rate constants for carrier-mediated transport of [^{14}C]-deoxyglucose and phosphorylation of [^{14}C]-deoxyglucose by hexokinase. The constants k_1, k_2 and k_3 are the equivalent rate constants for glucose. The dashed arrow represents the possibility of glucose-6-phosphate hydrolysis by glucose-6-phosphatase activity (Sokoloff et al. 1977).

Using this theoretical model (Figure 9) the rate of glucose utilisation can be described mathematically by the operational equation (Sokoloff et al. 1977). This equation (Figure 10) defines the rate of cerebral glucose utilisation in terms of the levels of glucose and [^{14}C]-2-deoxyglucose in arterial plasma during the experimental period (cp* and cp) and the total concentration of radioactivity within cerebral tissue at the end of the experiment (ci*) provided the values of certain predetermined constants are known. This method may be used to measure local rates of glucose utilisation under a variety of experimental conditions, provided that the following requirements are fulfilled.

(1) Tissue is homogenous within which the concentrations of [^{14}C]-2-deoxyglucose and glucose are uniform and exchange directly with plasma.

(2) [^{14C}]-2-Deoxyglucose and [^{14}C]-2-deoxyglucose-6-phosphate are present in tracer amounts.

(3) Plasma glucose concentration and local rates of glucose consumption remain constant throughout the experimental procedure.

(4) [^{14}C]-2-Deoxyglucose-6-phosphate, or its metabolites remain trapped within cerebral tissue for the duration of the sampling period.

$$Ri = \frac{Ci^*(T) - k_1^* e^{-(k_2^* + k_3^*)T} \int_0^T Cp^* e^{(k_2^* + k_3^*)t}\, dt}{K \cdot \left[\int_0^T (Cp^*/Cp)\, dt - e^{-(k_2^* + k_3^*)T} \cdot \int_0^T (Cp^*/Cp) e^{(k_2^* + k_3^*)t}\, dt\right]}$$

FIGURE 10
THE OPERATIONAL EQUATION

The rate of glucose utilisation Ri in any cerebral tissue is calculated from the total tissue concentration of ^{14}C in that tissue, Ci* (measured by densitometry) at time T, Cp* and Cp are the concentrations of [^{14}C]-deoxyglucose and glucose in the plasma and k_1^*, k_2^* and k_3^* are the rate constants for transport to and from plasma and tissue precursor pools and for phosphorylation of deoxyglucose by hexokinase. The lumped constant K, is composed of the relative distribution spaces for deoxyglucose and glucose, the ratio of the Michaelis-Menten constants, the maximal velocities of hexokinase for deoxyglucose and glucose and the fraction of glucose-6-phosphate which continues via the glycolytic pathway for further metabolism (Sokoloff et al. 1977).

1.2.2 Practice

Measurement of local cerebral glucose utilisation was performed using the [^{14}C]-2-deoxyglucose method in conscious rats in conjunction with quantitative autoradiography (Sokoloff et al. 1977).

[^{14}C]-2-Deoxyglucose (125μCi/kg, 50Ci/mmol) was injected intravenously at a constant rate over 30s. Fourteen timed arterial blood samples (~75μl) were withdrawn from the femoral cannulae and collected into plastic centrifuge tubes during the following 45 min. Over the first minute of the experiment, five arterial samples were taken to allow an accurate measurement of the history of the tracer in plasma to be determined during the time at which it is most rapidly changing. The volume of blood removed each time was replaced by an equal volume of Ringer's solution. In order to minimise haemolysis, each arterial sample was immediately centrifuged after withdrawal and the plasma separated from the cell fraction. Aliquots from each plasma sample (20μl) were pipetted from the centrifuge tubes into 1ml of distilled H_20 and the radioactivity in the plasma counted by liquid scintillation. A further aliquot of each plasma sample (10μl) was used to measure the glucose concentration (Glucose Analyser II, Beckman). The experiment was terminated at the end of the 45 min period when the rat was sacrificed by decapitation and the brain removed rapidly and processed for quantitative autoradiography (see Methods 3.4.1.1).

Rates of glucose utilisation within anatomically discrete regions of the rat brain were calculated using the operational equation from postmortem levels of ^{14}C measured by quantitative autoradiography together with the plasma histories of ^{14}C and glucose concentrations determined experimentally.

1.2.3 Methodological Considerations

The main limitations of the [^{14}C]-2-deoxyglucose technique are the degree of restraint necessary for plasma sampling and the long time constant required for the experimental measurement. Potential errors arising from uncertainty in the values of the rate constants K_1*, K_2* and K_3* which define the distribution of tracer between plasma and tissue compartments require the time between the pulse of labelled deoxyglucose and sacrifice of the animal to be sufficiently long to minimise the associated uncertainty in these measurements. Additionally, the experimental sampling procedure must be short enough to limit the depleting effects of the small amounts of phosphatases in cerebral tissue on 2-deoxyglucose-6-phosphate. However, an experimental time course of 45 minutes has been found to be sufficiently long enough to meet both these requirements.

The lumped constant is particularly stable over a wide range of experimental conditions. However, alterations in the lumped constant may occur in animals with severe hypoglycaemia (plasma glucose less than 5mM). In view of this, animals which had undergone surgical intervention were not

used unless their pre-operation weight was reached or increased. Additionally, prior to the sampling period, plasma glucose values were recorded. Animals which had undergone stereotactic surgery were allowed to survive for 21 days prior to performing the [^{14}C]-2-deoxyglucose technique to allow recovery of the animal to normal.

2. HUMAN POSTMORTEM STUDIES

2.1 Clinical Information

Autopsied brains of control and Alzheimer (AD) patients were obtained from Gartnavel Royal Hospital and Southern General Hospital, Glasgow. Alzheimer subjects had a clinical diagnosis of dementia which was subsequently confirmed as AD by criteria set by Khachaturian (1985). Control patients had no known history of neurological or neuropsychiatric impairment. All brains in both control and AD groups were free from gross tissue abnormalities such as tumours and infarcts. The characteristics of control and AD subjects are listed in Tables 2 and 3.

2.2 Brain Dissection

Brains were removed at autopsy and cut into multiple coronal slabs, approximately 1cm thick. Tissue blocks containing neuroanatomical regions of interest were dissected free, frozen by slow immersion in isopentane (-42°C) and transferred to storage at -80°C. Experimental studies described in this thesis focused on three brain regions: middle frontal gyrus (Brodmann area 9) at the level of the genu, middle temporal gyrus (Brodmann area 21) and the hippocampal formation both at the level of the lateral geniculate. Frozen blocks were later equilibrated to -20°C and 20μm thick cryostat sections cut serially and mounted onto gelatin-coated subbed slides in preparation for ligand binding autoradiography. In each block two sections were processed for histology and stained with cresyl violet. The remaining tissue was fixed in 10% formalin for neuropathological examination of the presence of plaques.

TABLE 2

SOURCES OF BRAINS FOR AUTORADIOGRAPHIC STUDY OF [^{3}H]-FORSKOLIN BINDING

	SEX	AGE (YEARS)	POSTMORTEM DELAY (HOURS)	CAUSE OF DEATH
CONTROLS				
C2	M	88	13.5	Septicaemia, Peritonitis
C3	F	72	13	Uraemia, Multiple Myeloma
C5	M	86	5.5	Myocardial Infarction, Small Pulmonary Emboli
C7	M	67	9	Pulmonary Congestion & Oedema
C8	F	80	23	Bronchopneumonia
C11	M	74	8	Bronchopneumonia
	Mean Age = 78 ± 3		Mean PM Delay = 12 ± 3	
AD PATIENTS				
4AD	F	78	4.5	Myocardial Infarction, Bronchopneumonia
5AD	M	67	6	Bronchopneumonia
7AD	F	74	14	Pulmonary Oedema and Atrial Fibrillation
8AD	M	67	3.5	Mesenteric Thrombosis
10AD	F	79	5	Bilateral Pulmonary Embolism
11AD	F	62	7	Bronchopneumonia
12AD	M	83	10	Bronchopneumonia, Myocardial Infarction
	Mean Age = 73 ± 3		Mean PM Delay = 7 ± 2	

TABLE 3

SOURCES OF BRAINS FOR AUTORADIOGRAPHIC STUDY OF [^{3}H]-PDBu BINDING

	SEX	AGE (YEARS)	POSTMORTEM DELAY (HOURS)	CAUSE OF DEATH
CONTROLS				
C16	M	76	17	Bronchopneumonia
C18	F	86	19	Carcinoma
C19A	F	84	7	Myocardial Infarction
C20	F	78	14.5	Myocardial Infarction
C21	F	90	11	Carcinoma
16AD	F	92	9	Renal Failure
C22	F	72	8	Bronchopneumonia
C23	M	74	4	Peritonitis
C25	M	67	12	Myocardial Infarction
		Mean Age = 80 ± 3	Mean PM Delay = 11 ± 2	
AD PATIENTS				
14AD	M	89	9.5	Obstruction of Colon
23AD	F	92	15	Bronchopneumonia
25AD	F	97	7	Bronchopneumonia
31AD	F	83	9	Pulmonary Congestion
33AD	F	71	8	Bronchopneumonia
44AD	F	75	19	Bronchopneumonia
43AD	M	77	13	Bronchopneumonia
45AD	F	76	14	Bronchopneumonia
36AD	F	76	7	Bronchopneumonia
		Mean Age = 82 ± 3	Mean PM Delay = 11 ± 1	

Brain dissection was carried out in a category II containment facility and only after brain tissue was cleared of HIV and Creutzfeld-Jacob disease. All experimental work was continued within a category II containment facility.

2.3 Quantification of Plaques

Plaque numbers were counted in sections taken from tissue blocks adjacent to those used for ligand binding autoradiography. Nominal 28μm thick sections were cut on a freezing microtome and stained using King's amyloid silver stain. Plaque numbers were counted using a Quantimet 520 (Cambridge Instruments) by outlining individual plaques manually. In cortex, mean plaque counts were obtained by making three individual readings on both the surface of the gyri and deep in the sulci, both in superficial (I-III) and deep (IV-VI) layers. In the hippocampal formation, mean counts were obtained from six different readings made in the subiculum.

2.4 Choline Acetyltransferase (ChAT) Activity

Grey matter was dissected carefully from the tissue blocks remaining after cryostat sections were cut for autoradiography. Part of this tissue was used for determination of ChAT activity as previously described by Fonnum (1975) and protein was estimated according to the method of Lowry (1951). Samples were assayed in triplicate.

2.5 In Vitro Ligand Binding

2.5.1 Practice

Protocols for [^{3}H]-forskolin and [^{3}H]-PDBu ligand binding autoradiography have been established in rat brain. However, at the outset of the thesis, ligands had not been applied in human postmortem tissue. Preliminary studies were undertaken to investigate the viability of using [^{3}H]-forskolin and [^{3}H]-PDBu as markers for second messenger systems in postmortem human tissue sections. Saturation analysis of both ligands was investigated in the presence of increasing concentrations of radioligand and the pharmacological profile of the ability of structurally-related compounds to inhibit the binding of these [^{3}H]-ligands determined.

Following investigation of the kinetics of [^{3}H]-forskolin and [^{3}H]-PDBu binding, the ligands could then be applied in autoradiographic studies according to the protocols outlined in Section 1.1 of this chapter. In one study, [^{3}H]-forskolin binding was examined in the presence and absence of 5'guanylimidodiphosphate (Gpp(NH)p). Gpp(NH)p is a non-hydrolyzable guanine-nucleotide which was purported to enhance the binding of [^{3}H]-forskolin. A concentration of 10μM Gpp(NH)p is believed to maximally stimulate [^{3}H]-forskolin (Gehlert, 1986).

On the same day, for each ligand, all control and AD sections were incubated, washed and dried. Radiolabelled sections from one brain region of a control and AD subject were apposed to [^{3}H]-Hyperfilm (Amersham) along with a set of precalibrated [^{3}H]-microscales (Amersham) in a light-

tight x-ray cassette. Exposure time for [^{3}H]-forskolin and [^{3}H]-PDBu was four weeks and one week respectively. Resultant autoradiograms were analysed using computer-assisted densitometry (Quantimet 970, Cambridge Instruments) as outlined in Section 3.4.2. of this chapter.

Ligand binding to each discrete region of interest on the autoradiogram was determined by reference to adjacent cresyl violet stained sections. The experimenter was blind to the identity of the sections and mean optical density measurements were averaged over a minimum of three total or non-specific sections; in each section at least 10 separate readings were made. Optical density measurements were converted to pmol/g tissue with reference to the standard curve generated by the [^{3}H]-microscales and the specific activity of the radiolabelled ligands.

2.5.2 Methodological Considerations

In human postmortem tissue, application of the ligand binding technique suffers certain problems. Predisposing factors such as age of patient, drug treatment history and postmortem delay in processing tissue may increase interindividual variability. This problem was minimised as far as possible in each ligand binding study by closely matching control and AD groups for age and postmortem delay.

Quantitative autoradiography employs ligands labelled with tritium. The low energy of the tritium β-emission is differentially quenched in brain regions exhibiting relative differences in the concentration of grey to white

matter. Moreover, in diseased tissue such as AD, the grey to white ratios may be affected in comparison to control brain. Efforts to correct for this quenching problem include the use of iodinated ligands whose high energy γ emissions are not significantly altered by the tissue. However, the ligands used in this thesis are relatively new and are as yet, unavailable in an iodinated form.

2.6 [^{3}H]-Phorbol 12,13 Dibutyrate Binding to Particulate and Cytosolic Homogenates

2.6.1 Separation of Particulate and Cytosolic Fractions

Procedures for the separation of the particulate and cytosolic fractions were carried out as previously described by Saitoh et al. 1986. Brain tissue retained from the ChAT studies was homogenised in 10 volumes of buffer (0.32M sucrose, 5mM HEPES, (pH 8.0), 5mM benzamidine, 2mM dithiothreitol, 3mM EGTA, 0.5mM $MgSO_4$, 0.5mM $ZnSO_4$, 0.1mM phenylmethyl- sulfonylfluoride, 0.1mg/ml leupeptin, 0.05 mg/ml pepstatin, 0.1mg/ml aprotonin) by two 5s strokes of a Polytron homogeniser. The homogenate was centrifuged for eight minutes at 10,000g (4°C) to precipitate nuclei and the cytoskeleton. The resultant supernatant was centrifuged for one hour at 100,000g (4°C) to separate the particulate from the cytosolic fraction. The pellet was reconstituted to its original volume with buffer.

2.6.2 [^{3}H]-Phorbol 12,13 Dibutyrate Binding Assay

[^{3}H]-PDBu binding was measured in a reaction mixture containing approximately 20µg protein in 1ml of the buffer 50mM Tris-HCl (pH 7.5) containing 10mM Mg-acetate, 1.4mM $CaCl_2$, 0.4mM EGTA, 50mM KCl, 4mg/ml bovine serum albumin, 100µg/ml phosphatidylserine and 2.5nM [^{3}H]-PDBu. Non-specific binding was defined in the presence of 2µM unlabelled PDBu. The assay was incubated for two hours at 4°C and stopped by filtration using a Brandell cell harvester to GF/B Whatman filter discs. The filter discs were washed five times with 5ml of the filtering solution 20mM Tris-HCl (pH 7.5) containing 10mM Mg acetate and 1mM $CaCl_2$, then placed in 10ml of scintillant and the radioactivity counted by liquid scintillation analysis (see Methods section 3.4.3). [^{3}H]-PDBu binding (pmol/mg protein) was calculated from the specific activity of the ligand and amount of protein in the sample.

2.6.3 Protein Determination

2.6.3.1 Practice

An aliquot of the tissue used in the homogenate binding of [^{3}H]-PDBu was retained for determination of the protein content. On ice, 200µl of the homogenate sample was made up to a volume of 950µl with distilled H_20 to this, 50µl of trichloroacetic acid (100%) was added, vortexed immediately and left for 15 min to allow precipitation of the proteins. The proteins were then pelleted by spinning in a Beckmann microfuge for 30s. The supernatant was discarded and the protein pellet suspended in 200µl 0.1M NaOH. The protein was determined using the method of Lowry (1951).

2.6.3.2 Methodological Considerations

Protein determination using the method of Lowry (1951) is unreliable in the presence of some compounds. The buffer in which brain tissue was homogenised and then separated to particulate and cytosolic fractions (see Methods section 2.6.1) contains several of these compounds.

This problem was highlighted in one study in which a standard amount of protein (10μg) was assayed for protein content in the presence of increasing concentrations of homogenisation buffer. Optical density measurement, (an index of protein concentration) of each sample, was found to increase linearly with increasing buffer concentration (Figure 11A). Additionally, the protein samples suspended in either H_20 or buffer gave completely different optical density values (Figure 11B). Even in the absence of protein, the buffer was separated from the protein sample by trichloracetic acid precipitation (see Methods section 2.6.3.1). The precipitated proteins could then be resuspended in H_20 and protein determined by the method of Lowry (1951).

2.7 Statistical Analysis

Ligand binding data and ChAT data from control and AD brain were compared using an unpaired, two-tailed Student's t-test. Correlations between ligand binding with ChAT activity or plaque numbers were carried out by linear regression analysis.

FIGURE 11
EFFECT OF BUFFER ON PROTEIN MEASUREMENT

A. Samples containing a constant amount of bovine serum albumin (10μg) in the presence of increasing concentrations of homogenisation buffer (as detailed in Methods section 2.6.1) were assayed for protein content using the method of Lowry (1951). Optical density (OD) measurements as shown on the graph are directly related to the concentration of protein. Samples were assayed in triplicate. Note the linear increase in OD values with increasing buffer concentration despite a constant concentration of protein.

B. Increasing concentrations, which had been predetermined, of bovine serum albumin were suspended in either distilled H_20 or homogenisation buffer (100%) and OD values, as an index of protein content, determined. A linear relationship is shown between protein content and OD measurement when the assay medium was H_20. In the absence of bovine serum albumin, the homogenisation buffer alone gave a high OD reading. The OD measurements for increasing concentrations of bovine serum albumin in the presence of homogenisation buffer are inconsistent.

FIGURE 11

A

EFFECT OF INCREASING BUFFER CONCENTRATION ON OPTICAL DENSITY MEASUREMENT OF PROTEIN SAMPLE.

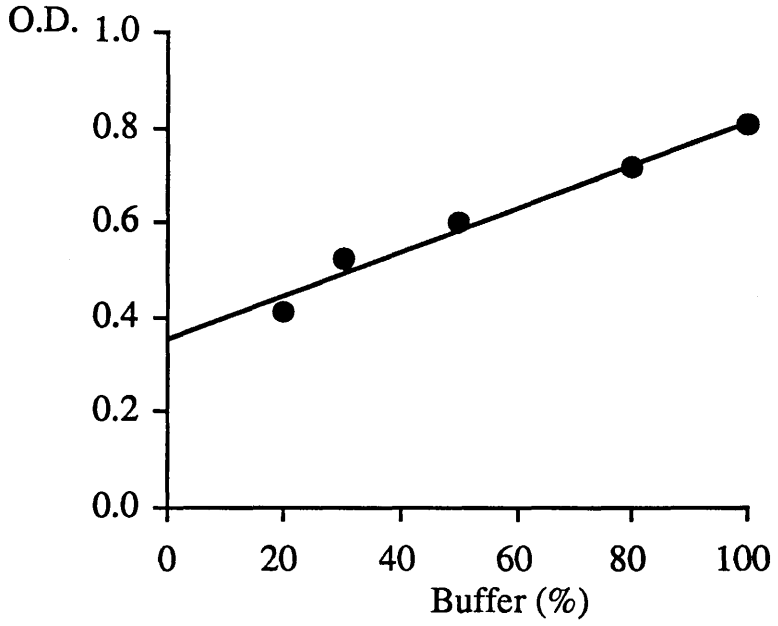

B

EFFECT OF INCREASING PROTEIN CONCENTRATION ON OPTICAL DENSITY MEASUREMENT

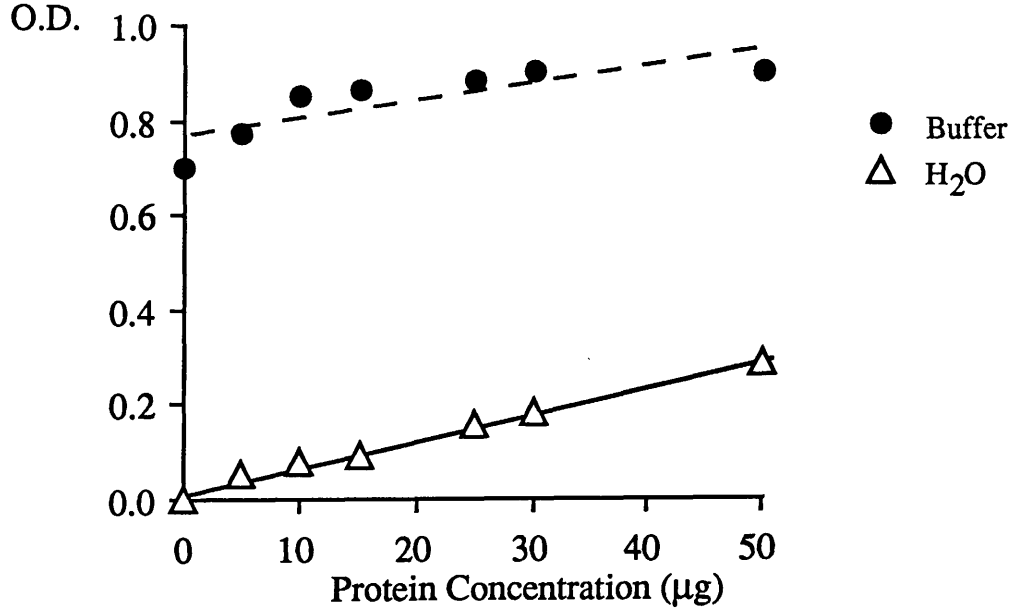

3. ANIMAL STUDIES

3.1 General

Animal studies utilised two experimental techniques, namely in vitro ligand binding autoradiography and [^{14}C]-2-deoxyglucose autoradiography. Animal surgery employed in these studies and experimental procedures are described in this section.

3.2 Animals

All studies of the rat visual system employed adult, male black-hooded PVG rats (250-400g). In the studies of the septo-hippocampal pathway, adult, male Sprague Dawley rats (250-400g) were used. Rats were supplied by Harlan Olac and on delivery were allowed to acclimatise for five days and nights before any surgical intervention was performed. In holding, rats were exposed to a natural day/night cycle at room temperature maintained at approximately 21°C. Food and water were freely available until the day of the experimental procedure.

3.3 Surgical Preparation of Animals

3.3.1 Unilateral Orbital Enucleation

Prior to surgery, animals were placed in a perspex box chamber into which 70% nitrous oxide and 30% 0_2 containing 5% halothane was flowing. During surgery, anaesthesia of the rat was maintained using a 1% halothane mixture administered through a face mask. The surgical procedure involved retraction of the eyelid muscles to expose the right eyeball. The underlying retractor occuli muscle, blood vessels and optic nerve were

clamped and the eyeball was then removed. Haemorrhage from the severed artery and vein was prevented by sealing the vessels with a bipolar coagulator. Antibiotic powder was applied to the wound and anaesthetic was withdrawn. The procedure did not last more than five minutes.

3.3.2 Stereotaxic Lesion of the Rat Visual Cortex

Anaesthesia was induced as outlined in Methods section 3.3.1. Long-term maintenance of anaesthesia (approximately one hour) was achieved by injection of Hypnovel/Hypnorm (3.3mg/kg, i.p.). Following injection, the rat was not handled for a further 15 minutes. The rat was then fixed on a David Kopf stereotaxic frame, a midline incision in the scalp was made and the membranes reflected to expose Bregma. A small burrhole in the skull was drilled and the right hemisphere at the level of the visual cortex injected through a stainless steel needle (30 gauge) attached to a Hamilton Syringe. The stereotaxic co-ordinates (-7.8mm anterior from Bregma; -3.0mm lateral to the right and -1.0mm below dura) were taken from the stereotaxic atlas, Paxinos and Watson (1985). Ibotenic acid (10mg/ml) was dissolved in phosphate-buffered saline (pH 7.4) and 1µl injected at a rate of 0.2µl/min. Following completion of the injection, the needle was left in place for five minutes to allow diffusion of the toxin and was then slowly withdrawn. Sham-operated animals were injected with an equal volume of saline. The wound was stitched using silk sutures and antibiotic powder applied. Glucose/saline (5ml) was administered subcutaneously to compensate for the loss of body fluids while the animal was recovering from the effects of anaesthesia. Following surgery, the animals survived for 21

days, at which time, autoradiographic measurements were recorded (see appropriate Methods sections 3.3.4 and 3.4.1).

3.3.3 Stereotaxic Lesion of the Medial Septum

Induction of anaesthesia was as outlined in Methods section 3.3.1. Anaesthesia was maintained by injection i.p. of chloral hydrate (400mg/kg) and diazepam (2mgkg). The procedure was similar to that described in Section 3.3.2 except the buffered ibotenic acid was delivered into the medial septum at stereotaxic co-ordinates 0.8mm anterior to Bregma, at the midline, and lowered 5.8mm below the surface of the dura. These co-ordinates have been previously defined (Wenk et al. 1984). A total volume of 0.6µl ibotenic acid was injected into the medial septum at a speed of 0.1µl min. Sham-operated rats were treated with a procedure identical to that outlined above, with the exception that phosphate-buffered saline only was injected into the medial septum. Following surgery, the animal survived for 21 days, at which time, the animal was sacrificed, the brain removed and processed for in vitro ligand binding autoradiography (see Methods section 1.1.2).

Following stereotaxic lesion of the visual cortex or medial septum, the rats were allowed to survive for 21 days at which time autoradiographic procedures were measured. This time-point was chosen for two main reasons; (1) surgical intervention by stereotaxic lesion of rats disrupts normal feeding and behavioral activity, the [^{14}C]-2-deoxyglucose technique requires that the glucose level in animals falls within certain limits, 21 days

allowed adequate recovery of the animals after surgery; (2) ligand binding to neurotransmitter receptors (Chalmers and McCulloch, 1990) and second messenger systems were found to be altered at 20 days following unilateral orbital enucleation.

3.3.4 Preparation of Animals for [^{14}C]-2-Deoxyglucose Measurement

Anaesthesia was induced and maintained as explained in Section 3.3.1. Small incisions were made on each side of the animal's groin and using blunt dissection, the connective tissue and fatty tissue was cleared to expose the femoral artery and vein. Polyethylene catheters (Portex: external diameter 0.96mm, internal diameter 0.58mm, 10cm long) containing heparinised saline (10 I.U./ml) were inserted a distance of 2cm into each artery and vein, tied off firmly using silk thread and the wound sutured closed. Anaesthetic gel was applied to the incision sites, covered in gauze pads and held in place by tape. The rat was enveloped in a surgical stocking and in a plaster of Paris bandage (Gypsona: 7.5cm wide) wrapped around the lower abdomen, pelvis and hindquarters. The plaster cast and the hindlimbs of the animal were taped on to a lead support brick which ensure the animal was completed immobilised. Core temperature was measured by a rectal probe and the arterial blood pressure was monitored by connecting the femoral artery to a pressure transducer (P23 ID Gould Stratham, Model 2202). The animals were then allowed to recover from the anaesthesia for at least two hours before the initiation of the experimental procedure by tracer administration.

3.4 Experimental Analysis

3.4.1 Preparation of Autoradiograms

3.4.1.1 [^{14}C]-2-Deoxyglucose Autoradiograms

At the end of the 45 minute sampling period, the animal was sacrificed by decapitation and the brain rapidly removed. A longitudinal midline incision was made at the level of the snout and extended caudally to the level of the forelimb. Skin and extracranial muscle were reflected to expose the skull. The dorsal cranium was removed and the dura reflected to facilitate excision of the intact brain. All adhering bone fragments and hair were removed and the brain frozen by slow immersion in isopentane which was precooled to -42°C. The time taken from sacrifice of the animal to freezing of the brain did not exceed five minutes. The brain was then fixed to a swivel-headed microtome chuck with plastic embedding medium (Lipshaw), over a bed of solid CO_2 and stored at -20°C for not more than two days. From each brain, 20μm thick coronal sections were cut from the level of the inferior colliculus to the level of the caudate putamen. One section in eight was picked onto a thin glass coverslip and dried immediately on a hotplate (70°C). Of the remaning seven sections, six of these were thaw-mounted onto gelatin-coated subbed slides and allowed to dry at room temperature for one hour in preparation for ligand binding. The last section was picked onto a glass slide for histological staining using cresyl violet. The glass coverslips were glued onto cards and placed, together with a set of precalibrated ^{14}C-labelled epoxy resin standards (18-1880μCi/g tissue equivalents) in light-tight cassettes. Autoradiograms were obtained by exposing x-ray film (Kodak-GRL-A) to the

brain sections and standards to 18 days. Films were then processed in a Kodak automatic presser.

3.4.1.2 Ligand Binding Autoradiograms

Tissue sections labelled with a specific radioligand were mounted securely on card along with a set of precalibrated tritium standards (1060 - 17720nCi/mg tissue equivalents). The brain sections and standards were apposed to tritium-sensitive film (Hyperfilm B_{MAX}, Amersham) in a light-tight cassette for one week and four weeks to generate PDBu and forskolin autoradiograms respectively. Films were manually developed in Kodak D-19 developer for five minutes at 17°C and the development stopped with a 30 second rinse in deionised water at 20°C. Films were fixed for 10 minutes at 20°C (Kodak, Kodafix), washed for 40 minutes in running filter water, rinsed in deionised water and suspended in a drying cabinet overnight.

3.4.2 **Quantitative Densitometric Analysis of Autoradiograms**

Analysis of resultant [^{14}C]-2-deoxyglucose or ligand binding autoradiograms was performed using a computer-assisted image analysis system (Quantimet 970, Cambridge Instruments).

Optical density measurements of autoradiograms were made under a constant light produced by four lamps (24W), the intensity of the light being computer controlled. The autoradiographic image was captured by a video-camera fitted with a zoom lens (2.5x) and digitised into an array of image

points (pixels) each with a grey level value in the range 1-255 (grey level = 255 corresponds to optical density =0; grey level = 1 corresponds to optical density 2.41). The image analyser was calibrated which allowed grey level values of each pixel to be converted into optical density values.

Following calibration, the optical densities of the precalibrated standards (^{3}H or ^{14}C) were measured, generating a calibration curve of optical density against isotope concentration and allowing quantification of isotope concentration in discrete brain regions. Optical density measurements were made by placing a measuring frame (9-900 pixels/frame) over the anatomical region of interest. The size of the frame was kept constant for each region between animals or humans. Optical density measurements in rat studies were made separately in the ipsilateral and contralateral hemisphere over two to six sections. Structures in rat brain were defined anatomically with reference to a stereotaxic atlas (Paxinos and Watson, 1986).

3.4.3 Liquid Scintillation Analysis

Liquid scintillation analysis was a necessary component of [^{14}C]-deoxyglucose and [^{3}H] ligand binding autoradiography.

The plasma history of [^{14}C]-2-deoxyglucose was determined by liquid scintillation. Aliquots from each plasma sample were pipetted into 1ml of distilled water in glass scintillation vials and residual radioactivity expelled by repeated flushing of the pipette with water. Prior to ligand binding

experiments, the concentration of the radioligand in the incubation medium was determined. Samples (10µl) were aliquotted into 1ml of distilled water in triplicate. To each vial 10ml of a proprietary scintillant (Ecoscint A, National Diagnostics) was added. In experiments where tissue sections were wiped from glass slides using filter discs, or the tissue was collected on filter discs, these were placed directly into 10ml scintillant. Each vial was counted for four minutes in a refrigerated scintillation counter. Counts per minute were converted to disintegrations per minute using the external channels ratio method (Peng, 1977) and a standard quench correction calibration curve.

3.4.4 Statistical Analysis

Rat Visual System Studies. The statistical design employed in analysis of ligand binding and glucose use following unilateral orbital enucleation and unilateral visual cortex lesion was similar. Asymmetries in ligand binding and glucose utilisation were determined using a Student's two-tailed paired t-test. The stability of ligand binding and glucose utilisation in brain regions of the control (intact) hemisphere was assessed using the analysis of variance (Scheffé, 1959) and the multiple comparisons method of Dunnett (1964). Statistical significance was taken to be $p<0.01$ to correct for the number of comparisons made in each group.

Septo-Hippocampal Studies. Ligand binding in the sham-operated rats and lesioned rats were taken as mean values of the left and right hemisphere. Data from the sham group was compared to the lesioned

group using a Student's two-tailed unpaired t-test. Statistical significance was taken to be $p<0.05$.

MATERIALS

[^{3}H]-Forskolin (38-40Ci/mmol) was obtained from Amersham and [^{3}H]-phorbol 12,13 dibutyrate (18-19.1Ci/mmol) from New England Nuclear. Forskolin; deacetylforskolin; phorbol 12,13 dibutyrate; phorbol 12, myristate 13, acetate; 4α phorbol 12,13 didecanoate; phorbol 12,13 diacetate; bovine serum albumin; phosphatidylserine; benzamidine; leupeptin; pepstatin; aprotonin and ibotenic acid were all obtained from Sigma Chemical Company. Dithiothreitol was obtained from BDH, 6β-[β-(piperidio) propionyl forskolin and 7β-deacetyl-7β-[γ-(morpholino) butyryl]-forskolin were obtained from Research Biochemicals Incorporated. All other reagents were of analytical grade.

CHAPTER III

RESULTS

1. QUANTITATIVE AUTORADIOGRAPHY OF [^{3}H]-FORSKOLIN BINDING IN POSTMORTEM HUMAN BRAIN

1.1 Scatchard Analysis of [^{3}H]-Forskolin Binding

Saturation experiments performed in frontal cortex sections of three controls (outwith subsequent studies) revealed that [^{3}H]-forskolin binding was of high affinity and saturable over the concentration range 2 - 100nM (Figure 12). Non-specific binding, defined in the presence of 20μM unlabelled forskolin, was linear with respect to the concentration of [^{3}H]-forskolin and, at 20nM [^{3}H]-forskolin, the specific binding was approximately 80%. The average dissociation constant (K_D) was approximately 33nM and the maximum number of binding sites in frontal cortex was 200fmol/section.

1.2 Displacement of [^{3}H]-Forskolin Binding

The pharmacological profile for inhibition of [^{3}H]-forskolin binding by forskolin analogues was examined in frontal cortex sections of two control and two AD patients (the patients were not included in subsequent studies). The ability of forskolin analogues to inhibit [^{3}H]-forskolin binding were found to be in the rank order of potency: 6β-[β-(piperidio) propionyl] forskolin >forskolin>7β-deacetyl-7β-[γ-morpholino)butyryl] forskolin >> deacetylforskolin (Table 4). The ability of forskolin analogues to inhibit [^{3}H]-forskolin binding was similar in control and AD tissue sections. The order of potency of forskolin analogues to inhibit [^{3}H]-forskolin binding in human brain correlates well with the ability of these analogues to stimulate adenylate cyclase and increase cAMP levels in cell lines, and to inhibit [^{3}H]-forskolin binding in rat brain membranes

FIGURE 12
SCATCHARD ANALYSIS OF [^{3}H]-FORSKOLIN BINDING IN HUMAN BRAIN

A. [^{3}H]-Forskolin binding in frontal cortex sections of 3 control subjects. Sections were incubated with increasing concentrations of [^{3}H]-forskolin (2-100nM) at 22°C for 20 minutes and the radioactivity counted by liquid scintillation. Non-specific binding (Δ) was defined in the presence of 20μM unlabelled forskolin. Specific binding (●) was determined from the subtraction of non-specific (Δ) from total (O) binding. Data points represent mean ± SEM.

B. Scatchard analysis of saturation data of [^{3}H]-forskolin binding in frontal cortex. Data points represent the mean ± SEM (n = 3). B_{MAX} and K_D values were determined using linear regression analysis.

FIGURE 12

SCATCHARD ANALYSIS OF ^{3}H-FORSKOLIN BINDING IN HUMAN BRAIN

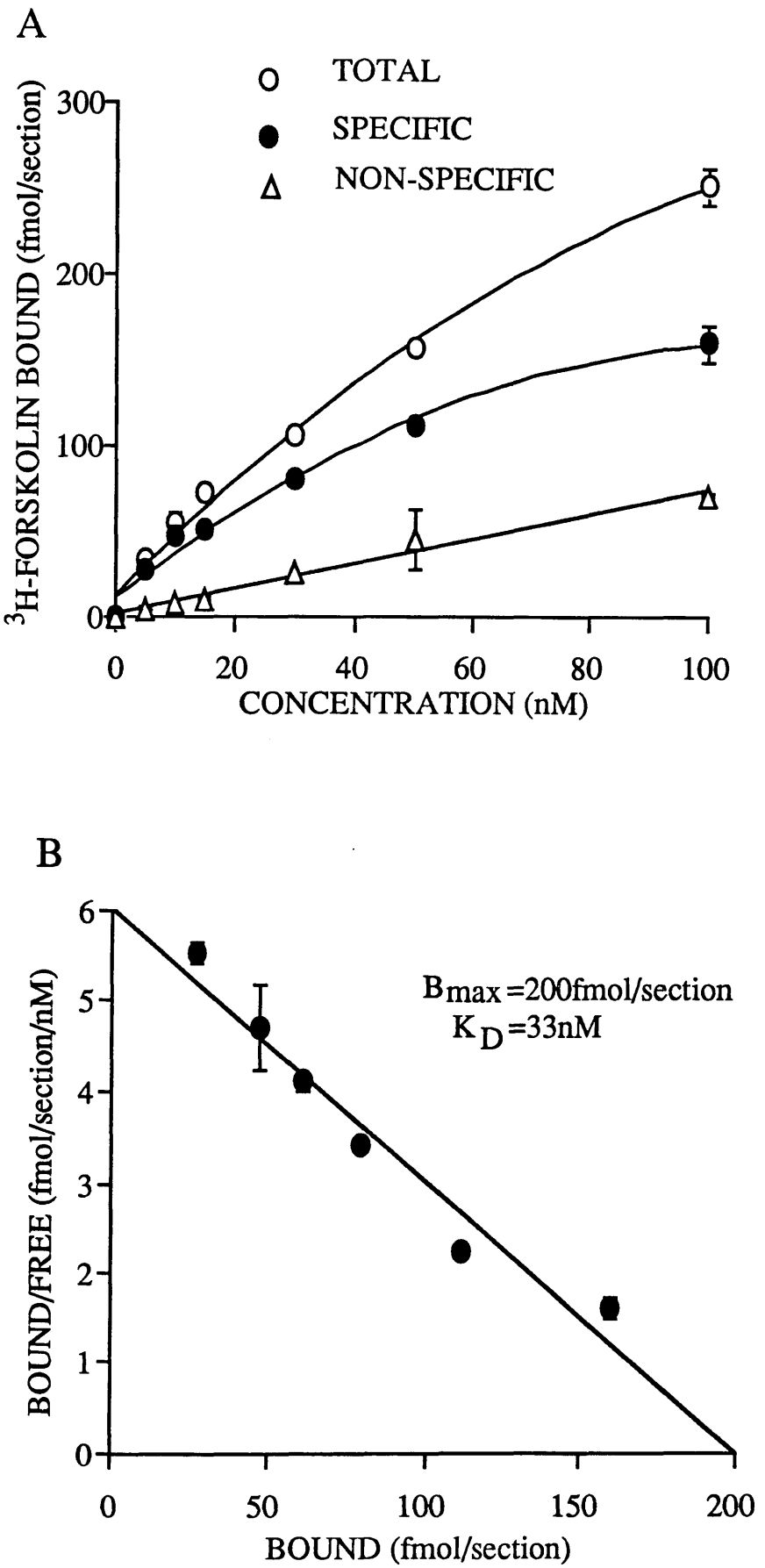

TABLE 4

INHIBITION OF [^{3}H]-FORSKOLIN BINDING IN HUMAN CORTEX

ANALOGUE CONCENTRATION (M)	% INHIBITION							
	ANALOGUE A		ANALOGUE B		ANALOGUE C		ANALOGUE D	
	CONTROL	AD	CONTROL	AD	CONTROL	AD	CONTROL	AD
10^{-10}	0	0	0	0	0	0	4	3
10^{-9}	0.9	12	0	6	16	15	24	32
10^{-8}	22	22	0	11	41	38	27	32
10^{-7}	74	72	27	17	76	78	46	59
10^{-6}	83	96	57	66	81	82	76	93
10^{-5}	91	99	72	84	88	89	81	87

Human frontal cortex sections of two control and two Alzheimer (AD) cases were labelled with 20nM [^{3}H]-forskolin. In adjacent sections, inhibition of [^{3}H]-forskolin binding was examined in the presence of increasing concentrations of unlabelled forskolin analogues ; A - forskolin, B - deacetylforskolin, C - 6β-[β-(piperidio)propionyl]forskolin, D - 7β-deacetyl-7β-[γ-(morpholino) butyryl]-forskolin. Sections were wiped from the glass slides using microfilters and the radioactivity bound counted by liquid scintillation. Inhibition of [^{3}H]-forskolin binding by each analogue was expressed as a percentage of the total [^{3}H]-forskolin binding.

(Laurenza et al. 1987). These data would indicate that [^{3}H]-forskolin binds to a pharmacological site involved in the activation of adenylate cyclase.

1.3 Anatomical Localisation of [^{3}H]-Forskolin Binding in Control Brain

[^{3}H]-Forskolin exhibited a heterogeneous pattern of binding in frontal and temporal cortex and in the hippocampal formation (see Figure 13 and also Figures 14, 15, and 16). The levels of [^{3}H]-forskolin binding were higher in middle frontal gyrus as compared to temporal gyrus. Within both cortical regions [^{3}H]-forskolin binding exhibited an obvious laminar distribution. Highest levels of binding were observed in layers I-III and layers V-VI with markedly less binding in layer IV. Within the hippocampal formation, the selective pattern of binding was striking. [^{3}H]-Forskolin binding was most prominent in the parahippocampal gyrus, CA4 field and molecular layer of the dentate gyrus whilst other hippocampal regions showed a lower degree of [^{3}H]-forskolin binding.

1.4 Quantitative Autoradiography of [^{3}H]-Forskolin Binding in Control and AD Brain

Quantitative analysis of [^{3}H]-forskolin binding was determined in six control and seven AD subjects (Table 2) in middle frontal and temporal cortex and the hippocampal formation.

[^{3}H]-Forskolin binding was markedly and significantly reduced in all layers of middle frontal cortex in AD brain compared to controls (Figures 13 and 14). The magnitude of the deficit was approximately 50% and was

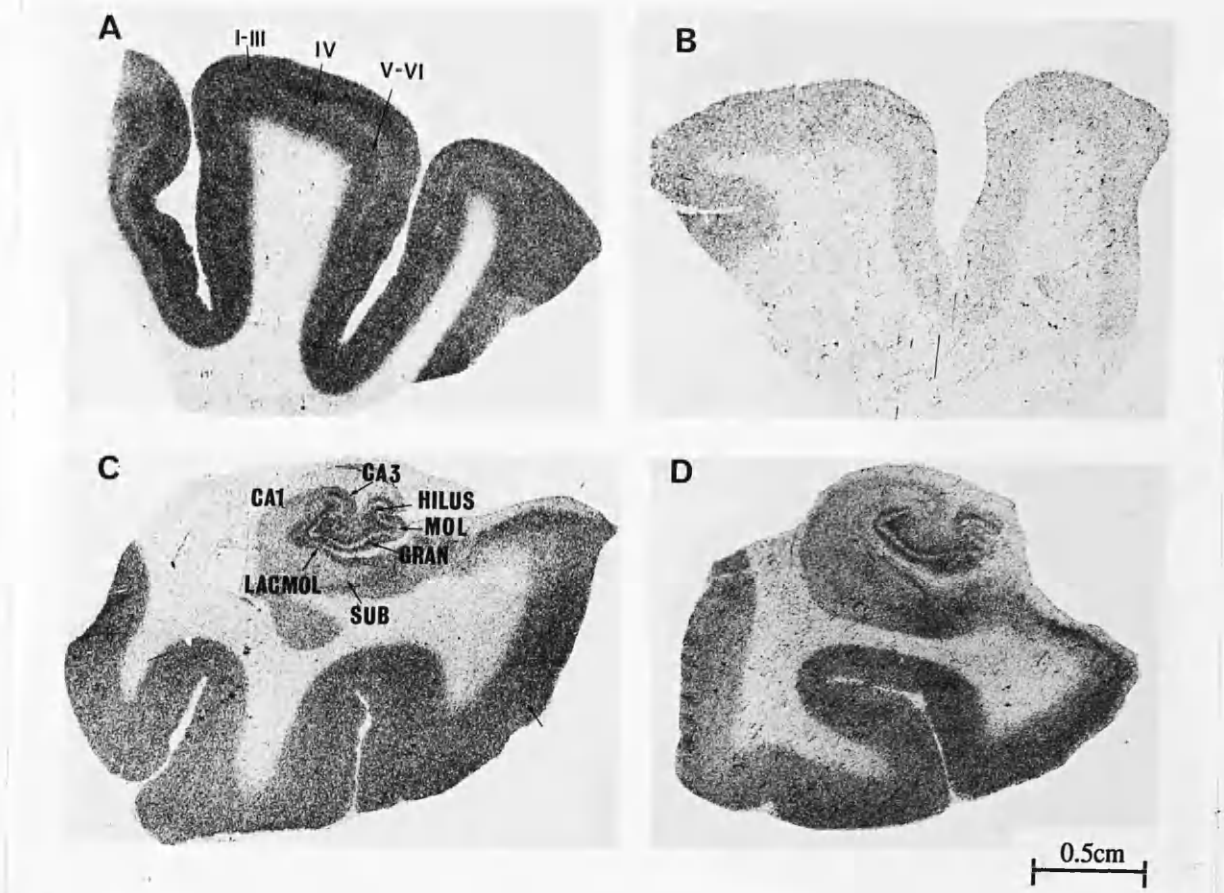

FIGURE 13
AUTORADIOGRAMS OF [^{3}H]-FORSKOLIN BINDING IN CONTROL AND AD BRAIN

Autoradiograms generated by incubating sections of human brain with 20nM [^{3}H]-forskolin. A and B are middle frontal cortex sections of a control subject (A) and an AD subject (B). Within the cortex [^{3}H]-forskolin binding sites are localised in three distinct bands corresponding to layers I-III, IV and V-VI which were determined by reference to adjacent sections stained with cresyl violet. Note the marked loss of [^{3}H]-forskolin binding throughout middle frontal cortex in the AD case. C and D and sections of the hippocampal region from a control (C) and an AD case (D). Autoradiographic measurements were made in the following regions: superficial (super) and deep layers of the parahippocampal gyrus (PHG); subiculum (SUB); stratum lacunosum moleculare (LACMOL); CA1, CA3 and CA4 fields of Ammon's Horn; in the dentate gyrus: hilus (HIL), molecular (MOL) and granular (GRAN) layers, with reference to cresyl violet-stained sections.

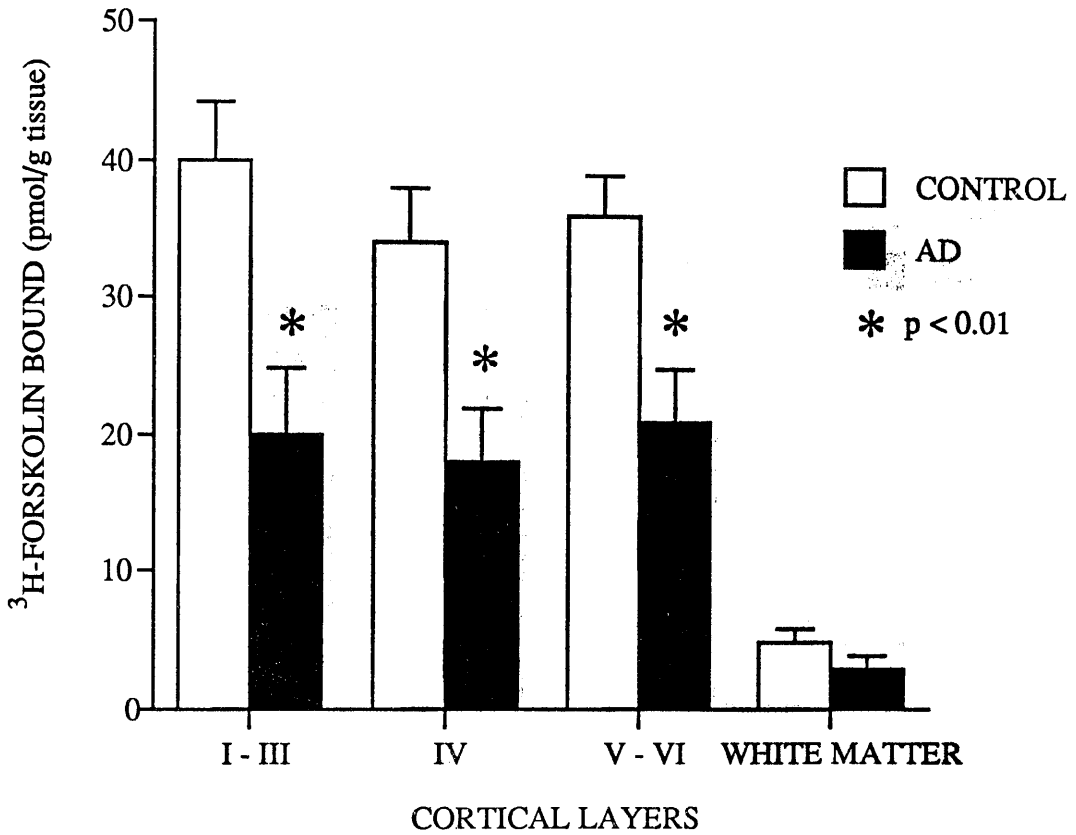

FIGURE 14
[^{3}H]-FORSKOLIN BINDING IN CONTROL AND AD MIDDLE FRONTAL CORTEX

Quantitative autoradiographic measurements of [^{3}H]-forskolin binding in middle frontal cortex. Cortical layers correspond to those in Figure 13A. Histograms are presented as mean ± SEM for control (n = 6) and AD (n = 5) subjects. Note the profound reduction in [^{3}H]-forskolin binding throughout the frontal cortex in AD. *p<0.01, Students unpaired t-test.

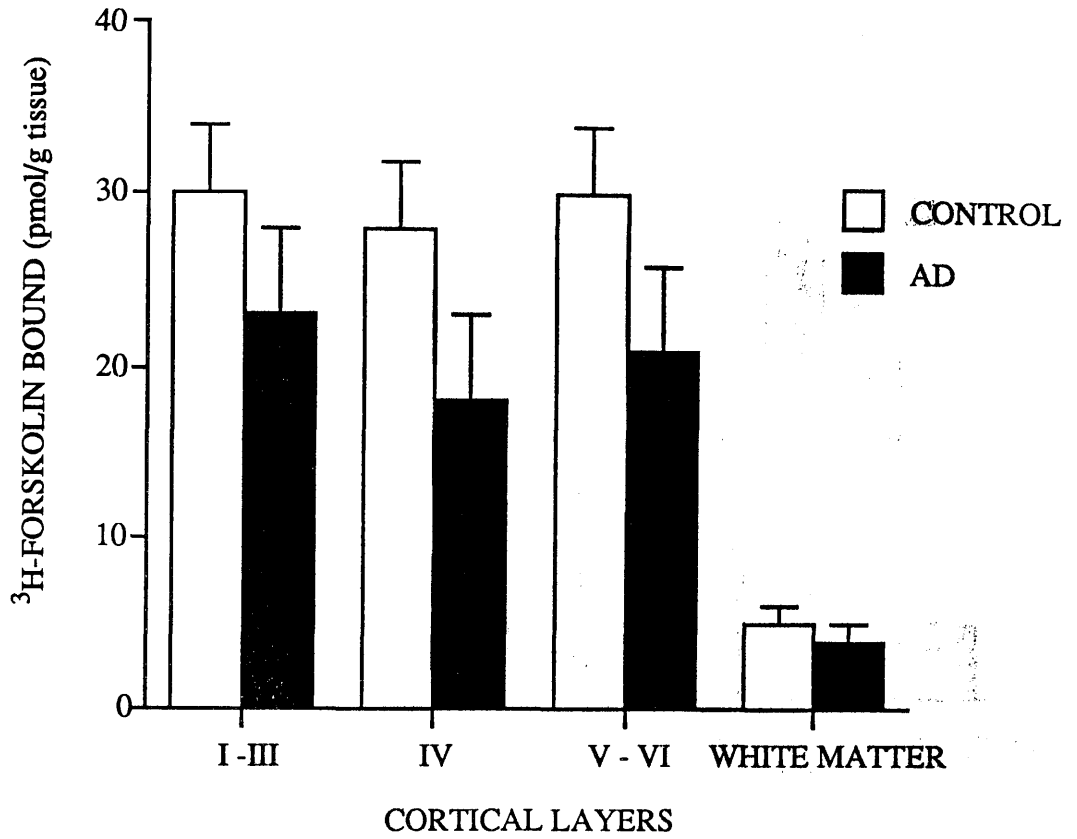

FIGURE 15
[^{3}H]-FORSKOLIN IN CONTROL AND AD MIDDLE TEMPORAL CORTEX

Quantitative autoradiographic measurement of [^{3}H]-forskolin binding in middle temporal cortex. The distribution of [^{3}H]-forskolin binding throughout the cortical layers was similar to that observed in middle frontal cortex (Figure 13). Histograms are presented as mean ± SEM for control (n = 6) and AD (n = 7) subjects. The apparent reduction in mean [^{3}H]-forskolin binding in the AD group was dominated by data from two AD cases (4AD and 7AD) while other AD cases had levels of binding similar to controls.

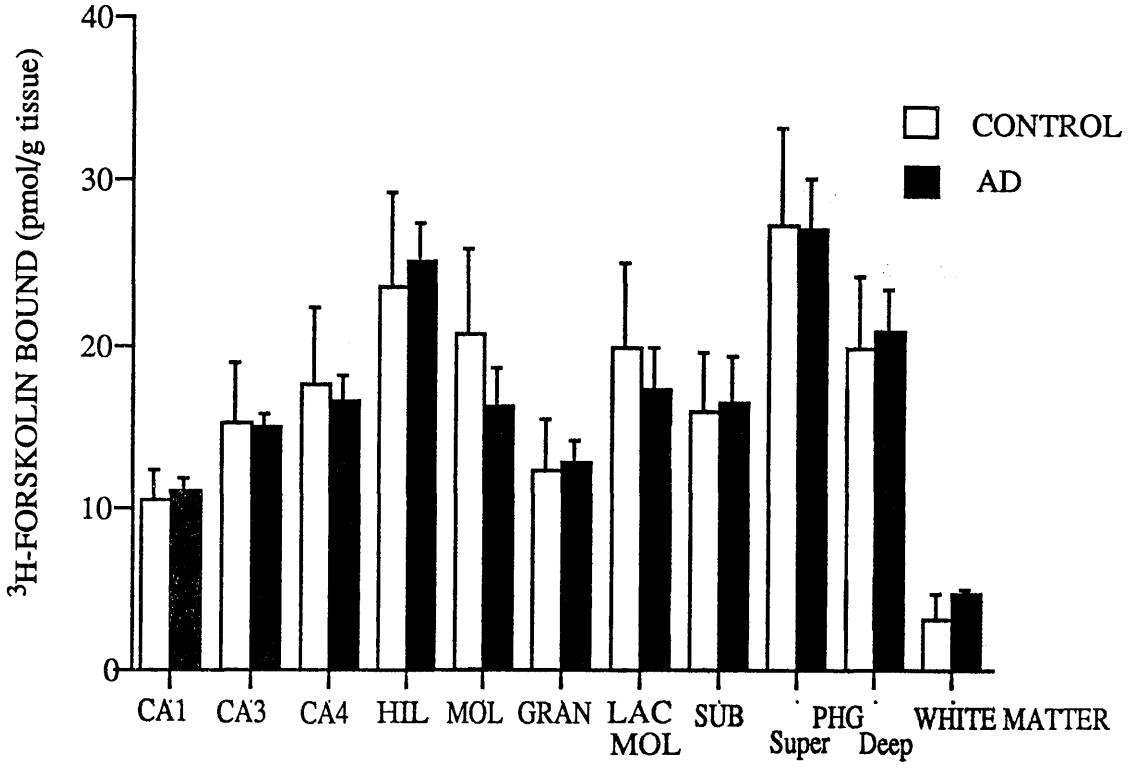

FIGURE 16
[^{3}H]-FORSKOLIN BINDING IN CONTROL AND AD HIPPOCAMPAL REGION

Quantitative autoradiographic measurement of [^{3}H]-forskolin binding in the hippocampal region. The areas examined are: CA1, CA3, CA4 fields of Ammon's Horn; hilus (HIL), molecular (MOL) and granular layer of the dentate gyrus; stratum lacunosum moleculare (LACMOL); subiculum (SUB); Superficial (super) and deep layers of the parahippocampal gyrus (PHG) and white matter (see Figure 13). Histograms are presented as mean ± SEM for control (n = 6) and AD (n = 6) subjects. There is no significant different between the control and AD group in each hippocampal region examined (Student's unpaired t-test).

consistent throughout the cortex.

A reduction in [^{3}H]-forskolin binding was observed in all layers of middle temporal gyrus in the AD group (Figure 15). This reduction did not achieve statistical significance. Analysis of individual data in the patient group revealed that two of the cases (4 AD and 7 AD) dominated the mean values for the AD group. The two cases exhibited extremely low levels of binding compared to the other five AD subjects which had levels of binding similar to mean control values.

[^{3}H]-Forskolin binding was not significantly different between the control and AD group in each of the anatomically-discrete regions of the hippocampal formation examined (Figures 16 and 13).

1.5 [^{3}H]-Forskolin Binding and ChAT Activity

Choline acetyltransferase (ChAT) activity was significantly reduced in both neocortex and the hippocampus in AD brain compared to controls (Table 5). The magnitude of this deficit was at least 40% of control values in all three brain regions examined.

Using least squares linear regression analysis in middle frontal cortex where [^{3}H]-forskolin binding was markedly reduced in AD brain, a positive correlation between [^{3}H]-forskolin binding and ChAT activity was observed when data from control and AD brains were combined (Figure 17). The correlation between binding and ChAT was consistent throughout the layers

TABLE 5

CHOLINE ACETYLTRANSFERASE ACTIVITY AND PLAQUE COUNTS
(SERIES 1)

Brain Area	CHOLINE ACETYLTRANSFERASE ACTIVITY Control	AD	PLAQUES IN AD BRAINS Layers I-III	Layers IV-VI
Middle Frontal Gyrus	16.8±2.0	9.1±1.8**	34±7	19±4
Middle Temporal Gyrus	7.7±1.2	2.5±0.9***	29±6	15±5
Hippocampus	13.3±2.3	6.1±1.7*	Subiculum:	8±3

For Choline acetyltransferase activity, values are mean ± SEM, nmol/mg protein/hr in grey matter dissected from brain areas in which [^{3}H]-forskolin autoradiography was carried out. **$p<0.01$, ***$p<0.001$.

For plaques, values are mean ± SEM, plaques/mm^2 in sections no more than 0.5cm caudal to sections used for [^{3}H]-forskolin autoradiography. Control brains had less than two plaques/mm^2 in each area.

of frontal cortex, layer I-III ($r = 0.662$, $p<0.05$), layer IV ($r = 0.809$, $p<0.05$), layer V-VI ($r = 0.717$, $p<0.05$).

There was no direct correlation between [^{3}H]-forskolin binding and ChAT activity in each cortical layer of middle temporal cortex ($r = 0.126 - 0.274$, $p>0.05$) (Figure 17). Those AD subjects which had reduced [^{3}H]-forskolin binding did not have levels of ChAT which were substantially different from the rest of the patient group (ChAT activity nmol/mg protein/hr : 4AD = 1.6, 7AD = 2.14, AD group = 25 0.9). In the hippocampal region, there was no significant correlation between [^{3}H]-forskolin binding and ChAT activity in each of the regions examined ($r = 0.42 - 0.6$ $p>0.05$).

1.6 [^{3}H]-Forskolin Binding and Local Neuropathology

Control brains had minimal numbers of plaques, less than two plaques per mm^2 in all brain regions examined while AD brains contained numerous plaques in cortical regions and the hippocampus (Table 5).

There was no direct correlation between [^{3}H]-forskolin binding and the number of plaques in AD brain in superficial and deep layers of middle frontal cortex ($r = 0.308$; $r = 0.095$, $p>0.05$) and middle temporal cortex ($r = 0.158$; $r = 0.56$, $p>0.05$). Similarly in the subiculum of the hippocampus there was no significant correlation between plaque numbers and [^{3}H]-forskolin binding ($r = 0.482$, $p>0.05$).

FIGURE 17
CORRELATION OF [^{3}H]-FORSKOLIN BINDING WITH ChAT ACTIVITY

Relationship between cholineacetyltransferase (ChAT) activity and [^{3}H]-forskolin binding in frontal (A) and temporal (B) cortex. Open circles represent control data and closed circles represent AD data. In middle frontal cortex (layer I-III) a significant correlation between ChAT activity and [^{3}H]-forskolin binding is shown ($r = 0.662$, $p<0.05$), the best fitting line generated by linear regression. There was also a significant correlation between ChAT activity and [^{3}H]-forskolin binding in layer IV ($r = 0.809$, $p<0.05$) and layers V-VI ($r = 0.712$, $p<0.05$). In middle temporal cortex there was no association between ChAT activity and [^{3}H]-forskolin binding.

FIGURE 17 CORRELATION OF ^{3}H-FORSKOLIN BINDING WITH CHAT ACTIVITY

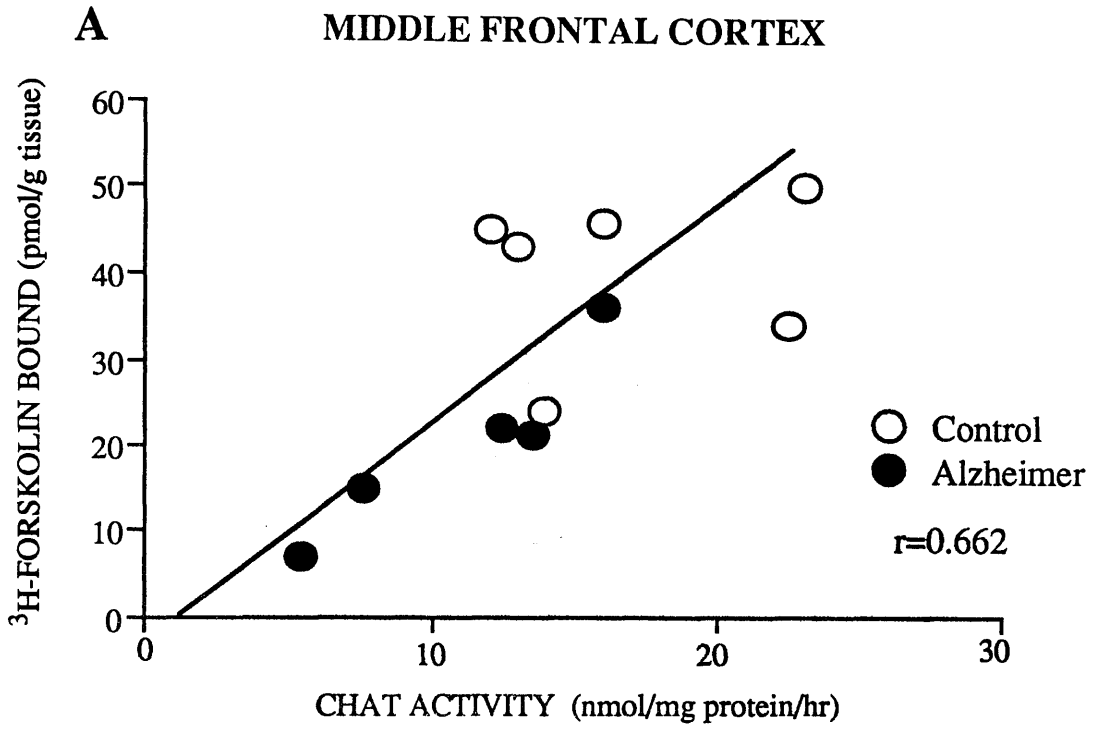

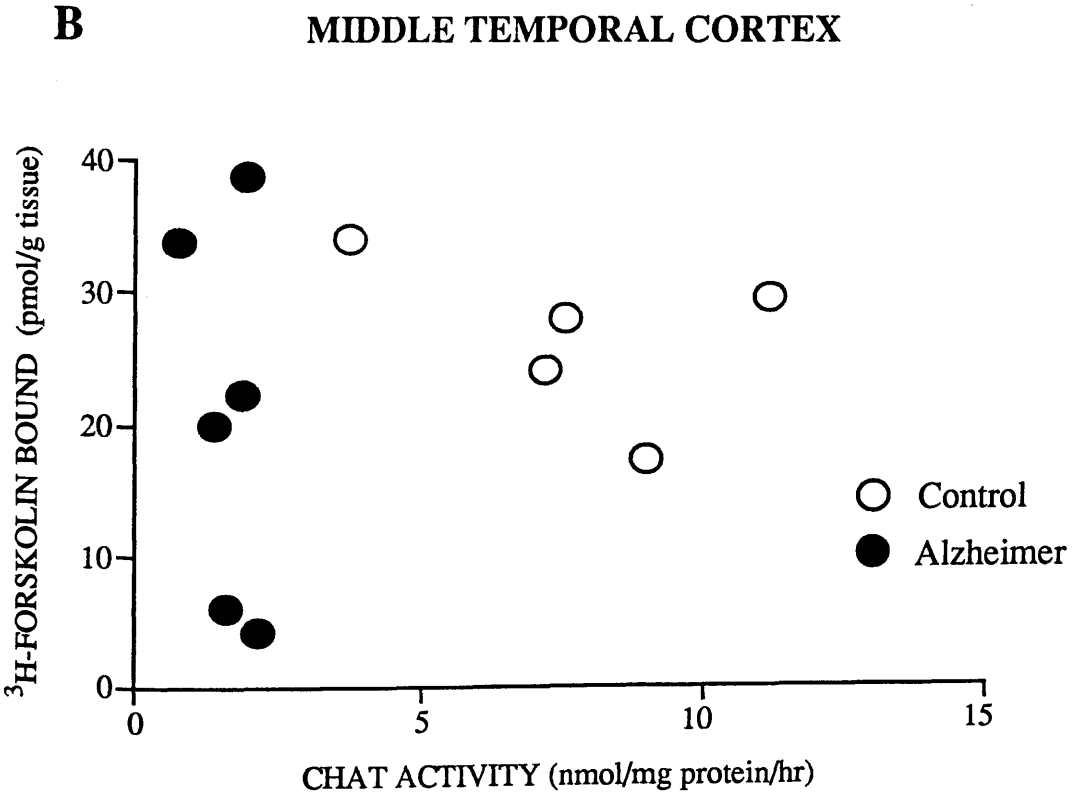

1.7 Effect of Gpp(NH)p on [^{3}H]-Forskolin Binding in Postmortem Human Brain

1.7.1 Effect of Gpp(NH)p on [^{3}H]-Forskolin Binding in Control Brain

The effect of Gpp(NH)p (10μM) on [^{3}H]-forskolin binding was investigated in adjacent sections to those used in the previous study (see Results section 1.1.4). In middle frontal cortex and temporal cortex of control subjects, [^{3}H]-forskolin binding was selectively increased in layers I-III of the gyri whilst the deeper cortical layers were unaffected by the inclusion of Gpp(NH)p in the incubation medium (Figures 19, 20, see also Figure 18). [^{3}H]-Forskolin binding was significantly increased in layers I-III of frontal cortex (28%) and temporal cortex (30%) compared to basal levels of [^{3}H]-forskolin binding.

In each discrete region analysed within the hippocampal formation of the control group, Gpp(NH)p had no effect on the level of [^{3}H]-forskolin binding (Figure 21).

1.7.2 Effect of Gpp(NH)p on [^{3}H]-Forskolin Binding in AD Brain

The differential effect of Gpp(NH)p to alter [^{3}H]-forskolin binding was conserved in AD brain as compared to controls. [^{3}H]-Forskolin binding was significantly increased in layers I-III in middle frontal cortex (25%) and in layers I-III of middle temporal cortex (33%), whilst Gpp(NH)p had no effect on [^{3}H]-forskolin binding in deep layers of both cortical regions of AD brain (Figures 19 and 20). It must be noted that although the percentage increase in [^{3}H]-forskolin binding, in the presence of Gpp(NH)p,

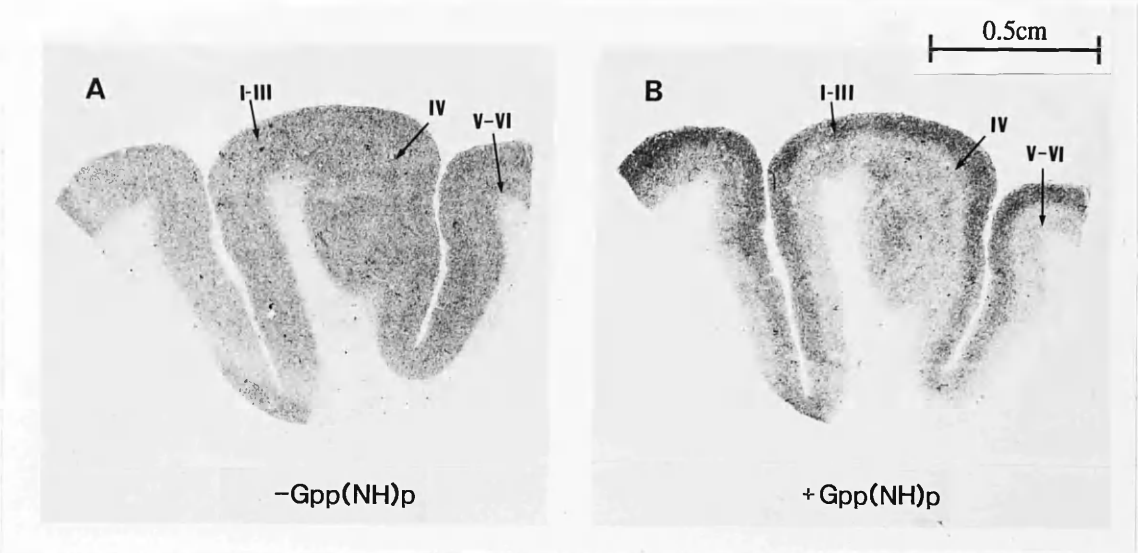

FIGURE 18
AUTORADIOGRAMS OF [^{3}H]-FORSKOLIN BINDING IN THE PRESENCE AND ABSENCE OF Gpp(NH)p

Autoradiograms generated by incubating sections of control human brain with 20nM [^{3}H]-forskolin in the presence and absence of Gpp(NH)p (10μM). A and B are adjacent sections of control middle frontal cortex incubated with [^{3}H]-forskolin alone (A) and [^{3}H]-forskolin in the presence of Gpp(NH)p (B). Note the marked increase in [^{3}H]-forskolin binding, in the presence of Gpp(NH)p, in cortical layers I-III from basal levels of [^{3}H]-forskolin binding.

was retained in AD brain compared to controls, the qualitative increase is approximately 50% of the magnitude of increase observed in control cortex. In the hippocampal formation, the basal levels of [^{3}H]-forskolin binding in each hippocampal region of AD brain was not significantly altered in the presence of Gpp(NH)p (Figure 21).

FIGURE 19
EFFECT OF Gpp(NH)p ON [^{3}H]-FORSKOLIN BINDING IN FRONTAL CORTEX

Quantitative autoradiographic measurement of [^{3}H]-forskolin binding in the presence and absence of Gpp(NH)p (10μM) in adjacent sections of middle frontal cortex. Histograms are presented as mean ± SEM of six controls (A) and five Alzheimer cases (B). [^{3}H]-Forskolin binding is significantly increased, in the presence of Gpp(NH)p, in cortical layers I-III compared to basal levels of [^{3}H]-forskolin in both control and AD frontal cortex. *$p<0.05$ Student's paired t-test.

FIGURE 19

EFFECT OF Gpp(NH)p ON ^{3}H-FORSKOLIN BINDING IN FRONTAL CORTEX

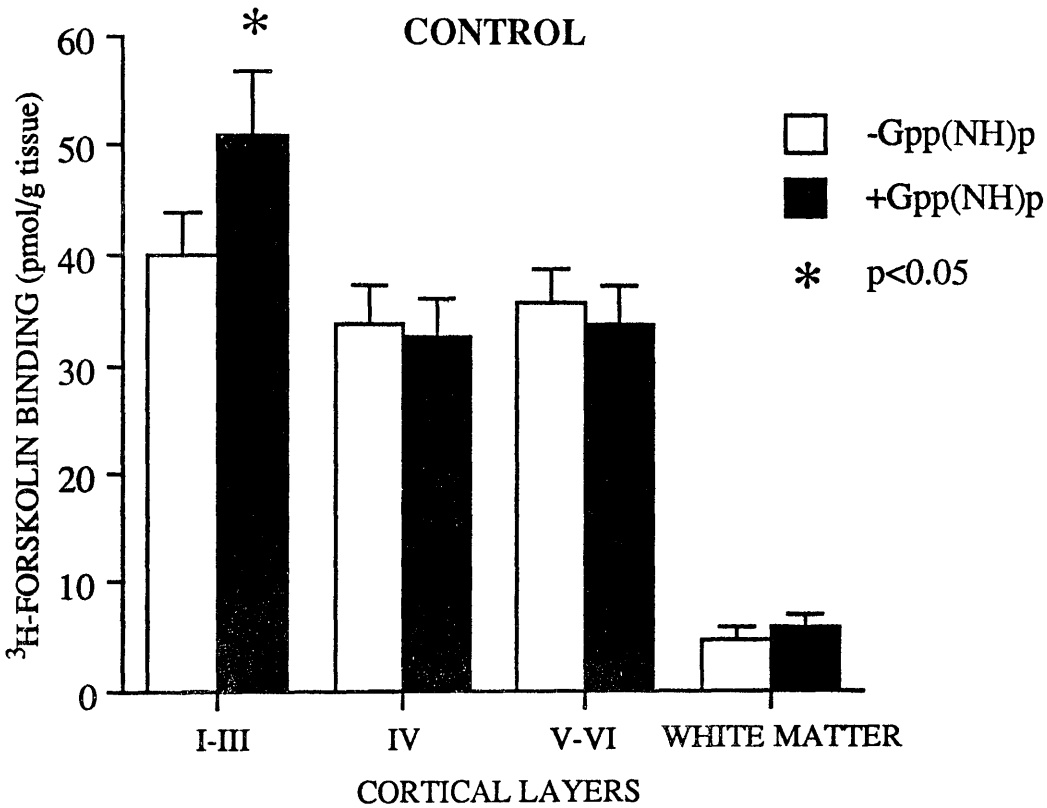

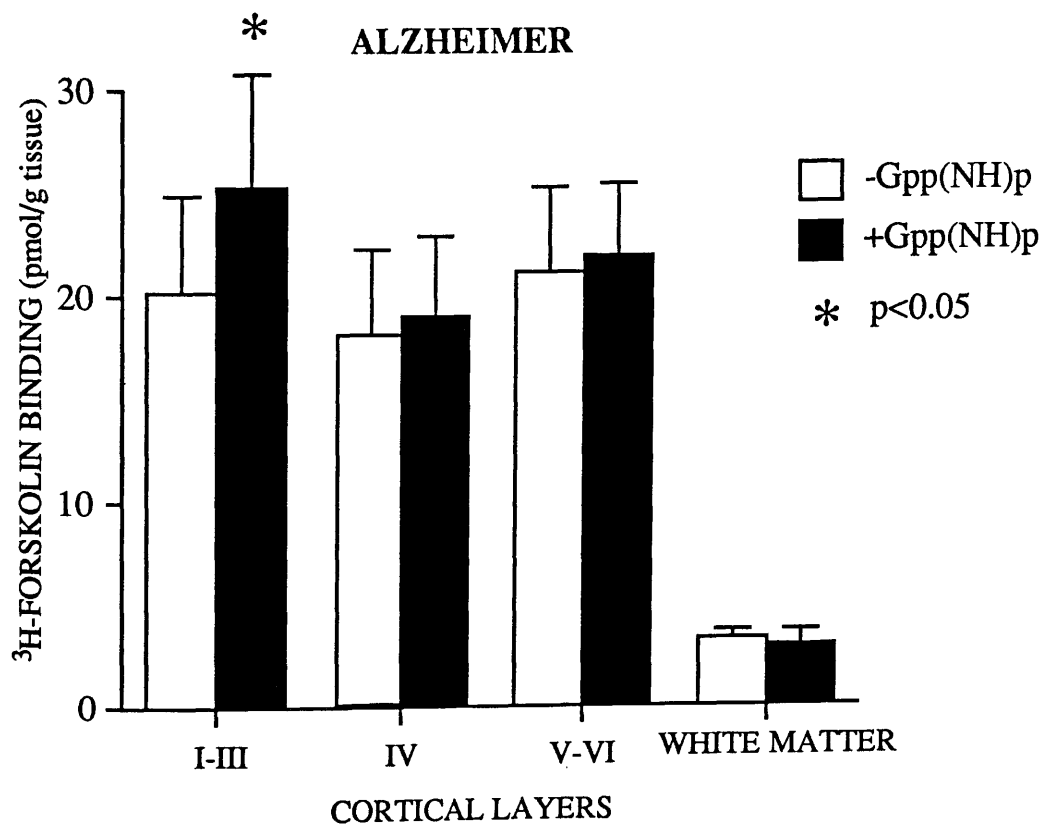

FIGURE 20
EFFECT OF Gpp(NH)p ON [^{3}H]-FORSKOLIN BINDING IN TEMPORAL CORTEX

Quantitative autoradiographic measurement of [^{3}H]-forskolin binding in the presence and absence of Gpp(NH)p (10μM) in adjacent sections of middle temporal cortex. Histograms are presented as mean ± SEM of six controls (A) and seven Alzheimer cases (B). [^{3}H]-Forskolin binding is significantly increased, in the presence of Gpp(NH)p, in cortical layers I-III compared to basal levels of [^{3}H]-forskolin in both control and AD middle frontal cortex. *$p<0.05$, Student's paired t-test.

FIGURE 20

EFFECT OF Gpp(NH)p ON ^{3}H-FORSKOLIN BINDING IN TEMPORAL CORTEX

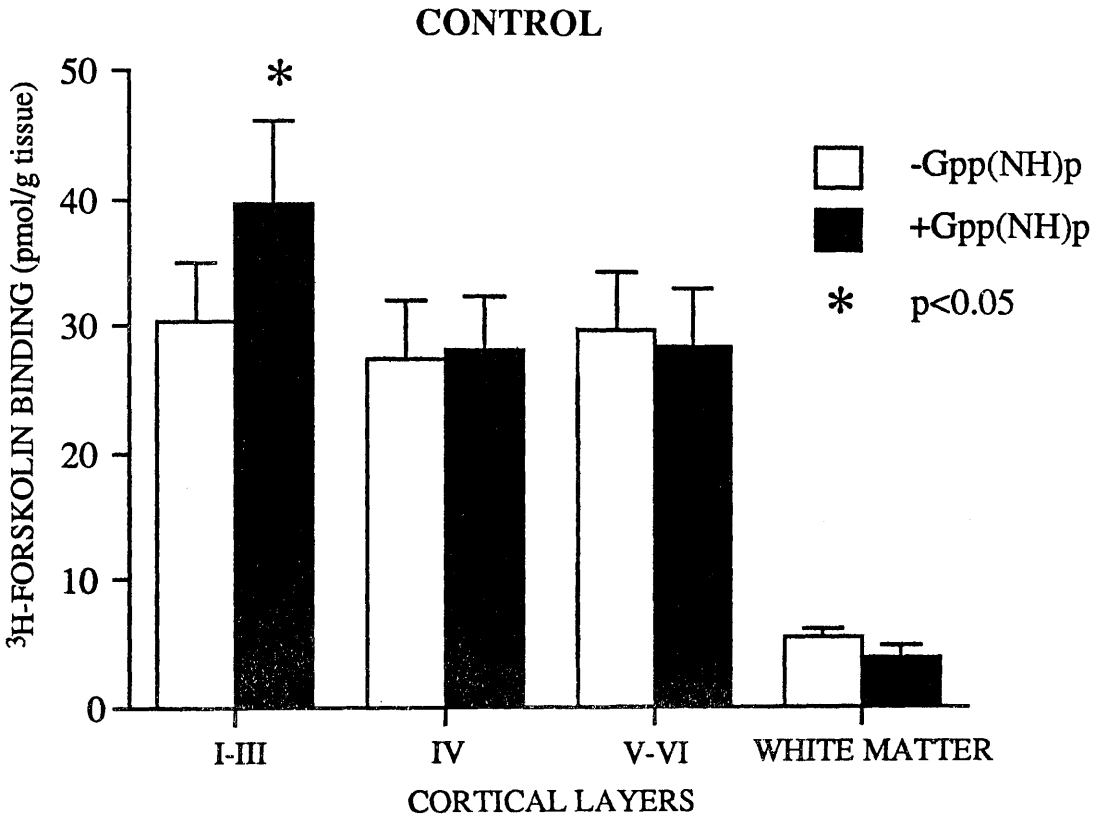

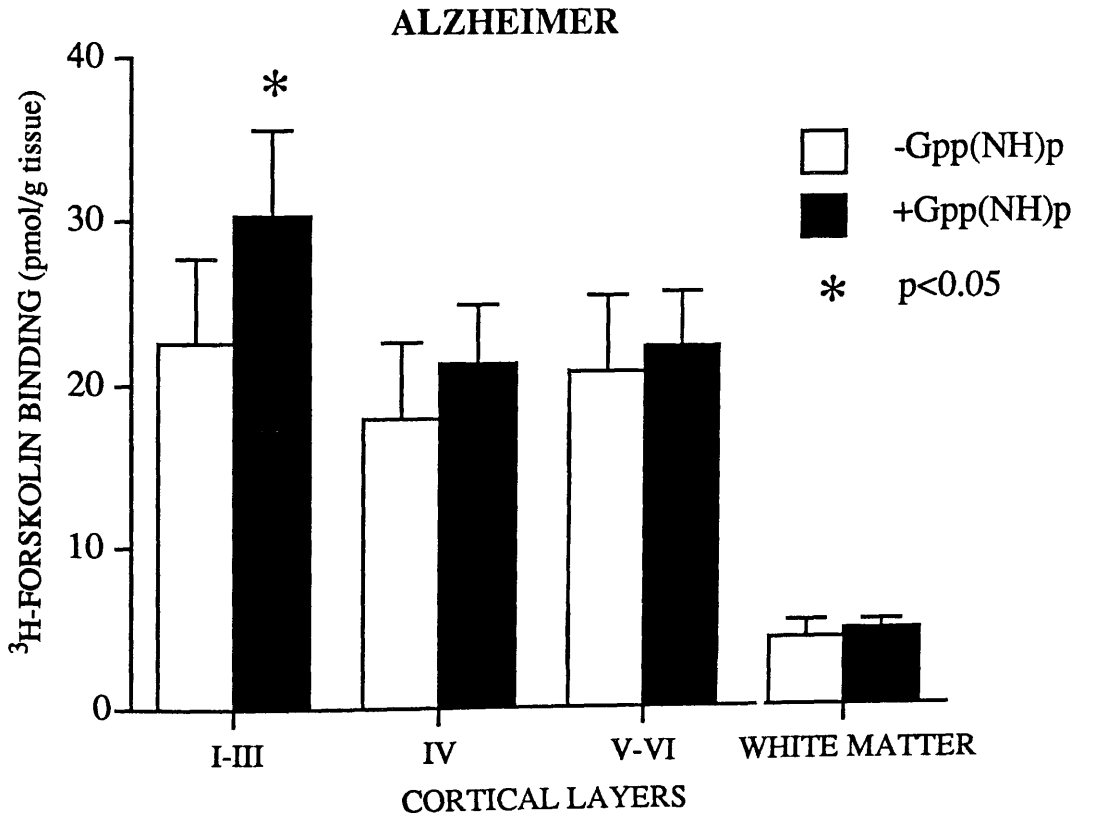

FIGURE 21
EFFECT OF Gpp(NH)p ON [^{3}H]-FORSKOLIN BINDING IN HIPPOCAMPAL REGION

Quantitative autoradiographic measurement of [^{3}H]-forskolin binding in the presence and absence of Gpp(NH)p (10μM) in adjacent sections of hippocampal region. Histograms are presented as mean ± SEM of six controls (A) and six Alzheimer cases (B). There was no significant difference between basal [^{3}H]-forskolin and [^{3}H]-forskolin in the presence of Gpp(NH)p, in any brain region examined in both control and AD groups by Student's paired t-test. Abbreviations are: molecular layer (MOL), granular layer (GRAN), hilus (HIL), stratum lacunosum moleculare (LACMOL), subiculum (SUB), superficial layer (super) of the parahippocampal gyrus (PHG).

FIGURE 21

EFFECT OF Gpp(NH)p ON ^{3}H-FORSKOLIN BINDING IN HIPPOCAMPAL REGION

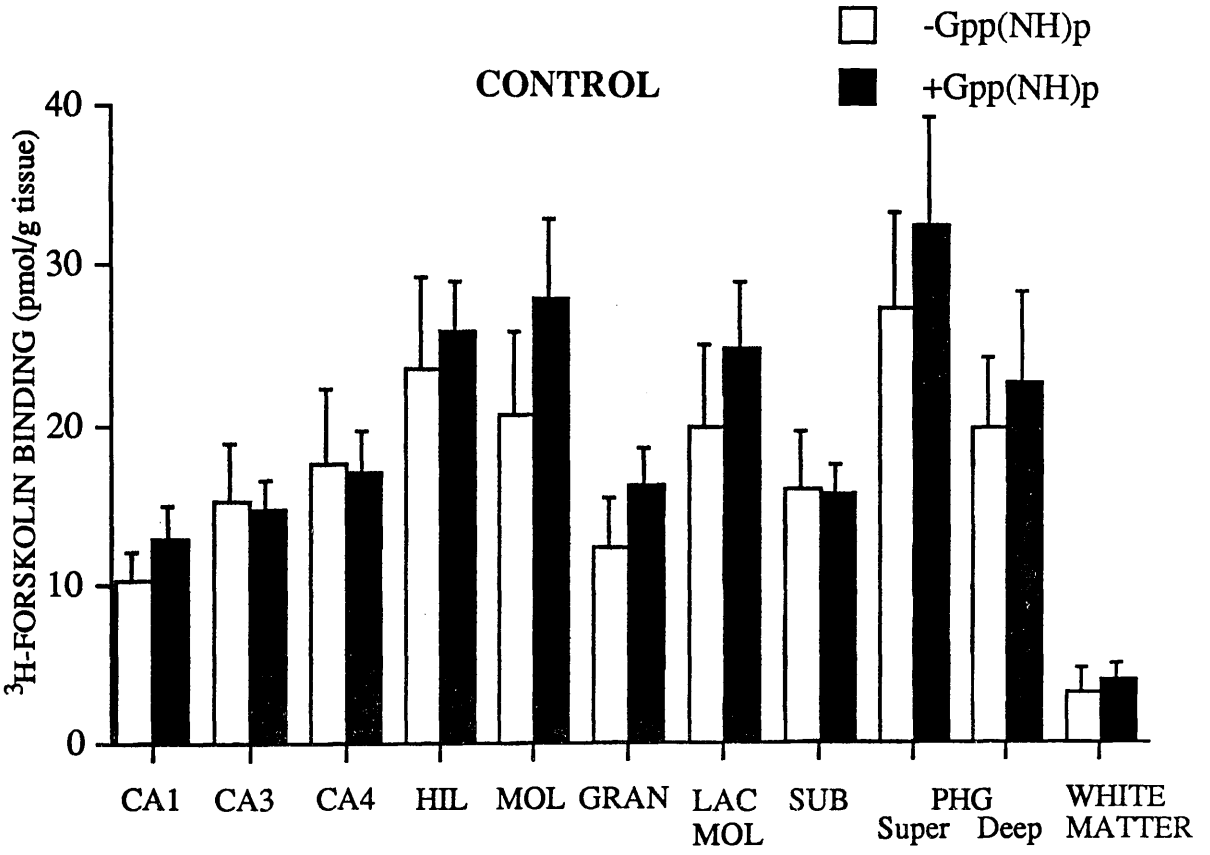

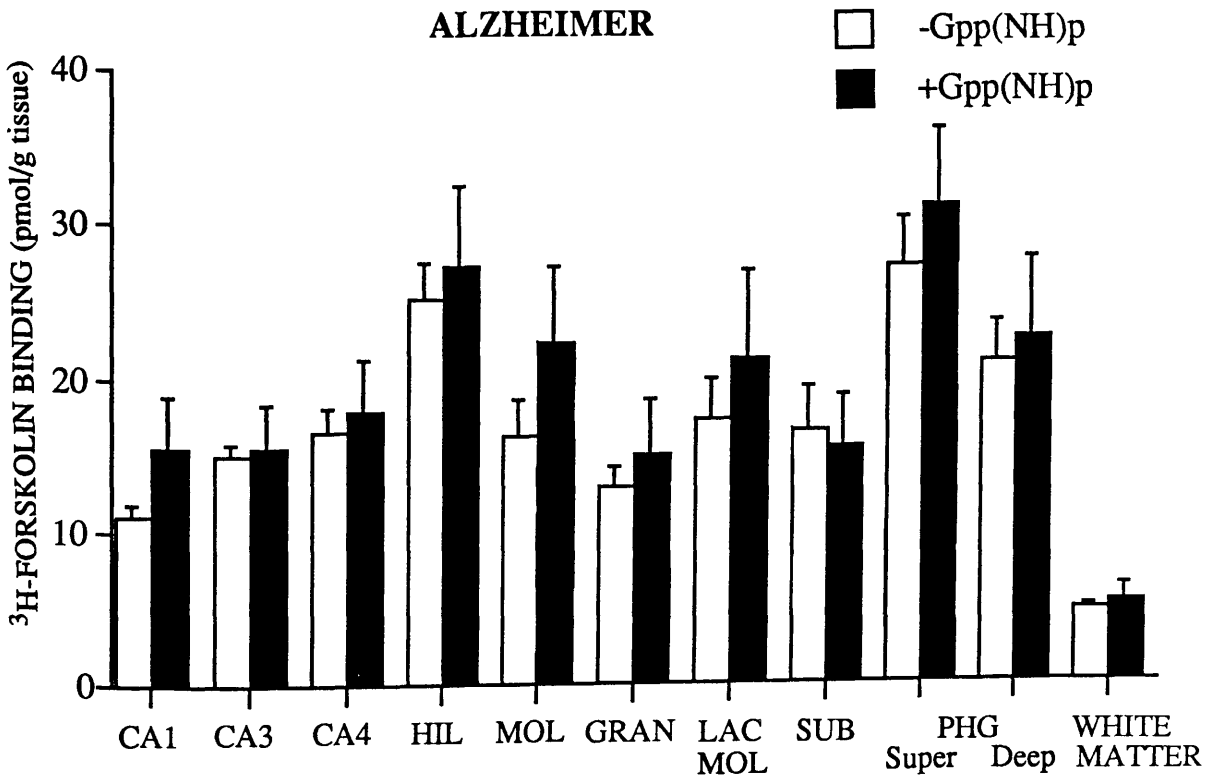

2. QUANTITATIVE AUTORADIOGRAPHY OF [^{3}H]-PDBu BINDING IN POSTMORTEM HUMAN BRAIN

2.1 Scatchard Analysis of [^{3}H]-PDBu Binding

In temporal cortex sections of four control subjects (not included in subsequent studies) saturation analysis revealed that [^{3}H]-PDBu specific binding was saturable and of high affinity (Figure 22). Non-specific binding, as measured in the presence of 2μM PDBu, was linear with respect to the concentration of [^{3}H]-PDBu and, at 2.5nM [^{3}H]-PDBu, the non-specific binding was only 5% of total binding. The average dissociation constant (K_D) of [^{3}H]-PDBu was 16nM and the maximum number of binding sites in temporal cortex was approximately 4pmol/section.

2.2 Displacement of [^{3}H]-PDBu Binding

Inhibition of [^{3}H]-PDBu binding by phorbol ester analogues was examined in temporal cortex sections of two control and two AD patients (outwith subsequent studies) (Table 6). Both phorbol 12,13 dibutyrate and phorbol 12, myristate 13-acetate were equipotent in their ability to inhibit [^{3}H]-PDBu binding. Phorbol 12,13-diacetate did not inhibit the binding of [^{3}H]-PDBu. The order of potency of the phorbol esters to inhibit [^{3}H]-PDBu binding was similar in control as compared to AD tissue sections. The ability of phorbol ester analogues to inhibit [^{3}H]-PDBu binding correlates well with their ability to stimulate protein kinase C and inhibit [^{3}H]-PDBu binding in rat brain (Driedger & Blumberg, 1980; Kikkawa et al. 1983; Blumberg et al. 1984). Thus [^{3}H]-PDBu binding in human brain would appear to reflect the distribution of protein kinase C.

FIGURE 22

SCATCHARD ANALYSIS OF [^{3}H]-PDBu BINDING IN HUMAN BRAIN

A. [^{3}H]-PDBu binding in temporal cortex sections of four control subjects. Sections were incubated with increasing concentrations of [^{3}H]-PDBu (1-250nM) at 22°C for 90 minutes and the radioactivity counted by liquid scintillation. Non-specific binding (▲) was defined in the presence of 2μM unlabelled PDBu. Specific binding (●) was determined from the subtraction of non-specific (▲) from total (O) binding.

B. Scatchard analysis of saturation data of [^{3}H]-PDBu binding in temporal cortex. Data points represent the mean ± SEM (n = 4). B_{MAX} and K_D values were determined using linear regression analysis.

FIGURE 22

SCATCHARD ANALYSIS OF ^{3}H-PDBu BINDING IN HUMAN BRAIN

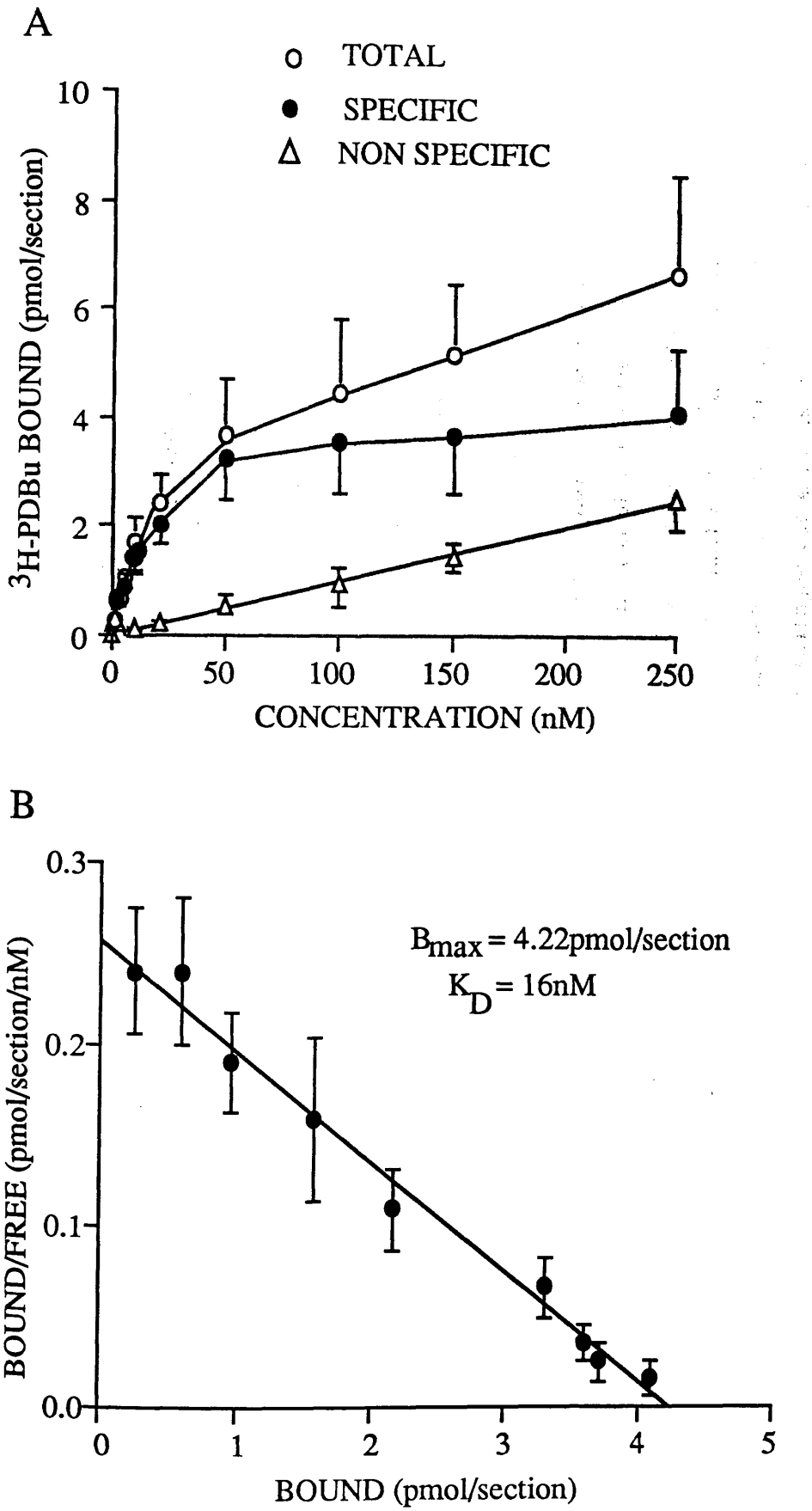

TABLE 6

INHIBITION OF [^{3}H]-PHORBOL 12,13 BINDING IN HUMAN CORTEX

ANALOGUE CONCENTRATION (M)	% INHIBITION							
	ANALOGUE A		ANALOGUE B		ANALOGUE C		ANALOGUE D	
	CONTROL	AD	CONTROL	AD	CONTROL	AD	CONTROL	AD
10^{-9}	6	28	9	12	11	3	12	7
10^{-8}	48	44	35	36	-	-	-	-
10^{-7}	86	76	72	67	12	1	2	4
10^{-6}	94	91	93	89	4	20	2	15
10^{-5}	96	91	95	91	12	25	74	64
10^{-4}	96	92	96	87	5	3	91	88

Human temporal cortex sections of two control and two Alzheimer (AD) cases were labelled with 2.5nM [^{3}H]-phorbol 12,13 dibutyrate (PDBu). In adjacent sections, inhibition of [^{3}H]-PDBu binding was examined in the presence of increasing concentrations of unlabelled phorbol ester analogues ; A - phorbol 12,13 dibutyrate, B - phorbol 12, myristate 13, acetate, C - 4α phorbol 12,13 didecanoate, D - phorbol 12,13 diacetate. Sections were wiped from the glass slides and the radioactivity bound counted by liquid scintillation. Inhibition of [^{3}H]-PDBu binding by each analogue was expressed as a percentage of the total [^{3}H]-PDBu binding.

2.3 Anatomical Localisation of [^{3}H]-PDBu Binding in Control Brain

[^{3}H]-PDBu exhibited a heterogeneous pattern of binding in tissue sections of control brain (Figure 23, see also Figures 24, 25 and 26), which was quite distinct from that of [^{3}H]-forskolin binding (see Figure 13). In neocortex, [^{3}H]-PDBu binding exhibited an obvious laminar distribution. In both frontal and temporal cortex, intense binding was observed in layers I-II with moderate levels of binding in layers III-IV and layers V-VI. [^{3}H]-PDBu binding was particularly high in the hippocampal formation. Within this region, binding was highest in the CA1 field and the superficial layer of parahippocampal gyrus. High densities were also noted in the CA3 field, hilus, molecular layer of the dentate gyrus and subiculum, with lower binding in the remainder of the hippocampal structures. There was minimal [^{3}H]-PDBu binding in white matter.

2.4 Quantitative Autoradiography of [^{3}H]-PDBu Binding in Control and AD Brain

[^{3}H]-PDBu binding was investigated in middle frontal and temporal cortex and the hippocampal formation of nine control and nine AD patients (Table 3) using quantitative autoradiography.

Statistical analysis of [^{3}H]-PDBu binding revealed that there was no significant difference in all regions of both frontal (Figure 24, see also Figures 23A and B) and temporal cortex (Figure 25) and in all hippocampal regions (Figure 26, see also Figures 23C and D) of the control group compared to the AD group.

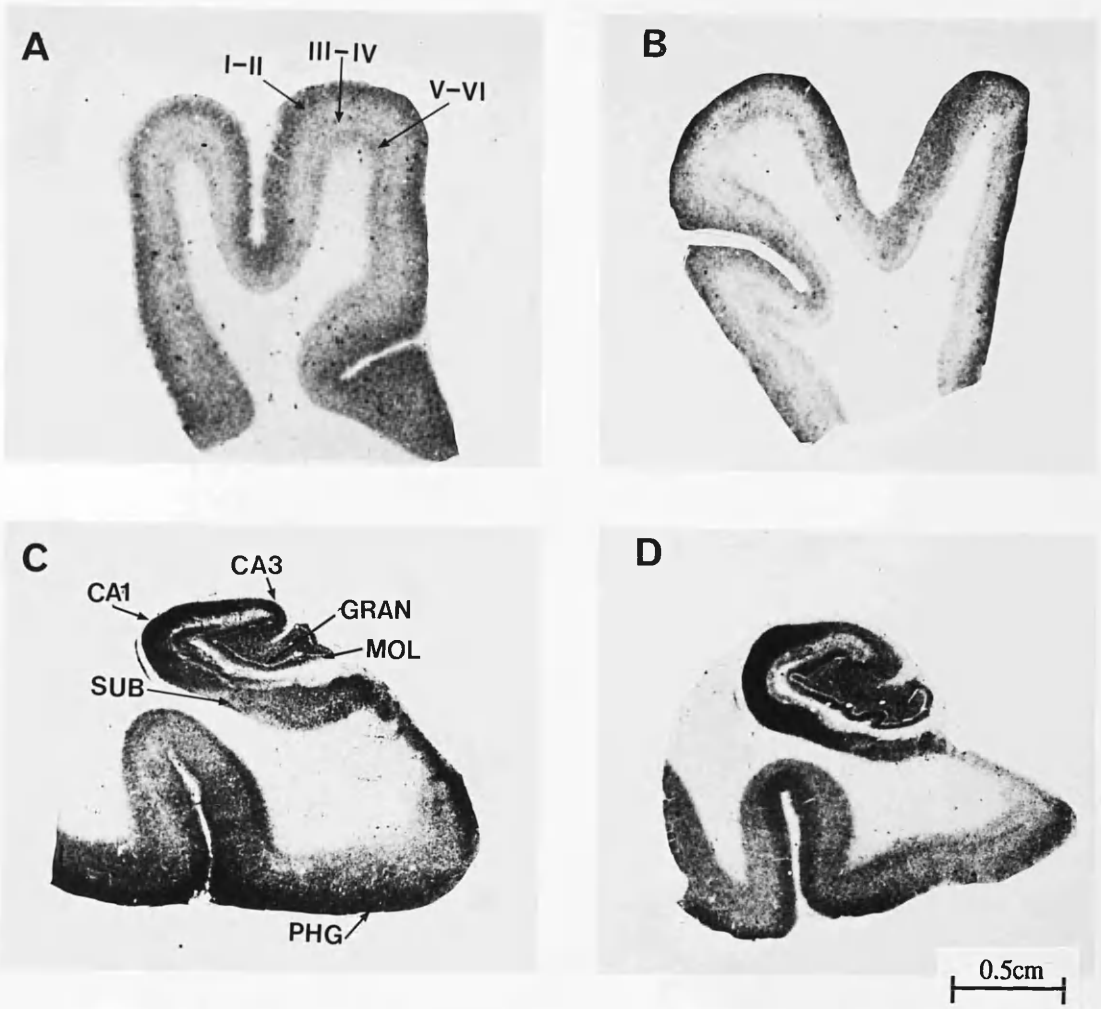

FIGURE 23
AUTORADIOGRAMS OF [^{3}H]-PDBu BINDING IN CONTROL AND AD BRAIN

Autoradiograms generated by labelling human sections with 2.5nM [^{3}H]-PDBu. A and B are middle frontal cortex sections of a control subject (A) and an AD subject (B). Within the cortex [^{3}H]-PDBu binding sites are localised in three distinct bands corresponding to layers I-II, III-IV and V-VI which were determined by reference to adjacent sections stained with cresyl violet. C and D are sections of the hippocampal region from a control (C) and an AD case (D). Autoradiographic measurements were made in the following regions: superficial (super) and deep layers of the parahippocampal gyrus (PHG); subiculum (SUB); stratum lacunosum moleculare (LACMOL); CA1, CA3 and CA4 fields of Ammon's Horn; in the dentate gyrus: hilus (HIL), molecular (MOL) and granular (GRAN) layers, with reference to cresyl violet-stained sections.

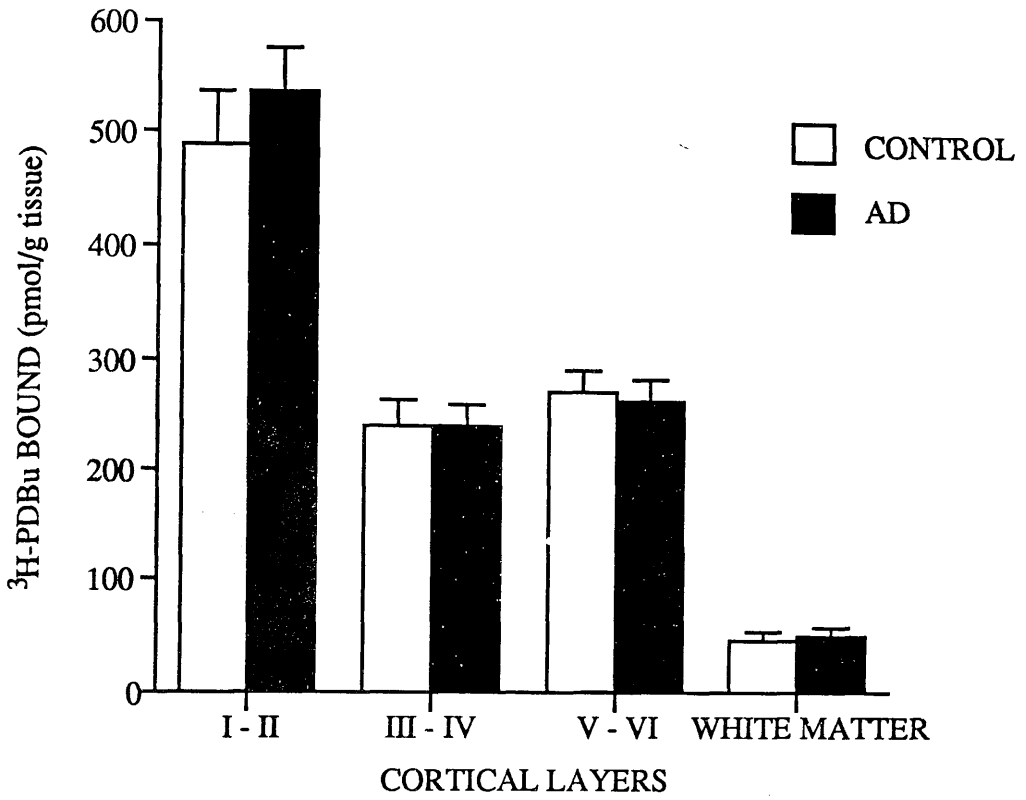

FIGURE 24
[^{3}H]-PDBu BINDING IN CONTROL AND AD MIDDLE FRONTAL CORTEX

Quantitative autoradiographic measurements of [^{3}H]-PDBu binding in middle frontal cortex. Cortical layers correspond to those in Figure 23A. Histograms are presented as mean ± SEM for control (n = 8) and AD (n= 9) subjects. There is no significant difference between the control and AD group in each cortical layer examined (Student's unpaired t-test).

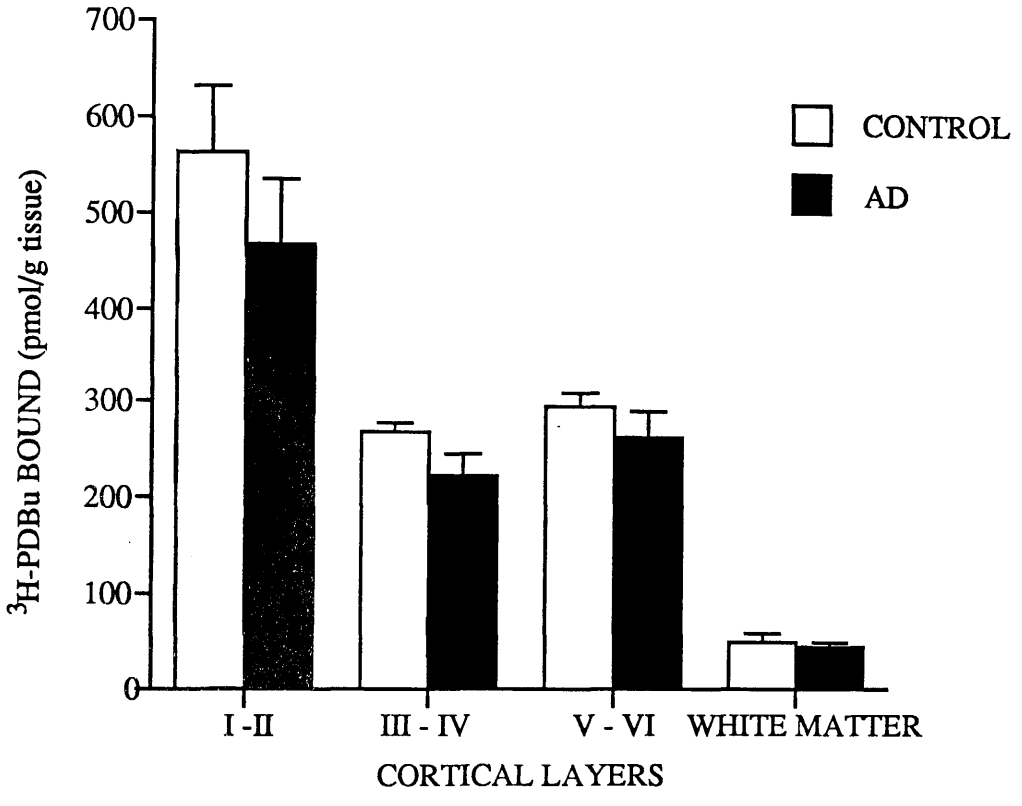

FIGURE 25
[^{3}H]-PDBu BINDING IN CONTROL AND AD MIDDLE TEMPORAL CORTEX

Quantitative autoradiographic measurement of [^{3}H]-PDBu binding in middle temporal cortex. The distribution of [^{3}H]-PDBu binding throughout the cortical layers was similar to that observed in middle frontal cortex (Figure 23A). Histograms are presented as mean ± SEM for control (n = 9) and AD (n = 9) subjects. There is no significant difference between the control and AD group in each control layer examined (Student's unpaired t-test).

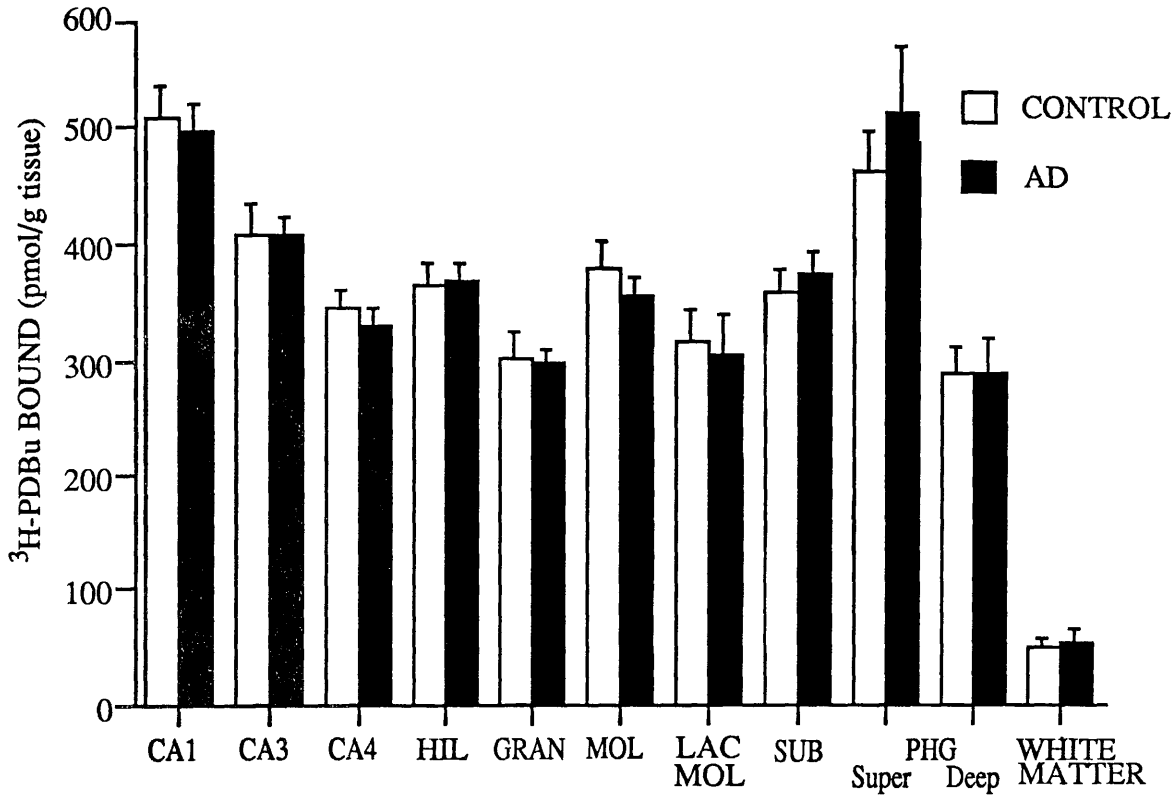

FIGURE 26
[^{3}H]-PDBu BINDING IN CONTROL AND AD HIPPOCAMPAL REGION

Quantitative autoradiographic measurement of [^{3}H]-PDBu binding in the hippocampal region. Abbreviations are: CA1, CA3, CA4 fields of Ammon's Horn; hilus (HIL), granular (GRAN) and molecular (MOL) layer of the dentate gyrus; stratum lacunosum moleculare (LACMOL); subiculum (SUB); superficial (super) and deep layers of the parahippocampal gyrus (PHG) (see Figure 23C). Histograms are presented as mean ± SEM for control (n = 9) and AD (n = 8) subjects. There is no significant different between the control and AD group in each hippocampal region examined (Student's unpaired t-test).

2.5 Quantitative Autoradiography of [^{3}H]-Forskolin Binding in Control and AD Brain

In the same control and AD subjects, in adjacent sections used for [^{3}H]-PDBu binding, quantitative autoradiographic analysis of [^{3}H]-forskolin binding was examined in middle frontal and temporal cortex and the hippocampal formation.

[^{3}H]-Forskolin binding was significantly reduced in all layers of middle frontal cortex, all layers of middle temporal cortex and the molecular layer of the dentate gyrus in this AD group compared to controls (full quantitative analysis of [^{3}H]-forskolin binding is presented in Appendix Va). The reductions in [^{3}H]-forskolin binding in neocortex and hippocampus in this AD group are consistent with the findings in a previous study, although the magnitude of change in [^{3}H]-forskolin binding between control and AD cases is different (see Results section 1.4). [^{3}H]-Forskolin binding was positively correlated with ChAT activity in all layers of middle frontal and temporal cortex (Appendix Vb).

2.6 [^{3}H]-PDBu Binding and ChAT Activity

ChAT activity was significantly reduced in the AD brain compared to the control group in middle frontal and temporal cortex and the hippocampal formation (Table 7). The deficit observed in the AD group was at least 60% of control values in all three brain regions examined.

TABLE 7

CHOLINE ACETYLTRANSFERASE ACTIVITY AND PLAQUE COUNTS
(SERIES 2)

Brain Area	CHOLINE ACETYLTRANSFERASE ACTIVITY		PLAQUES IN AD BRAINS	
	Control	AD	Layers I-III	Layers IV-VI
Middle Frontal Gyrus	6.3±0.8	2.5±0.5**	39±8	18±3
Middle Temporal Cortex	5.0±0.4	1.5±0.3***	38±7	22±4
Hippocampus	12.3±2.0	3.1±0.9**	Subiculum:	9±2

For Choline acetyltransferase activity, values are mean ± SEM, nmol/mg protein/hr in grey matter dissected from brain areas in which [^{3}H]-PDBu autoradiography and homogenate studies were carried out. **$p<0.01$, ***$p<0.001$.

For plaques, values are mean ± SEM, plaques/mm^2 in sections no more than 0.5cm caudal to sections used for [^{3}H]-PDBu autoradiography. Control brains had minimal plaques in each area.

Linear regression analysis of [^{3}H]-PDBu binding and ChAT activity demonstrated that there was no significant correlations between binding and ChAT in frontal cortex ($r = 0.155 - 0.192$, $p>0.05$), middle temporal cortex ($r = 0.263 - 0.288$, $p>0.05$), and the hippocampal formation ($r = 0 - 0.497$, $p>0.05$).

2.7 [^{3}H]-PDBu Binding and Local Neuropathology

All AD brains used in the autoradiographic study of [^{3}H]-PDBu binding contained numerous plaques in both cortical regions and the hippocampus, whilst controls had minimal plaques (Table 7). There were no significant correlations between [^{3}H]-PDBu binding and the number of plaques in superficial ($r = 0.148$, $p>0.05$) and deep ($r = 0.423$, $p>0.05$) layers of the middle frontal cortex; in the superficial ($r = 0.158$, $p>0.05$) and deep ($r = 0.212$, $p>0.05$) layers of temporal cortex and in the subiculum of the hippocampus ($r = 0.001$, $p>0.05$).

2.8 [^{3}H]-PDBu Binding to Particulate and Cytosolic Fractions in Control and AD Brain

Protein kinase C is differentially distributed within the cytosol and membrane of postmortem human brain (Saitoh & Dobkins, 1986). In the absence of significant alterations of [^{3}H]-PDBu binding in the autoradiographic study from the same control and AD subjects, the distribution of [^{3}H]-PDBu binding in particulate (membrane) and cytosolic fractions of homogenate preparations was investigated. There was no significant difference between control and AD brain in [^{3}H]-PDBu binding

to the particulate fraction (Figures 27A, B and C) in the middle frontal cortex (control = 11.8 ± 4.0, AD = 6.7 ± 1.9, p = 0.5); middle temporal cortex (control = 18.0 ± 7.2, AD = 9.4 ± 3.2, p = 0.461) and hippocampal region (control = 8.3 ± 1.8, AD = 9.7 ± 3.7, p = 0.5). Similarly, there was no significant difference between control and AD groups in the cytosolic fraction (Figures 27A, B and C) of middle frontal cortex (control = 7.1 ± 1.9, AD = 7.3 ± 2.6, p = 0.474); middle temporal cortex (control = 6.1 ± 1.7, AD = 5.4 ± 2.9, p = 0.474) and hippocampal region (control = 4.3 ± 1.4, AD = 4.9 ± 1.3, p =0.467).

FIGURE 27
SCATTERGRAM OF [^{3}H]-PDBu BINDING IN PARTICULATE AND CYTOSOLIC FRACTIONS OF CONTROL AND AD BRAIN

Scattergram of [^{3}H]-PDBu binding to particulate and cytosolic fractions of homogenate preparations from the middle frontal cortex (A), middle temporal cortex (B) and hippocampal formation (C). Individual points represent the amount of [^{3}H]-PDBu binding (pmol/mg protein) in each control or AD case. There is no significant difference between the control and AD group in the particulate or cytosolic fraction of each brain region (Student's unpaired t-test).

FIGURE 27 SCATTERGRAM OF ^{3}H-PDBu BINDING IN PARTICULATE AND CYTOSOLIC FRACTIONS OF CONTROL AND AD BRAIN

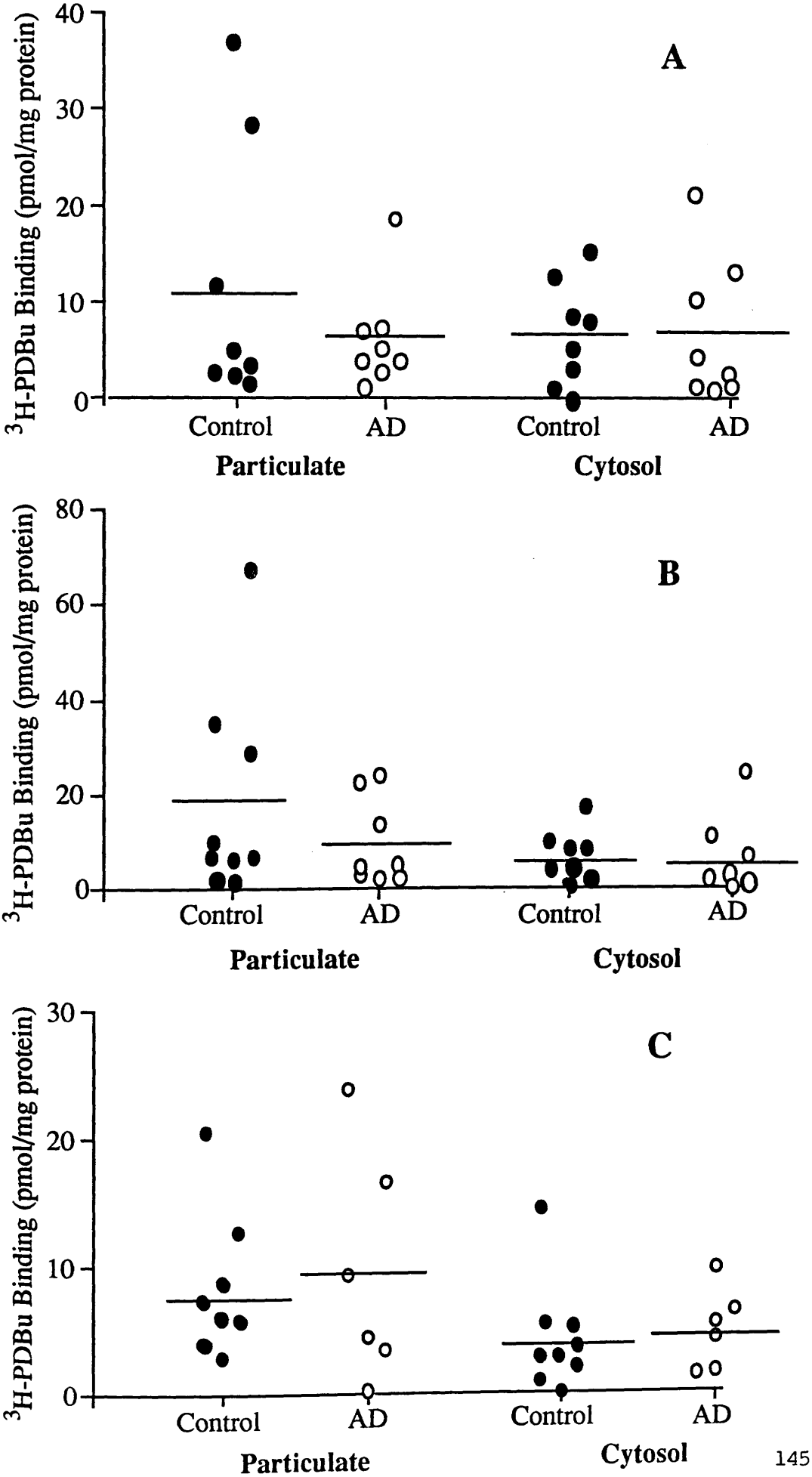

3. LESION OF RETINOFUGAL AND CORTICOFUGAL FIBRES IN THE RAT VISUAL SYSTEM

3.1 Anatomical Localisation of [^{3}H]-Forskolin and [^{3}H]-PDBu Binding in Rat Visual System

Both [^{3}H]-forskolin and [^{3}H]-PDBu exhibited distinct patterns of binding within the rat visual system (Figure 28). Additionally the hierarchy of binding levels within discrete anatomical components of the visual system was similar for both ligands.[^{3}H]-Forskolin binding was high in the visual cortex and superior colliculus. Lesser degrees of binding were observed in the remaining visual structures such as dorsal lateral geniculate, pretectal nuclei and lateral posterior nucleus. Within the visual cortex, a laminar distribution of [^{3}H]-forskolin binding was found. Layer IV of the visual cortex displayed slightly greater levels of [^{3}H]-forskolin binding in comparison to the superficial layers II-III and deeper layers V-VI.

Similarly, [^{3}H]-PDBu binding was markedly higher in the visual cortex and superior colliculus compared to other visual areas. However, the pattern of binding within the cortex was not exactly similar for [^{3}H]-PDBu compared to [^{3}H]-forskolin binding. [^{3}H]-PDBu binding was most marked in the superficial layers II-III of the visual cortex, whilst lower binding was associated in layers IV-VI.

NOTE: Preliminary results of Scatchard analysis of [^{3}H]-forskolin and [^{3}H]-PDBu binding in rat brain sections are presented in Appendix VIII(a) and VIII(b).

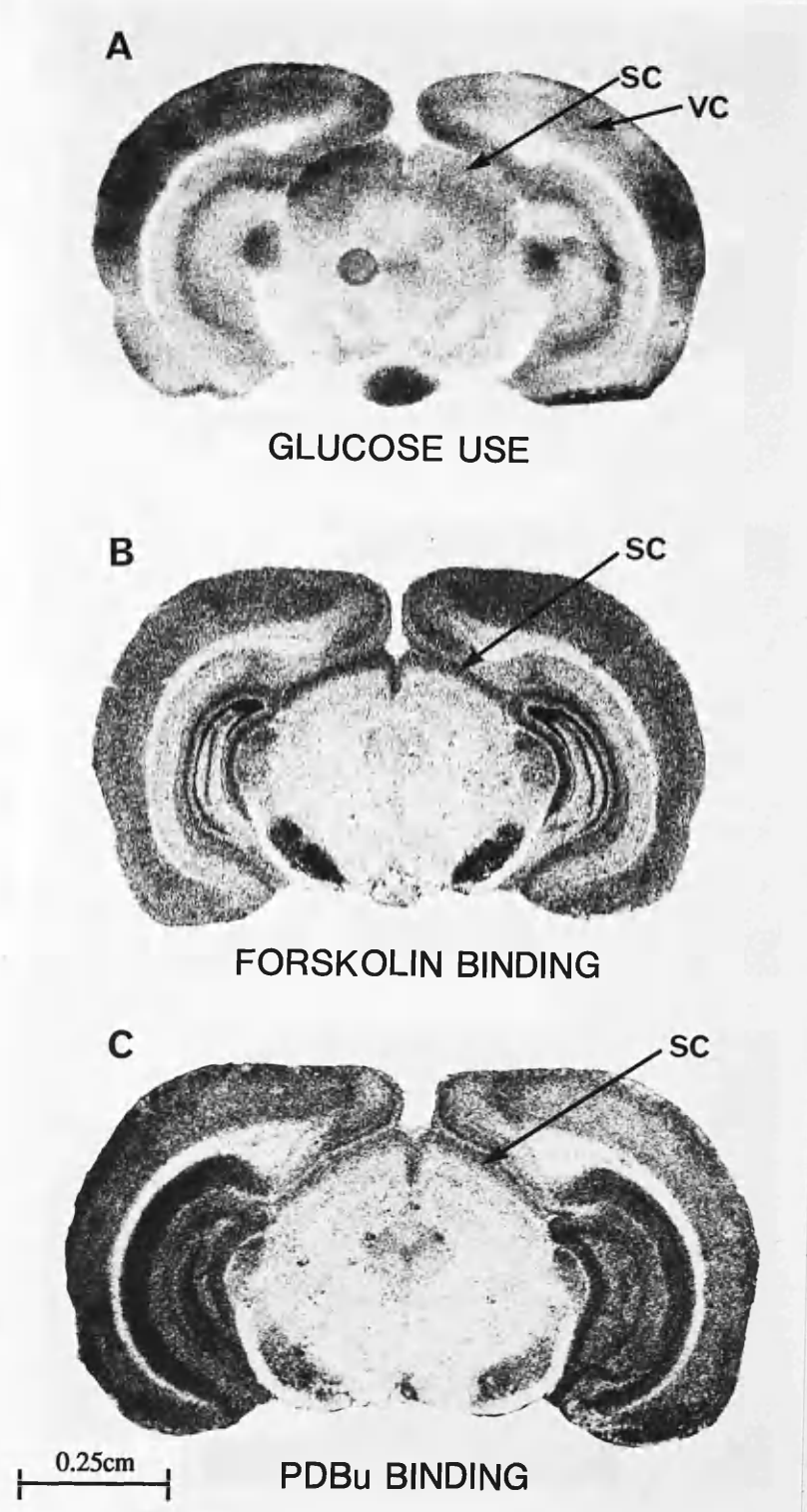

FIGURE 28
AUTORADIOGRAMS OF GLUCOSE USE, [^{3}H]-FORSKOLIN AND [^{3}H]-PDBu BINDING IN RAT BRAIN POST-ENUCLEATION

Representative autoradiograms of glucose use (A), [^{3}H]-forskolin binding (B) and [^{3}H]-PDBu (C) binding in the rat visual system at 10 days following unilateral orbital enucleation. Note the marked reduction in glucose use in the visually-deprived hemisphere of the visual cortex (VC) and superficial layers of the superior colliculus (SC). [^{3}H]-Forskolin binding is reduced in the visually-deprived SC and unaltered in the VC. [^{3}H]-PDBu binding is unaltered in both the SC and VC. The right hemisphere of the autoradiograms above is the visually-deprived hemisphere.

3.2 Ligand Binding to Second Messenger Systems and Glucose Use after Unilateral Orbital Enucleation

Full quantitative analysis of [^{3}H]-forskolin and [^{3}H]-PDBu binding and glucose use are presented in Appendix I.

3.2.1 [^{3}H]-Forskolin Binding After Unilateral Orbital Enucleation

There were no significant alterations in [^{3}H]-forskolin binding in any structure examined at one day post-enucleation. At 5, 10 and 20 days post-lesion, significantly lower levels of [^{3}H]-forskolin binding sites were present in the contralateral superior colliculus and dorsal lateral geniculate body (Figures 29 and 30, see also Figure 28). The magnitude of the deficit at 10 days post-lesion was -14% in the superior colliculus and -8% in the dorsal lateral geniculate. At any time point examined post-enucleation, no differences in any secondary visual structures were detected (Figure 31). [^{3}H]-Forskolin binding did not alter in the non-lesioned hemisphere post-enucleation (ANOVA) and there was no significant alteration in non-visual areas (Appendix I(a)).

3.2.2 [^{3}H]-PDBu Binding After Unilateral Orbital Enculeation

There were no significant differences in [^{3}H]-PDBu binding in either the primary (Figures 29 and 30, see also Figure 28) or secondary visual projections areas up to 20 days post-lesion (Figure 31). Non-visual structures remained unaltered and there was no significant difference in the non-lesioned hemisphere post-enucleation (ANOVA) (Appendix I(b)).

GLUCOSE USE, [^{3}H]-FORSKOLIN AND [^{3}H]-PDBu BINDING AT INCREASING SURVIVAL TIMES POST-ENUCLEATION

FIGURE 29 Superior Colliculus (superficial layer).

FIGURE 30 Dorsal Lateral Geniculate Body.

FIGURE 31 Visual Cortex (layer IV).

Interhemispheric differences are presented of glucose use, [^{3}H]-forskolin binding and [^{3}H]-PDBu binding at survival times 1, 5, 10 and 20 days after unilateral orbital enucleation. Data are expressed as the mean percentage change of the visually-deprived hemisphere (L) from the visually-intact hemisphere (R) ± SEM. *$p<0.01$, Student's paired t-test. (n = 3-6 per group)

FIGURE 29 GLUCOSE USE, ^{3}H-FORSKOLIN AND ^{3}H-PDBu BINDING AT INCREASING SURVIVAL TIMES POST-ENUCLEATION

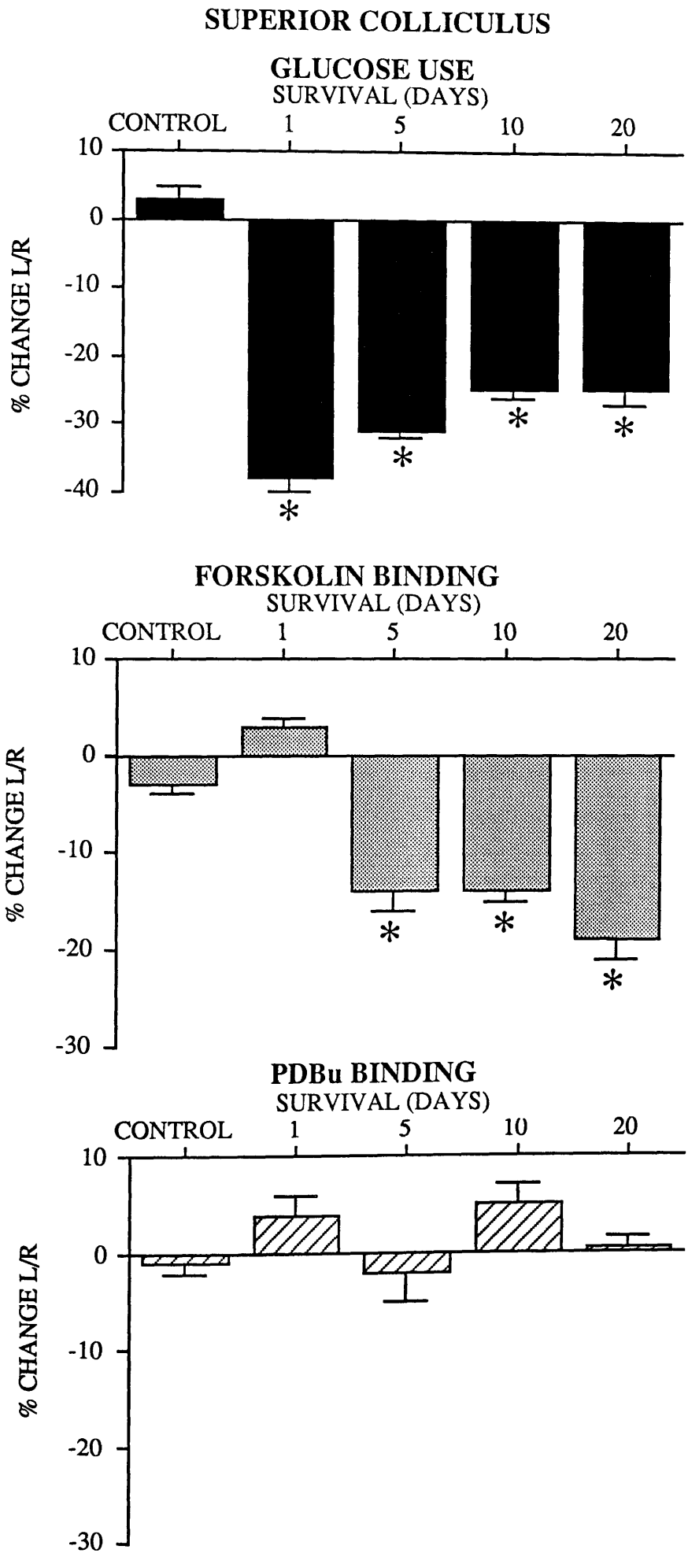

FIGURE 30 GLUCOSE USE ,^{3}H-FORSKOLIN AND ^{3}H-PDBu BINDING AT INCREASING SURVIVAL TIMES POST-ENUCLEATION

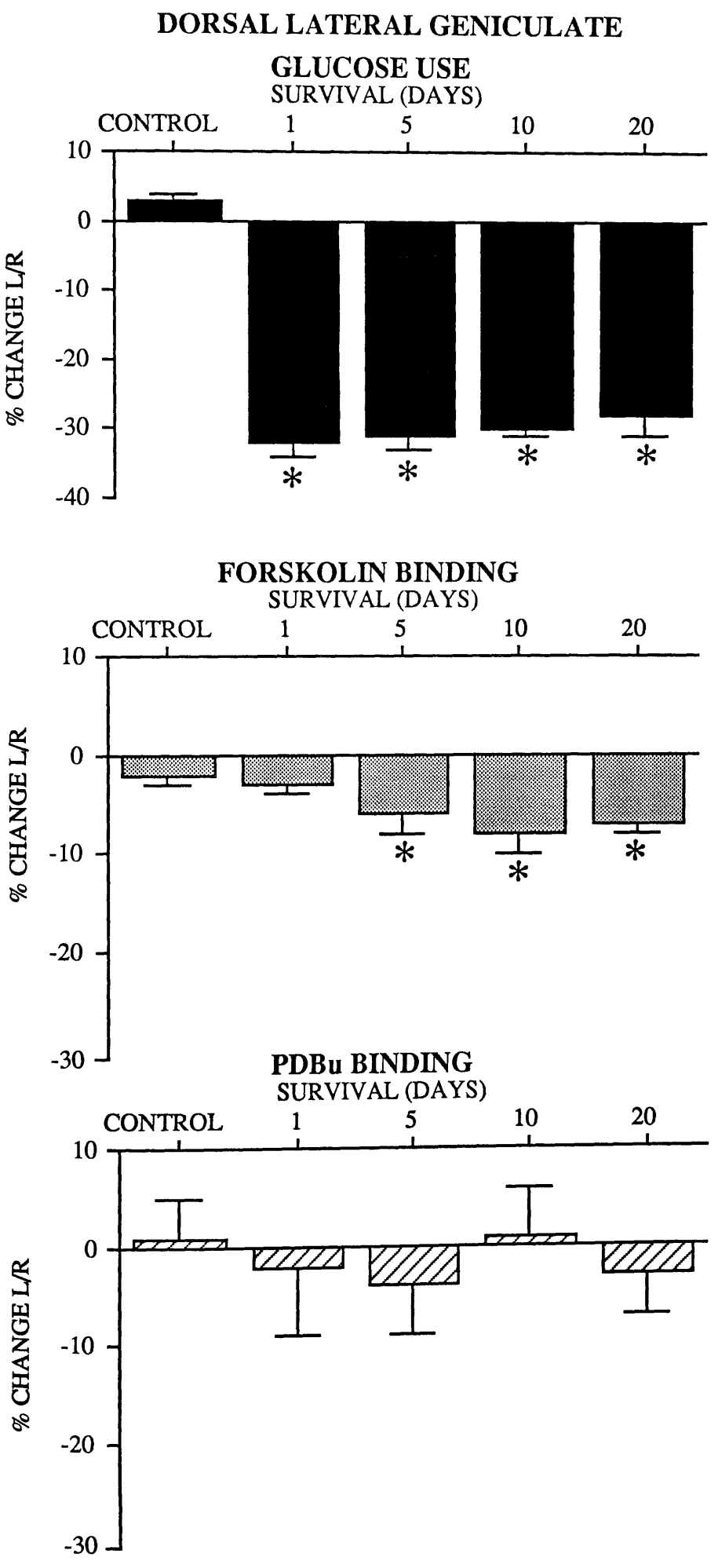

FIGURE 31 GLUCOSE USE, ^{3}H-FORSKOLIN AND ^{3}H-PDBu BINDING AT INCREASING SURVIVAL TIMES POST-ENUCLEATION

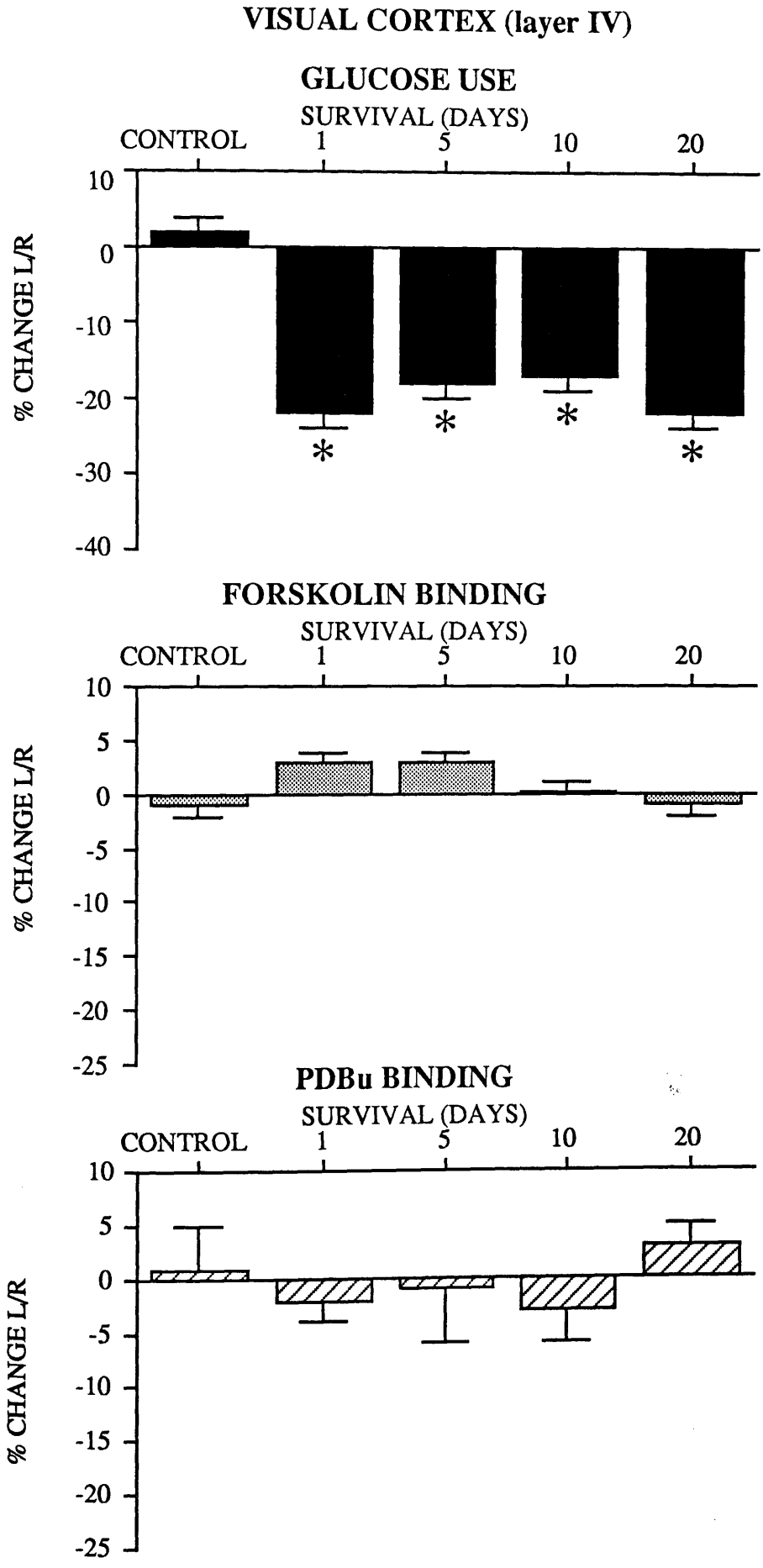

3.2.3 [^{14}C]-2-Deoxyglucose Utilisation After Unilateral Orbital Enucleation

In all visual structures examined there was a significant reduction in glucose use in the visually-deprived hemisphere of animals at each time point post-enucleation (Figures 29, 30, 31, see also Figure 28). The reduction in glucose use was most marked in the primary visual structures at 1 day post-lesion when the greatest deficit in the superior colliculus was 39% and dorsal lateral geniculate was 32%. Secondary visual structures were less affected by unilateral orbital enucleation, with the reduction in glucose use in the visually-deprived hemisphere of the visual cortex (layer IV) being 23%. Depression of metabolic activity in the deprived hemisphere of the superior colliculus at 10 and 20 days was less than the magnitude of the deficit in glucose use at one day. Glucose use was unaltered in the visually-intact hemisphere at any time point post-enucleation (ANOVA) and remained unchanged in the non-visual structures (Appendix I(c)).

3.3 Modulation of [^{3}H]-Forskolin Binding by Gpp(NH)p After Unilateral Orbital Enucleation

Full quantitative analysis of [^{3}H]-forskolin binding in the presence and absence of Gpp(NH)p is presented in Appendix II.

3.3.1 Effect of Gpp(NH)p on [^{3}H]-Forskolin Binding in the Rat Visual System

Adjacent sections from control rat brain were labelled with [^{3}H]-forskolin in the presence and absence of Gpp(NH)p (10μM). Differential effects of the levels of [^{3}H]-forskolin binding in the presence of Gpp(NH)p were observed in each of the areas examined. In both hemispheres of the

visual cortex, (layer IV), Gpp(NH)p significantly increased [^{3}H]-forskolin binding by 10% although basal levels of [^{3}H]-forskolin were unaltered in cortical layers II/III and layers V/VI. Similarly, in the superficial layer of the superior colliculus, [^{3}H]-forskolin binding was significantly increased (37%) in both hemispheres in the presence of Gpp(NH)p (see Figure 32). In contrast, Gpp(NH)p had no effect on [^{3}H]-forskolin binding in both hemispheres of the dorsal lateral geniculate body, pretectal nuclei and lateral posterior nucleus.

In non-visual structures, basal levels of [^{3}H]-forskolin binding in both hemispheres were markedly increased, in the presence of Gpp(NH)p in the caudate putamen by 81% and in the lateral habenula by 54%. [^{3}H]-Forskolin binding was unaffected by Gpp(NH)p in the medial geniculate, thalamus and molecular layer of the hippocampus (Appendix II).

3.3.2 Effect of Gpp(NH)p on [3H]-Forskolin Binding After Unilateral Orbital Enucleation

[^{3}H]-Forskolin binding was examined in the presence and absence of Gpp(NH)p in adjacent sections at 10 days following unilateral orbital enucleation. In a previous study (see Results section 3.2.1), [^{3}H]-forskolin binding deficits were demonstrated at 10 days post-enucleation, thus this time point was employed for the present study.

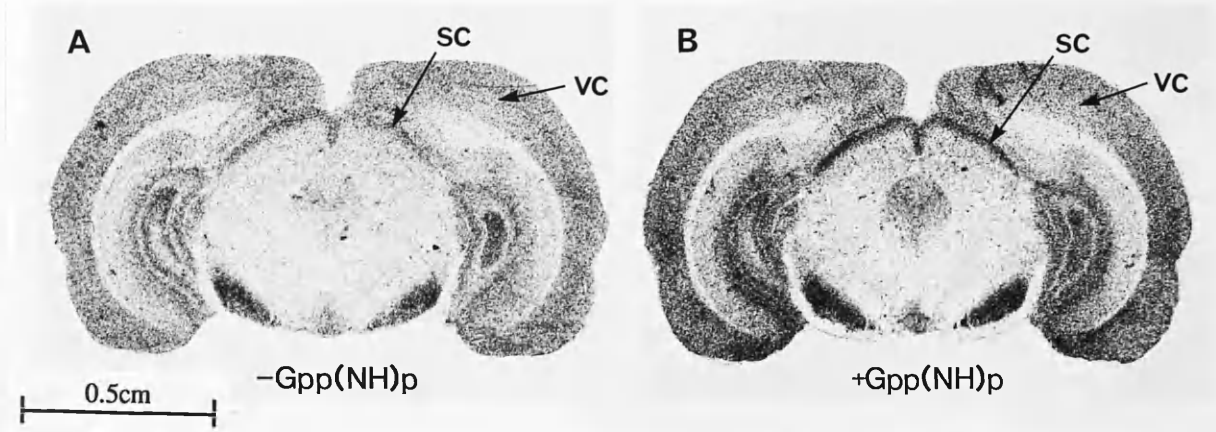

FIGURE 32
AUTORADIOGRAMS OF [^{3}H]-FORSKOLIN BINDING IN THE PRESENCE AND ABSENCE OF Gpp(NH)p POST-ENUCLEATION

Illustrative autoradiograms of [^{3}H]-forskolin binding in the absence (A) and presence (B) of Gpp(NH)p (10μM) at 10 days post-enucleation. Note the asymmetry in [^{3}H]-forskolin binding in the superior colliculus (SC) in A and B. [^{3}H]-Forskolin binding is enhanced in the presence of Gpp(NH)p (B) in the visual cortex and the superior colliculus compared to basal levels of [^{3}H]-forskolin binding (A) in these regions.

FIGURE 33
EFFECT OF Gpp(NH)p ON [^{3}H]-FORSKOLIN BINDING

Superior Colliculus (superficial layer)

Dorsal Lateral Geniculate Body and

Visual Cortex (layer IV).

Interhemispheric differences are presented of [^{3}H]-forskolin binding in the presence and absence of Gpp(NH)p (10μM) at 10 days post-enucleation. Data are expressed as the mean percentage change of the visually-deprived hemisphere (L) from the visually-intact hemisphere (R) ± SEM. *$p<0.01$, Student's paired t-test. (n = 5 per group)

Note the reduction in [^{3}H]-forskolin binding in the superior colliculus post-enucleation in both the presence and absence of Gpp(NH)p. In the dorsal lateral geniculate body post-lesion, [^{3}H]-forskolin binding alone was reduced and in the presence of Gpp(NH)p, symmetrical [^{3}H]-forskolin binding was restored. There was no significant alteration in [^{3}H]-forskolin binding in the visual cortex post-enucleation in the presence or absence of Gpp(NH)p.

FIGURE 33

EFFECT OF Gpp(NH)p ON ^{3}H-FORSKOLIN BINDING

SUPERIOR COLLICULUS (superficial layer)

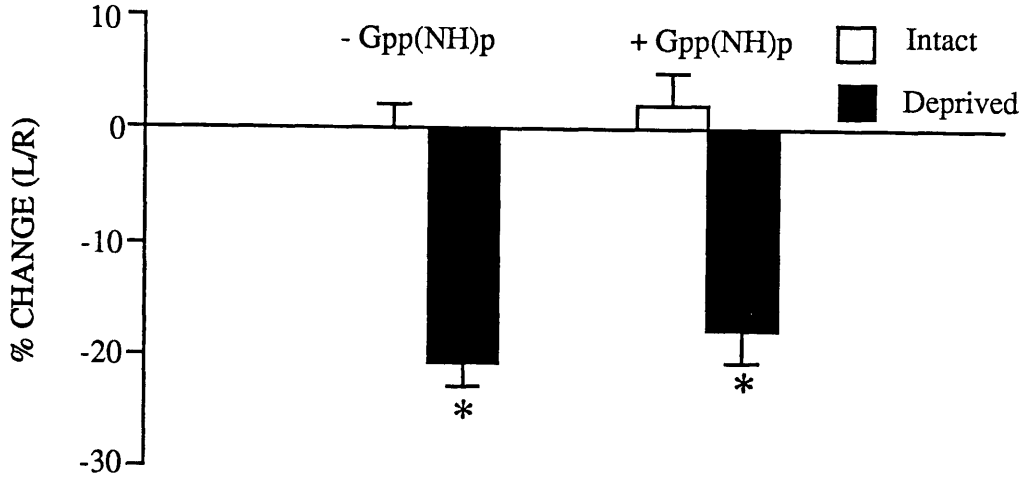

DORSAL LATERAL GENICULATE BODY

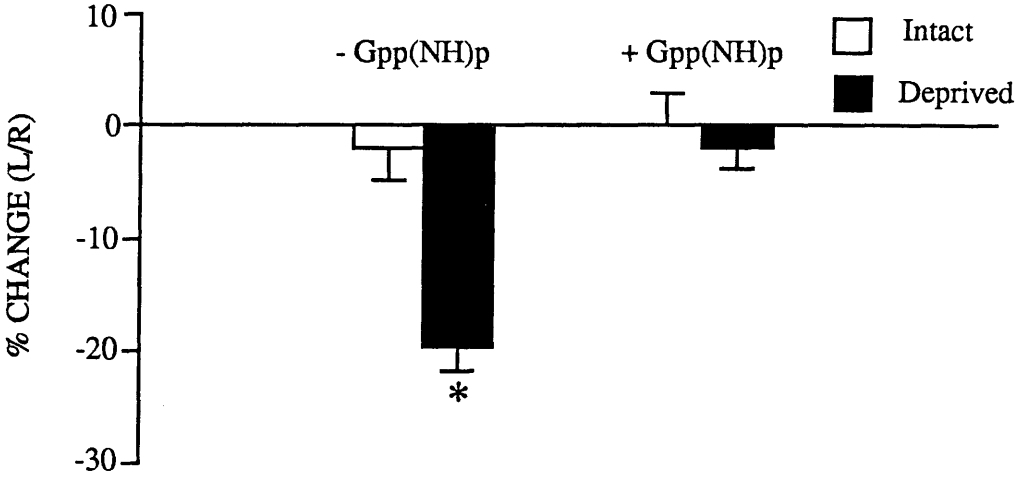

VISUAL CORTEX (Layer IV)

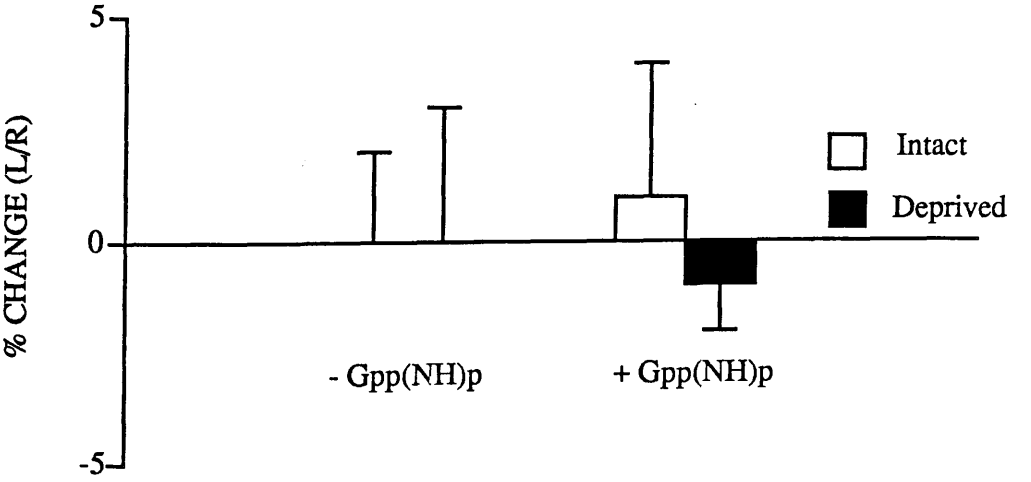

Post-enucleation, [^{3}H]-forskolin binding (in the absence of Gpp(NH)p) was significantly reduced in the visually-deprived superior colliculus (-20%) and the visually-deprived dorsal lateral geniculate body (-20%), compared to the visually-intact hemisphere (Figure 33). [^{3}H]-Forskolin binding was unaltered in secondary visual structures (e.g. visual cortex) following unilateral enucleation Figure 33). This study replicates the results of the previous examination of [^{3}H]-forskolin binding post-enucleation (Section 3.2.1).

In the presence of Gpp(NH)p, the asymmetry in [^{3}H]-forskolin binding in the visually-deprived superior colliculus post-enucleation was preserved (Figure 33, see also Figure 32). The magnitude of the deficit in the visually-deprived superior colliculus was maintained at approximately 18%. Following enucleation, in the presence of Gpp(NH)p, symmetrical [^{3}H]-forskolin binding appeared to be restored in the visually-deprived dorsal lateral geniculate despite enucleation (Figure 33). No asymmetry in [^{3}H]-forskolin binding was uncovered in the visual cortex post-lesion in the presence of Gpp(NH)p (Figure 33) (Appendix II).

3.4 Ligand Binding to Second Messenger Systems and Glucose Use After Unilateral Lesion of the Rat Visual Cortex

Full quantitative analysis of [^{3}H]-forskolin binding, [^{3}H]-PDBu binding and glucose use are presented in Appendix III.

3.4.1 Characterisation of Visual Cortex Lesions

Microscopic examination of cresyl violet-stained brain sections revealed that infusion of the right hemisphere of the rat visual cortex with ibotenic acid resulted in selective loss of neuronal cell bodies. Within the cortex, the lesion site was well defined in each rat brain being confined to area 17 of the visual cortex and there was no apparent diffusion of toxin to surrounding brain regions. There also appeared to be an abundance of glial elements surrounding the lesion and to a greater extent in the superficial layers of cortex. In most animals (80%), the extent of the lesion was apparent in all cortical areas and was the basic criteria for inclusion in autoradiographic studies. The remaining animals were excluded from subsequent studies. In sham-treated rats, there was minimal evidence of cortical disruption at the injection site, although in some animals, damage to the superficial cortical layers was observed.

3.4.2 [^{3}H]-Forskolin Binding After Unilateral Lesion of the Rat Visual Cortex

In the sham-treated animals, there was no significant alteration in [^{3}H]-forskolin binding between the ipsilateral (lesioned) hemisphere compared to the contralateral (intact) hemisphere. Following ibotenate lesion of the visual cortex, [^{3}H]-forskolin binding was significantly reduced in each cortical layer of the lesioned hemisphere of visual cortex (Figure 35, see also Figure 34). Significant reductions in [^{3}H]-forskolin binding were observed in the ipsilateral superior colliculus (Figure 36) and the ipsilateral dorsal lateral geniculate body (Figure 37). There were no significant alterations in [^{3}H]-forskolin binding in non-visual structures. [^{3}H]-Forskolin

binding was unchanged in each brain region in the contralateral hemisphere of the lesioned group compared to the sham-treated group (ANOVA) (Appendix III(a)).

3.4.3 [^{3}H]-PDBu Binding After Unilateral Lesion of the Rat Visual Cortex

[^{3}H]-PDBu binding was not significantly different between both hemispheres of the sham-treated animals in all structures. Post-lesion, the only significant alteration in [^{3}H]-PDBu binding was observed in layers V-VI of the lesioned visual cortex which was significantly reduced compared to the intact hemisphere. There was no significant difference in [^{3}H]-PDBu binding in all other visual structures (Figures 35, 36 and 37, see also Figure 34) or non-visual structures in the lesioned hemisphere compared to the intact hemisphere. [^{3}H]-PDBu binding was unaltered in the intact hemisphere of the lesioned compared to sham group (ANOVA) (Appendix III(b)).

3.4.4 [^{14}C]-2-Deoxyglucose Utilisation After Unilateral Lesion of the Rat Visual Cortex

In sham-treated animals, injection of buffered saline into the visual cortex caused a reduction in glucose utilisation. The deficit in glucose use was significant in visual cortex layer IV whilst there was a smaller, although not significant reduction in glucose use in layers II-III and layers V-VI in the ipsilateral hemisphere of visual cortex. All other structures exhibited no significant alterations in glucose-use post-lesion in the sham group.

Following infusion of ibotenate into the visual cortex, glucose use was markedly reduced in each layer of the lesioned cortex compared to the intact cortex (Figure 35, see also Figure 34). In the ipsilateral dorsal lateral geniculate body, a small yet consistently significant reduction in glucose use was demonstrated post-lesion (Figure 37). Although there appeared to be a reduction in glucose use in the ipsilateral superior colliculus, there was no significant difference between the lesioned and intact hemisphere (Figure 36). In any other structure examined there was no significant inter-hemispheric differences in glucose use. There was no alteration in glucose use in the intact hemisphere of the lesioned group compared to the sham group (ANOVA) (Appendix III(c)).

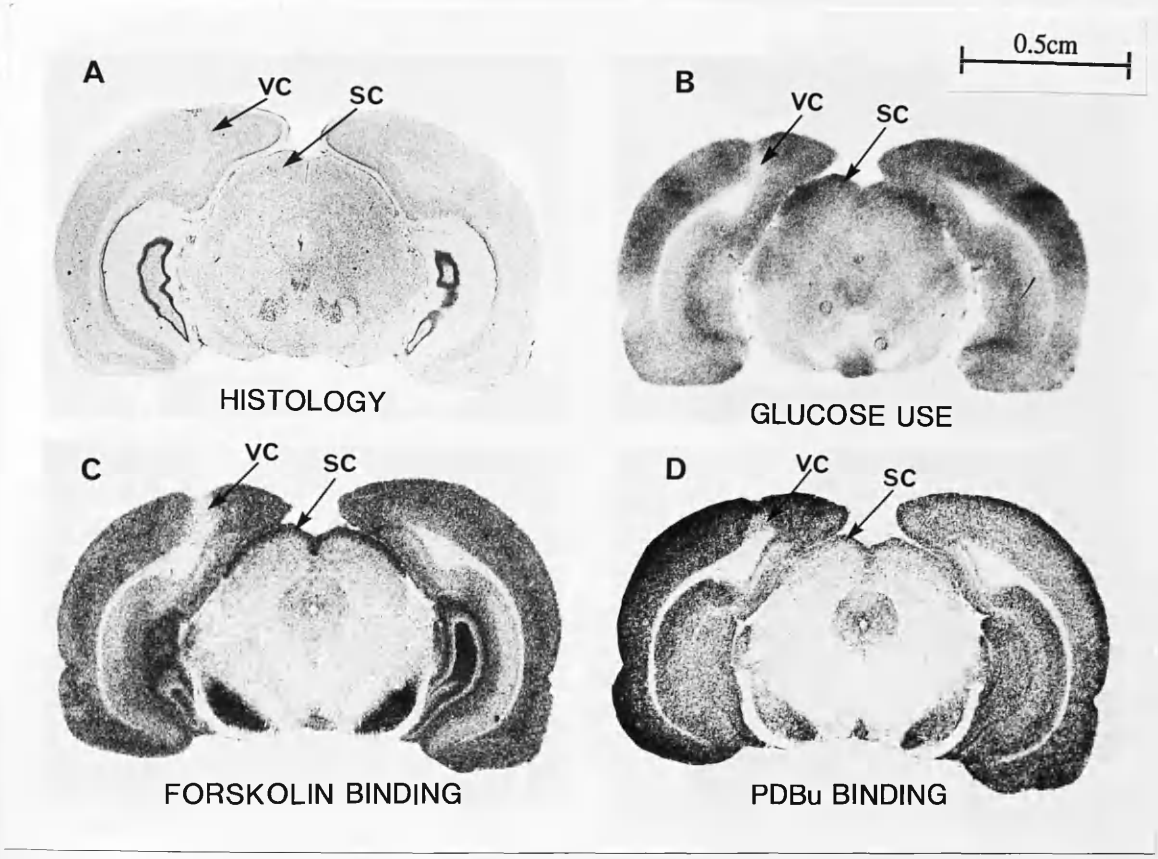

FIGURE 34
HISTOLOGY AND AUTORADIOGRAMS OF GLUCOSE USE, [^{3}H]-FORSKOLIN AND [^{3}H]-PDBu BINDING FOLLOWING LESION OF THE VISUAL CORTEX

Illustrative autoradiograms of (B) glucose use, (C) [^{3}H]-forskolin binding and (D) [^{3}H]-PDBu binding, in adjacent sections, following unilateral lesion of the visual cortex with ibotenic acid. In the same animal, histological verification of a loss of neuronal cell bodies in the visual cortex is shown (A). Note the reduction in glucose use (B) in the lesioned (left) visual cortex (VC). [^{3}H]-Forskolin binding (C) is reduced in the lesioned hemisphere of VC and superior colliculus (SC). [^{3}H]-PDBu binding is slightly reduced in VC but is unaltered in the SC.

Interhemispheric differences are presented of glucose use, [^{3}H]-forskolin binding and [^{3}H]-PDBu binding at 21 days following unilateral lesion of the visual cortex in a sham (n=6) and ibotenate-lesioned group (n=6). Data are expressed as the mean percentage change of the lesioned hemisphere (R) from the intact hemisphere (L) ± SEM. *$p<0.01$, Student's paired t-test.

Interhemispheric differences are presented of glucose use, [^{3}H]-forskolin binding and [^{3}H]-PDBu binding at 21 days following unilateral lesion of the visual cortex in a sham (n=6) and ibotenate-lesioned group (n=6). Data are expressed as the mean percentage change of the lesioned hemisphere (R) from the intact hemisphere (L) ± SEM. *$p<0.01$, Student's paired t-test.

FIGURE 35 GLUCOSE USE, ^{3}H-FORSKOLIN AND ^{3}H-PDBu BINDING FOLLOWING LESION OF THE VISUAL CORTEX

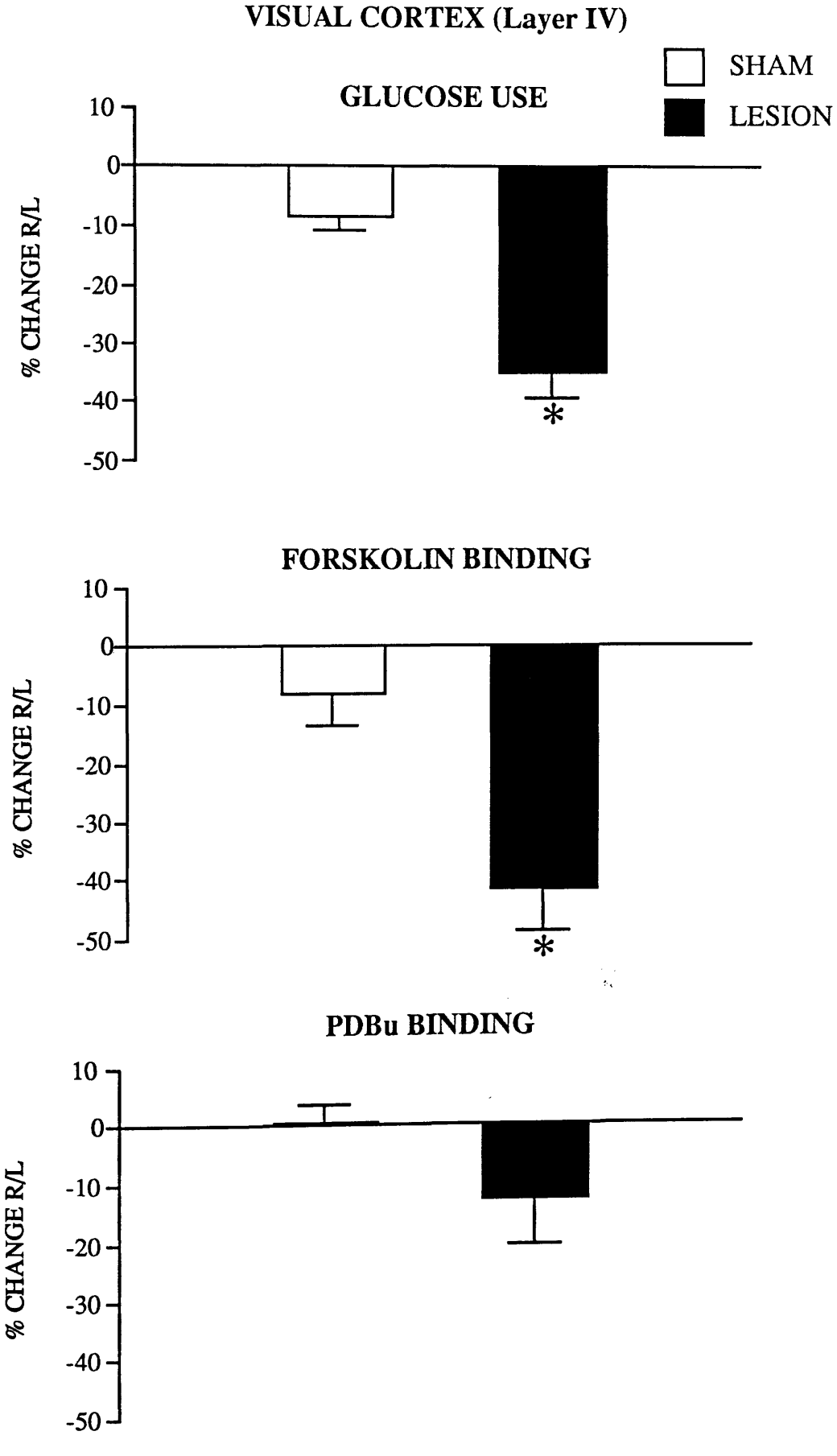

FIGURE 36 GLUCOSE USE, ^{3}H-FORSKOLIN AND ^{3}H-PDBu BINDING FOLLOWING LESION OF THE VISUAL CORTEX

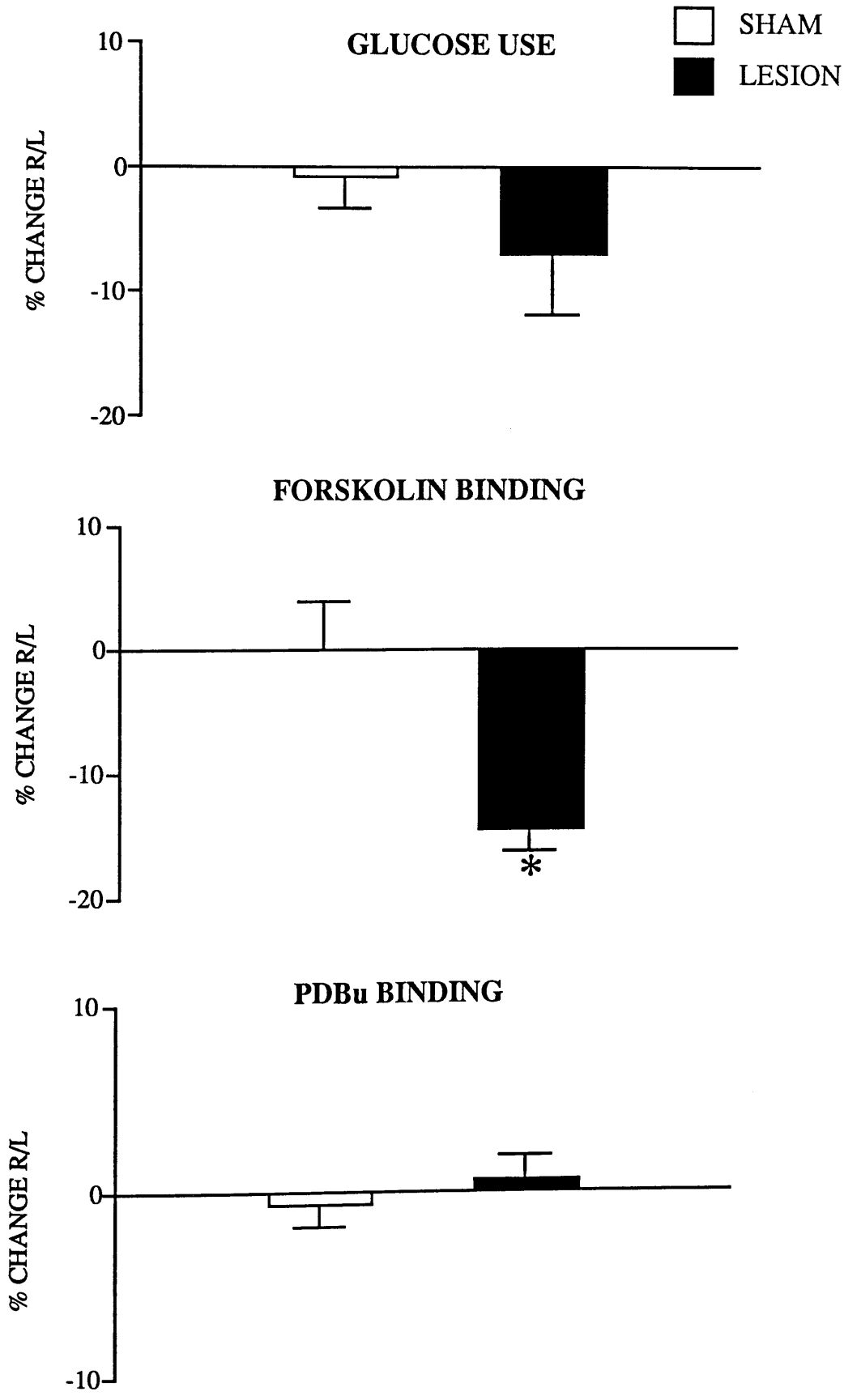

FIGURE 37 GLUCOSE USE, ^{3}H-FORSKOLIN AND ^{3}H-PDBu BINDING FOLLOWING LESION OF THE VISUAL CORTEX

DORSAL LATERAL GENICULATE BODY

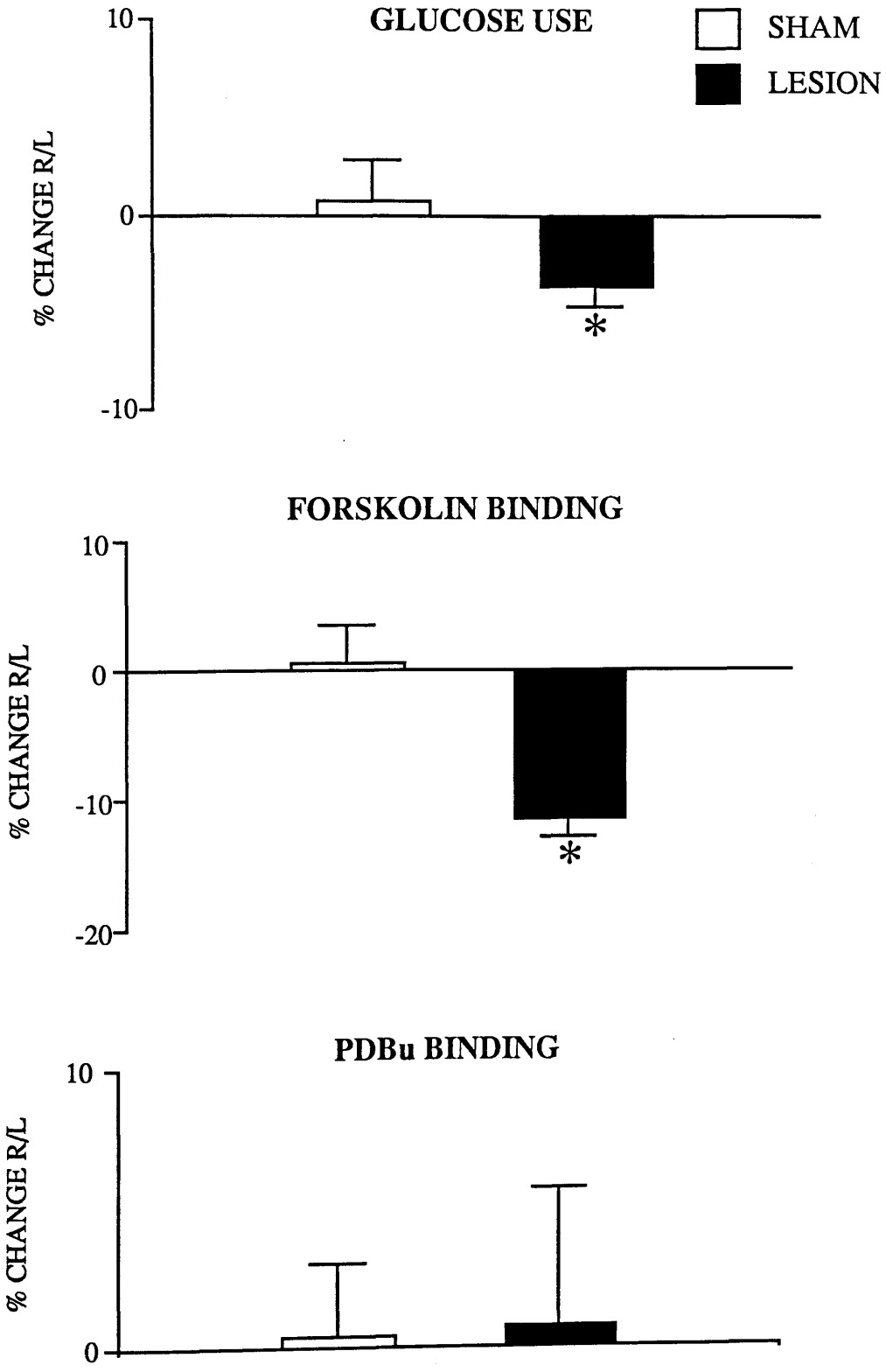

4. SEPTO-HIPPOCAMPAL STUDIES

4.1 Anatomical Localisation of [^{3}H]-Forskolin and [^{3}H]-PDBu Binding in Rat Septo-Hippocampal Pathway.

Both [^{3}H]-forskolin and [^{3}H]-PDBu exhibited a distinct pattern of binding in rat brain. Within the hippocampus the pattern of [^{3}H]-forskolin binding was striking (Figure 39). Intense binding was observed in the polymorph layer of the dentate gyrus with a moderate level of binding in the molecular layer. Dense labelling was also demonstrated in the pyramidal layer of CA3 subfield whilst the strata oriens had a very low density of [^{3}H]-forskolin binding. There were low levels of [^{3}H]-forskolin binding in the medial septum, lateral septum, vertical diagonal band and horizontal diagonal band.

[^{3}H]-PDBu binding was heterogeneous and was particularly dense in the hippocampal formation (Figure 39). The CA1 subfield exhibited the highests levels of binding, within this field [^{3}H]-PDBu binding was highly concentrated in the pyramidal layer. [^{3}H]-PDBu binding was moderate in the CA3 and CA4 subfield. Within the dentate gyrus the molecular layer had the highest [^{3}H]-PDBu binding densities compared to the granular layer. Low levels of [^{3}H]-PDBu binding were demonstrated in the medial septum, vertical diagonal band and horizontal diagonal band compared to the lateral septum which exhibited higher densities of [^{3}H]-PDBu binding. The entorhinal cortex demonstrated markedly high densities of [^{3}H]-PDBu binding compared to all other structures, [^{3}H]-PDBu binding being most concentrated in the superficial layers.

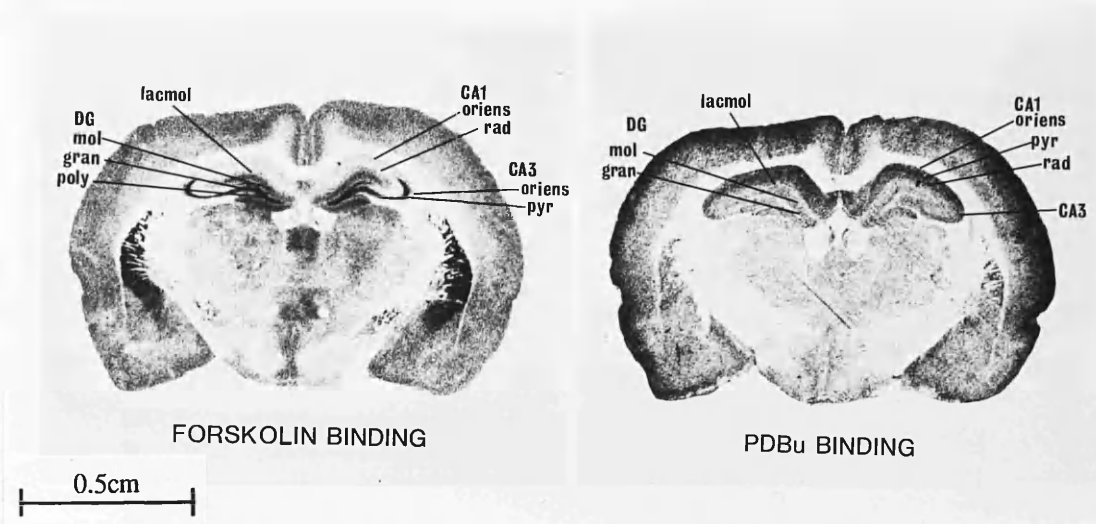

FIGURE 38
AUTORADIOGRAMS OF [^{3}H]-FORSKOLIN AND [^{3}H]-PDBu BINDING IN THE RAT HIPPOCAMPUS

Representative autoradiograms of [^{3}H]-forskolin and [^{3}H]-PDBu binding in rat brain sections at the level of the dorsal hippocampus. Abbreviations are: oriens, pyramidal (pyr) and radiatum (rad) layers of CA1, CA3 fields of Ammon's horn; molecular (mol), granular (gran) and polymorph (poly) layers of dentate gyrus (DG) and stratum lacunosum moleculare (lacmol).

4.2 Ligand Binding to Second Messenger Systems After Lesion of the Rat Septo-Hippocampal Pathway

Full quantitative analysis of [^{3}H]-forskolin and [^{3}H]-PDBu binding are presented in Appendix VI.

4.2.1 Characterisation of Medial Septum Lesion

Ibotenate lesion of the rat medial septum was confirmed histologically in cresyl-violet stained brain sections adjacent to those used in ligand binding studies. The lesion was confined to the medial septum with minimal damage to the lateral septum and vertical diagonal band and resulted in a selective loss of neuronal cell bodies. In sham-treated animals, neuronal cell bodies remained intact and there was minimal evidence of cellular disruption.

4.2.2 [^{3}H]-Forskolin Binding After Lesion of the Rat Septo-Hippocampal Pathway

Following ibotenate-lesion of the medial septum, [^{3}H]-forskolin binding was significantly decreased at the injection site (-19%) compared to the sham treated group. Further, a significant increase in [^{3}H]-forskolin binding was demonstrated in the polymorph layer of the dentate gyrus (19%) whilst [^{3}H]-forskolin binding remained unaltered in all other limbic structures post-lesion.

4.2.3 [^{3}H]-PDBu Binding After Lesion of the Rat Septo-Hippocampal Pathway

A significant increase in [^{3}H]-PDBu binding was demonstrated in the superficial layers (I-III) of the entorhinal cortex (27%) following lesion of the medial septum. There were no significant alterations in [^{3}H]-PDBu binding in any other brain region in the lesion group compared to the sham treated groups.

FIGURE 39
LIGAND BINDING TO SECOND MESSENGER SYSTEMS FOLLOWING MEDIAL SEPTAL LESION

Quantitative autoradiographic measurements are presented of [^{3}H]-forskolin binding and [^{3}H]-PDBu binding at 21 days following lesion of the medial septum in a sham (n = 7) and ibotenate-lesioned group (n = 7). Histograms are presented as mean ± SEM; *$p<0.05$, Student's unpaired t-test. Roman numerals indicate the cortical layers examined in entorhinal cortex whilst the polymorph layer of the dentate gyrus is abbreviated to DG poly.

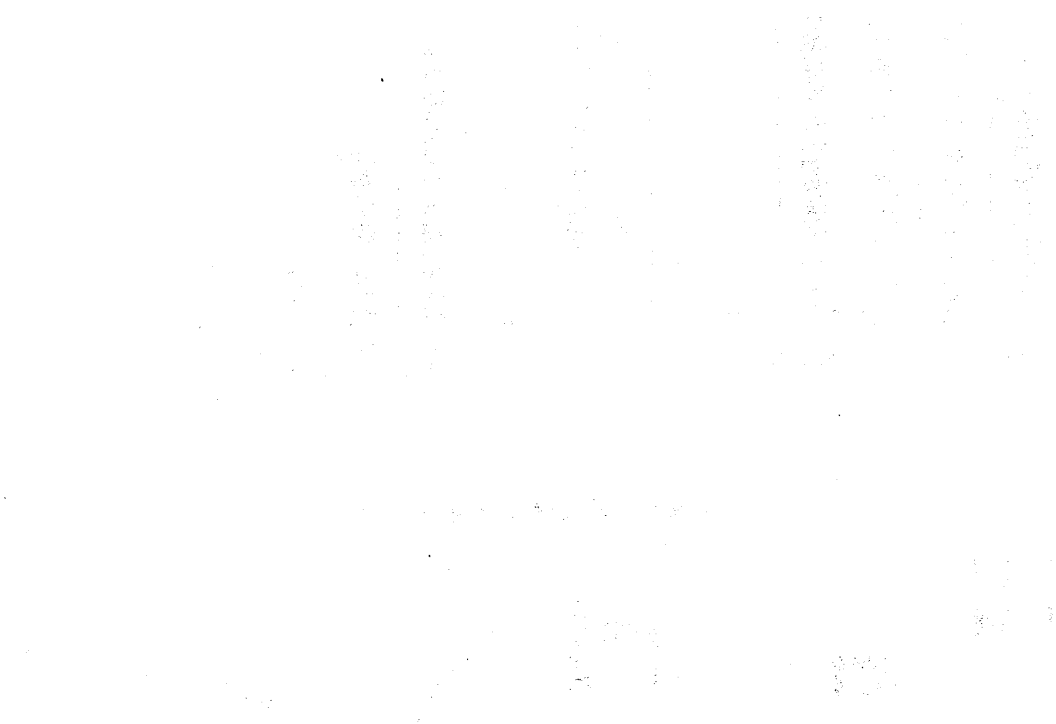

FIGURE 39 LIGAND BINDING TO SECOND MESSENGER SYSTEMS FOLLOWING MEDIAL SEPTAL LESION

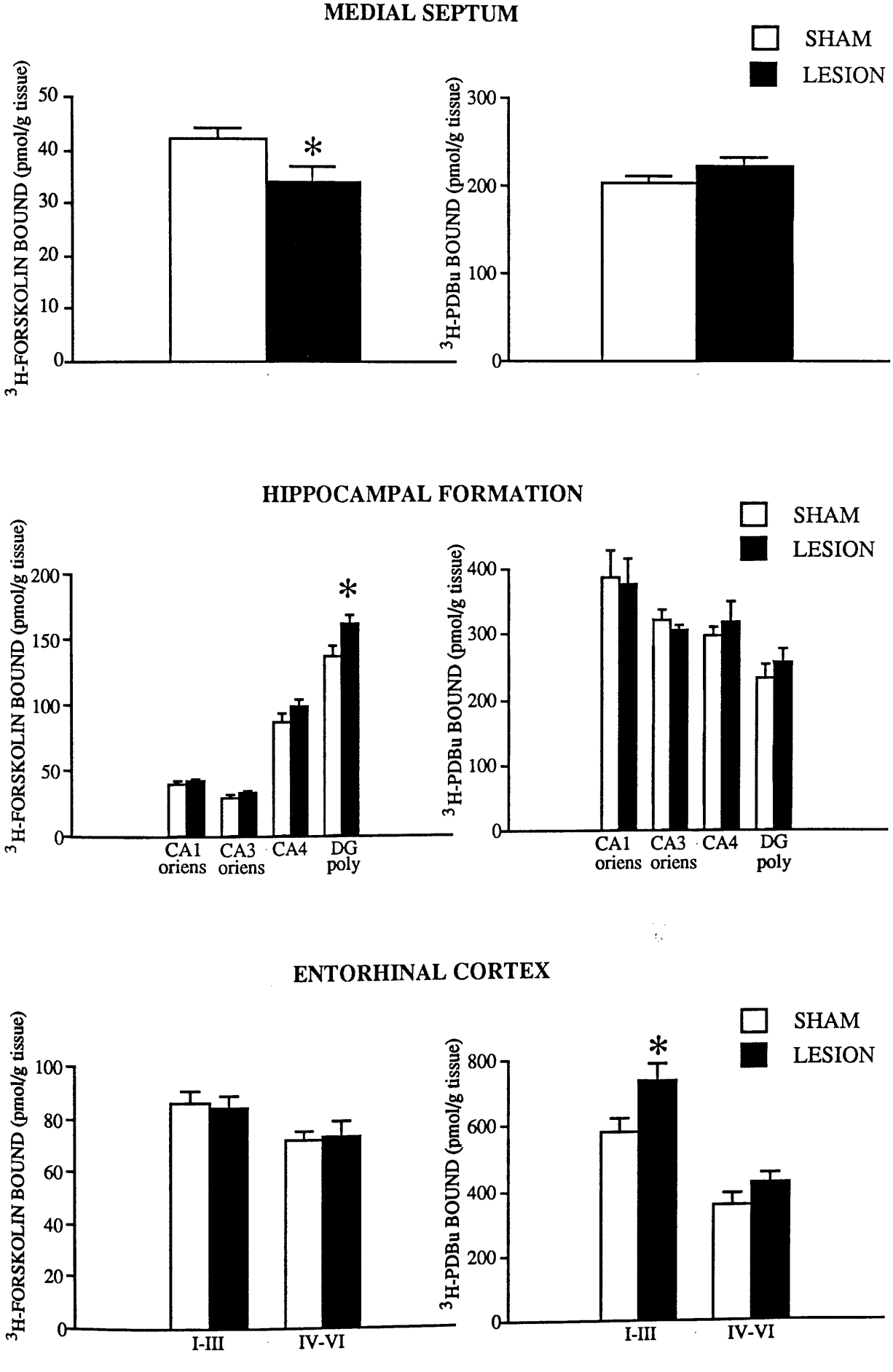

CHAPTER IV

DISCUSSION

1. SECOND MESSENGER LIGAND BINDING IN ALZHEIMER'S DISEASE

The classical hallmarks of Alzheimer's disease (AD) are characterised neuropathologically by the presence of numerous neuritic plaques and tangles. Although several neurochemical abnormalities have been demonstrated in AD, a profound reduction of presynaptic cholinergic innervation of cerebral cortex and hippocampus is consistently found in AD brain. In the past decade, neurotransmitter receptors have been the focus of intensive investigation in AD. Ligand binding techniques have demonstrated alterations in a number of neurotransmitter receptors in AD such as muscarinic (Perry et al. 1986; Smith et al. 1988); $5HT_2$ (Cross et al. 1986; Perry et al. 1984); $5HT_1$ (Bowen et al. 1983; Cross et al. 1988) and nicotinic (Nordberg et al. 1986). However, it is the integrity of neurotransmitter receptors with their associated signal transduction systems which determines normal cellular responses. There has been minimal attention directed towards transduction mechanisms in AD. In view of the ineffectiveness of receptor-targeted drug therapy in AD patients, the assessment of the functional capabilities of receptors (transduction mechanisms), as well as their distribution in AD, is vitally important if the possibilities of drug treatment for this condition are ever to be realised.

The present study represents a comprehensive examination of ligand binding to second messenger systems in AD. Quantitative autoradiography was used to map the distribution and density of [^{3}H]-forskolin binding to G_s-adenylate cyclase and [^{3}H]-phorbol 12,13 dibutyrate binding to protein kinase C (PKC) in three brain regions; middle frontal and temporal cortex and the

hippocampal formation, areas known to be severely affected by the neuropathological and neurochemical correlates of the disease.

1.1 [^{3}H]-Forskolin Binding in Alzheimer's Disease

In two separate series, [^{3}H]-forskolin binding was investigated in a total of 15 controls and 16 age-matched patients with AD in middle frontal and temporal cortices and in the hippocampal formation. [^{3}H]-Forskolin binding was differentially altered in AD brain despite all regions exhibiting significant AD neuropathology and neurochemical alterations. There appeared to be a regional hierarchy of [^{3}H]-forskolin binding reductions in AD brain ranging from the middle frontal cortex (in which it is consistently reduced in AD) to most of the hippocampal formation (in which it is minimally reduced) (Table 8). In the middle temporal cortex and the molecular layer of the dentate gyrus, there was evidence that [^{3}H]-forskolin binding was lower in AD patients compared to control subjects. Whether these changes achieved the probability level of 5% must be influenced to a certain extent by the group sizes, the variability of measurements and the errors of sampling a heterogeneous population.

Extrinsic factors such as temperature, pH and salt concentrations of buffer medium, differences in batches of radioistopes and methodological variations, may contribute to the amount of [^{3}H]-forskolin bound in brain tissue sections. In support of this, substantially elevated [^{3}H]-forskolin binding levels in the second population of control brain were demonstrated to be almost twice the levels detected in the previous control group. Since

TABLE 8

ALTERATIONS IN [^{3}H]-FORSKOLIN BINDING IN AD BRAIN IN TWO SEPARATE STUDIES

	SERIES 1	SERIES 2	
Middle Frontal Cortex			
Layers I/III	3.24 (-50%)	3.95 (-34%)	Consistently
Layer IV	2.89 (-46%)	2.74 (-28%)	Reduced
Layers V-VI	2.83 (-43%)	2.85 (-26%)	Significantly
Middle Temporal Cortex			
Layers I-III	0.70 (-18%)	3.36 (-36%)	
Layer IV	0.88 (-26%)	3.38 (-33%)	Inconsistently
Layers V-VI	0.85 (-21%)	3.31 (-30%)	Reduced
			Significantly
Hippocampal Region			
Molecular Layer	0.74 (-21%)	2.54 (-38%)	
Granular Layer	0.12 (3%)	1.27 (-21%)	
CA1	0.25 (1%)	0.35 (-5%)	
CA3	0.01 (0%)	1.02 (-17%)	
CA4	0.16 (-1%)	1.05 (-17%)	Not Reduced
Hilus	0.23 (1%)	1.97 (-28%)	Significantly
Lacunosum moleculare	0.49 (-14%)	1.79 (-29%)	
Subiculum	0.13 (4%)	1.05 (-19%)	
Parahippocampal Gyrus: Superficial layer	0.04 (0%)	1.37 (-19%)	
Deep layer	0.20 (-1%)	0.94 (-15%)	

p_3 values indicated above are derived from statistical comparison of [^{3}H]-forskolin binding in control and AD brain using Student's unpaired t-test. [^{3}H]-Forskolin binding was determined in two separate studies; Series 1 (see Results section 1.4) and Series 2 (see Results section 2.5). The magnitude of alterations between control and AD are indicated in brackets.

the second study was performed a year following completion of the first study, the technical improvement of [^{3}H]-forskolin autoradiography may contribute to the overall increase in specific [^{3}H]-forskolin binding and decrease the variability within control and AD groups.

The initial study was limited to six control and seven AD cases, and it was noted that the coefficient of variation of [^{3}H]-forskolin binding, in each brain region examined, was greater in comparison to the second study. The variability of neurochemical measures determines the magnitude of alterations required, between ligand binding in control and AD groups, at which statistical significance is achieved. Statistical power analysis (Cohen, 1977) indicates the variability of groups to be the prerequisite for detection of significant alterations in experimental procedures, with minimal importance placed on group size.

The heterogeneity of patient groups must go some way to explaining the differential alterations in [^{3}H]-forskolin binding in two separate cohorts of AD brain. The degree of neuropathological abnormalities, in terms of neuronal loss and the presence of neuritic plaques and neurofibrillary tangles between patients must influence inter-individuality and, to a certain extent, [^{3}H]-forskolin binding alterations. Direct evidence of this within the groups, was the demonstration of two patients, 4AD and 7AD, which exhibited markedly lower levels of binding in middle temporal cortex than the mean value of the other five AD patients, which was similar to control values.

Furthermore, both cases, 4AD and 7AD, were found to have high numbers of plaques in middle temporal cortex, compared to most of the remaining AD cases.

It is interesting that in the first cohort of AD patients, [^{3}H]-forskolin binding was profoundly reduced in middle frontal cortex to a greater extent than in middle temporal cortex. Yet in the second group of AD cases, reductions in [^{3}H]-forskolin binding were of a similar magnitude in both middle frontal and temporal cortex and these reductions in binding were not as pronounced as those previously demonstrated. These inconsistencies in differences between cortical regions are exemplified in in vivo neuroimaging studies of AD patients (Haxby et al. 1985 & 1988; Horwitz et al. 1987) and are demonstrative of the heterogeneity of AD. It has also been suggested that the earliest and most severe metabolic reductions in temporal and parietal cortex of AD patients progress to involve frontal cortex in more severely demented patients (Haxby et al. 1988). Thus, these discrepancies in [^{3}H]-forskolin binding may be a reflection of the different stages of AD within the patient groups. The degree of cholinergic deficit appears to be associated with the degree of cognitive impairment in AD (Perry et al. 1978; Wilcock et al. 1982). [^{3}H]-Forskolin binding was positively correlated with ChAT activity in cortical regions of AD brain which demonstrated significant reductions in binding sites. Thus, an association between the degree of cholinergic innervation and [^{3}H]-forskolin binding is evident in cortex which may imply a functional relationship between these parameters.

The question of whether [^{3}H]-forskolin binding simply reflects the degree of neuronal fallout should be addressed. A marked loss of neurons has been demonstrated in cortical (Mountjoy et al. 1983; Terry et al. 1981) and hippocampal (Probst et al. 1988) regions in AD brain. It may be suggested that the differential alterations in [^{3}H]-forskolin binding are simply a reflection of the severity of neuronal fallout in these AD brain areas. Loss of pyramidal cells from frontal cortex in AD has been estimated as 25 - 45% (Mountjoy et al. 1983; Terry et al. 1981). Such a loss may explain the deficit in [^{3}H]-forskolin binding demonstrated to be up to 50% in this brain region. However, this explanation would imply that almost all cortical pyramidal neurons in frontal cortex have [^{3}H]-forskolin binding sites. Whether this is true or not remains to be ascertained. Although this may be an explanation for events in frontal cortex, the demonstration of inconsistent reductions in [^{3}H]-forskolin binding in middle temporal cortex and the relative stability of binding in the hippocampal region (areas which exhibit severe neuronal loss) would argue that this association of [^{3}H]-forskolin binding losses with neuronal loss is over-simplistic.

In middle temporal cortex, neuronal loss is reported to be of a similar magnitude to that observed in frontal cortex (Mountjoy et al. 1983; Terry et al. 1981). Five of the AD group showed similar levels of [^{3}H]-forskolin binding compared with the controls, whilst the remaining two (4AD and 7AD) exhibited much lower levels of binding. A negative correlation has been demonstrated between neuronal counts and plaque numbers (Mountjoy et al. 1983). If neuronal loss was associated with [^{3}H]-forskolin binding, then cases

4AD and 7AD would be expected to have high numbers of plaques compared to the rest of the group. This indeed was shown to be the case in middle temporal cortex. However, another case had approximately double the number of plaques compared to the rest of the AD group but did not have excessively low levels of [^{3}H]-forskolin binding.

There was a reduction in [^{3}H]-forskolin binding in the molecular layer of the dentate gyrus in AD. This may be indicative of a loss of presynaptic input from the entorhinal cortex which often exhibits marked cell loss in AD (Hyman et al. 1984; Geddes et al. 1985; Hyman et al. 1987). In the present study, the status of entorhinal cortex as regards pathological abnormalities in this AD population was unclear. However, the robustness of [^{3}H]-forskolin binding in hippocampal regions exhibiting severe pathology implies that cellular loss is not always associated with [^{3}H]-forskolin binding reductions in AD. Neuronal loss in the hippocampal formation has been shown to be marked in the subiculum and in the CA1 fields of Ammon's Horn (Hyman et al. 1984), and can represent as much as up to 50% of control values (Probst et al. 1988). Despite this, [^{3}H]-forskolin binding remained unaltered in these hippocampal regions.

Under autoradiographic conditions, [^{3}H]-forskolin binding is purported to be associated with the coupling of a stimulatory guanine-nucleotide regulatory protein (G_s) with adenylate cyclase (Gehlert et al. 1985; Seamon & Daly, 1981; Worley et al. 1986a). A number of receptors, such as β-adrenergic, dopamine D_1, adenosine A_2 and vasoactive intestinal

polypeptide, mediate cellular responses via G_s activation (Levitzki, 1987). In the hippocampus, β-adrenergic receptors are altered - β_1 receptors are being reduced in AD whilst β_2 receptors are increased (Shimohama et al. 1987), individual events which could cancel each other out with regard to their effects on [^{3}H]-forskolin binding. In frontal cortex neither β_1 nor β_2-adrenergic receptors are altered (Shimohama et al. 1987). Similarly, total dopamine receptors (D_1 and D_2) as measured by [^{3}H]- spiroperidol binding are unchanged in AD frontal cortex (Reisine et al. 1978). Of the other receptors which are associated with G_s, such as adenosine A_2 or vasoactive intestinal polypeptide, it is unclear whether they are altered in AD. A loss of elements containing these receptors may contribute to the [^{3}H]-forskolin binding deficit. Alternatively, it may be that whilst the recognition sites (such as β-adrenergic and dopaminergic receptors) appear to be robust in AD frontal cortex, their associated intraneuronal mechanisms are disrupted. Interestingly, a recent study in rat brain has demonstrated that following transient forebrain ischaemia, dynamic alterations in [^{3}H]-forskolin binding occur in the absence of histological evidence of neuronal damage and minimal neurotransmitter receptor alterations (Onodera & Kogure, 1989).

[^{3}H]-Forskolin binding sites may not be identical in different brain regions. In some regions of rat brain, such as the striatum, [^{3}H]-forskolin binding is enhanced in the presence of Mg^{2+} and guanine nucleotides (Gehlert, 1986; Poat et al. 1988). In the present studies, [^{3}H]-forskolin binding was examined in the presence and absence of a non-

hydrolyzable guanine nucleotide, 5'guanylimidodiphosphate (Gpp(NH)p) which at 10μM is reported to maximally increase binding in the rat striatum (Gehlert, 1986). Gpp(NH)p showed a selective capacity to alter [^{3}H]-forskolin binding in specific regions of postmortem human brain. In both frontal and temporal cortex, in the presence of Gpp(NH)p, [^{3}H]-forskolin binding was significantly increased in the superficial layers I-III whilst there was no change in [^{3}H]-forskolin binding in deeper layers IV-VI. In the hippocampus, Gpp(NH)p had no effect on [^{3}H]-forskolin binding. Similarly in rat brain, [^{3}H]-forskolin binding in the hippocampus has been shown to be unaltered (Gehlert, 1986) and even reduced (Poat et al. 1988) in the presence of guanine nucleotides. This evidence may suggest that interactions between G_s and the catalytic subunit of adenylate cyclase are not mediated by identical molecular mechanisms in different brain regions. Gpp(NH)p stimulates both the stimulatory and inhibitory G-proteins (G_s and G_i). Perhaps, it is the case that in the presence of Gpp(NH)p, activation of G_i may alter the coupling of G_s with adenylate cyclase. Evidence already suggests that the $\beta\gamma$ subunits of G_i may inhibit G_s coupling with adenylate cyclase (Gilman, 1984). Depending on the abundance of G_i in different brain regions, this may be a predisposing factor to alterations in [^{3}H]-forskolin binding by Gpp(NH)p. It is now clear that there may exist different subspecies of both G_s (Bray et al. 1986; Kozasa et al. 1988) and adenylate cyclase (Mollner & Pfeuffer, 1988). The heterogeneity of G_s and adenylate cyclase may account for the non-uniform action of Gpp(NH)p stimulation on [^{3}H]-forskolin binding.

The ability of Gpp(NH)p to both enhance [^{3}H]-forskolin binding in control cortical sections, whilst having no effect on [^{3}H]-forskolin binding in the hippocampus, was conserved in AD brain. From this it could be inferred that the coupling mechanism of G_s with adenylate cyclase remains intact. However, one preliminary study has suggested a partial uncoupling of cerebral cortical muscarinic M_1 receptors from G-proteins in AD (Smith et al. 1987). Likewise, a similar type of receptor-G-protein uncoupling has been demonstrated in a detailed study of dopamine D_1 receptors in the amygdala of patients with Huntington's Disease (DeKeyser et al. 1989). In contrast, the integrity of the adenylate cyclase coupling with G-proteins has been suggested to be functionally preserved in the hippocampus and parietal cortex in AD patients (Danielsson et al. 1988). Signal transduction mechanisms may be funtionally impaired at the receptor-G-protein level but remain intact at the level of G-protein-adenylate cyclase interaction. This remains to be established. From the present studies, it would at least appear true that the capacity of Gpp(NH)p to alter [^{3}H]-forskolin binding is similar in AD brain compared with controls.

In summary, [^{3}H]-forskolin binding was differentially altered in three brain regions which were severely affected by the pathology normally associated with AD. It may be that there is a selective loss of elements to which forskolin binds in frontal cortex, or that in hippocampus (and in some cases in middle temporal cortex), compensatory mechanisms have come in to play to upregulate these elements. Finally, it is possible that forskolin binding sites are not identical in different regions of the human brain, and

that these differences may reflect different molecular mechanisms underlying G_s-adenylate cyclase interactions.

1.2 [^{3}H]-Phorbol 12,13 Dibutyrate Binding in Alzheimer's Disease

Quantitative autoradiography was employed to investigate [^{3}H]PDBu binding in parallel with homogenate binding to particulate and cytosolic fractions in a well-defined cohort of AD brains. Both studies clearly demonstrated that [^{3}H]-PDBu binding is preserved in middle frontal and temporal cortex and the hippocampal formation of an AD population which was markedly affected by the neuropathological and neurochemical correlates of the disease.

[^{3}H]-PDBu binds with high affinity to PKC (Kikkawa et al. 1983) and has provided a powerful tool for mapping the distribution and density of this enzyme in rat brain (Worley et al. 1986a, 1986b, 1987). This is the first systematic study which has investigated [^{3}H]-PDBu binding in both normal and AD postmortem brain using quantitative autoradiography. Evidence has now accumulated which implicates abnormalities in the phosphoinositide (PI) system in AD brain. An initial study (Stokes & Hawthorne, 1987) demonstrated a profound reduction of PI in temporal cortex preparations from AD patients. Ligand binding studies have since shown a marked loss of [^{3}H]-inositol 1,4,5 trisphosphate binding in parietal cortex and hippocampus AD brain tissue homogenates (Young et al. 1988). Significant reductions in PKC, as measured by [^{3}H]-PDBu binding, have now been reported in frontal cortex samples of AD brain (Cole et al. 1988). This reduction in

[^{3}H]-PDBu binding was demonstrated in the particulate fraction of AD cortex, but not in the cytosolic fraction. These results are in contrast to those reported here, where PKC has clearly been shown to be robust in both autoradiographic and homogenate binding studies in three brain regions. However, the investigation by Cole et al. (1988) was limited to one area of AD brain, frontal cortex, and the exact neuroanatomical location of the PKC deficit, if any, within the cortex was not known with precision.

In this present study, it was clear that all AD brain exhibited extensive signs of the pathology classically associated with the disease, namely numerous neuritic plaques and cholinergic hypofunction. In the study by Cole et al. (1988) which demonstrated a loss of PKC, there was no index as to the severity of the disease in their AD patient population. The heterogeneity of patient groups, especially in terms of neuropathological abnormalities, could have a major impact on postmortem studies.

Inconsistencies in the literature are exemplified by the studies of neurotransmitter receptors in AD brain. In particular, receptors which are linked with the PI system, such as muscarinic and $5HT_2$ receptors have been the subject of controversy in AD studies. Muscarinic receptors have been reported to be unchanged (Bartus et al. 1982; Davies & Verth, 1978; White et al. 1977) and reduced (Reisine et al. 1978; Shimohama, 1986; Wood et al, 1983) in AD. Selective alterations in muscarinic receptors have also been demonstrated with a reported decrease of M_2 receptors and no change in M_1 receptors in AD brain (Mash et al. 1985). It has also been suggested that

the number of muscarinic receptors per pyramidal cell may be increased in the hippocampus of AD subjects (Probst et al. 1988). One of the most consistent neurotransmitter receptor alterations in AD reported to date has been the repeated finding of a reduction in $5HT_2$ receptors (Cross et al. 1986, 1988; Perry et al. 1984; Sparks, 1989). Yet, a recent report has demonstrated that $5HT_2$ receptors may remain unchanged in a well-defined population of AD brains (Dewar et al. 1990). Differences in the methodology employed to characterise neurotransmitter receptors or indeed second messenger systems by using, for instance, homogenate binding as compared to quantitative autoradiography must go some way to explaining contrasting reports. This is exemplified by the study of [^{3}H]-kainate receptors in AD. Using quantitative autoradiography, a selective increase in [^{3}H]-kainate binding sites in AD frontal cortex, specifically localised only in deep cortical layers, has been demonstrated (Chalmers et al. 1990). This contrasts with ligand binding studies using homogenate preparations of AD brain tissue which showed no change in [^{3}H]-kainate binding sites (Cowburn et al. 1988). Furthermore, differences in the degree of local neuropathology such as neuronal loss, neurofibrillary tangles and neuritic plaques between different patient groups may influence alterations in binding sites. Associations between the extent of local neuropathology and neurochemical alterations are often observed (Mountjoy, 1986). It may be essential, in order to understand the functional significance of such a diversity of conflicting findings that patient populations be well-defined in terms of neuropathological and neurochemical alterations.

In the same AD patients and controls, selective reductions of [^{3}H]-AMPA and [^{3}H]-kainate binding sites were demonstrated in discrete regions of the hippocampal formation, using quantitative autoradiography in adjacent sections to those used for analysis of [^{3}H]-PDBu binding,(Dewar et al. 1991, in press). Moreover, the quisqualate metabotropic receptor associated with PI hydrolysis in the hippocampus (Sladeczek et al. 1988) was selectively reduced in the CA1 field and subiculum of the AD group - patients in which a preservation of [^{3}H]-PDBu binding to PKC has been clearly demonstrated. In AD, speculative hypotheses have implicated glutamatergic mechanisms in the aetiology of the disease (Greenamyre, 1986; Maragos et al. 1987). Increasingly evident is the important role PKC plays in mediating glutamate-induced neuronal death (Favaran et al. 1988, 1990; Manev et al. 1989). Prolonged glutamate receptor stimulation is associated with a translocation of PKC from the cytosol to the membrane. In the present study, homogenate binding of [^{3}H]-PDBu to PKC in particulate and cytosolic fractions showed there was no significant difference between AD hippocampus compared with control. Although this might indicate that there was no alteration in the translocation of PKC, this does not dismiss a regional-specific alteration of PKC translocation. However, if increased PKC translocation within the hippocampus was expected, then using quantitative autoradiography of [^{3}H]-PDBu binding to PKC which is suggested to map membrane-bound PKC (Onodera et al. 1989; Olds et al. 1989), an <u>increase</u> in [^{3}H]-PDBu binding would be expected. In addition, it may be significant that CA1 field and the subiculum of the hippocampus exhibit receptor losses, extensive neuronal fallout and the presence of numerous

plaques in AD, (Probst et al. 1988; Hyman et al. 1984) while PKC, which is highly concentrated in these regions, remains unchanged.

Furthermore, in the same population of AD and control patients, quantitative autoradiographic analysis of [^{3}H]-forskolin binding to G_s-adenylate cyclase demonstrated marked alterations in both cortical and hippocampal regions of AD brain (see Appendix V), whilst [^{3}H]-PDBu binding to PKC remained unaltered. Functional dysbalance of the adenylate cyclase system and phosphatidylinositol (PI) cycle has been proposed to occur in affective disorders. Hypofunction of the adenylate cyclase system with an absolute or relative dominance of PI-mediated responses has been demonstrated in depression whilst mania has been proposed to result from the converse (Wachtel, 1988, 1989). However, it remains to be established if the selective vulnerability of the G_s-adenylate cyclase system as opposed to the apparent stability of PKC is of any functional relevance in AD.

The densities of [^{3}H]-forskolin binding were compared with [^{3}H]-PDBu binding in the same control and AD patients (Figure 40). Comparison of ligand binding data indicated two main points. Firstly, there was a degree of association between [^{3}H]-forskolin binding and [^{3}H]-PDBu binding particularly in cortex, and secondly, the density of [^{3}H]-PDBu binding was variable within the control and AD groups in cortical regions. In middle temporal cortex there was an obvious association between the level of [^{3}H]-forskolin binding and [^{3}H]-PDBu binding. AD cases which exhibited significantly low [^{3}H]-forskolin binding densities in this region were similarly

FIGURE 40
COMPARISON OF [^{3}H]-FORSKOLIN BINDING WITH [^{3}H]-PDBu BINDING IN CONTROL AND AD BRAIN

Quantitative autoradiographic measurements are presented of [^{3}H]-forskolin binding and [^{3}H]-PDBu binding, in adjacent sections, in the same population of control and AD brain (series 2). Data is presented for measurements made in middle frontal cortex (layers I-II), middle temporal cortex (layers I-II) and the molecular layer of the dentate gyrus. Each of these brain regions exhibited significant reductions in [^{3}H]-forskolin binding in this AD group, whilst [^{3}H]-PDBu binding was unaltered. Note the association between [^{3}H]-forskolin and [^{3}H]-PDBu binding in middle temporal cortex.

FIGURE 40 COMPARISON OF ^{3}H-FORSKOLIN BINDING WITH ^{3}H-PDBu BINDING IN CONTROL AND AD BRAIN

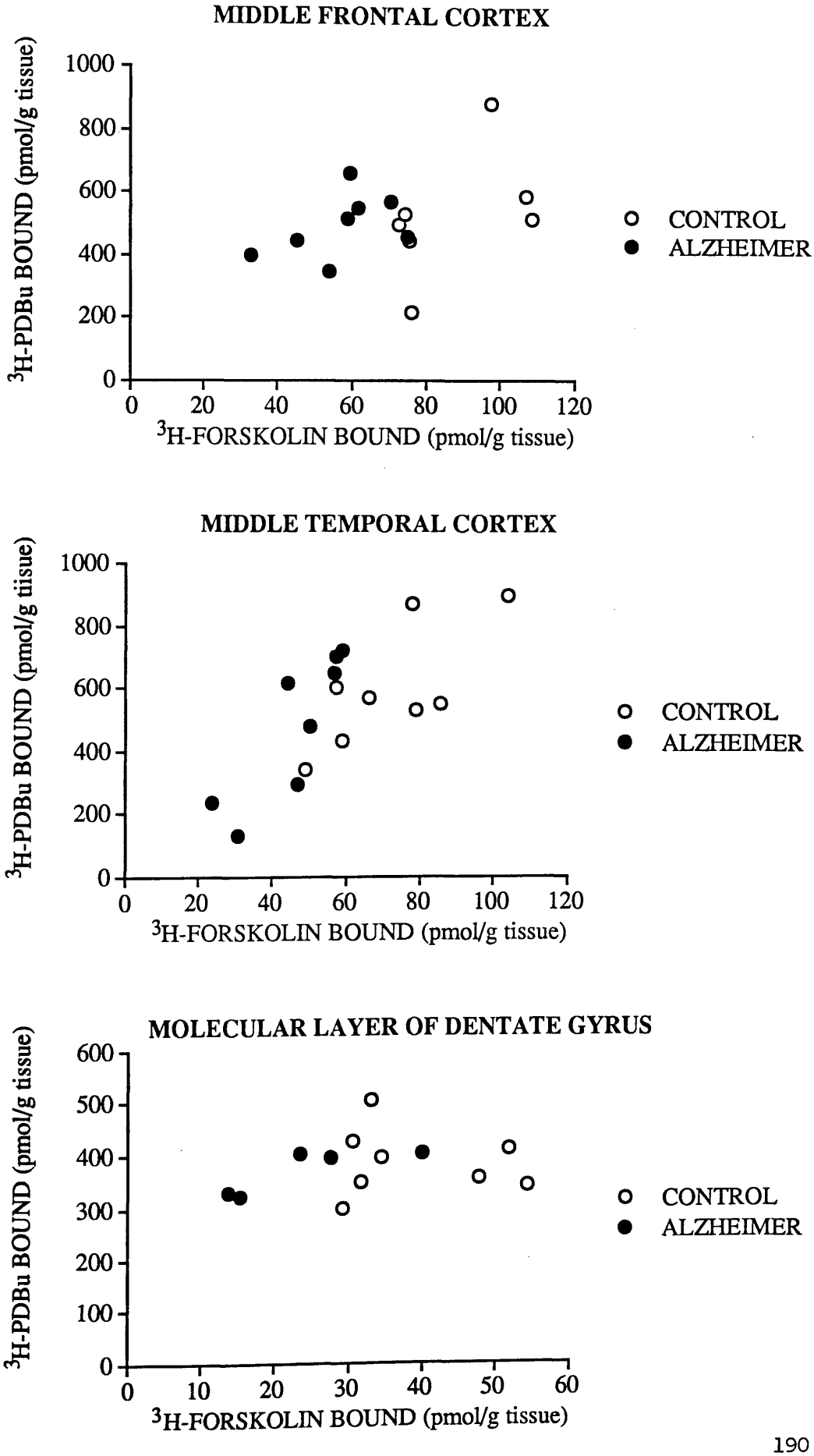

shown to have low densities of [^{3}H]-PDBu binding. However, in this cortical region, the variability of [^{3}H]-PDBu binding in addition to the limited number of control (n=8) and AD (n=8) cases would appear to preclude detection of significant alterations in this ligand binding site in AD compared with to controls. Three AD cases, 45AD, 31AD and 25AD, were found to have exceedingly low densities of [^{3}H]-PDBu binding compared to the remaining five AD cases. Perhaps if a greater number of AD patients had been examined, then an alteration in [^{3}H]-PDBu binding in AD compared to controls would have been more readily detectable. The heterogeneity of patient groups is undoubtedly a major factor influencing the outcome of ligand binding studies and will go some way to explaining the discrepancies between different laboratories. The inter-individuality of patient groups is likely to be the basis of the conflicting findings in the present study, showing PKC to be preserved, in comparison to a previous report demonstrating PKC to be profoundly reduced in AD brain (Cole et al. 1988).

It is interesting that the putative association of [^{3}H]-PDBu binding with [^{3}H]-forskolin binding in middle temporal cortex is not as obvious in middle frontal cortex. The reduction in [^{3}H]-forskolin binding is less marked in frontal cortex as compared to temporal cortex in this AD group, perhaps indicating differential extents of neuronal loss and neuropathological abnormalities between these cortical regions. It does appear that [^{3}H]-PDBu binding to PKC is altered in AD, but only in AD cases which exhibit profound losses of [^{3}H]-forskolin binding. This may imply that a threshold of neuronal fallout, corresponding to severe degrees of neuronal loss, is

required in AD brain, beyond which PKC is altered. There exists the possibility that intact neurons in AD brain may still be able to compensate by upregulating PKC, in response to the loss of this enzyme in degenerating neurons.

Experimentally-lesioned animal models have indicated that second messenger systems may be capable of adaptive change. Under normal conditions, it has been demonstrated that a close relationship exists between receptor occupancy by α_1-adrenergic, 5HT and muscarinic agonists, and the degree of inositol lipid turnover in the rat CNS (Fisher et al. 1983; Johnson & Minneman, 1985; Kendall & Nahorski, 1985). However, following denervation of specific neuronal pathways, this normal tight coupling between receptor occupancy and response is capable of adaptive change (Kendall et al. 1985). Further support is lent by the demonstration that the integrity of the coupling of excitatory amino acid receptors to PI hydrolysis may undergo alterations following denervation of putative glutaminergic pathways in the rat (Nicoletti et al. 1987). Dynamic alterations of [^{3}H]-PDBu binding have been demonstrated in rat brain using quantitative autoradiography. At one day after classical conditioning in rabbit (a form of associative memory), [^{3}H]-PDBu binding, as mapped autoradiographically was increased in CA1 field of the hippocampus (Olds et al. 1989). Additionally, following transient forebrain ischaemia, [^{3}H]-PDBu binding was demonstrated, using quantitative autoradiography, to be selectively increased in the CA1 subfield of the hippocampus before any histological evidence of ischaemic damage and neurotransmitter receptor alterations could be

detected (Onodera et al. 1989). This evidence provides support for the idea that PKC is capable of adaptive change in a variety of pathological states, including AD.

Phorbol ester binding has demonstrated an uneven distribution of PKC within the brain. PKC has also been shown to be distributed heterogeneously within different cell types. In rat brain this enzyme is predominantly localised in presynaptic terminals of particular neurons and within the neuronal nucleus (Wood et al. 1986). It is also known to be concentrated in astrocytes and related glial elements (Mobley et al. 1986; Neary et al. 1986). Increased gliosis in AD neocortex, seen most heavily in layers II-III and V (Beach et al. 1989), appears to mirror the preferential loss of large neurons in layers III and V (Terry et al. 1981). Since gliosis accompanies neuronal loss in AD tissue, it could be inferred that a loss of neuronal PKC is obscured by an increase in this enzyme manifested by astrocyte proliferation in AD. However, the majority of PKC resides in the cytosol of astrocytes (90%), while the remaining 10% is associated with the membrane. Using quantitative autoradiography of [^{3}H]-PDBu, which presumably maps the localisation of membrane bound PKC (see Olds et al. 1989), the increase in astrocytic PKC would have to be far in excess of neuronal PKC. Whether the extent of astrocyte proliferation is similar to the degreee of neuronal loss in AD remains to be established.

The overall view of the status of PKC in AD is further complicated by the identification of at least seven isoforms of PKC which are proposed to have distinct functions within specific neuronal compartments of the CNS (Coussens et al. 1986; Nishizuka, 1988; Parker et al. 1989; Tsujiino et al. 1990). The possibility then arises of one or more of these isoforms being differentially altered in pathologically-diseased tissue such as AD. Indeed, a recent study employed antibodies to four of these isoforms (α, βI, βII and γ) to determine possible alterations in AD brain (Masliah et al. 1990). They found a selective vulnerability of the β isoforms in frontal cortex, finding decreased levels in the particulate fraction, and significantly increased levels in the cytosolic fraction of AD brain. In AD hippocampus, α, βI, and βII isoforms were all significantly reduced, with a trend towards an increase in levels of these isoforms in the cytosolic fraction. PKC (γ) was shown to be relatively robust in AD brain. As yet, the stability of the remaining isoforms in AD is unclear. From the study by Masliah and colleagues (1990) it was interesting that the isoforms α, βI and βII were to some extent associated with plaque processes. In particular PKC (βII) was shown to be localised with the amyloid-containing portions of plaques. PKC has been proposed to be associated with abnormal phosphorylation and processing of the β amyloid precursor protein (Gandy et al. 1988; Buxbaum, 1990). In the present study no association of [^{3}H]-PDBu binding with plaques was found in either middle frontal cortex ($r<0.423$), middle temporal cortex ($r<0.212$) or in the subiculum of the hippocampus ($r = 0.001$). Nonetheless, there is increasing excitement surrounding the speculative hypothesis that PKC may play an integral role in abnormal production of amyloid and in addition,

may induce neuronal death (Saitoh et al. 1990).

This study clearly demonstrated that PKC is extremely robust in a well-defined cohort of AD patients. It may be significant that in the same brain regions, despite marked deficits in receptors, G_s-adenylate cyclase and gross neuropathological and neurochemical alterations, PKC remains preserved. The possibility exists that there may be mechanisms which have come in to force to upregulate this enzyme in brain areas severely disrupted by the disease process.

2. LESION OF RETINOFUGAL AND CORTICOFUGAL FIBRES IN THE RAT VISUAL SYSTEM

Glutamate is the main transmitter in retinofugal, corticofugal and intracortical fibres in the rat visual system. Lesion of these pathways, either by unilateral orbital enucleation or stereotaxic lesion of the visual cortex, allowed possible plastic modifications of second messenger systems following glutamatergic denervation to be examined. Quantitative ligand binding autoradiography in vitro and [^{14}C]-2-deoxyglucose autoradiography in vivo allowed measurement of second messenger ligand binding and function-related glucose use in anatomically discrete components of the visual system following unilateral orbital enucleation and lesion of the rat visual cortex.

2.1 Effect of Unilateral Orbital Enucleation on Glucose Use and Ligand Binding to Second Messenger Systems

[^{14}C]-2-Deoxyglucose autoradiography allows function-related alterations in glucose use to be assessed in vivo (Sokoloff et al. 1977). As the energy requirements and functional activity of cerebral tissue are intimately related, measurement of the local rate of [^{14}C]-2-deoxyglucose use provides a direct index of the local functional activity in anatomically-discrete regions of the CNS. Dynamic alterations in glucose use appear to be related predominantly to activity in neuronal terminals (Mata et al. 1980; Sejnowski et al. 1980). At all time points post-enucleation, significant reductions in glucose utilisation were selectively localised to neuroanatomical components of the visual pathway. Thus the deficits in

glucose use in the visually-deprived superior colliculus, dorsal lateral geniculate body and visual cortex presumably reflect decreased neuronal activity in these regions. Moreover, the deficit in glucose utilisation in each visual structure appeared to be directly related to the level of retinal input. Thus, primary visual structures such as the superior colliculus and dorsal lateral geniculate body exhibited a greater reduction in glucose use post-enucleation compared with secondary visual structures such as visual cortex which receives no direct retinal input. In the superficial layers of the superior colliculus metabolic depression appeared to recover with increased survival time post-enucleation. The magnitude of the deficit in glucose use in the superior colliculus at 20 days was different from that observed at one day post-lesion. A previous study has demonstrated similar diaschisis (Cooper & Thurlow, 1985) in the superior colliculus following enucleation and attributed their findings to either increased gliosis or shrinkage of the superior colliculus in response to denervation. However, ablation of the visual cortex enhances the metabolic depression observed in the superior colliculus post-enucleation (Thurlow & Cooper, 1985) and would seem to suggest that there is some cortical control over metabolic activity in the colliculus. Clearly, the [^{14}C]-2-deoxyglucose method provides a sensitive measurement of functional activity in the visual system post-enucleation.

Although local glucose utilisation was markedly reduced in all visual structures post-enucleation, ligand binding to second messenger systems was differentially altered. [^{3}H]-Forskolin binding was selectively reduced in the

visually-deprived superior colliculus and dorsal lateral geniculate body from five days post-lesion, but remained intact in secondary visual structures (e.g. visual cortex) up to 20 days post-enucleation. In contrast, [^{3}H]-PDBu binding remained unaltered in all brain regions at all time points despite enucleation. Meaningful interpretation of the heterogeneous alterations of ligand binding to second messenger systems must be based on their cellular localisation.

The most conservative explanation for the deficit in [^{3}H]-forskolin binding in primary visual structures would be the localisation of these binding sites on retinal efferents. However, other retino-recipient areas such as the pretectal nuclei and lateral posterior nucleus may be expected to exhibit a similar loss of [^{3}H]-forskolin binding post-lesion. The contralateral pretectal nuclei and lateral posterior nucleus receive approximately 13% and 4% of the retinal input respectively, whilst the dorsal lateral geniculate body and superficial layer of the superior colliculus receive approximately 15% and 65% of retinal efferent fibres respectively (Toga & Collins, 1981). It is conceivable that the proportionately lower degree of retinal input to the lateral posterior nucleus precludes detection of small binding deficits. However, this seems unlikely in the pretectal nuclei which receive a similar percentage of input compared to the dorsal lateral geniculate body.

[^{3}H]-Forskolin binding, under autoradiographic conditions, is associated with the coupling of a stimulatory guanine nucleotide regulatory protein (G_s) with adenylate cyclase (Gehlert et al. 1985; Seamon et al. 1984; Worley

et al. 1986a). A number of receptors such as β-adrenergic, dopamine D_1, adenosine A_2 and vasoactive intestinal polypeptide mediate cellular responses via G_s activation (Levitski, 1987). Reductions in β-adrenergic receptors, as mapped by [^{3}H]-DHA autoradiography, were reported in the superior colliculus (-23%) and dorsal lateral geniculate body (-30%) in the visually-deprived hemisphere of rats post-enucleation (Chalmers & McCulloch, 1990). Moreover, the time-course of [^{3}H]-DHA loss parallels the reduction in [^{3}H]-forskolin binding. Both are reduced at five days post-enucleation and maintained thereafter at reduced levels, 10 and 20 days post-lesion. It must be noted that the superior colliculus exhibited a smaller deficit in [^{3}H]-DHA binding compared to the dorsal lateral geniculate body which is in contrast to that observed for [^{3}H]-forskolin binding. Thus, [^{3}H]-forskolin binding losses are not simply the result of β-adrenergic receptor deficits. It is interesting that another study demonstrated an increase in β-adrenergic receptors in response to monocular deprivation in the dorsal lateral geniculate body of both the deprived and non-deprived eye (Schliebs et al. 1982). Thus, receptor and possibly second messenger system alterations are dependent on the type of visual impairment. As yet, the effect of visual deprivation on other receptors associated with G_s, such as D_1, A_2 and vasoactive intestinal polypeptide, remains to be established.

Alterations in receptor populations and second messenger systems are clearly delayed compared to the functional deficits post-enucleation. Alterations in either neurotransmitter receptors (Chalmers & McCulloch, 1990) or [^{3}H]-forskolin binding were not apparent until five days post-

enucleation whilst local cerebral glucose utilisation is maximally reduced at one day post-lesion. Receptor and second messenger system reductions occur at the time when the metabolic activity in the deafferentated superior colliculus appears to recover. It has been suggested that selective receptor alterations within the visual circuitry may contribute to the functional re-organisation post-enucleation (Chalmers & McCulloch, 1990). Thus alterations in [^{3}H]-forskolin binding may be indicative of altered receptor function in visual structures post-enucleation.

The interaction of G_s with adenylate cyclase might not involve identical molecular mechanisms or G_s-proteins in all brain regions (Poat et al. 1988). In some brain areas, [^{3}H]-forskolin binding is differentially regulated by Mg^{2+} and guanine nucleotides which normally act to promote coupling of G_s with adenylate cyclase. The stable guanine nucleotide, 5′guanylimidodiphosphate (Gpp(NH)p) has previously been shown to maximally enhance [^{3}H]-forskolin binding in the caudate at a concentration of 10μM (Gehlert, 1986; Poat et al. 1988). Thus, this concentration was used in the present study to examine the effect of Gpp(NH)p on [^{3}H]-forskolin binding. [^{3}H]-Forskolin binding was markedly enhanced in the presence of Gpp(NH)p in areas such as the superior colliculus, caudate putamen and lateral habenula, whilst other regions such as the visual cortex, dorsal lateral geniculate body, molecular layer of the hippocampus and thalamus were unaffected or minimally increased. These results are similar to those reported by Gehlert (1986) although some regions such as the thalamus and medial geniculate were previously shown to exhibit an increased density of

[^{3}H]-forskolin binding by Gpp(NH)p. In different brain regions the ability of Gpp(NH)p to alter [^{3}H]-forskolin binding is not the same. Furthermore, following unilateral orbital enucleation, the characteristics of [^{3}H]-forskolin binding are altered in the visually-deprived dorsal lateral geniculate body in the presence of Gpp(NH)p. [^{3}H]-Forskolin binding alone was significantly reduced in the visually-deprived dorsal lateral geniculate body post-lesion (-20%); in the presence of Gpp(NH)p this asymmetry was apparently restored (-2%). These results extend original observations (Poat et al. 1988) which suggested G_s-adenylate cyclase interactions may <u>not</u> be mediated by identical mechanisms in different brain regions. Following denervation, it seems likely that the molecular mechanisms underlying [^{3}H]-forskolin binding are further altered. Similarly, in ethanol-fed mice, [^{3}H]-forskolin binding was differentially altered in the presence of Gpp(NH)p (Valverius et al. 1989). In some brain regions such as hypothalamus, cerebellar vermis and paraventricular nucelus of the thalamus, [^{3}H]-forskolin binding was unaltered in control compared to ethanol-treated mice, while significantly less [^{3}H]-forskolin bound to these brain regions in ethanol-fed mice in the presence of Gpp(NH)p. Interpretation of results solely as a loss of G_s-associated elements cannot be made until further examination of the molecular mechanisms underlying changes in [^{3}H]-forskolin binding are made.

Another distinct but key second messenger, protein kinase C (PKC) was mapped by the phorbol ester ligand [^{3}H]-PDBu. Despite chronic depression of functional activity in visually-deprived areas, [^{3}H]-PDBu binding was preserved. This apparent stability of [^{3}H]-PDBu binding may infer that these

binding sites are absent from degenerating retinofugal fibres and are instead localised post-synaptically in the dorsal lateral geniculate body. α_1-mediation of phosphoinositide and as a result, PKC activity, has been shown to be wholly post-synaptic (Kemp & Downes, 1986). However, the precise cellular localisation of PKC in other visual structures is unclear.

PKC isoforms are proposed to have distinct functions within specific neuronal compartments of the CNS (Nishizuka, 1988; Parker et al. 1989; Tsujiino et al. 1990). Conflicting reports as to the exact cellular localisation of PKC subspecies is evident. Some studies have demonstrated the prevalence of PKC in presynaptic neuronal terminals (Girard et al. 1985; Wood et al. 1986) whilst others have shown some PKC isoforms to be predominantly post-synaptic (Tsujiino et al. 1990). In the visual cortex (area 17) immunocytochemistry of PKC isoenzymes demonstrated a high density of PKC in cortical layers II/III which is similar to that observed in the present autoradiographic study of [^{3}H]-PDBu binding to PKC. Localisation of PKC isoenzymes within the visual cortex (Stichel & Singer, 1988) appeared to suggest that PKC was associated with cortical projection and local circuit neurons which would explain the relative stability of PKC in the visually-deprived cortex. Overall though, it would seem unlikely that all isoforms of PKC are either pre- or postsynaptic in location and, as a result, it is perhaps simplistic to attribute intact [^{3}H]-PDBu binding to the dominance of these sites on post-synaptic terminals. There appears a greater possibility that some of the PKC isoforms are differentially altered in visually-deprived areas, the additive effect of which cannot be detected

using [^{3}H]-PDBu autoradiography. Selective vulnerability of some PKC isoforms to alter has been demonstrated in neurodegenerative systems such as Alzheimer's disease (Masliah et al. 1990) and following lesion of the fimbria-fornix in rat (Shimohama et al. 1988).

Neurotransmitter receptors which regulate cellular responses via activation of PKC include α_1-adrenergic, muscarinic, serotonergic $5HT_2$ receptors and glutamate receptors. Glutamate is the main neurotransmitter in both retinofugal (Crunelli et al. 1985, 1987) and corticofugal fibres (Fosse et al. 1986) to the superior colliculus and dorsal lateral geniculate body and within visual cortex (Baughman & Gilbert, 1981). Post-enucleation, glutamate remains unaltered in the visually-deprived superior colliculus and dorsal lateral geniculate (Chalmers & McCulloch, 1989) although the uptake of glutamate in these structures has been shown to be affected (Lund-Karlsen & Fonnum, 1978). However, a profound reduction in [^{3}H]-glutamate binding was observed in the visually-deprived visual cortex at one day following denervation of the visual pathway (Chalmers & McCulloch, 1989). It is unlikely that a "transynaptic" alteration in [^{3}H]-PDBu binding has occurred in the present study in view of the time-frame of the glutamate response (1 day) and the survival periods at which [^{3}H]-PDBu binding was examined (1-20 days). Additionally, α_1-adrenergic, muscarinic and serotonergic receptors are not altered in visually-deprived areas following enucleation (Chalmers & McCulloch, 1990).

2.2 Effect of Unilateral Lesion of the Rat Visual Cortex on Glucose Use and Ligand Binding to Second Messenger Systems

The [^{14}C]-2-deoxyglucose autoradiographic technique can be used successfully to map the functional consequences of manipulation of simple sensory pathways such as the auditory system (Sokoloff, 1977; Sharp et al. 1982) following stimulation and deprivation. In the present study, the effect of removal of a specific neuronal population in the rat visual cortex on the functional activity within the visual circuitry was examined.

Intracortical injection of saline alone caused a marked disturbance in glucose use in the ipsilateral hemisphere of sham animals. This finding confirms previous reports (Kurumaji & McCulloch, 1990; Kelly & McCulloch, 1987) which demonstrate alterations in glucose use following mechanical damage either to the tympanic membrane induced by the use of stereotactic frames with ear bars or by placement of the guide cannula into the cortex. Additionally, the injection of 1µl of saline into the cortex will upset the normal homeostasis of cellular function by diluting extracellular concentrations of neurotransmitters which may precipitate subtle alterations in glucose use near the injection site. Asymmetries in glucose use were confined to the area of injection.

Ibotenic acid has been widely used as a neurotoxin in morphological and functional analyses of the CNS. Intracerebral injection of ibotenic acid produces a discrete loss of nerve cell bodies and dendrites in the injection area, sparing axons of passage and nerve terminals of extrinsic origin

(Schwarcz et al. 1979). Injection of ibotenic acid into the visual cortex (area 17) in the present study was associated with a loss of nerve cell bodies which was not observed in the sham group treated with saline, as verified histologically. The lesion was reproducible and extended from superficial layers to the deep cortical layers confined to visual cortex (area 17). Local cerebral glucose utilisation was markedly reduced in the ipsilateral visual cortex (layers II-VI). Further, glucose use was significantly reduced in the ipsilateral dorsal lateral geniculate body and there was a trend towards a reduction in glucose use in the ipsilateral superior colliculus. These results extend previous observations (Toga & Collins, 1981; Thurlow & Cooper, 1985) in non-quantitative assessment of glucose utilisation following visual cortex lesions. However, the magnitude of alterations in glucose use in the present study appear to be to a lesser extent to those previously demonstrated. Most likely, the basis for the discrepancies lies in differences in the procedures for lesioning the visual cortex. In the present study, a discrete lesion of cortex was produced by focal injection of neurotoxin compared to ablation of visual cortex by suction (Thurlow & Cooper, 1985) and electrical stimulation (Toga & Collins, 1981). These latter two procedures would ensure complete destruction of visual cortex removing nerve terminals and fibres en passage in addition to cell bodies and moreover, the extent of damage to the visual cortex in these studies appears to be greater.

Perhaps a more crucial difference may be the timing of glucose use measurement following visual cortex lesions, 21 days in the present study compared to one day or less previously (Toga & Collins, 1981; Thurlow &

Cooper, 1985). Ablation of the visual cortex is associated with axonal sprouting in subcortical visual structures (Goodman & Horel, 1966) and reactive gliosis (Mathewson & Berry, 1985). The minimal alterations in glucose use in cortical projection areas may be due to a functional reorganisation within the visual pathways. Many of the visual structures receive a modulatory control from other non-visual structures. For example, the dorsal lateral geniculate body receives a projection from the locus coeruleus and the parabigeminal nucleus innervates the superficial layers of the superior colliculus. It is possible that compensatory mechanisms have tried to restore the disturbance of visual circuitry. As already demonstrated, following enucleation, recovery in functional activity in the denervated superior colliculus involves an increase in cortical control over metabolic activity (Thurlow & Cooper, 1985). In other experimentally-lesioned animal models a metabolic recovery with increasing survival time is seen in areas which have shown alterations in glucose use previously at earlier time points (Orzi et al. 1988; London et al. 1984).

Although function-related alterations in glucose use were minimal following ibotenate-induced visual cortex lesion, in the same animals [^{3}H]-forskolin binding was profoundly deficient in the lesioned hemisphere of visual cortex, dorsal lateral geniculate body and the superficial layers of the superior colliculus. Thus, it would appear that a major proportion of [^{3}H]-forskolin binding is associated with intrinsic cortical neurons and presynaptic terminals of cortical efferents to the superior colliculus and dorsal lateral geniculate. These findings are consistent with a presynaptic localisation

of [^{3}H]-forskolin binding sites. In the previous study which examined [^{3}H]-forskolin binding after unilateral orbital enucleation, these sites were determined to be principally located on retinal efferent fibres.

The adenylate cyclase system, as mapped by [^{3}H]-forskolin, does appear to have some functional role within the visual circuitry. Evidence has indicated that the adenylate cyclase system coupled to β-adrenergic receptors may play an important role in the maintenance of cortical plasticity during the critical period. Intraventricular injection (Kasamatsu & Pettigrew, 1976, 1979) or cortical microperfusion (Kasamatsu et al. 1981) of the neurotoxin 6-hydroxydopamine (6OHDA) which is known to destroy catecholaminergic terminals and hence deplete catecholamines, preserved binocular responses of neurons in the visual cortex of monocularly-deprived kittens. Microperfusion with noradrenaline (Kasamatsu et al. 1979) or dibutyryl cAMP (Kasamatsu, 1980) of the visual cortex restores neuronal plasticity in kittens previously treated with 6OHDA and to a certain degreee in adult cats which were no longer susceptible to monocular deprivation. cAMP-dependent phosphorylation of MAP2 in homogenates prepared from cat visual cortex was found to increase after a brief exposure of dark-reared animals to light (Aoki & Siekevitz, 1985).

It is interesting that functional mapping of the visual circuitry does not appear to be indicative of any major alterations within this pathway following cortical lesions. Clearly the profound loss of [^{3}H]-forskolin binding in visual structures receiving cortical efferents would appear to contradict

this. Perhaps, as suggested earlier, there is a functional recovery within the visual pathway post-lesion as mapped by [^{14}C]-2-deoxyglucose autoradiography but an altered receptor function as indicated by [^{3}H]-forskolin binding.

In the same study, [^{3}H]-PDBu binding to protein kinase C (PKC) was minimally altered after visual cortex lesion. The only difference in [^{3}H]-PDBu binding was confined to the lesioned cortex where [^{3}H]-PDBu binding was significantly decreased in deep cortical layers although there was a trend to a reduction in binding in the remaining layers of visual cortex.

PKC is localised to a certain extent on astrocytes (Mobley et al. 1986; Neary et al. 1986). Since vigorous gliosis accompanies cortical lesion as verified histologically and from previous observations (Mathewson & Berry, 1985), it would seem likely that the lack of asymmetry in [^{3}H]-PDBu binding in the superficial layers of visual cortex was masked by an increase in astrocyte proliferation which is seen to a lesser extent in deep cortical layers.

A loss of [^{3}H]-PDBu binding in response to ibotenate-induced lesion of the visual cortex would be consistent with immunocytochemical localisation of PKC on intrinsic neurons (Stichel & Singer, 1988). However, the robustness of PKC in the superior colliculus and dorsal lateral geniculate is at variance with the association of PKC with cortical projection terminals (Stichel & Singer, 1988). Ablation of the visual cortex markedly reduces

the levels of glutamate, associated with PKC, in the ipsilateral dorsal lateral geniculate body and superior colliculus (Lund-Karlsen & Fonnum, 1978) and thus alterations in the levels of [^{3}H]-PDBu binding in these visual areas might be expected. However, denervation of the glutamatergic pathway from frontal cortex to the striatum is associated with a potentiation of excitatory amino acid-induced stimulation of PI hydrolysis (Nicoletti et al. 1987). This may be indicative of an upregulation of PKC following denervation. Whether this applies for [^{3}H]-PDBu binding following denervation of a major glutamatergic pathway in the visual system is unclear.

In summary, selective lesioning of two major glutamatergic pathways in the rat visual system, either by orbital enucleation or neurotoxin-induced lesion of the visual cortex, has demonstrated the differential alterations of ligand binding to second messenger systems in visual structures exhibiting functional deficits. [^{3}H]-Forskolin binding was consistently reduced post-lesion and may be indicative of alterations in receptor function within the visual circuitry. Following chronic depression of functional activity within the visual pathways, [^{3}H]-PDBu binding to PKC was extremely robust suggesting that this transduction system is not susceptible to lesion-induced modulation or perhaps the persistence of PKC is indicative of a homeostatic role for this pathway in maintaining cellular function with the visual system.

3. LESION OF THE RAT SEPTO-HIPPOCAMPUS

The rat septo-hippocampal pathway provided a model system in which to examine ligand binding to second messenger systems following denervation of a principally cholinergic pathway. The most striking findings in this study were an increase in both [^{3}H]-forskolin and [^{3}H]-PDBu binding in discrete and anatomically distinct regions of the septo-hippocampal pathway following lesion of the medial septum. [^{3}H]-Forskolin binding was significantly increased in the polymorph layer of the dentate gyrus (19%) whilst [^{3}H]-PDBu binding was increased in the superficial layers (I-III) of entorhinal cortex (27%) post-lesion.

3.1 Ligand Binding to Second Messenger Systems in Lesioned Rat Septo-Hippocampal Pathway

Loss of the septal cholinergic innervation to the hippocampal formation, as a result of medial septum lesion, is associated with an enormous degree of reorganisation within the hippocampal circuitry. Sympathetic axons sprout and grow into the dentate-CA3 region of the hippocampal formation (Crutcher et al. 1979). This restricted distribution of sympathetic fibres to dentate-CA3 region appears to correlate with the distribution of dentate granule cells and their axons, the mossy fibres (Crutcher & Davis, 1982). [^{3}H]-Forskolin binding was most dense in the polymorph layer of the dentate gyrus and the pyramidal layer of CA3, associated with granule cells and mossy fibre terminals (Worley et al. 1986a). Following medial septal lesion, a significant increase in [^{3}H]-forskolin binding was evident in the polymorph layer of dentate gyrus. Further, there was a marked increase in [^{3}H]-

forskolin binding in the pyramidal layer of CA3 (21%) indicating the association of [^{3}H]-forskolin binding with cell bodies in the medial septum. Thus, this trend in [^{3}H]-forskolin binding to be increased in discrete brain regions distal to the lesion site infers an upregulatory response to deafferentation which may be putatively linked to axonal sprouting. In the hippocampus, there is evidence that noradrenaline stimulation of adenylate cyclase mediated through β-adrenergic receptors is important for long-term potentiation in the dentate gyrus (Stanton & Sarvey, 1985). Reductions in long-term potentiation of the perforant path granule cell synapse caused by depeletion of noradrenaline can be reversed by application of forskolin (Stanton & Sarvey, 1985). Long-term potentiation is used as a possible model of the cellular mechanisms involved in learning and memory. A proposed functional role for the adenylate cyclase system in learning and memory is also indicated in animal behavioral studies. In rats, delayed memory dysfunction is markedly ameliorated by post-treatment with forskolin (Ando et al. 1987). Additionally, blockade of β-adrenergic linked adenylate cyclase inhibits the learning and retention of an active avoidance task in mice (Laborit & Zerib, 1987).

In the present study it is unclear whether this increase in [^{3}H]-forskolin binding is associated with a parallel increase in associated neurotransmitter receptors. Denervation-induced supersensitivity of neurotransmitter receptors is often linked to a concomitant increase in receptor-mediated adenylate cyclase activity. Well documented is the enhanced stimulation by dopamine of striatal adenylate cyclase (Mishra et al. 1980; Parenti et al.

1982) mediated through D_1 receptors (Herve et al. 1989) after lesion of central dopaminergic projections. Following electroconvulsive shock therapy in the rat, [^{3}H]-forskolin binding is increased in the substantia nigra in parallel with an upregulation of D_1 receptors in this region (Fochtmann et al. 1988). Although supersensitivity of muscarinic receptors has been demonstrated in the hippocampus (Bird & Aghajanian, 1975; Westlind et al. 1981), this has been contradicted by studies showing muscarinic receptors to be unaltered following medial septal lesion (Yamamura & Snyder, 1974; Fisher et al. 1980; Overstreet et al. 1980). Investigation of muscarinic receptor subtypes has indicated an upregulation of muscarinic (M_2) receptors in the stratum oriens of CA2-4 fields with relatively minor changes in M_1 receptors following lesion of the medial septum (Dawson & Wamsley, 1989). Although there has been intensive investigation of muscarinic receptors in the hippocampus post-lesion, as yet, there is minimal evidence of alterations in other neurotransmitter receptors especially those linked to adenylate cyclase. This does not exclude the possibility, however, of denervation-induced supersensitivity as the basis of the increase in [^{3}H]-forskolin binding. In addition, it is important to recognise that [^{3}H]-forskolin binding in the hippocampus may behave in a qualitatively different manner to binding in other brain regions, e.g. striatum (Gehlert, 1986; Poat et al. 1988) in particular, following denervation.

In contrast, [^{3}H]-PDBu binding was extremely robust within all regions of the hippocampus yet was increased in the entorhinal cortex after lesion of the medial septum. This result is in contradiction with a previous study

which demonstrated an upregulation of cholinergic mediated phosphoinositide (PI) hydrolysis in the deafferentated hippocampus by electrolytic lesion (Connor & Harrell, 1989). This attenuated PI response after lesion of the septo-hippocampal pathway was only evident in response to cholinergic and not noradrenergic stimulation. Thus, the expansion of sympathetic fibres in the hippocampus following medial septum lesion does not appear to be associated with changes in the PI system. A similar study has shown α_1-adrenergic mediated PI breakdown to be unaltered in the hippocampus after selective noradrenergic denervation (Fowler et al. 1986). However, the enhanced PI response to cholinergic stimulation (Connor & Harrell, 1989) would suggest [^{3}H]-PDBu binding to protein kinase C (PKC) should be increased in the hippocampus. An upregulation of the PI response to carbachol has been noted in the cerebral cortex five days after cholinergic deafferentation via nucleus basalis lesions (Reed & de Belleroche, 1988). However, this response was short-lived as it was partially reversed at 14 days post-lesion and completely reversed by 50 days. In the present study, [^{3}H]-PDBu binding to PKC was examined at only one time-point, 21 days following septal lesion. It is possible that any changes in PKC, in the hippocampal formation, have occurred previous to this time. Another group have demonstrated muscarinic stimulation of PI hydrolysis to be unaltered at 21 days following nucleus basalis of Meynert lesion (Raulli et al. 1988). Discrepancies with the study by Connor and Harrell (1989) may also be due to the extent and type of the lesion. In their study, the vertical diagonal band of Broca, which has a cholinergic input to the hippocampus, in addition to the medial septum, was destroyed by electrolytic lesion. In the present

study, a chemical lesion was produced by the neurotoxin ibotenic acid and was mainly confined to the medial septum. Thus, the extent of cholinergic denervation to the hippocampus would be qualitatively and quantitatively different; electrolytic lesion of the medial septum would remove all nerve fibre tracts in addition to cell bodies and ensure a more complete disruption of the cholinergic pathways to the hippocampus unlike ibotenate lesion which is discrete. Many of these reasons for the apparent stability of PKC found in the hippocampus may go some way to explaining the controversy surrounding the status of muscarinic receptors in the hippocampus post-lesion.

This apparent stability of PKC may also be due to selective alterations of PKC isoforms in the hippocampus. Following denervation of the septo-hippocampal pathway, a decrease in PKC-α immunoreactivity was noted in CA1 and CA2 fields with a parallel increase in PKC-β and PKC-λ in these regions (Shimohama et al. 1988). The additive effect of these selective changes in PKC isoforms may have the overall effect of cancelling out any alterations which may be expected in [^{3}H]-PDBu binding to PKC.

Although [^{3}H]-PDBu binding was not altered in the hippocampal formation, there was a significant increase in binding in the superficial layers of entorhinal cortex following cholinergic deafferentation. The entorhinal cortex receives a major input from the medial septum terminating in cortical layers II, IV and VI. In turn entorhinal cortex projects from layer II primarily to the molecular layer of the dentate gyrus via the perforant

pathway. Intensive investigation has focused on the hippocampal formation following medial septal lesion examining receptor dynamics, morphological changes, electrophysiological events and the anatomical interconnectivity. However, minimal importance has been placed on the entorhinal cortex following medial septal lesion. Destruction of the entorhinal cortex and hence the input to the hippocampus, via the perforant pathway, causes a rapid degeneration of synaptic terminals that end in the outer dentate gyrus molecular layer (Mathews et al. 1976). A small number of remaining acetylcholinesterase axons proliferate rapidly and reinnervate the deafferented area (Lynch et al. 1972) manifested by increased acetyl cholinesterase (AChE) staining. Lesion of the medial septum abolishes this response (Lynch et al. 1972). However, combined lesions of the septum and entorhinal cortex induce a different set of AChE terminals to sprout into the deafferented region, yielding a similar but slightly different distribution of AChE staining (Chen et al. 1983). Since the entorhinal area receives a substantial input from the medial septum and is functionally important within the hippocampal circuitry, it may be suggested that this increase in [^{3}H]-PDBu binding is indicative of synaptic alterations in the entorhinal cortex or may be akin to axonal sprouting observed in the hippocampus following medial septum lesion (and entorhinal cortex lesion). In the entorhinal cortex, local cerebral glucose utilisation, as an index of functional activity, is unaltered following denervation of the septo-hippocampal pathway (Inglis, unpublished observations). Thus, it would appear alterations in the functional activity of entorhinal cortex may not underlie the increase in [^{3}H]-PDBu binding in this region.

In the present study, the heterogeneous alterations in ligand binding to second messenger systems and the direction of these responses (an increase as opposed to a decrease) may be supportive of plastic modifications of second messenger systems following denervation. It remains unclear whether these changes in ligand binding to second messenger systems represent an upregulation in response to neurotransmitter receptor alterations or are associated with axonal sprouting in areas distant from the primary lesion.

OVERVIEW

In the past, simple biochemical assays have been employed to examine second messenger systems in homogenate preparations of CNS tissue, usually the turnover of second messengers being measured in response to agonist stimulation. However, given the intricate cellular and anatomical complexity of the brain, a fuller understanding of second messenger systems in brain warrants techniques with higher anatomical resolution. Quantitative ligand binding autoradiography offered a novel and sensitive approach to the study of second messenger systems allowing key components of transduction mechanisms such as protein kinase C (PKC) and adenylate cyclase to be mapped in well-defined neuroanatomical components of human and rat CNS. Further, the possible plasticity of second messenger systems, as mapped using quantitative ligand binding, could be investigated in discrete brain areas of pathologically-diseased tissue such as Alzheimer (AD) brain.

The application of autoradiographic techniques to human postmortem brain encounters many of the problems faced in other neurochemical studies. Intrinsic variables such as the patient's age, sex, agonal state, pre-mortem drug history and postmortem delay may influence alterations in second messenger systems and increase interindividuality. Groups of control and AD patients were closely matched for age and postmortem delay to minimise these differences. The majority of neurotransmitter receptors appear to be stable over very long postmortem delay intervals (Hardy & Dodd, 1983). However, studies have demonstrated markedly increased basal levels of second messenger activities with relatively short postmortem intervals in human brain (Candy et al. 1984; Saitoh

& Dobkins, 1986; Danielsson et al. 1988) which may be indicative of second messenger instability in brain with longer periods of postmortem delay. Ligand binding of [^{3}H]-forskolin was determined to be relatively stable over increasing periods of postmortem delay in rat brain (Appendix VIII). Further, in human brain there was no correlation between postmortem delay and either [^{3}H]-forskolin or [^{3}H]-PDBu binding in all brain regions of control and AD brain (Appendix VIa and VIb). Thus, the stability of ligand binding to second messenger systems over relatively long periods of postmortem delay affords an advantage of using quantitative autoradiography over homogenate preparations in the study of second messenger systems. There was some association between ligand binding densities and the age of patient in brain regions of control and AD brain (Appendix VIa and VIb). In particular, a positive correlation between [^{3}H]-forskolin binding and age in AD middle frontal cortex was noted. [^{3}H]-Forskolin binding was demonstrated to be markedly reduced in AD frontal cortex compared to controls. Although it is unclear whether the age of the AD patients influenced the amount of [^{3}H]-forskolin binding in AD cortex compared to controls, it cannot be dismissed that there may be an ageing effect in addition to the neurodegenerative effects of AD influencing [^{3}H]-forskolin binding. However, since the probability of spurious associations between two measures may be increased considerably when correlating several parameters in a number of brain regions, caution must be taken before placing importance on correlation data.

Inter-individual variability may, however, preclude detection of small changes in ligand binding densities in AD compared to control brain. This problem can be dealt with to a certain extent statistically. Power analysis (Cohen, 1977) allows determination of either the patient group size necessary to detect a certain magnitude of change or vice versa in ligand binding in a group of AD cases compared to controls. Autoradiographic analysis of [^{3}H]-PDBu binding demonstrated that PKC was preserved in a population of AD brain in contrast to a previous study which reported a significant reduction in PKC in AD frontal cortex (Cole et al. 1988). While the numbers of subjects in control and AD groups were smaller in the present study compared to Cole et al. (1988), the magnitude of the reported deficit (50%) strongly suggested that such a loss of binding would have been detected, if it was present. The use of statistical power analysis indicated that quantitative [^{3}H]-PDBu binding autoradiography was capable of demonstrating changes of approximately 30% in binding levels at a probability level of 5% and a power of 80% of AD individuals (assuming a consistent variation). The patient group size (n=9) was adequate to detect such a change (50%) in [^{3}H]-PDBu binding.

The heterogeneity of patients groups especially in terms of neuropathological abnormalities is most likely to have a major impact on postmortem studies. Neurochemical markers for cholinergic muscarinic receptors (Lang & Henke, 1983; Reinikainen et al. 1987; Probst et al. 1988), $5HT_2$ receptors (Cross et al. 1988; Perry et al. 1984; Dewar et al. 1990) and N-methyl-D-aspartate receptors (Maragos et al. 1987; Monaghan et al. 1987) have been the subjects of controversy as regards their status in AD. The severity of neuropathological abnormalities

such as neuronal loss, neurofibrillary tangles and plaques between different groups of patients may have some bearing on these conflicting results. This was seen to a certain extent in two separate studies of [^{3}H]-forskolin binding which demonstrated differential alterations in binding in AD brain. In one study, [^{3}H]-forskolin binding was profoundly reduced in all layers of middle frontal cortex, was inconsistently reduced in middle temporal cortex and unchanged in the hippocampal formation of an AD group. In a different cohort of AD cases, [^{3}H]-forskolin binding was significantly decreased in all layers of middle frontal cortex, middle temporal cortex and the molecular layer of dentate gyrus. It was noted that the deficit in choline acetyltransferase (ChAT) activity and the presence of neuritic plaques was of a greater magnitude in the second AD group (Table 2) (exhibiting reductions in [^{3}H]-forskolin binding in three brain regions) in comparison to the other population of AD brain (Table 5) (in which [^{3}H]-forskolin binding was significantly reduced only in frontal cortex). Thus, although there was a consistent trend for [^{3}H]-forskolin binding to be decreased in neocortex and the molecular layer of dentate gyrus in AD brain, the degree of binding deficits may be influenced by the extent of local neuropathological and neurochemical abnormalities.

The level of complexity introduced in human postmortem investigations of neurochemical parameters is not encountered in animal models. Experimental lesions of specific neuronal pathways in rat brain were used as a basis on which to compare alterations in ligand binding to second messenger systems following denervation of glutamatergic and cholinergic pathways to those alterations found in AD brain. Loss of presynaptic input was consistently associated with

reductions in [^{3}H]-forskolin binding in recipient brain regions. Most notably [^{3}H]-forskolin binding deficits were observed in AD brain regions to which the cholinergic innervation is disrupted and in rat visual structures following denervation of retinal or cortical input to those regions. Further, the loss of [^{3}H]-forskolin binding appeared to be associated with alterations in the functional activity of these brain regions. Following unilateral orbital enucleation, [^{3}H]-forskolin binding was significantly reduced in visually-deprived retinorecipient brain regions (superior colliculus, dorsal lateral geniculate body) in which the functional activity, as measured by 2-deoxyglucose (2DG) autoradiography, was depressed. After lesion of the visual cortex, marked reductions in [^{3}H]-forskolin binding were observed in the superior colliculus and dorsal lateral geniculate body, regions which exhibited minimal alterations in the level of functional activity. Indeed, in this study, the use of [^{3}H]-forskolin binding autoradiography would appear to map "functional" alterations in denervated brain regions to a greater ability than the 2DG method. AD brains, in which [^{3}H]-forskolin binding was examined, exhibited a profound cholinergic hypofunction. In cortical regions which exhibited a profound reduction in [^{3}H]-forskolin binding in AD, there was a consistent and positive correlation between the level of binding and the level of ChAT activity. The degree of cholinergic deficit appears to be associated with the degree of cognitive impairment in elderly people (Perry et al. 1978; Wilcock et al. 1982). Forskolin, by increasing adenylate cyclase stimulation of cAMP, has been suggested to facilitate memory function by enhancing cerebral blood flow (Ando et al. 1987). Increased levels of cAMP have also been shown to restore neuronal transmission supressed by hypoxia (Okada et al. 1989). Since in AD, neuroimaging studies have indicated reductions in regional metabolism and blood

flow in frontal and temporal lobes (Haxby et al. 1985; Horwitz, 1987) it may be of value to examine [^{3}H]-forskolin binding deficits in postmortem AD brain in patients in which the premortem status of blood flow and metabolism were known by in vivo imaging. It is important to recognise that, as yet, it remains unclear whether deficits in regional blood flow and metabolism in AD neocortex are true functional alterations or are simply an indication of brain atrophy.

It does not appear that in all brain regions loss of presynaptic input will precipitate a parallel reduction in [^{3}H]-forskolin binding, in particular the hippocampus, following denervation. The hippocampus receives a major cortical projection from the perforant pathway arising in entorhinal cortex to terminate on the outer granule cell dendrites of the dentate gyrus molecular layer and on pyramidal cell dendrites of the hippocampus and subiculum. The trend in [^{3}H]-forskolin to be reduced in the molecular layer of the dentate gyrus in AD hippocampus may be indicative of a loss of cortical input from the entorhinal area which often exhibits extensive cell losses in AD (Hyman et al. 1984). However, [^{3}H]-forskolin binding was preserved in the subiculum and CA1 field of AD hippocampus, areas in which marked cell losses and severe neuropathological abnormalities are characteristic (Hyman et al. 1984; Probst et al. 1988) which may indicate an upregulation of [^{3}H]-forskolin in these regions. AD hippocampus has been demonstrated to undergo plastic modifications. Deafferentation of the dentate gyrus by neuropathological changes in entorhinal cortex may induce sprouting of septal afferents as demonstrated by enhanced acetylcholinesterase (AChE) activity in the dentate gyrus molecular layer (Hyman et al. 1987). Further, an enhanced AChE staining in the entire perforant pathway zone,

particularly in the molecular layer of the subiculum, has been observed in AD cases in which entorhinal and septal cell losses were evident in AD brain (Hyman et al. 1987). Lesion of the cholinergic projection of the rat medial septum to the hippocampus induced an increase in [^{3}H]-forskolin binding indicative of the ability of this second messenger system to adapt in deafferentated hippocampus. Although the extent of disease-related cellular damage in the entorhinal cortex and septum was unknown in the AD cases used in ligand binding studies, the preservation of [^{3}H]-forskolin binding in hippocampal areas severely affected by the pathological correlates of AD would suggest an upregulation of this system in response to neuronal loss.

Whilst [^{3}H]-forskolin binding appeared to be consistently reduced in AD brain, autoradiographic imaging of [^{3}H]-PDBu binding to PKC demonstrated this enzyme to be extremely robust in all areas of AD neocortex and hippocampus. Further, following experimental lesions of cholinergic and glutamatergic pathways in rat brain, there were minimal alterations in [^{3}H]-PDBu binding in recipient brain regions, perhaps indicative of a post-synaptic location of PKC. Dynamic alterations in [^{3}H]-PDBu binding have previously been mapped following transient forebrain ischaemia in rats (Onodera et al. 1989) and associative memory conditioning in rabbits (Olds et al. 1989). Indeed, a number of studies have demonstrated lesion-induced denervation of putatitve glutamatergic and cholinergic pathways to induce an upregulation of agonist-mediated PI hydrolysis (Nicoletti et al. 1987; Reed & de Belleroche, 1988; Connor & Harrell, 1989). In the present studies, there was some indication that [^{3}H]-PDBu can alter in response to denervation. After lesion of the rat medial septum, a marked

increase in [^{3}H]-PDBu binding was observed in entorhinal cortex. It seems remarkable, though, that in AD brain which exhibited gross neuropathological and neurochemical abnormalities, loss of glutamate receptor subtypes and [^{3}H]-forskolin binding reductions, PKC was preserved. In particular, quisqualate metabotropic receptors which mediate PI hydrolysis in the hippocampus (Sladeczek et al. 1988) were profoundly reduced in the CA1 field and subiculum of AD hippocampus in adjacent sections to those used for [^{3}H]-PDBu binding autoradiography. Thus, it seems unlikely that the preservation of [^{3}H]-PDBu binding in AD hippocampus is explained by the maintenance of cellular elements to which [^{3}H]-PDBu binds in AD brain. It is possible that PKC has been upregulated in intact neurons in response to neurotransmitter receptor loss. This compensation, however, may not be possible beyond a threshold of neuronal fall-out, corresponding to severe degrees of neuronal loss. Comparison of [^{3}H]-PDBu binding to [^{3}H]-forskolin binding in the same control and AD patients (Figure 40) demonstrated the level of [^{3}H]-PDBu and [^{3}H]-forskolin binding to be positively associated in middle temporal cortex, that is AD patients in which [^{3}H]-forskolin binding was markedly reduced, exhibited low levels of [^{3}H]-PDBu binding compared to the control values. This association was less obvious in middle frontal cortex. It is interesting to note that the magnitude of [^{3}H]-forskolin binding reduction in AD middle frontal cortex was to a lesser extent than that seen in AD middle temporal cortex compared to controls, perhaps indicative of differing severities of neuronal loss and neuropathology in these cortical regions.

The complexity of Alzheimer's disease in terms of symptomatology, neuropathological and neurochemical abnormalities makes the functional evaluation of the status of neurotransmitter receptors and second messenger systems somewhat difficult. Quantitative autoradiography of ligand binding to second messenger systems demonstrated the selective vulnerability of G_s-adenylate cyclase, being consistently reduced in AD brain, in comparison to protein kinase C, which was extremely robust. Such data suggest that the loss of G_s-adenylate cyclase in discrete brain areas may contribute to the pathology in AD and complicate the use of treatments targeted at cyclase-linked receptors. However, the preservation of PKC would suggest the possibility of directing drugs, such as muscarinic agonists, which are coupled to this system. Although there was no conclusive evidence of plastic modifications of second messenger systems in AD, the magnitude of the reduction in [^{3}H]-forskolin binding in the primary area of degeneration in AD, coupled with the preservation of [^{3}H]-PDBu binding, warrants future research.

APPENDIX I

Full Quantitative Analysis of
[^{3}H]-Forskolin Binding (a),
[^{3}H]-PDBu Binding (b) and
Local Cerebral Glucose Utilisation (c)
following Unilateral Orbital Enucleation.

APPENDIX I (a)

[^{3}H]-FORSKOLIN BINDING FOLLOWING UNILATERAL ENUCLEATION

	CONTROL Intact/Deprived	1 DAY Intact/Deprived	5 DAY Intact/Deprived	10 DAY Intact/Deprived	20 DAY Intact/Deprived
Visual Structures					
Visual Cortex II/III	74±5 / 72±4	75±3 / 73±3	65±3 / 68±3	81±2 / 81±2	83±4 / 82±4
Visual Cortex IV	75±4 / 76±4	76±3 / 73±3	70±3 / 73±3	87±2 / 86±2	89±3 / 88±3
Visual Cortex V/VI	62±3 / 66±4	63±3 / 60±3	61±3 / 64±3	74±2 / 74±2	74±7 / 73±2
Superior Colliculus (Superficial layer)	80±5 / 78±5	76±3 / 78±4	69±3 / 55±2*	87±3 / 73±2	91±4 / 72±5*
Dorsal Lateral Geniculate Body	41±3 / 39±2	42±2 / 40±3	41±3 / 35±2*	51±2 / 43±2*	49±3 / 41±2*
Pretectal Nuclei	28±4 / 28±4	34±3 / 33±3	32±3 / 31±3	36±2 / 35±2	36±3 / 35±4
Lateral Posterior Nucleus	52±8 / 52±8	59±5 / 58±4	51±5 / 52±6	60±3 / 59±3	60±4 / 60±4
Non-Visual Structures					
Medial Geniculate	40±5 / 40±6	44±4 / 42±3	39±5 / 40±6	55±4 / 58±4	52±4 / 51±2
Lateral Habenula	30±5 / 28±5	29±4 / 29±4	32±3 / 33±4	30±5 / 28±5	29±5 / 30±4
Hippocampus Molecular Layer	67±9 / 69±9	75±6 / 78±6	66±8 / 66±8	84±4 / 84±3	82±14/ 79±12
Parietal Cortex IV	78±5 / 79±6	80±4 / 78±3	74±4 / 74±5	79±6 / 80±4	83±5 / 85±5
Caudate Putamen	107±15/109±16	138±22/138±25	98±10/ 99±10	103±4 /110±7	111±8 /112±9
Thalamus	49±12/ 49±12	55±5 / 56±5	52±7 / 53±8	57±4 / 56±4	59±2 / 58±3

Forskolin binding pmoles/g tissue. Roman numerals indicate the cortical layer examined. Data are derived from 23 animals and presented as mean ± SEM (n=3-6 per group). *$p<0.01$ significant difference between intact and deprived hemisphere by paired t-test. $F<1.6$ ($p>0.5$) for all structures in intact hemisphere between control and enucleated animals by ANOVA.

APPENDIX I (b)

[^{3}H]-PDBu BINDING FOLLOWING UNILATERAL ENUCLEATION

	CONTROL Intact/Deprived	1 DAY Intact/Deprived	5 DAY Intact/Deprived	10 DAY Intact/Deprived	20 DAY Intact/Deprived
Visual Structures					
Visual Cortex II/III	611±39/603±46	502±23/483±17	631±43/625±35	653±33/628±29	560±30/566±34
Visual Cortex IV	544±40/550±47	432±19/422±20	556±38/541±29	555±33/540±39	477±16/493±20
Visual Cortex V/VI	502±34/526±44	417±18/418±20	530±34/524±30	566±28/590±39	459±19/481±18
Superior Colliculus (Superficial layer)	425±23/424±26	374±11/387±12	477±26/437±24	461±28/484±33	390±18/391±18
Dorsal Lateral Geniculate Body	314±19/315±19	288±17/276±14	306±29/291±26	313±26/316±31	267±25/255±11
Pretectal Nuclei	175±4 /180±16	155±2 /154±10	200±17/205±16	173±17/169±14	143±14/148±17
Lateral Posterior Nucleus	369±31/387±35	356±10/351±22	400±61/395±62	375±41/376±35	317±27/329±22
Non-Visual Structures					
Medial Geniculate	341±23/339±28	343±30/342±32	383±107/393±130	356±56/392±55	336±42/320±43
Lateral Habenula	174±14/158±11	146±14/143±10	168±17/171±25	166±15/151±11	138±15/121±9
Hippocampus Molecular Layer	667±59/658±74	535±39/526±44	768±66/766±61	708±40/758±47	548±20/579±34
Parietal Cortex IV	540±80/568±79	484±19/489±16	549±70/572±66	650±74/662±72	613±48/645±43
Caudate Putamen	496±90/487±80	351±37/363±42	506±87/544±96	539±88/589±101	367±33/364±32
Thalamus	433±42/408±50	367±24/351±22	415±61/421±69	429±56/433±54	338±23/340±23

PDBu binding pmoles/g tissue. Roman numerals indicate the cortical layer examined. Data are derived from 23 animals and presented as mean ± SEM (n=3-6 per group). *$p<0.01$ significant difference between intact and deprived hemisphere by paired t-test. $F<1.7$ ($p>0.5$) for all structures in intact hemisphere between control and enucleated animals by ANOVA.

APPENDIX I (c)

GLUCOSE UTILISATION FOLLOWING UNILATERAL ENUCLEATION

	CONTROL Intact/Deprived	1 DAY Intact/Deprived	5 DAY Intact/Deprived	10 DAY Intact/Deprived	20 DAY Intact/Deprived
Visual Structures					
Visual Cortex II/III	85±3 / 88±4	92±2 / 75±2*	87±4 / 70±3*	91±3 / 74±2*	83±2 / 66±2*
Visual Cortex IV	96±3 / 98±4	102±2 / 79±2*	93±3 / 75±2*	101±3 / 83±3*	93±3 / 72±2*
Visual Cortex V/VI	82±3 / 84±4	88±2 / 73±1*	82±3 / 70±2*	89±2 / 74±2*	79±2 / 67±1*
Superior Colliculus (Superficial layer)	93±3 / 95±4	95±2 / 58±1*	90±2 / 62±2*	92±2 / 68±1*	87±2 / 65±2*
Dorsal Lateral Geniculate Body	102±5 / 98±4	102±2 / 69±2*	99±4 / 68±4*	107±2 / 75±1*	100±2 / 72±2*
Pretectal Nuclei	96±3 / 98±4	96±3 / 84±3*	88±4 / 73±3*	97±1 / 87±2*	91±2 / 81±2*
Lateral Posterior Nucleus	98±4 / 99±4	96±2 / 75±2*	92±4 / 72±3*	98±2 / 77±3*	96±4 / 78±4*
Non-Visual Structures					
Medial Geniculate	105±9 /112±15	107±4 /107±2	104±7 /106±6	108±3 /114±5	101±2 /103±2
Lateral Habenula	104±10/104±8	111±4 /113±3	112±7 /111±8	110±4 /111±5	111±3 /114±4
Hippocampus Molecular Layer	77±4 / 77±5	82±2 / 80±2	77±4 / 76±4	81±1 / 82±2	73±1 / 71±2
Parietal Cortex IV	99±12/ 99±13	100±2 / 99±3	97±5 / 94±5	98±4 / 97±4	93±4 / 89±3
Caudate Putamen	79±6 / 79±7	82±1 / 80±2	76±6 / 74±5	84±11/ 87±11	78±2 / 78±2
Thalamus	96±3 / 98±3	102±3 /102±3	104±5 /106±6	115±5 /114±5	103±2 /104±2

Glucose utilisation: μmol $100g^{-1}min^{-1}$. Roman numerals indicate the cortical layer examined. Data are derived from 30 animals and presented as mean ± SEM (n=6 per group). *$p<0.01$ significant difference between intact and deprived hemisphere by paired t-test. $F<1.1$ ($p>0.5$) for all structures in intact hemisphere between control and enucleated animals by ANOVA.

APPENDIX II

Full Quantitative Analysis of [^{3}H]-Forskolin Binding in the Presence and Absence of Gpp(NH)p in Control Animals and Following Unilateral Orbital Enucleation

APPENDIX II

EFFECT OF GPP(NH)P ON [^{3}H]-FORSKOLIN BINDING FOLLOWING UNILATERAL ORBITAL ENUCLEATION

	-GPP(NH)p		+Gpp(NH)p	
	CONTROL Intact/Deprived	ENUCLEATED Intact/Deprived	CONTROL Intact/Deprived	ENUCLEATED Intact/Deprived
Visual Structures				
Visual Cortex II/III	62±4 / 62±3	56±7 / 56±6	63±5 / 63±4	56±3 / 56±4
Visual Cortex IV	64±4 / 64±4	60±5 / 60±6	†70±5 / 69±5	65±3 / 63±4
Visual Cortex V/VI	55±4 / 54±4	51±5 / 54±4	59±5 / 60±5	54±4 / 52±4
Superior Colliculus (Superficial layer)	60±3 / 60±2	61±3 / 48±4*	†82±3 / 84±5	82±4 / 67±3*
Dorsal Lateral Geniculate Body	42±3 / 41±3	40±2 / 32±2*	42±3 / 42±3	43±2 / 42±1
Pretectal Nuclei	33±3 / 32±2	26±4 / 26±4	39±3 / 38±2	39±6 / 38±6
Lateral Posterior Nucleus	57±3 / 56±3	47±3 / 46±3	48±3 / 48±2	50±2 / 50±1
Non-Visual Structures				
Medial Geniculate	41±4 / 41±4	39±5 / 44±6	47±4 / 45±5	45±4 / 46±3
Lateral Habenula	26±3 / 29±3	31±3 / 32±3	†40±1 / 38±2	42±1 / 42±1
Hippocampus Molecular Layer	68±3 / 64±3	63±5 / 60±6	75±6 / 72±6	66±4 / 63±4
Parietal Cortex IV	65±3 / 62±3	57±6 / 57±5	71±4 / 68±5	64±6 / 69±5
Caudate Putamen	116±17/118±18	113±13/115±14	†210±17/204±17	194±17/191±22
Thalamus	51±4 / 52±5	47±4 / 47±4	51±5 / 50±4	46±3 / 46±3

Forskolin binding pmoles/g tissue. Roman numerals indicate the cortical layer examined. Data are mean ± SEM (n=5 per group). *$p<0.01$ significant difference between intact and deprived hemisphere by paired t-test. † $p<0.01$ significant difference between [^{3}H]-forskolin binding in the absence and presence of Gpp(NH)p.

APPENDIX III

Full Quantitative Analysis of
[^{3}H]-Forskolin Binding (a),
[^{3}H]-PDBu Binding (b) and
Local Cerebral Glucose Utilisation
Following Visual Cortex Lesion

APPENDIX III(a)

[^{3}H]-FORSKOLIN BINDING FOLLOWING VISUAL CORTEX LESION

	SHAM Ipsilateral/Contralateral	LESION Ipsilateral/Contralateral
Visual Structures		
Visual Cortex II/III	64±4 / 73±7	**44±6 / 74±4
Visual Cortex IV	69±5 / 77±7	***45±6 / 77±3
Visual Cortex V/VI	61±4 / 63±4	**34±5 / 63±3
Superior Colliculus (Superficial layer)	74±5 / 75±6	***70±4 / 82±4
Dorsal Lateral Geniculate Body	49±3 / 49±4	***46±2 / 52±2
Pretectal Nuclei	34±3 / 34±3	37±2 / 38±1
Lateral Posterior Nucleus	59±3 / 61±3	61±3 / 64±3
Non-Visual Structures		
Medial Geniculate	48±4 / 51±3	46±2 / 49±2
Lateral Habenula	32±2 / 33±2	41±3 / 40±2
Hippocampus Molecular Layer	85±9 / 75±7	77±6 / 79±6
Parietal Cortex IV	80±7 / 78±7	81±4 / 81±5
Caudate Putamen	131±8 /135±10	140±8 /144±12
Thalamus	63±3 / 65±4	64±4 / 64±3

Forskolin binding: pmoles/g tissue. Roman numerals indicate the cortical layer examined. Data are derived from six sham and six lesion animals and presented as mean ± SEM.

**$p<0.005$, ***$p<0.001$ significant difference between contralateral and ipsilateral hemisphere by paired t-test.

$F<1.5$ ($p>0.5$) for all structures in contralateral hemisphere between sham and lesion animals by ANOVA.

APPENDIX III(b)

[^{3}H]-PDBu BINDING FOLLOWING VISUAL CORTEX LESION

	SHAM Ipsilateral/Contralateral	LESION Ipsilateral/Contralateral
Visual Structures		
Visual Cortex II/III	429±24/476±44	380±11/405±36
Visual Cortex IV	314±18/315±23	239±6 /286±26
Visual Cortex V/VI	311±14/315±24	*185±14/279±19
Superior Colliculus (Superficial layer)	289±17/291±18	262±26/260±25
Dorsal Lateral Geniculate Body	187±14/187±14	181±11/180±4
Pretectal Nuclei	124±11/126±9	136±16/133±13
Lateral Posterior Nucleus	212±14/208±12	228±10/230±10
Non-Visual Structures		
Medial Geniculate	194±13/197±11	182±16/180±14
Lateral Habenula	104±17/ 98±17	124±13/110±13
Hippocampus Molecular Layer	270±15/281±22	280±16/294±19
Parietal Cortex IV	284±35/257±36	308±28/314±28
Caudate Putamen	258±12/263±19	252±26/260±23
Thalamus	229±8 /227±9	222±12/223±13

PDBu binding: pmoles/g tissue. Roman numerals indicate the cortical layer examined. Data are derived from five sham and six lesion animals and presented as mean ± SEM.

*$p<0.01$ significant difference between contralateral and ipsilateral hemisphere by paired t-test.

$F<1.94$ ($p>0.5$) for all structures in contralateral hemisphere between sham and lesion animals by ANOVA.

APPENDIX III(c)

GLUCOSE UTILISATION FOLLOWING VISUAL CORTEX LESION

	SHAM Ipsilateral/Contralateral	LESION Ipsilateral/Contralateral
Visual Structures		
Visual Cortex II/III	†79±10/ 84±9	**63±10/ 83±7
Visual Cortex IV	*87±8 / 95±9	***63±10/ 95±8
Visual Cortex V/VI	†75±7 / 83±3	**59±9 / 82±8
Superior Colliculus (Superficial layer)	91±9 / 93±11	84±8 / 91±8
Dorsal Lateral Geniculate Body	93±6 / 92±6	*91±11/ 94±11
Pretectal Nuclei	83±5 / 83±6	83±8 / 86±9
Lateral Posterior Nucleus	86±7 / 87±8	86±10/ 88±10
Non-Visual Structures		
Medial Geniculate	97±10/101±10	92±10/ 97±12
Lateral Habenula	96±6 / 97±7	95±9 / 98±10
Hippocampus Molecular Layer	72±5 / 70±5	72±8 / 72±8
Parietal Cortex IV	91±7 / 92±8	82±9 / 83±6
Caudate Putamen	67±5 / 68±4	66±4 / 67±4
Thalamus	78±4 / 78±5	85±5 / 83±5

Glucose utilisation: μmol $100^{-1}min^{-1}$. Roman numerals indicate the cortical layer examined. Data are derived from six sham and six lesion animals and presented as mean ± SEM.

†<0.05, *$p<0.01$, **$p<0.005$, ***$p<0.001$ significant difference between contralateral and ipsilateral hemisphere by paired t-test.

$F<0.261$ ($p>0.5$) for all structures in contralateral hemisphere between sham and lesion animals by ANOVA.

APPENDIX IV

Full Quantitative Analysis of
[^{3}H]-Forskolin Binding (a),
[^{3}H]-PDBu Binding (b)
Following Lesion of the Rat Medial Septum

APPENDIX IV(a)

[^{3}H]-FORSKOLIN BINDING FOLLOWING MEDIAL SEPTAL LESION

	SHAM	LESION
Medial Septum	42 ± 2	34 ± 3*
Lateral Septum	52 ± 6	43 ± 5
Vertical Diagonal Band	32 ± 3	34 ± 3
Horizontal Diagonal Band	28 ± 2	31 ± 3
HIPPOCAMPUS:		
CA1 Field: Stratum oriens	40 ± 2	42 ± 2
Pyramidal	-	-
Radiatum	33 ± 2	36 ± 1
Lacunosum Moleculare	52 ± 3	57 ± 3
CA3 Field: Stratum oriens	30 ± 2	33 ± 2
Pyramidal	75 ± 4	91 ± 10
CA4 Field:		
Dentate Gyrus: Molecular Layer	73 ± 4	83 ± 3
Granular Layer	67 ± 4	77 ± 4
Polymorph Layer	136 ± 8	162 ± 6*
Entorhinal Cortex:		
Layer I-III	86 ± 5	84 ± 5
Layer IV-VI	72 ± 3	73 ± 6
Caudate Putamen	154 ± 6	157 ± 9
Frontal Cortex layer IV	65 ± 3	73 ± 3
Superior Colliculus	77 ± 2	84 ± 3
Dorsal Lateral Geniculate Body	49 ± 2	55 ± 2
Medial Geniculate	47 ± 2	48 ± 3

Forskolin Binding: pmoles/g tissue. Roman numerals indicate the cortical layer examined. Data are presented as mean ± SEM where n=7 in each group. *$p<0.05$ significant difference between sham and lesion group by unpaired t-test.

APPENDIX IV(b)

[^{3}H]-PDBu BINDING FOLLOWING MEDIAL SEPTAL LESION

	SHAM	LESION
Medial Septum	203 ± 8	223 ± 11
Lateral Septum	344 ± 28	381 ± 62
Vertical Diagonal Band	234 ± 10	228 ± 15
Horizontal Diagonal Band	166 ± 13	151 ± 13
HIPPOCAMPUS:		
CA1 Field: Stratum oriens	387 ± 42	377 ± 39
Pyramidal	463 ± 43	473 ± 46
Radiatum	371 ± 31	384 ± 32
Lacunosum Moleculare	255 ± 18	255 ± 16
CA3 Field: Stratum oriens	321 ± 16	306 ± 9
Pyramidal	340 ± 21	334 ± 21
CA4 Field:	297 ± 15	319 ± 32
Dentate Gyrus: Molecular Layer	315 ± 14	322 ± 33
Granular Layer	280 ± 14	287 ± 18
Polymorph Layer	233 ± 20	256 ± 21
Entorhinal Cortex:		
Layer I-III	583 ± 37	737 ± 53*
Layer IV-VI	355 ± 39	421 ± 33
Caudate Putamen	210 ± 11	216 ± 9
Frontal Cortex layer IV	275 ± 16	276 ± 19
Superior Colliculus	282 ± 16	316 ± 12
Dorsal Lateral Geniculate Body	204 ± 21	211 ± 4
Medial Geniculate	205 ± 14	206 ± 7

PDBu Binding: pmoles/g tissue. Roman numerals indicate the cortical layer examined. Data are presented as mean ± SEM where n=7 in each group. *$p<0.05$ significant difference between sham and lesion group by unpaired t-test.

APPENDIX V

(a) Full Quantitative Analysis of [^{3}H]-Forskolin Binding in Control and AD Brain. [^{3}H]-Forskolin Binding was performed in Adjacent Sections to Those Used for [^{3}H]-PDBu Binding as Shown in Results Section 2.

(b) Linear Correlation Coefficients of [^{3}H]-Forskolin Binding with ChAT Activity.

APPENDIX V(a)

[^{3}H]-FORSKOLIN BINDING IN CONTROL AND AD BRAIN

	[^{3}H]-FORSKOLIN BINDING	
	CONTROL	AD
Middle Frontal Cortex		
Layers I/III	88 ± 6	57 ± 5 *
Layer IV	71 ± 6	52 ± 5 *
Layers V-VI	76 ± 5	57 ± 5 *
White Matter	14 ± 1	15 ± 1
Middle Temporal Cortex		
Layers I-III	72 ± 6	46 ± 5 *
Layer IV	65 ± 5	44 ± 4 *
Layers V-VI	67 ± 5	47 ± 4 *
White Matter	14 ± 1	11 ± 1
Hippocampal Region		
CA1	24 ± 2	22 ± 3
CA3	29 ± 3	24 ± 3
CA4	35 ± 3	29 ± 4
Hilus	45 ± 3	33 ± 6
Molecular Layer	39 ± 4	24 ± 5 *
Granular Layer	29 ± 3	23 ± 5
Lacunosum moleculare	41 ± 4	29 ± 6
Subiculum	29 ± 3	24 ± 5
Parahippocampal Gyrus: Superficial layer	54 ± 4	43 ± 7
Deep layer	43 ± 3	36 ± 7
White Matter	13 ± 2	12 ± 2

Forskolin Binding: pmol/g tissue. Roman numerals indicate the cortical layer examined.

Data are derived from nine control and nine Alzheimer (AD) cases and presented as mean ± SEM. *$p<0.05$ significant difference by unpaired t-test.

FOOTNOTE: The levels of [^{3}H]-forskolin binding, presented here, are markedly different to those in a separate study (see Results section 1.4). These disparate levels of [^{3}H]-forskolin binding in two different series of experiments reinforces the absolute requirement that all ligand binding in control and AD brain be performed on the same day.

APPENDIX V(b)

LINEAR CORRELATION COEFFICIENTS OF [^{3}H]-FORSKOLIN BINDING WITH ChAT ACTIVITY

	r VALUES	p VALUES
Middle Frontal Cortex		
Layers I/III	0.711	<0.01
Layer IV	0.683	<0.01
Layers V-VI	0.619	<0.05
Middle Temporal Cortex		
Layers I-III	0.735	<0.01
Layer IV	0.723	<0.01
Layers V-VI	0.727	<0.01
Hippocampal Region		
CA1	0.032	NS
CA3	0.032	NS
CA4	0.077	NS
Hilus	0.257	NS
Molecular Layer	0.305	NS
Granular Layer	0.290	NS
Lacunosum moleculare	0.336	NS
Subiculum	0.141	NS
Parahippocampal Gyrus: Superficial layer	0.469	NS
Deep layer	0.363	NS

Correlation analysis, using linear regression analysis, was determined between [^{3}H]-forskolin binding and ChAT activity when data from control and AD brains were combined. r Values are indicated above and the significance level (p value). NS indicates no significant correlation.

APPENDIX VI

Linear Correlation Coefficient of
[^{3}H]-Forskolin Binding (a) and
[^{3}H]-PDBu Binding (b)
with Postmortem Delay and Age

APPENDIX VI(a)

LINEAR CORRELATION COEFFICIENTS OF [^{3}H]-FORSKOLIN BINDING WITH POSTMORTEM DELAY AND AGE IN HUMAN BRAIN

BRAIN REGION	POSTMORTEM DELAY		AGE	
	CONTROL	AD	CONTROL	AD
MIDDLE FRONTAL CORTEX				
Layer I-III	0.000	0.270	0.055	-0.955*
IV	0.155	0.145	0.423	-0.959*
V-VI	0.266	0.152	0.444	-0.972*
MIDDLE TEMPORAL CORTEX				
Layer I-III	0.467	0.363	0.000	0.329
IV	0.486	0.397	0.109	0.055
V-VI	0.564	0.359	0.221	0.359
HIPPOCAMPAL FORMATION				
CA1	0.253	0.428	0.554	0.000
CA3	0.285	0.045	0.483	0.348
CA4	0.182	0.207	0.457	0.293
Hilus	0.000	0.361	0.589	0.305
Granular Layer	0.063	0.192	0.550	0.192
Molecular Layer	0.122	0.158	-0.700*	0.045
Lacunosum moleculare	0.286	0.000	-0.710*	0.000
Subiculum	0.313	0.210	-0.710*	0.000
Parahippocampal Gyrus:				
Superficial	0.396	0.592	0.503	0.263
Deep	0.604	0.540	0.265	0.339

r Values are presented as determined using least squares fit linear regression analysis. *$p<0.05$ significant correlation, the direction of the correlation is shown.

[^{3}H]-Forskolin binding is taken from series 1 (see Results section 1.4).

APPENDIX VI(b)

LINEAR CORRELATION COEFFICIENTS OF [^{3}H]-PDBu BINDING WITH POSTMORTEM DELAY AND AGE IN HUMAN BRAIN

BRAIN REGION	POSTMORTEM DELAY		AGE	
	CONTROL	AD	CONTROL	AD
MIDDLE FRONTAL CORTEX				
Layer I-II	0.543	0.164	0.644	0.141
III-IV	0.327	0.319	0.367	0.257
V-VI	0.349	0.155	0.285	0.268
MIDDLE TEMPORAL CORTEX				
Layer I-II	0.447	0.486	-0.847*	0.283
III-IV	0.286	0.263	-0.754*	0.077
V-VI	0.564	0.359	0.221	0.359
HIPPOCAMPAL FORMATION				
CA1	0.621	0.632	0.263	0.356
CA3	0.170	0.286	0.351	0.176
CA4	0.696	0.200	0.355	0.495
Hilus	0.513	0.540	0.539	0.045
Granular Layer	0.138	0.581	0.249	0.110
Molecular Layer	0.239	0.443	0.270	0.063
Lacunosum moleculare	0.478	0.575	0.286	0.148
Subiculum	0.608	0.495	0.228	0.482
Parahippocampal Gyrus:				
Superficial	0.286	0.352	0.228	0.482
Deep	0.628	0.509	0.243	0.032

r Values are presented as determined using least squares fit linear regression analysis. *$p<0.05$ significant correlation, the direction of the correlation is shown.

APPENDIX VII

Effect of Postmortem Delay
on [^{3}H]-Forskolin Binding in Rat Brain

APPENDIX VII

EFFECT OF POSTMORTEM DELAY ON [^{3}H]-FORSKOLIN BINDING IN RAT BRAIN

Postmortem Delay (hours)	Total	Non-Specific	Specific	% Specific
0	93 ± 3	6 ± 1	87 ± 3	93
2	95 ± 1	8 ± 1	87 ± 1	92
5	98 ± 1	12 ± 1	86 ± 1	88
15	84 ± 4	12 ± 1	71 ± 4	86

Rats were decapitated and the intact brain inside the skull left at room temperature for increasing periods of time after which the brain was frozen in isopentane and sectioned. Brain sections were labelled with 20nM [^{3}H]-forskolin. Non-specific binding was defined in the presence of 20μM unlabelled forskolin. Specific binding was determined by subtraction of non-specific from total binding. Radioactivity was measured using liquid scintillation analysis. Data are presented as mean ± SEM (n=2 at each time point).

APPENDIX VIII

Scatchard Analysis of [^{3}H]-Forskolin Binding (VIIIa) and [^{3}H]-PDBu (VIIIb) in Rat Brain

VIIIa

A. [^{3}H]-Forskolin binding was examined in rat brain sections at the level of the caudate putamen in three rats. Sections were incubated with increasing concentrations of [^{3}H]-forskolin (2 - 100nM) at 22°C for 20 minutes and the radioactivity counted by liquid scintillation. Non-specific binding was defined in the presence of 20μM unlabelled forskolin.

B. Scatchard analysis of saturation data of [^{3}H]-forskolin binding.

VIIIb

A. [^{3}H]-PDBu binding was examined in rat brain sections at the level of the caudate putamen in three rats. Sections were incubated with increasing concentrations of [^{3}H]-PDBu (2.5 - 150nM) at 22°C for 90 minutes and the radioactivity counted by liquid scintillation. Non-specific binding was defined in the presence of 2μM unlabelled forskolin.

B. Scatchard analysis of saturation data of [^{3}H]-PDBu binding.

APPENDIX VIII(a)

SCATCHARD ANALYSIS OF ^{3}H-FORSKOLIN BINDING IN RAT BRAIN

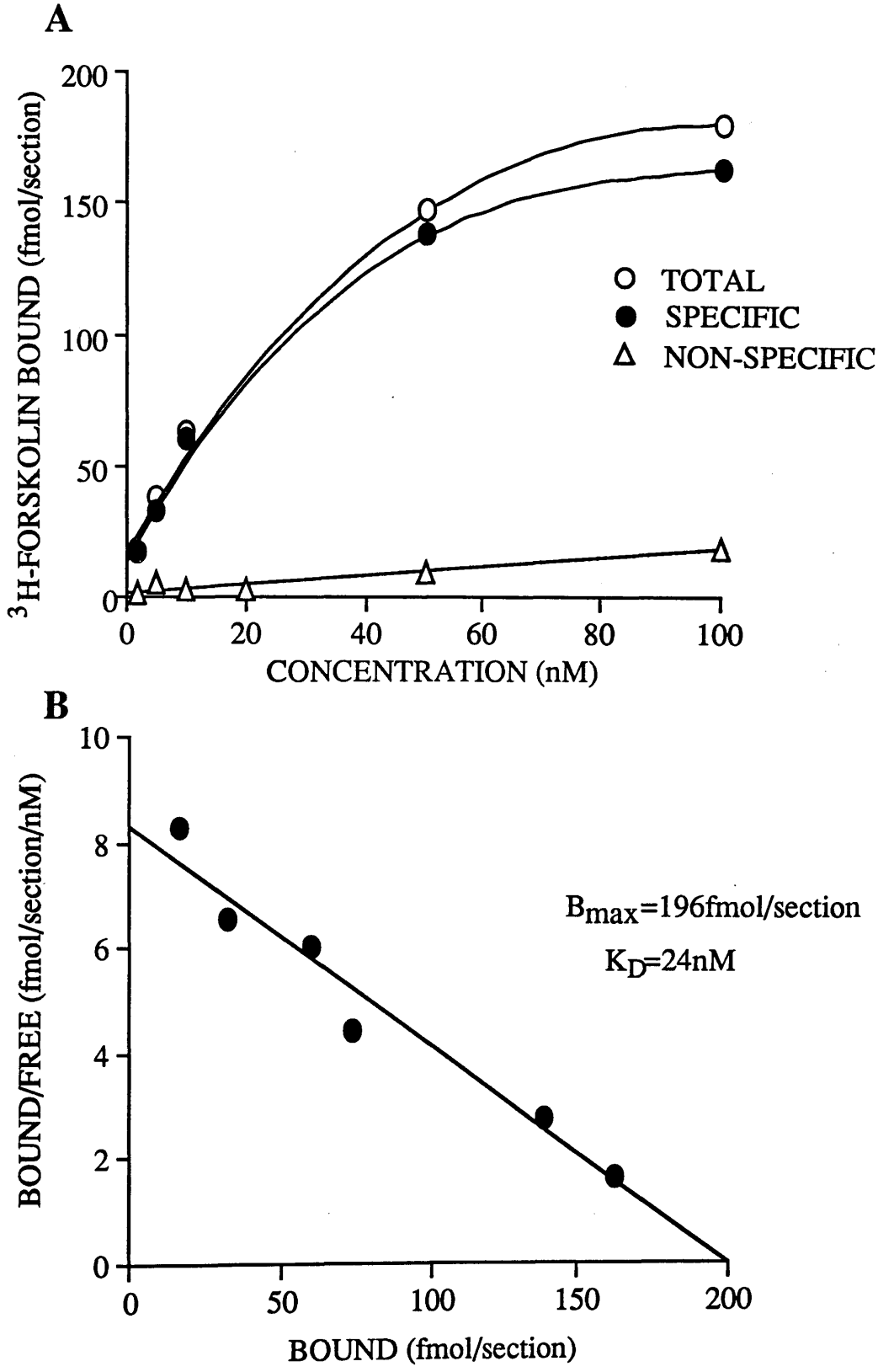

APPENDIX VIII(b)

SCATCHARD ANALYSIS OF ^{3}H-PDBu BINDING IN RAT BRAIN

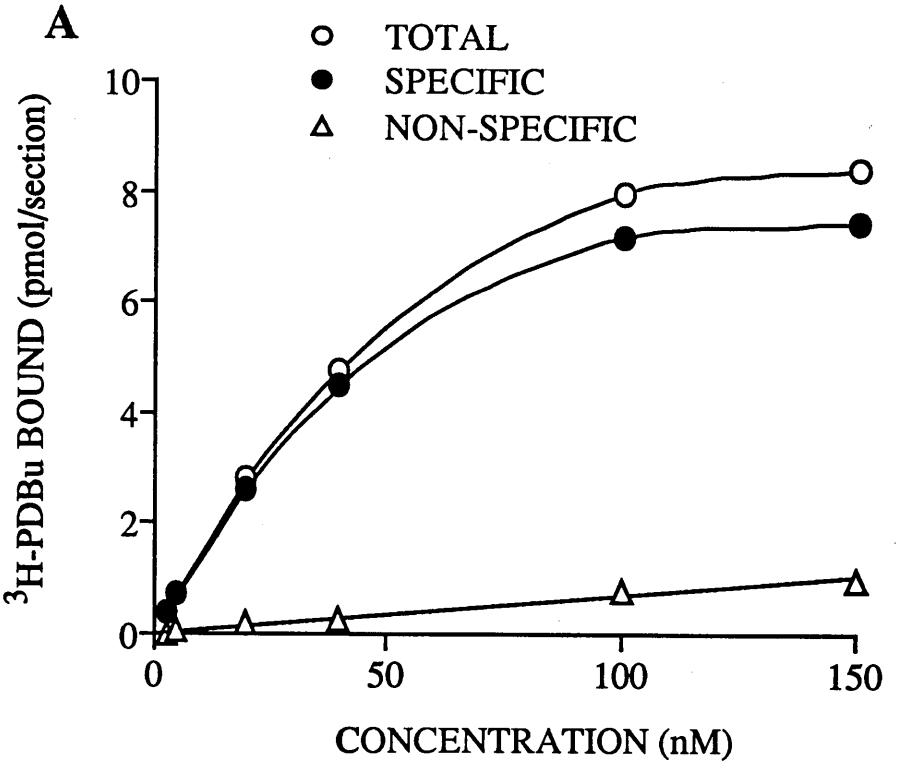

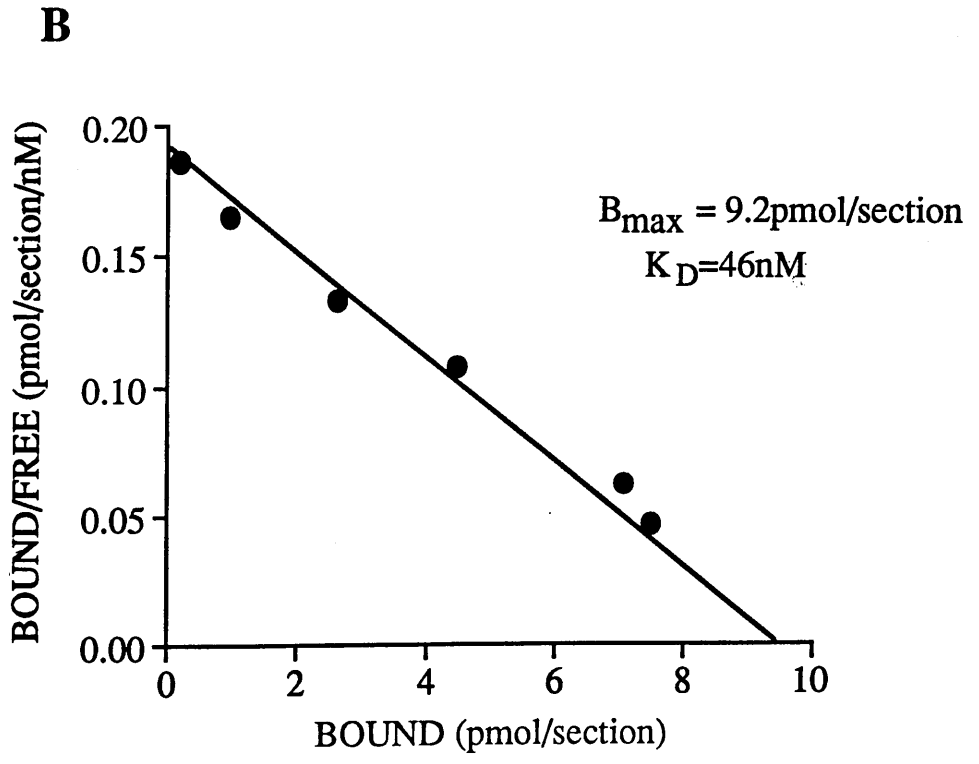

REFERENCES

Alonso, A. & Köhler, C. (1984) A study of the reciprocal connections between the septum and the entorhinal area using anterograde and retrograde axonal transport methods in the rat brain, *Journal of Comparative Neurology*, **225**, 327-343.

Ando, S., Kametani, H., Osada, H., Iwamoto, M. & Kimura, N. (1987) Delayed memory dysfunction by transient hypoxia and its prevention with forskolin, *Brain Research*, **405**, 371-374.

Aoki, C. & Siekevitz, P. (1985) Ontogenetic changes in the cyclic adenosine 3'-5' monophosphate stimulatable phosphorylation of cat visual cortex proteins, particularly of microtubule associated protein 2 (MAP2): effects of normal and dark rearing and of exposure to light, *Journal of Neuroscience*, **5**, 2465-2483.

Artola, A. & Singer, W. (1987) Long-term potentiation and NMDA receptors in rat visual cortex, *Nature*, **330**, 649-652.

Avissar, S., Schreiber, G., Danon, A. & Belmaker, R.H. (1988) Lithium inhibits adrenergic and cholinergic increase in GTP binding in rat cortex, *Nature*, **331**, 440-442.

Barnes, D.M. (1986) Neurotransmitters regulate growth cones, *Science*, **234**, 1325-1326.

Barovsky, K., Pedone, C. & Brooker, G. (1983) Distinct mechanisms of forskolin-stimulated cyclic AMP accumulation of forskolin-potentiated hormone responses in C6-2B cells, *Molecular Pharmacology*, **25**, 256-260.

Bartus, R.T., Dean III, R.L., Beer, B. & Lippa, A.S. (1982) The cholinergic hypothesis of geriatric memory dysfunction, *Science*, **217**, 408-417.

Baughman, R.W. & Gilbert, C.D. (1981) Aspartate and glutamate as possible neurotransmitters in the visual cortex, *Journal of Neuroscience*, **1**, 427-439.

Beach, T.G., Walker, R. & McGeer, E.G. (1989) Patterns of gliosis in Alzheimer's disease and aging cerebrum. *Glia*, **2**, 420-436.

Beal, M.G. & Martin, J.B. (1986) Neuropeptides in neurological disease, *Annals of Neurology*, **20**, 547-565.

Bear, M.F. & Singer, W. (1986) Modulation of visual cortical plasticity by acetylcholine and noradrenaline, *Nature*, **320**, 172-176.

Berridge, M.J. (1984) Inositol trisphosphate and diacylglycerol as second messengers, *Biochemical Journal*, **220**, 345-360.

Berridge, M.J. & Irvine, R.F. (1984) Inositol trisphosphate, a novel second messenger in cellular signal transduction, *Nature*, **312**, 315-321.

Bhat, S.V., Bajwa, B.S., Dornauer, H. & De Souza, N.J. (1977) Structures and stereochemistry of new labdane diterpenoids from coleus forskohlii briq. *Tetrahedron Letters*, **19**, 1669-1672.

Bird, S.J. & Aghajanian, G.K. (1975) Denervation supersensitivity in the cholinergic septo-hippocampal pathway: a microiontophoretic study, *Brain Research*, **100**, 355-370.

Blumberg, P.M., Jaken, S., König, B., Sharkey, N.A., Leach, K.L., Jeng, A.Y. & Yeh, E. (1984) Mechanism of action of the phorbol ester tumor promoters: specific receptors for lipophilic ligands, *Biochemical Pharmacology*, **33**, 933-940.

Bowen, D.M., Allen, S.J., Benton, J.S., Goodhardt, M.J., Haan, E.A., Palmer, A.M., Sims, N.R., Smith, C.C.T., Spillane, J.A., Esiri, M.M., Neary, D., Snowdon, J.S., Wilcock, G.K. & Davison, A.M. (1983) Biochemical assessment of serotonergic and cholinergic dysfunction and cerebral atrophy in Alzheimer's disease, *Journal of Neurochemistry*, **41**, 266-272.

Brashear, H.R., Zaborszky, L. & Heimer, L. (1986) Distribution of GABAergic and cholinergic neurons in the rat diagonal band, *Neuroscience*, **17**, 439-451.

Bray, P., Carter, A., Simons, C., Guo, V., Puckett, C., Kamholz, J., Speigel, A. & Nirenberg, M. (1986) Human cDNA clones for four species of $G_{\alpha S}$ signal transduction protein, *Proceedings of National Academy of Sciences* USA, **85**, 2081-2085.

Brostrom, C.O., Huang, Y.C., Breckenridge, B.M. & Wolff, D.J. (1975) Identification of a calcium-binding protein as a calcium-dependent regulator of brain adenylate cyclase, *Proceedings of the National Academy of Sciences*, **72**, 64-68.

Brun, A. (1983) An overview of light and electron microscope changes. In *Alzheimer's Disease, The Standard Reference*, ed. Reisberg, B., pp 37-47, New York, Free Press.

Buxbaum, J.D., Gandy, S.W. Cicchetti, P., Ehrlich, M.E., Czernok, A.J., Fracasso, R.P., Ramabhadran, T.V., Unterbeck, A.J. & Greengard, P. (1990) Processing of Alzheimer β/A4 amyloid precursor protein: modulation by agents that regulate protein phosphorylation, *Proceedings of the National Academy of Sciences USA*, **87**, 6003-6006.

Candy, J.M., Court, J.A., Perry, R.H. & Smith, C.J. (1984) Carbachol-stimulated phosphatidylinositol hydrolysis in the cerebral cortex after freezing and postmortem delay, *British Journal of Pharmacology*, **83**, 356P.

Cassel, D. & Selinger, Z. (1978) Mechanism of adenylate cyclase activation through the β-adrenergic receptor: catecholamine induced displacement of bound GDP by GTP, *Proceedings of the National Academy of Sciences* USA, **75**, 4155-4159.

Chalmers, D.T. & McCulloch, J. (1989) Reduction in [^{3}H]glutamate binding in the visual cortex after unilateral orbital enucleation, *Neuroscience Letters*, **97**, 298-304.

Chalmers D.T., Dewar D., Graham D.I., Brooks D.N. & McCulloch J. (1990) Differential alterations of cortical glutaminergic binding sites in senile dementia of the Alzheimer Type, *Proceedings of the National Academy of Sciences, USA*, **87**, 1352-2356.

Chalmers, D.T. & McCulloch, J. (1990) Alterations in Neurotransmitter Receptors and Glucose Use after Unilateral Orbital Enucleation, *Brain Research*, (in press).

Chen, L.L., Van Hoesen, G.W., Barnes, C.L. & West, J.R. (1983) Enhanced acetylcholinesterase staining in the hippocampal perforant pathway zone after combined lesions of the septum and entorhinal cortex, *Brain Research*, **272**, 354-359.

Cheung, W.Y., Bradham, L.S., Lynch, T.J., Lin, Y.M. & Tallant, E.A. (1975) Protein activator of cyclic 3'-5'-nucleotide phosphodiesterase of bovine or rat brain also activates its adenylate cyclase, *Biochemistry and Biophysiology Research Communications*, **66**, 1055-1062.

Chu, D.C.M., Penney Jr., J.B. & Young, A.B. (1987) Cortical $GABA_B$ and $GABA_A$ receptors in Alzheimer's disease: a quantitative autoradiographic study, *Neurology*, **37**, 1454-1459.

Cockroft, S. & Gomperts, B.D. (1985) Role of guanine nucleotide binding protein in the activation of polyphosphoinositide phosphodiesterase, *Nature*, **314**, 534-536.

Cohen, J. (1977) *Statistical Power Analysis for the Behavioural Sciences*, Revised Edition, Academic Press, New York.

Cole G., Dobkins K.R., Hansen L.A., Terry R.D. & Saitoh T. (1988) Decreased levels of protein kinase C in Alzheimer brain. *Brain Research*, **452**, 165-174.

Collingbridge, G.L. & Bliss, T.V.P. (1987) NMDA receptors - their role in long-term potentiation, *Trends in Neurosciences*, **10**, 288-293.

Collingbridge, G.L. & Singer, W. (1990) Excitatory amino acid receptors and synaptic plasticity, *Trends in Pharmacological Sciences*, **11**, 290-296.

Connor, D.J. & Harrell, L.E. (1989) Chronic septal lesions cause upregulation of cholinergic but not noradrenergic hippocampal phosphoinositide hydrolysis, *Brain Research*, **488**, 387-389.

Cooper, D.M.F., Boyajian, C.L., Goldsmith, P.K., Unson, C.G. & Spiegel, A. (1990) Differential expression of low molecular weight form of $G_{S\alpha}$ in neostriatum and cerebellum: correlation with expression of calmodulin-independent adenylyl cyclase, *Brain Research*, **523**, 143-146.

Cooper, R.M. & Thurlow, G.A. (1985) Depression and recovery of metabolic activity in rat visual system after eye removal, *Experimental Neurology*, **89**, 322-336.

Coussens, L., Park, P.J., Rhee, L., Yang Feng, T.L., Chen, E., Waterfield, M.D., Francke, U. & Ullrich, A. (1986) Multiple distinct forms of bovine and human protein kinase C suggest diversity in cellular signalling pathways, *Science*, **233**, 859-866.

Cowburn, R., Hardy, J., Roberts, P. & Briggs, R. (1988) Presynaptic and postsynaptic glutamatergic function in Alzheimer's Disease, *Neuroscience Letters*, **86**, 109-113.

Cross, A.J., Crow, T.J., Ferrier, I.N. & Johnson, J.A. (1986) The selectivity of the reduction of serotonin S_2 receptors in Alzheimer-type dementia, *Neurobiology of Aging*, **7**, 3-7.

Cross, A.J., Slater, P., Perry, E.K. & Perry, R.H. (1988) An autoradiographic analysis of serotonin receptors in human temporal cortex: changes in Alzheimer-type dementia, *Neurochemistry International*, **13**, 89-96.

Crunelli, V., Leresche, N. & Pirchio, M. (1985) Non-NMDA receptors mediate the optic nerve input to the rat lateral geniculate nucleus in vitro, *Journal of Physiology*, **365**, 40P.

Crunelli, V., Kelly, J.S., Leresche, N. & Pirchio, M. (1987) On the Excitatory Post-Synaptic Potential Evoked by Stimulation of the Optic Tract in the Rat Lateral Geniculate Nucleus, *Journal of Physiology*, **384**, 603-518.

Crutcher, K.A., Brothers, L. & Davis, J.N. (1979) Sprouting of sympathetic nerves in the absence of afferent input, *Experimental Neurology*, **66**, 778-783.

Crutcher, K.A. & Davis, J.N. (1982) Target regulation of sympathetic sprouting in the rat hippocampal formation, *Experimental Neurology*. **75**, 347-359.

Curtis, D.R. & Davies, R. (1962) Pharmacological studies upon neurones of the lateral geniculate nucleus of the cat, *British Journal of Pharmacology*, **18**, 217-246.

Cusick, C.G. & Lund, R.D. (1981) The distribution of the callosal projection to the occipital visual cortex in rats and mice, *Brain Research*, **214**, 239-259.

Daly, J.W., Padgett, W. & Seamon, K.B. (1982) Activation of cyclic AMP-generating systems in brain membranes and slices by diterpene forskolin: augmentation of receptor-mediated responses, *Journal of Neurochemistry*, **38**, 532-544.

Daniellson, E., Eckernäs, S., Westlind-Danielsson, A., Nordström, O., Bartfai, T., Gottfries, C. & Wallin, A. (1988) VIP-sensitive adenylate cyclase, quanylate cyclase, muscarinic receptors, choline acetyltransferace and acetylcholinesterase, in brain tissue afflicted by Alzheimer's Disease/senile dementia of the Alzheimer type, *Neurobiology of Aging*, **9**, 153-162.

Davies, P. (1979) Neurotransmitter-related enzymes in senile dementia of the Alzheimer type, *Brain Research*, **171**, 319-327.

Davies, P. & Verth, A.H. (1978) Regional distribution of muscarinic acetylcholine receptor in normal and Alzheimer's type dementia brains, *Brain Research*, **138**, 385-392.

Dawson, V.L. & Wamsley, J.K. (1989) Differential upregulation of hippocampal M-1 and M-2 muscarinic receptors after cholinotoxin (AF64A) lesion of the medial septum or diagonal band, *Society for Neuroscience Abstracts*, **15**, S226.4.

De Boni, U. & Crapper-McLachlan, D.R. (1985) Controlled induction of paired helical filaments of the Alzheimer type in cultured human neurons by glutamate and aspartate, *Journal of Neurological Sciences*, **68**, 105-118.

De Keyser, J., De Backer, J., Ebinger, G. & Vauquelin, G. (1989) Coupling of D_1 dopamine receptors to the guanine nucleotide binding protein G_s is deficient in Huntington's disease, *Brain Research*, **496**, 327-330.

De Souza, E.B. Whitehouse, P.J., Kuhar, M.J., Price, D.L. & Vale, W.W. (1986) Reciprocal changes in corticotropin releasing factor (CRF)-like immunoreactivity and CRF receptors in cerebral cortex of Alzheimer's disease, *Nature*, **319**, 593-595.

Dewar, D., Graham, D.I. & McCulloch, J. (1990) $5HT_2$ receptors in dementia of the Alzheimer type: A quantitative autoradiographic study of frontal cortex and hippocampus, *Journal of Neural Transmission*, **2**, 129-137.

Dewar, D.D., Chalmers, D.T., Graham, D.I. & McCulloch, J. (1991) Metabotropic glutamate receptors in human hippocampus: Alterations in Alzheimer's disease, *Brain Research*, (in press).

Dodd, P.R., Hambley, J.W. Cowburn, R.F. & Hardy, J.A. (1988) A comparison of methodologies for the study of functional transmitter neurochemistry in human brain, *Journal of Neurochemistry*, **50**, 1333-1345.

Driedger, P.E. & Blumberg, P.M. (1980) Specific binding of phorbol ester tumor promoters, *Proceedings of the National Academy of Sciences* USA, **77**, 567-571.

Dunnett, C.W. (1964) New Tables for multiple comparisons with a control, *Biometrics*, **20**, 482-491.

Etienne, P. (1983) Treatment of Alzheimer's Disease with Lecithin. In *Alzheimer's Disease*, ed. Reisberg, B. New York: Free Press.

Favaron, M., Maner, H., Alho, H., Bertolino, M., Ferret, B., Guidotti, A. & Costa, E. (1988) Gangliosides prevent glutamate and kainate neurotoxicity in primary neuronal cultures of neonatal rat cerebellum and cortex, *Proceedings of the National Academy of Sciences* USA, **85**, 7351-7355.

Favaron, M., Maner, H., Suman, R., Bertolino, M., Szekely, A.M., DeEvausiquin, G., Guidotti, A. & Costa, E. (1990) Down-regulation of protein kinase C protects cerebellar granule neurons in primary culture from glutamate-induced neuronal death, *Proceedings of the National Academy of Sciences* USA, **87**, 1983-1987.

Feldman, M.L. & Peters, A. (1978) The forms of non-pyramidal neurons in the visual cortex of the rat, *Journal of Comparative Neurology*, **179**, 761-794.

Fisher, S.K., Boast, C.A. & Agranoff, B.W. (1980) The muscarinic stimulation of phospholipid labeling in hippocampus is independent of its cholinergic input, *Brain Research*, **189**, 284-288.

Fisher, S.K., Klinger, P.D. & Agranoff, B.W. (1983) Muscarinic agonist binding and phospholipid turnover in brain, *Journal of Biological Chemistry*, **258**, 7358-7363.

Fitzpatrick, D., Penny, G.R. & Schmechal, D.E. (1984) Glutamic acid decarboxylase-immunoreactive neurons and terminals in the lateral geniculate nucleus of the rat, *Journal of Neuroscience*, **4**, 1809-1829.

Fochtmann, L.J., Gutkind, J.S. & Potter, W.Z. (1988) Electroconvulsive shock increases [^{3}H]-forskolin binding in substantia nigra in the rat, *Society for Neuroscience Abstracts*, **14**, S35.13, p80.

Fonnum, F. (1975) A rapid radiochemical method for the determination of choline acetyltransferase, *Journal of Neurochemistry*, **24**, 407-409.

Fosse, V.M. & Fonnum, F. (1987) Biochemical evidence for glutamate and/or aspartate as neurotransmitters in fibers from the visual cortex to the lateral posterior thalamic nucleus (pulvinar) in rats, *Brain Research*, **400**, 219-224.

Fosse, V.M., Iversen, E. & Fonnum, F. (1986) A bioluminescence method for the measurement of L-glutamate: applications to the study of changes in the release of L-glutamate from lateral geniculate nuculeus and superior colliculus after visual cortex ablation in rats, *Journal of Neurochemistry*, **47**, 340-349.

Fowler, C.J., Magnusson, O., Mohammed, A.K., Danysz, W. & Archer, T. (1986) The effect of selective noradrenergic lesions upon the stimulation by noradrenaline of inositol phospholipid breakdown in rat hippocampal miniprisms, *European Journal of Pharmacology*, **123**, 401-407.

Fox, K., Sato, H. & Daw, N. (1989) The location and function of NMDA receptors in cat and kitten visual cortex, *Journal of Neuroscience*, **9**, 2443-2454.

Gandy, S., Czernik, A.J. & Greengard, P. (1988) Phosphorylation of Alzheimer disease amyloid precursor peptide by protein kinase C and Ca^{2+}/calmodulin-dependent protein kinase II, *Proceedings of the National Academy of Sciences USA*, **85**, 6218-6221.

Geddes, J.W., Monaghan, D.T., Cotman, C.W., Lott, I.T., Kim, R.C. & Chang Chui, H. (1985) Plasticity of hippocampal circuitry in Alzheimer's disease, *Science*, **230**, 1179-1181.

Gehlert, D. R. (1986) Regional modulation of [^{3}H]-forskolin binding in the rat brain by guanylyl-5'-imidodiphosphate and sodium fluoride: comparison with the distribution of guanine nucleotide binding sites, *Journal of Pharmacology and Experimental Therapeutics*, **239**, 952-958.

Gehlert, D.R., Dawson, T.M., Yamamura, H.I. & Wamsley, J.K. (1985) Quantitative autoradiography of [^{3}H]-forskolin binding sites in the rat brain, *Brain Research*, **361**, 351-360.

Gilman, A.G. (1984) G proteins and dual control of adenylate cyclase, *Cell*, **36**, 577-579.

Gilman, A.G. (1989) G Proteins and regulation of adenylyl cyclase, *Journal of American Medical Association*, **262**, 1819-1825.

Girard, P.R., Mazzei, G.J., Wood, J.G. & Kuo, J.F. (1985) Polyclonal antibodies to phospholipid/Ca^{2+}-dependent protein kinase and immunocytochemical localization of the enzyme in rat brain, *Proceedings of the National Academy of Sciences USA*, **82**, 3030-3034.

Goodman, D.C. & Horel, J.C. (1966) Sprouting of optic tract projections in the brain stem of the rat, *Journal of Comparative Neurology*, **127**, 71-88.

Graziano, M.P. & Gilman, A.G. (1987) Guanine nucleotide-binding regulatory proteins: mediators of transmembrane signalling, *Trends in Pharmacological Sciences*, **8**, 478-481.

Greenamyre, J.T. (1986) The role of glutamate in neurotransmission and in neurologic disease, *Archives of Neurology*, **43**, 1058-1063.

Greenamyre, J.T., Olsen, J.M.M., Penney, J.B. & Young, A.B. (1985) Autoradiographic characterization of N-methyl-D-aspartate-, quisqualate- and kainate-sensitive glutamate binding sites, *Journal of Pharmacology and Experimental Therapeutics*, **233**, 254-263.

Greenamyre, J.T., Penney, J.B., D'Amato, C.J. & Young, A.B. (1987) Dementia of the Alzheimer's type: changes in hippocampal L-[^{3}H]-glutamate binding, *Journal of Neurochemistry*, **48**, 543-551.

Hale, P.J., Sefton, A.J., Bauer, L.A. & Cottee, L.J. (1982) Interrelations of the rat's thalamic reticular and dorsal lateral geniculate nuclei, *Experimental Brain Research*, **45**, 217-229.

Hallcher, L.M. & Sherman, W.R. (1980) The effect of lithium ion and other agents on the activity of myo-inositol-1-phosphatase from bovine brain, *Journal of Biological Chemistry*, **225**, 10896-10901.

Hara, H., Onodera, H., Yoshidomi, M., Matsuda, Y. & Kogure, K. (1990) Staurosporine, a novel protein kinase C inhibitor, prevents postischemic neuronal damage in the gerbil and rat, *Journal of Cerebral Blood Flow and Metabolism*, **10**, 646-653.

Hardy, J.A. & Dodd, P.R. (1983) Metabolic and functional studies on post-mortem human brain, *Neurochemistry International*, **5**, 253-266.

Hardy, J., Adolfsson, R., Alafuzoff, I., Bucht, G., Marcusson, J., Nyberg, P., Perdahl, E., Wester, P. & Winblad, B. (1985) Transmitter deficits in Alzheimer's Disease, *Neurochemistry*, **7**, 545-563.

Harrison, J.K., Hewlett, G.H.K. & Greigy, M.E. (1989) Regulation of calmodulin-sensitive adenylate cyclase by the stimulatory G-protein, G_S, *Journal of Biological Chemistry*, **264**, 15880-15885.

Haxby, J.V., Duara, R., Grady, C.L. Cuther, N.R. & Rapoport, S.I. (1985) Relations between neuropsychological and cerebral metabolic asymmetries in early Alzheimer's disease, *Journal of Cerebral Blood Flow and Metabolism*, **5**, 193-200.

Haxby, J.V., Grady, C.L., Koss, E., Horwitz, B., Shapiro, M., Friedland, R.P. & Rapoport, S.I. (1988) Heterogeneous anterior-posterior metabolic patterns in dementia of the Alzheimer type, *Neurology*, **38**, 1853-1863.

Hebb, C.O. & Silver, A. (1956) Choline acetyltransferase in the central nervous system of man and some other mammals, *Journal of Physiology (Lond)*, **134**, 718-728.

Henderson, A.S. (1986) The epidemiology of Alzheimer's Disease, *British Medical Bulletin*, **42**, 3-10.

Herve, D., Trovero, F., Blanc, G., Thierry, A.M., Glowinski, J. & Tassin, J.P. (1989) Nondopaminergic prefrontocortical efferent fibers modulate D1 receptor denervation supersensitivity in specific regions of the rat striatum, *Journal of Neuroscience*, **9**, 3699-3708.

Hokin, L.E. (1985) Receptors and phosphoinositide-generated second messengers, *Annual Review of Biochemistry*, **54**, 205-235.

Hokin, M.R. & Hokin, L.E. (1953) Enzyme secretion and the incorporation of ^{32}P into phospholipids of pancreatic slices, *Journal of Biological Chemistry*, **203**, 967-977.

Hoover, D.B. & Jacobowitz, D.M. (1979) Neurochemical and histochemical studies of the effect of a lesion of nucleus cuneformis on the cholinergic innervation of discrete areas of the rat brain, *Brain Research*, **170**, 113-122.

Horwitz, B., Grady, C.L., Schlageter, N.L., Duara, R. & Rapoport, S.I. (1987) Intercorrelations of regional cerebral glucose metabolic rates in Alzheimer's Disease, *Brain Research*, **407**, 294-306.

Houser, C.R., Crawford, G.D., Barber, R.P., Salvaterra, P.M. & Baugh, J.E. (1983) Organization and morphological characteristics of cholinergic neurons: an immunocytochemical study with a monoclonal antibody to choline acetyltransferase, *Brain Research*, **266**, 97-119.

Houser, C.R., Vaughn, J.E., Hendry, S.H.C., Jones, E.G. & Peters, A. (1984) GABA neurons in the cerebral cortex. In *Cerebral Cortex, Vol. 2, Functional Properties of Cortical Cells*, eds. Jones, E.G. & Peters, A., pp 63-89, New York: Academic Press.

Huang, K.P., Nakabayashi, H. & Huang, F.L. (1986) Isozymic forms of rat brain Ca^{2+}-activated and phospholipid-dependent protein kinase, *Proceedings of the National Academy of Sciences* USA, **83**, 8535-8539.

Hubel, D.H. & Wiesel, T.N. (1970) The period of susceptibility to the physiological effects of unilateral eye closure in kittens, *Journal of Physiology* (Lond), **206**, 419-436.

Huber, G.C. & Crosby, E.D. (1943) A comparison of the mammalian and reptilian tecta, *Journal of Comparative Neurology*, **78**, 133-169.

Hughes, A. (1977) The pigmented-rat optic nerve: fibre count and fibre diameter spectrum, *Journal of Comparative Neurology*, **176**, 263-268.

Hyman, B.T., Van Hoesen, G.W., Damasio, A.R. & Barnes, C.L. (1984) Alzheimer's disease: cell-specific pathology isolates the hippocampal formation, *Science*, **225**, 1168-1170.

Hyman, B.T., Kromer, L.J. & Van Hoesen, G.W. (1987) Reinnervation of the hippocampal perforant pathway zone in Alzheimer's Disease, *Annals of Neurology*, **21**, 259-267.

Inoue, M., Kishimoto, A., Takai, Y. & Nishizuka, Y. (1977) Studies on a cyclic nucleotide-independent protein kinase and its proenzyme in mammalian tissues, *Journal of Biological Chemistry*, **252**, 7610-7616.

Ishii, D.N. (1978) Effect of tumor promoters on the response of cultured embryonic chick ganglia to nerve growth factor, *Cancer Research*, **38**, 3886-3893.

Itoh, H., Toyama, R., Kozasa, T., Tsukamoto, T., Matsuoka, M. & Kaziro, Y. (1988) Presence of three distinct molecular species of G_i protein α subunit: structure of rat cDNA and human genomic DNAs, *Journal of Biological Chemistry*, **263**, 6656-6664.

Izumi, Y., Miyakama, H., Itoh, K. & Kato, H. (1987) Quisqualate and N-methyl-D-aspartate (NMDA) receptors in induction of hippocampal long-term facilitation using conditioning solution, *Neuroscience Letters*, **83**, 201-206.

Jeffrey, G. (1984) Retinal ganglion cell death and terminal field retraction in the developing rodent visual system, *Developmental Brain Research*, **13**, 81-96.

Johnson, E.S. & Minneman, K.P. (1985) α-Adrenergic receptors and stimulation of [^{3}H]-inositol metabolism in rat brain: regional distribution and parallel inactivation, *Brain Research*, **341**, 7-15.

Jones, E.G. (1981) In *Anatomy of cerebral cortex: columnar input-output organisation in the organisation of the cerebral cortex*, eds. Schmitt, F.O., Worden, F.G., Adelman, G. & Dennis, S.G., pp 199-235, MIT Press, Cambridge MA.

Kandel, E.R. & Schwartz, J.H. (1982) Molecular biology of learning: modulation of transmitter release, *Science*, **218**, 433-436.

Kasamatsu, T. (1980) A possible role of cyclic nucleotides in plasticity of visual cortex, *Society for Neuroscience Abstracts*, **6**, S494.

Kasamatsu, T. & Pettigrew, J.D. (1976) Depletion of brain catecholamines: failure of occular dominance shift after monocular occlusion in kittens, *Science*, **194**, 206-209.

Kasamatsu, T. & Pettigrew, J.D. (1979) Preservation of binocularity after monocular deprivation in the striate cortex of kittens treated with 6-hydroxydopamine, *Journal of Comparative Neurology*, **185**, 139-162.

Kasamatsu, T., Pettigrew, J.D. & Ary, M. (1981) Cortical recovery from effects of monocular deprivation: Acceleration with norepinephrine and suppresion with 6-hydroxydopamine, *Journal of Neurophysiology*, **45**, 254-266.

Katada, T., Kusabe, K., Oinuma, M. & Ui, M. (1987) A novel mechanism for the inhibition of adenylate cyclase via inhibitory GTP-binding proteins, *Journal of Biological Chemistry*, **262**, 11879-11900.

Kayama, Y. (1985) Ascending, descending and local control of neuronal activity in the rat lateral geniculate nucleus, *Vision Research*, **25**, 339-347.

Kelly, P.A.T. & McCulloch, J. (1987) Cerebral glucose utilisation following striatal lesions: the effects of the GABA agonist, muscimol, and the dopaminergic agonist, apomorphine, *Brain Research*, **425**, 290-300.

Kemp, J.A. & Downes, C.P. (1986) Noradrenaline-stimulated inositol phospholipid breakdown in rat dorsal lateral geniculate nucleus neurones, *Brain Research*, **371**, 314-318.

Kemp, J.A. & Sillito, A.M. (1981) The nature of the excitatory transmitter mediating 'X' and 'Y' cell inputs to the cat dLGN, *Journal of Physiology (Lond)*, **323**, 377-391.

Kendall, D.A., Brown, E. & Nahorski, S.R. (1985) α_1-Adrenoceptor-mediated inositol phospholipid hydrolysis in rat cerebral cortex: relationship between receptor occupany and response and effects of denervation, *European Journal of Pharmacology*, **114**, 41-52.

Kendall, D.A. & Nahorski, S.R. (1985) 5-Hydroxytryptamine-stimulated inositol phospholipid hydrolysis in rat cerebral cortex slices: pharmaclogical characterisation and effects of antidepressants, *Journal of Pharmacology and Experimental Therapeutics*, **233**, 473-479.

Khachaturian, Z.S. (1985) Diagnosis of Alzheimer's disease, *Archives of Neurology*, **42**, 1097-1104.

Kidd, M. (1963) Paired helical filaments in electron microscopy of Alzhiemer's disease, *Nature*, **197**, 192-193.

Kikkawa, U., Takai, Y., Minakuchi,R., Inohara, S. & Nishizuka, Y. (1982) Calcium-activated, phospholipid-dependent protein kinase from rat brain. Subcellular distribution, purification and properties, *Journal of Biological Chemistry*, **257**, 13341-13348.

Kikkawa, U., Takai, Y., Tanaka, Y., Miyake, R. & Nishizuka, Y. (1983) Protein kinase C as a possible receptor protein of tumor-promoting phorbol esters, *Journal of Biological Chemistry*, **258**, 11442-11445.

Kozasa, T., Itoh, H., Tsukamoto, T. & Kaziro, Y. (1988) Isolation and characterisation of the human G_{Sa} gene, *Proceedings of the National Academy of Sciences* USA, **85**, 2081-2085.

Kraft, A.S. & Anderson, W.G. (1983) Phorbol esters increase the amount of Ca^{2+}, phospholipid-dependent protein kinase associated with plasma membrane, *Nature*, **301**, 621-623.

Kromer, L.F. & Moore, R.Y. (1980) A study of the organization of the locus coeruleus projections to the lateral geniculate nuclei in the albino rat, *Neuroscience*, **5**, 255-271.

Kuo, J.F., Andersson, R.G.G., Wise, B.D., Mackerlova, L., Salomonsson, I., Brackett, N.L., Katoh, N., Shoji, M. & Wrenn, R.W. (1980) Calcium-dependent protein kinase: widespread occurrence in various tissues and phyla of the animal kingdom and comparison of effects of phospholipid, calmodulin and trifluoperazine, *Proceedings of the National Academy of Sciences* USA, **77**, 7039-7043.

Kurumaji, A. & McCulloch, J. (1990) Effects of MK-801 upon local cerebral glucose utilisation in conscious rats following unilateral lesion of caudate entorhinal cortex, *Brain Research*, **531**, 72-82.

Laborit, H. & Zerib, R. (1987) Role of various second messengers in the memorization of a passive or active avoidance, *Research Communications in Psychology, Psychiatry and Behavior*, **12**, 193-204.

Lai, J., Makous,W.L., Quock, R.M. & Horita, A. (1978) Visual deprivation affects serotonin levels in the visual system, *Journal of Neurochemistry*, **30**, 1187-1189.

Lang, W. & Henke, H. (1983) Cholinergic receptor binding and autoradiography in brain of non-neurological and senile dementia of Alzheimer-type patients, *Brain Research*, **267**, 271-280.

Laurenza, A., Khandelwal, Y., De Souza, N.J., Kupp, R.H., Metzger, H. & Seamon, K.B. (1987) Stimulation of adenylate cyclase by water-soluble analogues of forskolin molecular pharmacology, **32**, 133-139.

Levitzki, A. (1987) Regulation of hormone-sensitive adenylate cyclase, *Trends in Pharmacological Science*, **8**, 299-303.

Lewis, P.R., Shute, C.C.D. & Silver, A. (1967) Confirmation from choline acetylase analyses of a massive cholinergic innervation to the rat hippocampus, *Journal of Physiology (London)*, **191**, 215-224.

London, E.D., McKinney, M., Dam, M., Ellis, A. & Coyle, J.T. (1984) Decreased cortical glucose utilisation after ibotenate lesion of the rat ventromedial globus pallidus, *Journal of Cerebral Blood Flow and Metabolism*, **3**, 381-390.

Lowe, S.L., Francis, P.T., Procter, A.W., Palmer, A.M., Davison, A.N. & Bowen, D.M. (1988) Gamma-aminobutyric acid concentration in brain tissue at two stages of Alzheimer's disease, *Brain*, **111**,789-799.

Lowry, O.H., Rosebrough, N.J., Farr, A.L. & Randall, R.J. (1951) Protein measurement with the Folin phenol reagent, *Journal of Biological Chemistry*, **193**, 265-275.

Lund-Karlsen, R. & Fonnum, F. (1978) Evidence for glutamate as a neurotransmitter in the cortico fugal fibres to the dorsal lateral geniculate body and the superior colliculus in rats, *Brain Research,* **151**, 457-467.

Lynch, G., Mathews, D., Mosko, S., Parks, T. & Cotman, C. (1972) Induced acetylcholinersterase-rich layer in rat dentate gyrus following entorhinal lesions, *Brain Research*, **42**, 311-318.

MacKay-Sim, A., Sefton, A.J. & Martin, P.R. (1983) Subcortical projections to lateral geniculate and thalamic reticular nuclei in hooded rat, *Journal of Comparative Neurology*, **213**, 24-35.

Manev, H., Favaron, M., Guidotti, A. & Costa, E. (1989) Delayed increase of Ca^{2+} influx elicited by glutamate: role in neuronal death, *Molecular Pharmacology*, **36**, 106-112.

Mann, D.M.A. (1988) Neuropathological and neurochemical aspects of Alzheimer's disease. In *Handbook of Psychopharmacology,* Vol 20, eds. Iversen, L.L., Iversen, S.D. & Snyder, S.H., pp 1-67, Plenum Press.

Mann, D.M.A., Yates, P.O. & Marcyniuk, B. (1985) Some morphometric observations on the cerebral cortex and hippocampus in presenile Alzheimer's Disease, senile dementia of the Alzheimer type and Down's syndrome in middle age. *Journal of Neurological Sciences*, **69**, 139-159.

Mann, D.M.A., Yates, P.O., Marcyniuk, B. & Ravindra, C.R. (1986) The topography of plaques and tangles in Down's syndrome patients of different ages, *Neuropathology and Applied Neurobiology*, **2**, 447-457.

Maragos, W.F., Chu, D.C.M., Young, A.B., d'Amato, C.J, & Penney, J.B. (1987) Loss of hippocampal [^{3}H]TCP binding in Alzheimer's disease, *Neuroscience Letters*, **74**, 371-376.

Mash, D.C., Flynn, D.D. & Potter, L.T. (1985) Loss of M_2 muscarinic receptors in the cerebral cortex in Alzheimer's disease and experimental cholinergic denervation, *Science*, **228**, 1115-1117.

Masliah, E., Cole, G., Shimohama, S., Hansen, L., DeTeresa, R., Terry, R. & Saitoh, T. (1990) Differential involvement of protein kinase C isozymes in Alzheimer's Disease, *Journal of Neuroscience,* **10**, 2113-2124.

Mata, M., Fink, D.J., Gainer, H., Smith, C.B., Davidsen, L., Savaki, H., Schwartz, W.J. & Sokoloff, L. (1980) Activity dependent energy metabolism in rat posterior pituitary primarily reflects sodium-pump activity, *Journal of Neurochemistry*, **34**, 213-215.

Mathews, D.A., Cotman, C. & Lynch, G. (1976) An electron microscopic study of lesion-induced synaptogenesis in the dentate gyrus of the adult rat. 1. Magnitude and time course of degeneration, *Brain Research*, **115**, 1-21.

Mathewson, A.J. & Berry, M. (1985) Observations on the astrocyte response to a cerebral stab wound in adult rats, *Brain Research*, **327**, 61-69.

Mattson, M.P. (1988) Neurotransmitters in the regulation of neuronal cytoarchitecture, *Brain Research Review*, **13**, 179-212.

Mattson, M.P., Taylor-Hunter, A. & Kater, S.B. (1988) Neurite outgrowth in individual neurons of a neuronal population is differentially regulated by calcium and cyclic AMP, *Journal of Neuroscience*, **8**, 1704-1711.

Melander, T., Staines, W.A., Hökfelt, T., Rökaeus, A., Eckenstein, F., Salvaterra, P.M. & Wainer, B.H. (1985) Galanin-like immunoreactivity in cholinergic neurons of the septum-basal forebrain complex projecting to the hippocampus of the rat, *Brain Research*, **360**, 130-138.

Mellgren, S.I. & Srebro, B. (1973) Changes in acetylcholinesterase and distribution of degenerating fibers in the hippocampal region after septal lesions in the rat, *Brain Research*, **52**, 19-36.

Michell, R.H. (1975) Inositol phospholipids and cell surface receptor function, *Biochimica et Biophysica Acta*, **415**, 81-147.

Mishra, R.K., Marshall, A.M. & Yarmuza, S.L. (1980) Supersensitivity in rat caudate nucleus: effects of 6-hydroxydopamine on the time course of dopamine receptor and cyclic AMP changes, *Brain Research*, **200**, 47-57.

Mize, R.R., Spencer, R.F. & Sterling, P. (1982) Two types of GABA-accumulating neurons in the superficial gray layer of the cat superior colliculus, *Journal of Comparative Neurology*, **206**, 180-192.

Mobley, P.L., Scott, S.L. & Cruz, E.G. (1986) Protein kinase C in astrocytes: a determinant of cell morphology, *Brain Research*, **398**, 366-369.

Mollner, S. & Pfeuffer, T. (1988) Two different adenylyl cyclases in brain distinguished by monoclonal antibodies, *European Journal of Biochemistry*, **171**, 265-271.

Monaghan, D.T., Yao, D & Cotman, C.W. (1985) L-[^{3}H]-glutamate binds to kainate-, NMDA- and AMPA-sensitive binding sites: an autoradiographic analysis, *Brain Research*, **340**, 378-383.

Monaghan, D.T., Geddes, J.W., Yao, D., Chung, C. & Cotman, C.W. (1987) [^{3}H]TCP binding sites in Alzheimer's disease, *Neuroscience Letters*, **73**, 197-200.

Mountjoy, C.Q. (1986) Correlations between neuropathological and neurochemical changes, *British Medical Bulletin*, **42**, 81-85.

Mountjoy, C.Q., Roth, M., Evans, N.J.R. & Evans, H.M. (1983) Cortical neuronal counts in normal elderly controls and demented patients, *Neurobiology of Aging*, **4**, 1-11.

Mountjoy, C.Q., Rossor, M.N., Iversen, L.L. & Roth, M. (1984) Correlation of cortical cholinergic and GABA deficits with quantitative neuropathological findings in senile dementia. *Brain*, **107**, 507-518.

Neary, J.T., Norenberg, L.B. & Norenberg, M.D. (1986) Calcium-activated, phospholipid-dependent protein kinase and protein substrates in primary cultures of astrocytes, *Brain Research*, **385**, 420-424.

Newman, M.E. & Belmaker, R.H. (1987) Effects of lithium in vitro and ex vivo on components of the adenylate cyclase system in membranes from the cerebral cortex of the rat, *Neuropharmacology*, **26**, 211-217.

Newman, M.E., Klein, E., Birmaker, B., Feinsod, M. & Belmaker, R.H. (1983) Lithium at therapeutic concentrations inhibits human brain noradrenaline-sensitive cAMP accumulation, *Brain Research*, **278**, 380-381.

Newman, M.E. & Belmaker, R.H. (1987) Effects of lithium in vitro and ex vivo on components of the adenylate cyclase system in membranes from the cerebral cortex of the rat, *Neuropharmacology*, **26**, 211-217.

Nicoletti, F., Wrobleswki, J.T., Alho, H., Eva, C., Fadda, E. & Costa, E. (1987) Lesions of putative glutaminergic pathways potentiate the increase of inostiol phospholipid hydrolysis elicited by excitatory amino acids, *Brain Research*, **436**, 103-112.

Niedel, J.E., Kuhn, L.J. & Vanderbank, G.R. (1983) Phorbol diester receptor co-purifies with protein kinase C, *Proceedings of the National Academy of Sciences* USA, **80**, 36-40.

Ninomiya, H., Taniguchi, T. & Fujiwara, M. (1990) Phosphoinositide breakdown in rat hippocampal slices: sensitivity to glutamate induced by in vitro anoxia, *Journal of Neurochemistry*, **55**, 1001-1007.

Nishizuka, Y. (1984) Turnover of inositol phospholipids and signal transduction, *Science*, 225, 1365-1370.

Nishizuka, Y. (1988) The molecular heterogeneity of protein kinase C and its implications for cellular regulation, *Nature*, 334, 661-665.

Nordberg, A. & Winblad, B. (1988) Reduced number of [^{3}H]-nicotine and [^{3}H]acetylcholine binding sites in the frontal cortex of Alzheimer brains, *Neuroscience Letters*, 72, 115-119.

Northup, J.K., Sternweis, P.C., Smigel, M.D., Schliefer, L.S., Ross, E.M. & Gilman, A.G. (1980) Purification of the regulatory component of adenylate cyclase, *Proceedings of the National Academy of Sciences* USA, 77, 6516-6520.

Ogura, A., Miyamoto, M. & Kudo, Y. (1988) Neuronal death in vitro: parallelism between survivability of hippocampal neurones and sustained elevation of cytosolic Ca^{2+} after exposure to glutamate receptor agonist, *Experimental Brain Research*, 73, 447-0458.

Okada, M., Mine, K. & Fujiwara, M. (1989) Relationship of calcium and adenylate cyclase messenger systems in rat brain synaptosomes, *Brain Research*, 501, 23-31.

Olds, J.L., Anderson, M.L., McPhie, D.L., Staten, L.D. and Alkon, D.L. (1989) Imaging of memory-specific changes in the distribution of protein kinase C in the hippocampus, *Science*, **245**, 866-869.

Olivarria, J. & Van Sluyters, R. (1982) The projection from striate and extrastriate cortical areas to the superior colliculus in the rat, *Brain Research*, **242**, 332-336.

Onodera, H., Araki, T. & Kogure, K. (1989) Protein kinase C activity in the rat hippocampus after forebrain ischaemia: autoradiographic analysis by [^{3}H]-phorbol 12,13 dibutyrate, *Brain Research,* **481**, 1-7.

Onodera, H. & Kogure, K. (1989) Mapping second messenger systems in the rat hippocampus after transient forebrain ischaemia: in vitro [^{3}H]forskolin and [^{3}H]inositol 1,4,5 trisphosphate binding, *Brain Research,* **487**, 343-347.

Onodera, H., Sato, G. & Kogure, K. (1986) Lesions of Schaffer collaterals prevent ischemic death of CA_1 pyramidal cells, *Neuroscience Letters*, **68**, 169-174.

Orzi, F., Diana, G., Casamenti, F., Palombo, E. & Fieschi, C. (1988) Local cerebral glucose utilisation following unilateral and bilateral lesions of the nucleus basalis magnocellularis in the rat, *Brain Research*, **462**, 99-103.

Overstreet, D.H., Speth, R.C., Hruska, R.E., Ehlert, F., Dumont, Y. & Yamamura, H.I. (1980) Failure of septal lesions to alter muscarinic cholinergic or benzodiazepine binding sites in hippocampus of rat brain, *Brain Research*, **195**, 203-207.

Parenti, M., Gentleman, S., Olianas, M.C. & Neff, N.H. (1982) The dopamine receptor adenylate cyclase complex: evidence for post recognition site involvement for the development of supersensitivity, *Journal of Neurchemical Research*, 7, 115-124.

Parker, P.J., Kour, G., Marais, R.M., Mitchell, F., Pears, C., Schaap, D., Stabel, S. and Webster, C. (1989) Protein kinase C - a family affair, *Molecular and Cellular Endocrinology,* **65**, 1-11.

Parnavelas, J.G., Lieberman, A.R. & Webster, K.E. (1977) Organization of neurons in the visual cortex, area 17, of the rat, *Journal of Anatomy*, **124**, 305-322.

Pasquier, D.A. & Villar, M.J. (1982) Subcortical projections to the lateral geniculate body in the rat, *Experimental Brain Research*, **48**, 409-419.

Paxinos, G. & Watson, C. (1986) *The Rat Brain in Stereotaxic Co-ordinates* (2nd Ed.) Academic Press, Australia.

Pearson, R.C.A., Esiri, M.M., Hiorns, R.W., Wilcock, G.K. & Powell, T.P.S. (1985) Anatomical correlates of the distribution of the pathological changes in the neocortex in Alzheimer disease, *Proceedings of the National Academy of Sciences*, USA, **82** 4531-4534.

Peng, C.T. (1977) Sample preparation of liquid scintillation, *Radiochemical Centre Review*, **17.**

Perry, E.K. (1986) The cholinergic hypothesis, *British Medical Bulletin*, **42**, 63-69.

Perry, E.K., Atack, J.R., Perry, R.H., Hardy, J.A., Dodd, P.R., Edwardson, J.A., Blessed, G., Tomlinson, B.E. & Fairbairn, A.F. (1984) Intralaminar neurochemical distributions in human mid-temporal cortex - comparison between Alzheimer's disease and the normal, *Journal of Neurochemistry*, **42**, 1402-1410.

Perry, E.K., Perry, R.H., Candy, J.M., Fairbairn, A.F., Blessed, G., Dick, D.J. & Tomlinson, B.E. (1984) Cortical serotonin S_2 receptor binding abnormalities in patients with Alzheimer's disease: comparisons with Parkinson's disease, *Neuroscience Letters*, **51**, 353-357.

Perry, E.K., Perry, E.H., Smith C.J., Purohit, D., Bonham, J., Dick, D.J., Candy, J.M., Edwardson, J.A. & Fairbairn, A. (1986) Cholinergic receptors in cognitive disorders, *Canadian Journal of Neurological Sciences*, **13**, 521-527.

Perry, E.K., Tomlinson, B.E., Blessed, A., Bergmann, K., Gibson, P.H. & Perry, R.H. (1978) Correlation of cholinergic abnormalities with senile plaques and mental test scores in senile dementia, *British Medical Journal*, **2**, 1457-1459.

Perry, R.H. (1986) Recent advances in neuropathology. *British Medical Bulletin*, **42**, 34-41.

Perry, R.H. & Perry, E.K. (1982) in *The Psychiatry of Late Life*, eds. Levy, R. & Post, F., pp 1-67. Oxford: Blackwell Scientific.

Peters, A. & Feldman, M.L. (1976) The projection of the lateral geniculate nucleus to area 17 of the rat cerebral cortex. I. General description, *Journal of Neurocytology*, **5**, 63-84.

Peters, A. & Feldman, M.L. (1977) The projection of the lateral geniculate nucleus to area 17 of the rat cerebral cortex. IV. Terminations upon spiny dendrites, Journal of Neurocytology, **6**, 669-689.

Peters, A., Proskauer, C.C. & Ribak, C.E. (1982) Chandelier cells in rat visual cortex, *Journal of Comparative Neurology*, **206** 387-416.

Pfeuffer, T. & Metzger, H. (1982) 7-0-Hemisuccinyl-deacetyl forskolin-sepharose: a novel affinity support for purification of adenylate cyclase, *Federation of European Biochemical Societies Letters*, **146**, 369-375.

Phillis, J.W., Tebecis, A.K. & York, D.N. (1967) A study of cholinoceptive cells in the lateral geniculate nucleus, *Journal of Physiology (Lond)*, **192**, 695-713.

Poat, J.A., Cripps, H.E. & Iversen, L.L. (1988) Differences between high-affinity forskolin binding sites in dopamine-rich and other regions of rat brain, *Proceedings of the National Academy of Sciences USA*, **85**, 3216-3220.

Probst, A., Cortes, R., Ulrich, J. & Palacios, J.M. (1988) Differential modification of muscarinic cholinergic receptors in the hippocampus of patients with Alzheimer's disease: an autoradiographic study, *Brain Research*, **450**, 190-201.

Quirion, R., Martel, J.C., Robitaille, Y., Etienne, P., Wood, P., Nair, N.P.V. & Gauthier, S. (1986) Neurotransmitter and receptor deficits in senile dementia of the Alzheimer type, *Canadian Journal of Neurological Sciences*, **13**, 503-510.

Rakic, P., Goldman-Rakic, P.S. & Gallager, D. (1988) Quantitative autoradiography of major neurotransmitter receptors in the monkey striate and extrastriate cortex, *Journal of Neuroscience*, **8**, 3670-3690.

Rall, T.W., Sutherland, E.W. & Berthet, J. (1957) The relationship of epinephrine and glucogon to liver phosphorylase IV: effect of epinephrine and glucagon on the reactivation of phosphorylase in liver homogenates, *Journal of Biological Chemistry*, **224**, 463-475.

Raulli, R.E., Arendash, G. & Crews, F.T. (1988) Effects of nBM lesions on muscarinic-stimulation of phosphoinositide hydrolysis, *Neurobiology of Aging*, **10**, 191-197.

Reed, L.J. and de Belleroche, J. (1988) Increased polyphosphoinositide responsiveness in the cerebral cortex induced by cholinergic denervation, *Journal of Neurochemistry*, **50**, 1566-1571.

Reinikainen, K.J., Reikkinen, P.J., Halonen, T. & Laakso, M. (1987) Decreased muscarinic receptor binding in cerebral cortex and hippocampus in Alzheimer's Disease, *Life Sciences*, **41**, 453-461.

Reisine, T.D., Yamamura, H.I., Bird, E.D., Spokes, E. & Enna, S.J. (1978) Pre- and postsynaptic neurochemical alterations in Alzheimer's disease, *Brain Research*, **159**, 477-481.

Richter, J.A., Perry, E.K. & Tomlinson, B.E. (1980) Acetylcholine and choline levels in postmortem brain tissue: preliminary observations in Alzheimer's disease, *Life Sciences*, **26**, 1683-1689.

Rodbell, M., Kraus, H.M.J., Pohl, S.L. & Birnbaumer, L. (1971) The glucagon-sensitive adenylate cyclase system in plasma membranes of rat liver, V: an obligatory role of guanine nucleotides in glucagon action, *Journal of Biological Chemistry*, **246**, 1877-1882.

Rogawski, M.A. & Aghajanian, G.K. (1980) Norepinephrine and serotonin: opposite effects on the activity of lateral geniculate neurons evoked by optic pathway stimulation, *Experimental Neurology*, **69**, 678-694.

Rose, A.M., Hatton, T. & Fibiger, H.C. (1976) Analysis of the septo-hippocampal pathway by light and electron microscopic autoradiography, *Brain Research*, **108**, 170-174.

Ross, E.M., Howlett, A.C., Ferguson, K.M. & Gilman, A.G. (1978) Reconstitution of hormone sensitive adenylate cyclase activity with resolved components of the enzyme, *Journal of Biological Chemistry*, **253**, 6401-6412.

Rossor, M.N., Emson, P.C., Mountjoy, C.W., Roth, M. & Iversen, L.L. (1980) Reduced amounts of immunoreactive somatostatin in the temporal cortex in senile dementia of the Alzheimer type, *Neuroscience Letters*, **20**, 373-377.

Rossor, M. & Iversen, L.L. (1986) Non-cholinergic neurotransmitter abnormalities in Alzheimer's disease, *British Medical Bulletin*, **42**, 70-74.

Routtenberg, A. (1986) Synaptic plasticity and protein kinase C. In *Progress in Brain Research.* Vol 69, eds. Gispen, W.H. & Routtenberg, A., pp 221-234, Elsevier Science Publishers.

Rye, D.B., Wainer, B.H., Mesulam, M.-M., Mufson, E.J. & Saper, C.B. (1984) Cortical projections arising from the basal forebrain: a study of cholinergic and noncholinergic components employing combined retrograde tracing and immunohistochemical localisation of choline acetyltransferase, *Neuroscience*, **13**, 627-643.

Rylett, R.J., Ball, M.J., & Colhoun, E.M. (1983) Evidence for high affinity choline transport in synaptosomes prepared from hippocampus and neocortex of patients with Alzheimer's disease, *Brain Research*, **284**, 169-175.

Saitoh, T., Cole, G. & Huynh, T.V. (1990) Aberrant protein kinase C cascades in Alzheimer's disease. In *Molecular Aspects of Development and Aging of the Nervous System*, ed. Lauder, J.M., pp 301-310, Plenum Press, New York.

Saitoh, T. & Dobkins, K.R. (1986) Protein kinase C in human brain and its inhibition by calmodulin, *Brain Research*, **379**, 196-199.

Sara, S. & Lefevre, D. (1972) Hypoxia-induced amnesia in one trial learning and pharmacological protection by piracetam, *Psychopharmacologia*, **25**, 32-40.

Sato, H. & Kayama, Y. (1983) Effects of noradrenaline applied iontophoretically on rat superior colliculus neurons, *Brain Research Bulletin*, **10**, 453-457.

Scalia, F. (1972) The termination of retinal axons in the pretectal region of mammals, *Journal of Comparative Neurology*, **145**, 223-258.

Scatchard, G. (1949) The attraction of protein for small molecules and ions, *Annals of the New York Academy of Sciences*, **51**, 660-672.

Scheffé, H. (1959) The Analysis of Variance, John Wiley, New York.

Schliebs, R., Burgoyne, R.D. & Bigl, V. (1982) The effect of visual deprivation on β-adrenergic receptors in the visual centres of the rat brain, *Journal of Neurochemistry*, **38**, 1038-1043.

Schliebs, R., Kunert, E. & Bigl, V. (1984) Effect of monocular deprivation on uptake and binding of [^{3}H]-glutamate in the visual system of rat brain, *Journal of Neurochemistry*, **43**, 1490-1493.

Schliebs, R., Kullman, E. & Bigl, V. (1986) Development of glutamate binding sites in the visual structures of the rat brain. Effect of visual pattern deprivation, *Biomedical Biochimica Acta* **45**, 495-506.

Schwarcz, R., Hökfelt, T., Fuxe, K., Jonsson, G., Goldstein, M. & Terenius, L. (1979) Ibotenic acid-induced neuronal degeneration: a morphological and neurochemical study, *Experimental Brain Research*, **37**, 199-216.

Schwartz, W.J., Smith, C.B., Davidsen, L., Savaki, H., Sokoloff, L., Mata, M., Fink,D.J. & Gainer, H. (1979) Metabolic mapping of functional activity in the hypothalamo-neurohypophysial system of the rat, *Science*, **205**, 723-725.

Seamon, K. & Daly, J.W. (1981) Activation of adenylate cyclase by the diterpene forskolin does not require the guanine nucleotide regulatory protein, *Journal of Biological Chemistry*, **256**, 9799-9801.

Seamon, K.B., Padgett, W. & Daly, J.W. (1981) Forskolin: unique diterpene activator of adenylate cyclase in membranes and in intact cells, *Proceedings of National Academy of Sciences* USA, **78**, 3363-3367.

Seamon, K.B., Vaillancourt, R., Edwards, M. & Daly J.W. (1984) Binding of [^{3}H]-forskolin to rat brain membranes, *Proceedings of the National Academy of Sciences* USA, **81**, 5081-5085.

Sefton, A.J. & Dreher, B. (1984) Visual system. In *The Rat Nervous System.* ed. Paxinos, G., Vol. 1, pp 169-221, Academic Press.

Sefton, A.J., MacKay-Sim, A., Baur, L.A. & Cottee, L.J. (1981) Cortical projections to visual centres in the rat: An HRP study, *Brain Research*, **215**, 1-13.

Sejnowski, T.J., Reingold, S.C., Kelley, D.P. & Gelperin, A. (1980) Localisation of [^{3}H]-2-deoxyglucose in single molluscan neurons, *Nature*, **287**, 449-451.

Shapiro, D.L. (1973) Morphological and biochemical alterations in foetal rat brain cells culture in the presence of monobutyryl cyclic AMP, *Nature*, **241**, 203-204.

Sharp, F.R., Ryan, A.F., Goodwin, P. & Woolf, N.K. (1982) Increasing intensities of wide band noise increase [^{124}C]2-deoxyglucose uptake in gerbil central auditory structures, *Brain Research*, **230**, 87-96.

Shimohama, S., Taniguchi, T., Fujiwara, M. & Kameyama, M. (1986) Biochemical characterisation of α-adrenergic receptors in human brain and changes in Alzheimer-type dementia, *Journal of Neurochemistry*, **47**, 1294-1301.

Shimohama, S., Taniguchi, T., Fujiwara, M. & Kameyama, M. (1986) Changes in nicotinic and muscarinic cholinergic receptors in Alzheimer-type dementia, *Journal of Neurochemistry*, **46**, 288-293.

Shimohama, S., Taniguchi, T., Fujiwara, M. & Kameyama, M. (1987) Changes in β-adrenergic receptor subtypes in Alzheimer-type dementia, *Journal of Neurochemistry*, **48**, 1215-1221.

Shimohama, S., Saitoh, T. & Gage, F.H. (1988) Protein Kinase C in hippocampus and septum following fimbria-fornix transection, *Society of Neuroscience, Abstract* **14**, S12.10. p19.

Shimohama, S., Taniguchi, T., Fujiwara, M. & Kameyama, M. (1988) Changes in benzodiazepene receptors in Alzheimer-type dementia, *Annals of Neurology*, **23**, 404-406.

Sims, N.R., Bowen, D.M., Smith, C.C.T., Flack, R.H.A., Davison, A.N., Snowden, J.S. & Neary, D. (1980) Glucose metabolism and acetylcholine synthesis in relation to neuronal activity in Alzheimer's disease, *Lancet*, **i**, 333-335.

Sladeczek, F., Recasens, M. & Bockaert, J. (1988) A new mechanism for glutamate receptor action: Phosphoinositide hydrolysis, *Trends in Neuroscience*, **11**, 545-549.

Smigel, M.D. (1986) Purification of the catalyst of adenylate cyclase, *Journal of Biological Chemistry*, **261**, 1976-1982.

Smith, C.D., Cox, C.C. & Snyderman, R. (1986) Receptor-coupled activation of phosphoinositide-specific phospholipase C by an N protein, *Science*, **232**, 97-100.

Smith, C.J., Perry, E.K., Perry, R.H., Fairbairn, A.F. & Birdsall, N.J.M. (1987) Guanine nucleotide modulation of muscarinic cholinergic receptor binding in postmortem human brain - a preliminary study in Alzheimer's disease, *Neuroscience Letters*, **50**, 847-856.

Smith, C.J., Perry, E.K., Perry, R.H., Candy, J.M., Johnson, M., Bonham, J.R., Dick, D.J., Fairbairn, A., Blessed, G. & Birdsall, N.J. (1988) Muscarinic cholinergic receptor subtypes in hippocampus in human cognitive disorders, *Journal of Neurochemistry*, **50**, 847-850.

Sofroniew, M.V. & Pearson, R.C.A. (1985) Degeneration of cholinergic neurons in the basal nucleus following kainic of N-methyl-D-aspartate acid application to the cerebral cortex in the rat, *Brain Research*, **339**, 186-190.

Sokoloff, L. (1977) Relation between physiological function and energy metabolism in the central nervous system, *Journal of Neurochemistry*, **29**, 13-26.

Sokoloff, L. (1982) The radioactive deoxyglucose method. Theory, procedure and applications for the measurement of local glucose utilisation in the central nervous system, In *Advances in Neurochemistry*, eds. Agranoff, B.W. & Aprison, M.H., Vol. 4, pp 1-82, Plenum, New York.

Sokoloff, L., Reivich, M., Kennedy, C., Des Rosiers, M.H., Patlak, C.S., Pettigrew, K.D., Sakurada, O. & Shinohara, M. (1977) The [^{14}C]deoxyglucose method for the measurement of local cerebral glucose utilization theory, procedure and normal values in the conscious and anesthetized albino rat, *Journal of Neurochemistry,* **28**, 897-916.

Sparks, D.L. (1989) Aging and Alzheimer's Disease, *Archives of Neurology*, **46**, 138-140.

Spiegel, A.M., Levine, M.A., Marx, S.J. & Aurbach, G.D. (1982) Pseudohypoparathyroidism: the molecular basis for hormone resistance - a retrospective, *New England Journal of Medicine*, **307**, 679-681.

Spiegel, A.M., Gierschik, P., Levine, M.A. & Downs, R.W. (1985) Clinical implications of guanine nucleotide-binding proteins as receptor-effector couplers, *New England Journal of Medicine*, **312**, 26-33.

Spinelli, W. & Ishii, D.N. (1983) Tumor promoter receptor regulation of neurite formation in cultured human neuroblastoma cells, *Cancer Research*, **43**, 4119-4125.

Stanton, P.K. & Sarvey, J.M. (1985) Depletion of norepinephrine but not serotonin, reduces long term potentiation in the dentate gyrus of rat hippocampal slices, *Journal of Neuroscience*, **5**, 2169-2176.

Stein, B.E. (1981) Organisation of the rodent superior colliculus: some comparisons with other mammals, *Behavioural Brain Research*, **3**, 175-188.

Sternweis, P.C., Northup, J.K., Smigel, M.D. & Gilman, A.G. (1981) The regulatory component of adenylate cyclase: purification and properties, *Journal of Biological Chemistry*, **256**, 11517-11526.

Steward, O. (1976) Topographic organization of the projections from the entorhinal area to the hippocampal formation of the rat, *Journal of Comparative Neurology*, **167**, 285-314.

Stichel, C.C. & Singer, W. (1988) Localization of isoenzymes II/III of protein kinase C in the rat visual cortex (area 17), hippocampus and dentate gyrus, *Experimental Brain Research,* **72**, 443-449.

Stokes, C.E. & Hawthorne, J.N. (1987) Reduced phosphoinositide concentrations in anterior temporal cortex of Alzheimer-diseased brains, *Journal of Neurochemistry*, **48**, 1018-1021.

Storm-Mathisen, J. (1970) Quantitative histochemistry of acetylcholinesterase in rat hippocampal region correlated to histochemical staining, *Journal of Neurochemistry*, **17**, 739-750.

Storm-Mathisen, J. (1977) Glutamic acid and excitatory nerve endings: reduction of glutamic acid uptake after axotomy, *Brain Research*, **120**, 379-386.

Swanson, L.W. & Cowan, W.M. (1979) The connections of the septal region in the rat, *Journal of Comparative Neurology*, **186**, 621-665.

Swanson, L.W., Köhler, C. & Björklund, A. (1987) The limbic region. 1: The septohippocampal system. In *Handbook of Chemical Neuroanatomy Vol. 5*, eds. Björklund, A., Hökfelt, T. & Swanson, L.W., pp 125-255, Elsevier, Amsterdam.

Takahashi, T. (1985) The organisation of the lateral thalamus of the hooded rat, *Journal of Comparative Neurology*, **231**, 281-309.

Terry, R.D., Peck, A., DeTeresa, R., Schechter R. & Horoupian, D.S. (1981) Some morphometric aspects of the brain in senile dementia of the Alzheimer type, *Annals of Neurology*, **10**, 184-192.

Thandroyen, F.T., McCarthy, J., Burton, K.P. & Opie, L.H. (1988) Ryanodine and caffeine prevent ventricular arrythmias during acute myocardial ischemia and reperfusion in rat heart, *Circulation Research*, **62**, 306-314.

Thurlow, G.A. & Cooper, R.M. (1985) Increased dependence of superior colliculus metabolic activity on visual cortex after eye enucleation, *Experimental Neurology*, **90**, 594-600.

Toga, A.W. & Collins, R.C. (1981) Metabolic response of optic centers to visual stimuli in the albino rat: anatomical and physiological considerations. *Journal of Comparative Neurology*, **199**, 443-464.

Tsujiino, T., Kose, A., Saitoh, N. & Tanaka, C. (1990) Light and electronic microscopic localization of β1-, β11 and γ sub-species of protein kinase C in rat cerebral neocortex, *Journal of Neuroscience*, **10**, 870-884.

Unnerstall, J.R., Niehoff, D.L., Kuhar, M.J. & Palacios, J.M. (1982) Quantitative receptor autoradiography using [^{3}H] Ultro films: application to multiple benzodiazepene receptors, *Journal of Neuroscience Methods*, **6**, 59-73.

Valverius, P., Hoffmann, P.L. & Tabakoff, B. (1989) Brain forskolin binding in mice dependent on and tolerant to ethanol, *Brain Research,* **503**, 38-43.

Wasterlain, C.G. & Dwyer, B.E. (1983) Brain metabolism during prolonged seizures in neonates. In *Status Epilepticus, Advances in Neurology Vol 4.*, eds. Delgado-Escveta, A.V., Wasterlain, C.G., Treuman, D.M. & Pocter, R.J. pp 241-260. New York: Raven Press.

Wasterlain, C. (1989) Epileptic seizures. In *Basic Neurochemistry*, eds. Siegel, G., Agranoff, B., Albers, R.W. & Molinoff, P., 4th Ed., pp 797-810, New York: Raven Press.

Wachtel, H. (1988) Defective second-messenger function in the etiology of endogenous depression: novel therapeutic approaches. In *New Concepts in Depression*, eds. Briley, M., Fillion, G., pp 277-293, MacMillan Press.

Wachtel, H. (1989) Dysbalance of neuronal second messenger function in the aetiology of affective disorders: a pathophysiological concept hypothesising defects beyond first messenger receptors, *Journal of Neural Transmission*, **75**, 21-29.

Wenk, G.L., Cribbs, B. & McCall, L. (1984) Nucleus basalis magnocellularis: optimal co-ordinates for selective reduction of choline acetyltransferase in frontal neocortex by ibotenic acid injections, *Experimental Brain Research*, **56**, 335-340.

Westlind, A., Grynfarb, M., Hedlund, B., Bartfai, T. & Fuxe, K. (1981) Muscarinic supersensitivity induced by septal lesion or chronic atropine treatment, *Brain Research*, **225**, 131-141.

White, P., Hiley, C.R., Goodhart, M.J., Carrasco, L.H., Keet, J.P., Williams, I.E.I. & Bowen, D.M. (1977) Neocortical cholinergic neurons in elderly people, *Lancet*, **i**, 668-671.

White, W.F., Nadler, J.V., Hamberger, A., Cotman, C.W. & Cummins, J.T. (1977) Glutamate as a transmitter of hippocampal perforant path, *Nature (London)*, **270**, 356-357.

Wilcock, G.K., Esiri, M.M., Bowen, D.M. & Smith, C.C.T. (1982) Alzheimer's disease: correlation of cortical choline acetyltransferase activity with the severity of dementia and histological abnormalities, *Journal of Neurological Sciences*, **57**, 407-417.

Wisniewski, H.M. & Terry, R.D. (1973) Re-examination of the pathogenesis of the senile plaque. In *Progress in Neuropathology*, ed. Zimmerman, H.M. Vol. 2, pp 1-26, New York and London, Grune and Stratton.

Witter, M.P., Groenewegen, H.J., Lopes da Silva, F.H. & Lohman, A.H.M. (1989) Functional organization of the extrinsic and intrinsic circuitry of the parahippocampal region, *Progress in Neurobiology*, **33**, 161-253.

Wood, P.L., Etienne, P., Lal, S., Nair, N.P.V., Finlayson, M.H., Gauthier, S., Palo, J., Haltio, M., Paetan, A. & Bird, E.D. (1983) A postmortem comparison of the cortical cholinergic system in Alzheimer's disease and Pick's disease, *Journal of Neurological Science*, **61**, 211-217.

Wood, J.G., Girard, P.R., Mazzei, G.J. & Kuo, J.K. (1986) Immunocytochemical localization of protein kinase C in identified neuronal compartments of rat brain, *Journal of Neuroscience,* **6**, 1571-2577.

Woolf, N.J., Eckenstein, F. & Butcher, L.L. (1984) Cholinergic systems in the rat brain. 1. Projection to the limbic telencephalon, *Brain Research Bulletin*, **13**, 751-784.

Worley, P.F., Baraban, J.M., De Souza, E.B. & Snyder, S.H. (1986a) Mapping second messenger systems in the brain: Differential localization of adenylate cyclase and protein kinase C, *Proceedings of the National Academy of Sciences USA,* **83**, 4053-4057.

Worley, P.F., Baraban, J.M. & Snyder, S.H. (1986b) Heterogeneous localization of protein kinase C in rat brain: autoradiographic analysis of phorbol ester receptor binding, *Journal of Neuroscience,* **6**, 199-207.

Worley, P.F., Baraban, J.M., Colvin, J.S., & Snyder, S.H. (1987) Inositol trisphosphate receptor localization in brain : variable stoichiometry with protein kinase C, *Nature*, **325**, 159-161.

Yamamura, H.I. & Snyder, S.H. (1974) Postsynaptic localisation of muscarinic cholinergic receptor binding in rat hippocampus, *Brain Research*, **78**, 320-326.

Yankner, B.A., Dawes, L.R., Fisher, S., Villa-Komaroff, L., Oster-granite, M. & Neve, R.L. (1989) Neurotoxicity of a fragment of the amyloid precursor associated with Alzheimer's Disease, *Science*, **245**, 417-420.

Yeager, R.E., Heideman, W., Rosenberg, G.B. & Storm, D.R. (1985) Purification of the calmodulin-sensitive adenylate cyclase from bovine cerebral cortex, *Biochemistry*, **24**, 3776-3783.

Young, L.T., Kish, S.J., Li, P.P. & Warsh, J.J. (1988) Decreased brain [^{3}H]-inositol 1,4,5-triphosphate binding in Alzheimer's disease, *Neuroscience Letters*, **94**, 198-202.

Young, W.S. III & Kuhar, M.J. (1979) A new method for receptor autoradiography: [^{3}H] opiod receptors in rat brain, *Brain Research*, **179**, 255-270.

PUBLICATIONS

Papers

D. Dewar, K. Horsburgh, D.I. Graham, D.N. Brooks, J. McCulloch (1990) Selective alterations of high affinity ^{3}H-forskolin in Alzheimer's Disease: a quantitative autoradiographic study. Brain Res. **511**: 241-248.

K. Horsburgh, I. Jansen, L. Edvinsson, J. McCulloch. (1990) Second messenger systems: functional role in cerebrovascular smooth muscle regulation. European J. Pharmac. (in press).

K. Horsburgh, D. Dewar, D.I. Graham, J. McCulloch (1990) Autoradiographic imaging of [^{3}H]-phorbol 12,13 dibutyrate binding to protein kinase C in Alzheimer's disease. J. Neurochem. (in press).

K. Horsburgh, J. McCulloch (1990) Alterations of functional glucose use and ligand binding to second messengers following unilateral orbital enucleation. Brain Res. (in submission).

S.E. Browne, K. Horsburgh, D. Dewar, J. McCulloch (1990) An autoradiographic comparison of D-[^{3}H]-Aspartate and [^{3}H]-cyclohexyladenosine as potential markers of glutamate terminals in the rat visual system. Neuroscience Letters (in submission).

Book Chapters

L. Edvinsson, B. Fallgren, I. Jansen, K. Horsburgh (1989) Mechanisms of action and interaction of perivascular peptides and non-peptides in cerebral vasoconstriction. In *Neurotransmission and Cerebrovascular Function I* (eds J. Seylaz and E.T. MacKenzie) pp 131-135, Elsevier Science Publishers B.V.

ABSTRACTS

K. Horsburgh, D.T. Chalmers, J. McCulloch (1988) ^{3}H-Forskolin binding in the visual system of the rat after unilateral orbital enucleation. Br. J. Pharmac. **95**: 902P.

D. Dewar, K. Horsburgh, D.N. Brooks, J. McCulloch (1989) Quantitative autoradiographic measurement of [^{3}H]-forskolin binding sites in human brain : deficits in Alzheimer's Disease. Br. J. Pharmac. **96**: 349P.

D. Dewar, K. Horsburgh, D.I. Graham, D.N. Brooks, J. McCulloch (1989) Selective alterations of [^{3}H]-forskolin binding sites in Alzheimer's Disease assessed by quantitative autoradiography. Neuropathol. App. Neurobiol. **15**: 273.

D. Dewar, K. Horsburgh, D.I. Graham, J. McCulloch (1989) Heterogeneous alterations of ^{3}H-forskolin binding sites in Alzheimer Brain. J. Cereb. Blood Flow Metab. Suppl. **1**: S571

K. Horsburgh, D.T. Chalmers, J. McCulloch (1989) Modulation of [^{3}H]-forskolin binding by 5'guanylimidodiphosphate in the rat visual system after unilateral orbital enucleation. J. Cereb. Blood Flow Metab. Suppl. **1**: S704.

K. Horsburgh, I. Jansen, L. Edvinsson, J. McCulloch (1989) Vasomotor responses of feline cerebral arteries in situ and in vitro to forskolin and phorbol 12,13 dibutyrate. J. Cereb. Blood Flow Metab. Suppl. **1**: S461.

K. Horsburgh, D. Dewar, D. Graham, J. McCulloch (1990) Quantitative autoradiography of protein kinase C levels in Alzheimer's Disease. Neurobiol. Aging. **11**: S359.

K. Horsburgh, D. Dewar, D.I. Graham, J. McCulloch (1990) [^{3}H]-Phorbol 12,13 dibutyrate binding to protein kinase C in Alzheimer's disease: a quantitative autoradiography study - in submission for presentation at XVth International Symposium on Cerebral Blood Flow and Metabolism.

S.E. Brown, K. Horsburgh, D. Dewar, J. McCulloch (1990) An autoradiographic comparison of D-[^{3}H]-aspartate and [^{3}H-cyclohexyladenosine binding in the rat visual system after orbital enucleation, Br. J. Pharmacology, .. S128.

S.E. Brown, K. Horsburgh, D. Dewar, J. McCulloch (1990) D-[^{3}H]-Aspartate binding does not map glutamate terminals in the rat visual system - an autoradiographic study - in submission for presentation at XVth International Symposium on Cerebral Blood Flow and Metabolism.